The Effect of IKKbeta on Estrogen Receptor Positive Breast Cancer Phenotypes

BY

LAMIAA KHAMIES MOHAMED ALI EL-SHENNAWY
B.S., University of Alexandria, Egypt, 1997
M.S., University of Alexandria, Egypt, 2008

THESIS

Submitted as partial fulfillment of the requirements
for the degree of Doctor of Philosophy in Biopharmaceutical Sciences
in the Graduate College of the
University of Illinois at Chicago, 2015

Chicago, Illinois

Defense Committee:

Jonna Frasor, Chair and Advisor
Debra Tonetti
Leslyn Hanakahi, Medicinal Chemistry and Pharmacognosy
Gail Prins, Urology
Steven Swanson, University of Wisconsin-Madison

This thesis is dedicated to breast cancer patients and breast cancer survivors.

ACKNOWLEDGMENTS

It is with great pleasure that I record my deepest gratitude and special appreciation to Dr. Jonna Frasor, who taught me how to be a scientist. I am truly thankful for the valuable time she devoted in planning and supervising this work. I am gratefully acknowledging her continuous encouragement, support, and constructive criticism.

I would like to thank the members of my dissertation committee: Dr. Debra Tonetti, Dr. Gail Prins, Dr. Leslyn Hanakahi, and Dr. Steven Swanson, for their invaluable insight, comments, and advice. I really appreciate their intellectual contributions to the development of this work.

To my current and former lab mates: Dr. Irida Kastrati, Dr. Dana Felice-Podwol, Dr. Shuangping Zhao, Gergana Georgieva, and Jeanne Danes, thanks for your help, support, and encouragement.

Finally, I would like to point out that I could not have accomplished this work without the support of my beloved parents and the tremendous care and encouragement of my wonderful husband and children. Thank you, my family, for standing by my side.

LES

TABLE OF CONTENTS

TABLE OF CONTENTS (continued)

CHAPTER **PAGE**

TABLE OF CONTENTS (continued)

LIST OF TABLES

LIST OF FIGURES

LIST OF FIGURES (continued)

FIGURE **PAGE**

LIST OF FIGURES (continued)

FIGURE **PAGE**

LIST OF ABBREVIATIONS

AF-1	Activation function 1
AF-2	Activation function 2
AP-1	Activator protein 1
AURKA	Aurora kinase A
BSA	Bovine serum albumin
CA-IKKβ	Constitutively active IκB kinase β
CBP	CREB-binding protein
CD40L	CD40 ligand
CDK	Cyclin-dependent kinase
cIAP1/2	Cellular inhibitor of apoptosis protein 1 and 2
CK	Cytokeratin
Dox	Doxycycline
DPBS	Dulbecco's phosphate-buffered saline
E2	17-β estradiol
ECM	Extracellular matrix
EGFR	Epidermal growth factor receptor
EMT	Epithelial mesenchymal transition
ER	Estrogen receptor α
ER-	Estrogen receptor α negative
ER+	Estrogen receptor α positive
EREs	Estrogen response elements
EZH2	Enhancer of zeste homolog 2
FADD	Fas-associated death domain

LIST OF ABBREVIATIONS (continued)

FBS	Fetal bovine serum
FDR	False discovery rate
FITC	Fluorescein isothiocyanate
GFP	Green fluorescent protein
GO	Gene ontology
GSEA	Gene set enrichment analysis
H&E	Hematoxylin and eosin
HER2	Human epidermal growth factor receptor 2
IHC	Immunohistochemistry
IκBα-DN	Dominant negative IκBα
IKK	IκB kinase
IKKα	IκB kinase α
IKKβ	IκB kinase β
IL-1β	Interleukin-1β
IVIS	In vivo imaging system
MAPKs	Mitogen-activated protein kinases
MMPs	Matrix metalloproteinases
MSigDB	Molecular signatures database
NCoR1	Nuclear receptor corepressor 1
NEMO	NF-κB essential modulator
NES	Normalized enrichment analysis
NF-κB	Nuclear factor kappa-light-chain-enhancer of activated B cells
NIK	NF-κB-inducing kinase

LIST OF ABBREVIATIONS (continued)

NLS	Nuclear localization signal
NSAIDs	Nonsteroidal anti-inflammatory drugs
PBS	Phosphate-buffered saline
PR	Progesterone receptor
RHD	Rel homology domain
RIP1	Receptor-interacting protein 1
SRC	Steroid receptor coactivator
TAK1	Transforming growth factor β-activated kinase 1
TNFR1	Tumor necrosis factor receptor 1
TNFα	Tumor necrosis factor-α
TRADD	TNFR1-associated death domain
TRAF2	TNFR-associated factor 2
TRAF3	TNFR-associated factor 3
UPR	Unfolded protein response
βTRCP	β-transducin repeat-containing protein

SUMMARY

Breast cancer is the second cause of cancer-related deaths of women in the US. Almost 75% of breast tumors are of the luminal subtype and express the estrogen receptor alpha (ER) at the time of diagnosis. Estrogen receptor positive (ER+) breast tumors depend on estrogens for cell proliferation, survival, and overall tumor progression. Endocrine therapy targets ER and is effective in treating the disease; however, almost 50% of women receiving endocrine therapy will experience relapse and late recurrence from 5 to more than 20 years after initial diagnosis. The recurrent tumors are often aggressive, resistant, and metastatic.

A growing body of evidence suggests that an inflammatory microenvironment and activation of the proinflammatory NF-κB pathway are highly associated with the progression of ER+ tumors to more aggressive stages. It has been reported that ER+ tumors with constitutively active NF-κB represent a subset of patients with increased risk of recurrence, metastasis, and poor overall survival. However, it is unknown whether NF-κB is a driver or a consequence of aggressive ER+ breast cancer.

In order to study this, we developed MCF-7 and T47D ER+ breast cancer cell lines expressing a Doxycycline (Dox)-inducible constitutively active form of IκB kinase β (CA-IKKβ), a key kinase in the canonical NF-κB pathway. Treating the cells with Dox results in the expression of CA-IKKβ which can activate the NF-κB pathway and regulate the expression of NF-κB target genes. Thus, the Dox-inducible system allowed us to specifically activate the canonical arm of the NF-κB pathway in a controlled fashion.

One of the main hallmarks of aggressive ER+ breast tumors is high proliferation, yet, we found that activation of IKKβ inhibited E2-dependent cell proliferation in vitro and tumor growth in vivo. However, IKKβ enhanced E2-induced cell survival. This was particularly evident in vivo because the cells survived for up to 60 days at the implantation site despite the absence of

palpable tumors. The effect of CA-IKKβ on cell proliferation and tumor growth was reversible, suggesting that CA-IKKβ induces dormant ER+ breast cancer. Intriguingly, coactivation of ER and IKKβ promoted cell migration and invasion in vitro as well as both spontaneous and experimental metastasis in vivo.

Cell-based studies revealed that coactivation of ER and CA-IKKβ does not induce epithelial mesenchymal transition, yet, ER and NF-κB work together to expand a basal-like cell population responsible for invasion, suggestive of collective motility. Generally, we observed that activation of IKKβ and treatment with E2 induced a global inhibition in differentiation regulators and shifted the cells away from the luminal, epithelial, differentiated state with the gain of some progenitor properties. However, that occurred without full differentiation to the basal or mesenchymal state.

Taken together, this study suggests that coactivation of ER and the canonical arm of NF-κB pathway may induce a dormant metastatic ER+ breast cancer phenotype. This proposes IKKβ as a driver of some features of aggressive ER+ breast cancer and suggests it as a biomarker and a novel therapeutic target in ER+ breast cancer.

I. INTRODUCTION

1.1 Estrogen receptor positive breast cancer

1.1.1 Breast cancer facts and subtypes

Breast cancer is a global problem, accounting for almost one quarter of all cancers in women worldwide (1). In the US, it is the most commonly diagnosed cancer in women besides skin cancer. Moreover, it is considered as the second cause of cancer-related mortalities in women after lung cancer. Based on 2010-2012 data, approximately 13.3% of US women will be diagnosed with the disease at some point in their lifetime. In 2015, an estimate of 292,130 women will be diagnosed with breast cancer, and 40,730 women will die of the disease (2-4).

There are risk factors associated with breast cancer, some of which depend on life style, such as obesity, physical inactivity, heavy smoking, alcohol consumption, and the use of hormone replacement therapy comprising combined estrogen and progesterone. Other factors do not depend on life style, such as: benign breast conditions (e.g. atypical hyperplasia), high breast density, and exposure to chest radiation for cancer treatment at young age (e.g. in cases of Hodgkin lymphoma). Family history, in particular, having one or more affected first degree relatives, constitutes another risk factor. There are also reproductive risk factors including long menstrual history, nulliparous or having the first child after the age of 30, and the use of oral contraceptives (3).

Breast cancer is a heterogeneous disease, comprising a number of subtypes that differ in terms of histology, patterns of distant metastasis, patient outcomes, and disease free survival (5). Perou and colleagues were the first to describe molecular subtypes of breast cancer by mapping the phenotypic diversity observed in patients to particular gene expression patterns (6). There are five established breast cancer intrinsic subtypes: luminal A, luminal B, HER2-

enriched, claudin-low, and basal-like. Subsequent studies related the different subtypes to prognosis, clinical outcomes, and response to chemotherapy (7-9).

Luminal tumors are typically positive for the biomarker estrogen receptor alpha (ER) and /or progesterone receptors (PR), whereas the HER2 subtype of tumors are generally negative for ER and PR but positive for human epidermal growth factor receptor 2 (HER2). Basal and claudin-low subtypes are negative for the three receptors, with claudin-low tumors exhibiting reduced expression of genes involved in tight junctions and cell-cell adhesion (6,8,10,11).

Almost 75% of breast tumors are of the luminal A and B subtypes and express ER at the time of diagnosis (12,13). Patients with ER-positive (ER+) tumors usually have better prognosis compared to ER-negative (ER-) tumors. Luminal B tumors express lower ER compared to luminal A. In terms of patient outcome, women with luminal B tumors have significantly shorter relapse-free and overall survival times. Thus, the luminal B subtype is considered to be more aggressive than luminal A (8,10).

1.1.2 Estrogen receptor alpha

ER is a nuclear receptor that functions as a ligand activated transcription factor. It is composed of six domains, designated A-F. The N-terminal (A/B domain) comprises a region responsible for the transcriptional activity of the receptor in the absence of the ligand; it is termed activation function 1 (AF-1). The C domain is the DNA-binding domain (DBD), comprising a two zinc-finger structure important for receptor dimerization and DNA binding. A hinge region, the D domain, contains a signal for nuclear localization. The E domain is the ligand binding domain (LBD), consisting of a twelve-helix region involved in ligand binding, and an activation function domain (AF-2) responsible for ligand-dependent activation of the receptor. It also contains a dimerization site and a nuclear localization signal. The F domain is located at

the C-terminal, which is considered not necessary for the transcriptional activity, yet, modulates both AF-1 and AF-2 activity (14).

ER function involves both genomic and non-genomic mechanisms of action. In the direct/classic genomic action of ER pathway, a ligand, such as the agonist 17-β estradiol (E2), binds to ER resulting in conformational changes. The receptor then dimerizes and directly binds to DNA sequence of target genes, known as estrogen receptor elements (EREs), to either induce or repress gene expression. Direct ER binding to EREs at gene enhancers is facilitated via pioneer factors, such as FoxA1 and Gata3, which act to facilitate chromatin opening and thus provides access for the liganded receptor (15). Indirect genomic activity, however, involves the binding of ER to other transcription factors, such as specificity protein 1 (SP-1), activator protein 1 (AP-1) Fos/Jun complexes (16-18). This leads to the recruitment of ER to transcriptional sites other than EREs where it can influence gene transcription.

Direct or indirect binding of ER recruits coactivators and coregulators (e.g. steroid receptor coactivator (SRC) and p300/CBP) to enhancers resulting in the regulation of RNA polymerase II (Pol II) recruitment or activity, and subsequent regulation of target gene expression. The majority of ER binding sites are distant from the transcription start sites of regulated genes (15). The regulation of ER target genes can take place via short-range interactions, as in the case of promoter proximal enhancers, as well as long range interactions, as in the case of promoter distal enhancers. The latter involves DNA looping with target gene promoters in order to connect ER activity to promoter engaged polymerase II and the transcriptional machinery (19).

Ligand-independent ER transcriptional activity has also been reported. Phosphorylation of the receptor or its coregulators causes ligand-independent ER activation. This modulation is

induced by different kinases (e.g. protein kinase A), growth factors signaling pathways (e.g. insulin-like growth factor and epidermal growth factor), and other extracellular signals, such as neurotransmitters and cell cycle regulators. Ligand-independent ER transcriptional activity can contribute to hormone-independence of breast tumors (20,21).

Estrogen can also elicit rapid responses mediated via receptors localized near or at the plasma membrane, such as G protein-coupled estrogen receptor 1 (GPER1) and certain variants of ER. This involves the interaction between plasma membrane ER and many other proteins, such as c-Src, G proteins, growth factor receptors (e.g. epidermal growth factor receptor (EGFR)), cytoplasmic kinases (e.g. mitogen-activated protein kinases (MAPKs), phosphoinositide 3-kinase (PI3K) and AKT), or signaling enzymes (e.g. adenyl cyclase). Thus, E2 mediates different mechanisms independent of gene transcription (22). The molecular mechanisms underlying the non-genomic pathway are diverse and cell type specific, since they depend on the availability of signal transduction molecules and their downstream targets (23).

1.1.3 Estrogen receptor as a therapeutic target

Estrogen receptor positive breast tumors are generally estrogen-dependent, which means that they depend on estrogens for cell proliferation, survival, and overall tumor growth and progression. Because it mediates the effects of estrogens in breast cancer, ER has historically been an attractive therapeutic target. The activity of ER can be inhibited either directly by blocking signaling through ER or indirectly by reducing estrogens levels. Selective estrogen receptor modulators (SERMs, e.g. tamoxifen and raloxifene) compete with estrogen for binding to ER (24). In contrast, selective estrogen receptors downregulators (SERDs, e.g. ICI 182,780/fulvestrant) induce destabilization and subsequent proteosomal degradation of ER (25). Estrogen synthesis inhibitors (e.g. aromatase inhibitors (AIs), such as exemestane,

anastrozole, or letrozole) inhibit the aromatase enzyme responsible for the conversion of androgen to estrogen, thus inhibiting the level of local estrogen in the tumor microenvironment (26).

Endocrine therapy, particularly tamoxifen and aromatase inhibitors, has proven to be effective in treating ER+ breast cancer (27). Endocrine therapy is also approved for breast cancer prevention in women with high risk for the disease (28). A major obstacle in using endocrine therapy is resistance. Some patients do not respond to first line treatment, and this is known as *de novo* resistance. Other patients experience relapse, despite an initial positive drug response, and this is known as acquired resistance (14). It is estimated that almost 50% of women with ER+ disease will experience recurrence. The tumors that recur are often therapy-resistant, aggressive and metastatic tumors (12,13,29,30).

Extensive studies have attributed endocrine therapy resistance to a number of mechanisms: (i) loss of ER expression (31), (ii) availability of coactivator/corepressor of ER complex formation necessary for DNA accessibility (32), (iii) non genomic ER signaling (33), iv) ligand-independent phosphorylation and activation of ER and ER-accessory protein by different kinases (34,35), and (v) crosstalk between ER and other growth factor signaling pathways (36). Thus, finding predictive markers of therapy resistance and effectively treating women with recurrent/resistant ER+ tumors mandate a better understanding of the molecular factors and pathways modulating ER.

One important and understudied aspect of metastatic recurrence in ER+ disease, is that ER+ tumors tend to relapse after a prolonged period of dormancy. Estrogen receptor positive metastatic recurrence can occur from 5 years to more than 20 years after primary diagnosis and/or surgery (37-39). A study reported that the median 15-year distant relapse rates were 27.8% and 42.9% for luminal A and luminal B tumors, respectively (13). This is in contrast to

ER- tumors, which relapse early (~2 years after diagnosis), and then the recurrence rate diminishes after 5 years (30,40). The Early Breast Cancer Trialists' Collaborative Group reported the long term value of 5 years of tamoxifen, through 15 years of follow-up. The annual risk of recurrence in years 0 through 4 was 3-4% per year. Late recurrence in years 5 through 9 was 2-3%. After 10 years, the annual risk of recurrence was ~2% (39,41,42). Similarly, adjuvant trials of aromatase inhibitors, tamoxifen or combination of both revealed that the annual recurrence was ~2-4% (42-45). The risk for late recurrence indicates that women with clinically undetectable cancer can have disseminated ER+ tumor cells that survive in a non-proliferating/dormant state for up to decades. While proliferating disseminating tumor cells are targets of endocrine therapy and chemotherapy, non-proliferating cells, however, are not effectively targeted by such therapy (46).

Breast cancer mortalities are mainly due to metastasis and not the primary tumor. It is estimated that ~90% breast cancer mortalities are a consequence of metastatic disease, whether the tumor was metastatic at diagnosis or metastatic recurrence developed later (1). Approximately 70% of late distant recurrent metastatic breast tumors are ER+ (13,47). Recently, preclinical mouse models have shown that ER+ breast cancer metastases are likely to be dependent on estrogen signaling (47). Interestingly, 65-70% of distant metastases and greater than 80% of the lymph node metastases arising from human ER+ tumors retain ER expression (48,49). Moreover, ER mutations have been identified in metastatic and endocrine resistant patient tumors. The mutations were shown to play a role in therapy resistance and enhanced ER activity (50,51). This indicates that ER remains a main player in the progression to resistance and metastatic recurrence.

1.2 NF-κB pathway and estrogen receptor positive breast cancer

1.2.1 NF-κB pathway

Nuclear factor kappa-light-chain-enhancer of activated B cells (NF-κB) is an evolutionarily conserved pathway, which controls the expression of genes involved in multiple physiological processes, including the development, function, and maintenance of the innate and adaptive immune system, inflammation, cell survival and apoptosis. Constitutive activation of the pathway is a driver of chronic inflammation, which underlies the development and progression of multiple diseases including cancer (52-54).

NF-κB transcription factors are divided into two classes. The first class comprises RelA/p65, RelB, and c-Rel family members, which contain a transcriptional activation domain at their C-terminus and are synthesized in their mature form. The second class comprises NF-κB1/ p105 and NF-κB2/p100 family members, which lack the transcriptional activation domain and contain C-terminal series of ankyrin repeats. The mature p50 and p52 subunits are synthesized from their longer precursors, p105 and p100, respectively, through ubiquitin-dependent proteolytic processing of the C-terminus. NF-κB family members can form homo and heterodimers to activate transcription of their target genes. RelB is different from the other members in that it binds DNA as a heterodimer only. The N-terminal region of NF-κB family members shares homology with the v-Rel oncoprotein and is termed Rel homology domain (RHD). All NF-κB proteins contain (RHD), which is responsible for their dimerization, nuclear translocation, and DNA binding. The carboxyl terminus of RHD contains a nuclear localization signal (NLS), which is recognized and blocked by inhibitory IκB proteins. These inhibitory proteins include IκBα, IκBβ, IκBε, and the carboxy termini of p105 and p100. Binding of IκB proteins to the RHD interferes with the function of the NLS and inhibits nuclear localization. Thus, IκBs maintain NF-κB in the cytoplasm and are crucial for signal responsiveness (55,56).

The IκB kinase (IKK) complex is an essential upstream player that is required for activation of the transcription factors. It comprises two serine specific catalytic subunits IKKβ and IKKα, as well as non-enzymatic regulatory proteins NEMO (NF-κB essential modulator) or IKKγ. NF-κB activation is regulated by two different pathways, the canonical pathway and the non-canonical pathway (Figure 1).

1.2.1.a <u>The canonical pathway of NF-κB activation</u>

In the canonical pathway, NF-κB activation is induced by various stimuli, including proinflammatory cytokines (e.g. tumor necrosis factor-α (TNFα) and interleukin-1β (IL-1β)), bacterial products (e.g. lipopolysacharides) and others. When TNFα, for example, binds to its receptor, tumor necrosis factor receptor 1 (TNFR1), adaptor proteins TNFR1-associated death domain (TRADD), Fas-associated death domain (FADD), TNFR-associated factor 2 (TRAF2) and receptor-interacting protein 1 (RIP1) are recruited and a complex is assembled at the TNFR1. This promotes RIP1 polyubiquitination, which then becomes a docking site for TAB2 and TAB3. These are essential components in the transforming growth factor β-activated kinase 1 (TAK1) complex. The IKK complex is brought to close proximity with TNFR1 signalosome via NEMO, which can recognize ubiquitinylated RIP1. This facilitates the phosphorylation and activation of IKKβ molecule on Ser177 and 181 by TAK1 (56-59).

Activated IKKβ then phosphorylates its substrate the NF-κB inhibitor, IκBα at Ser32 and Ser36. This induces IκBα ubiquitination by the Skp1, Cdc53/Cullin1, and F-box protein (SCF)-β transducin repeat-containing protein (βTRCP) complex, targeting it for rapid degradation by the 26S proteasome. Consequently, NF-κB dimers translocate to the nucleus, bind to their DNA motifs in target gene promoters, and induce gene expression (56-58) (Figure 1).

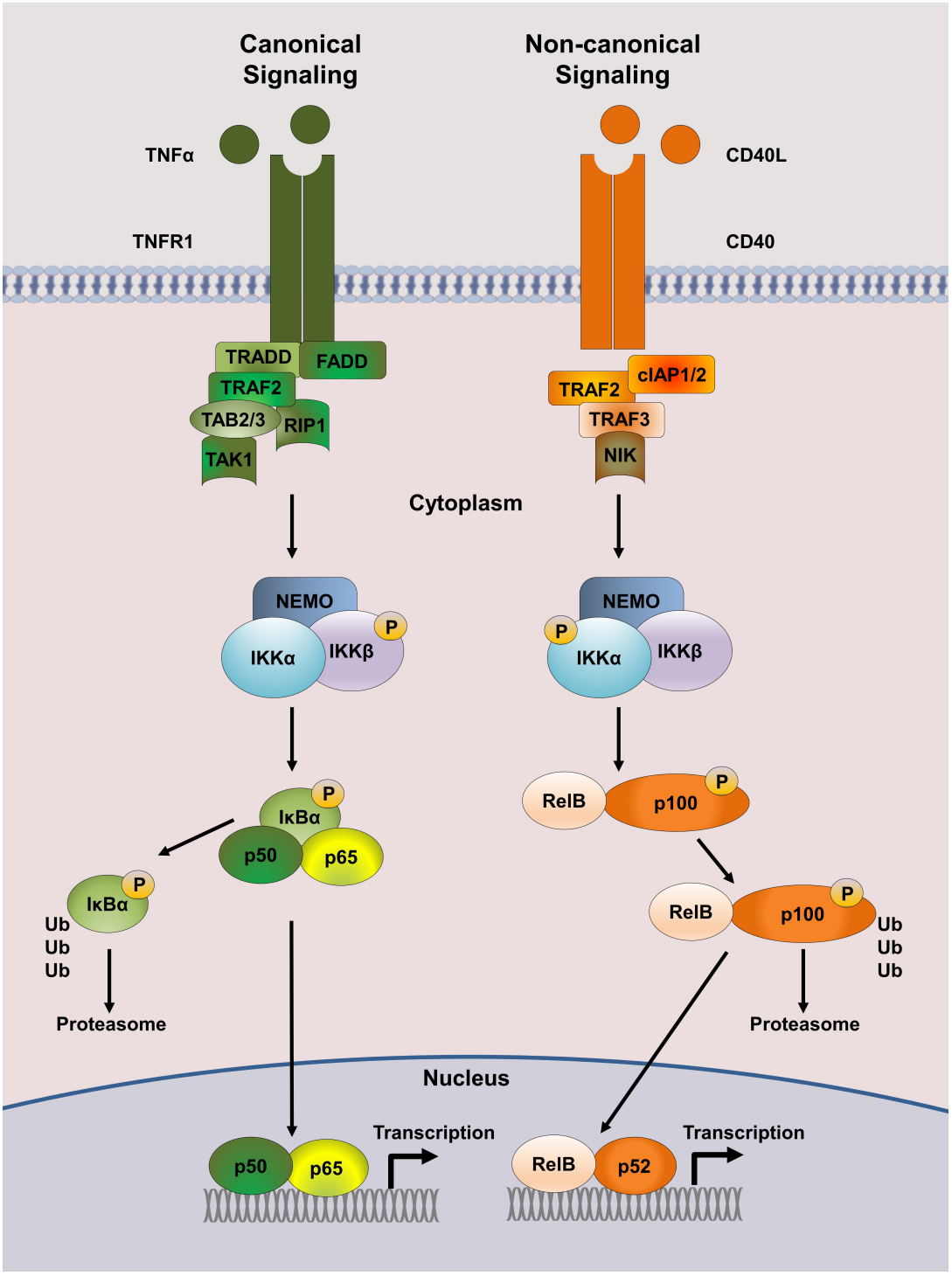

Figure 1: The NF-κB pathway (Adapted and modified from Oeckinghaus et al., 2011 (57)).

1.2.1.b The non-canonical pathway of NF-κB activation

IKKα is activated by certain TNF family members (e.g. lymphotoxin-β (LT-β) and CD40 ligand (CD40L)). IKKα activation is independent of IKKβ or the other regulatory subunits of the IKK complex. In resting, non-activating cells, TNFR-associated factor 3 (TRAF3) links NF-κB-inducing kinase (NIK) to TRAF2 and cellular inhibitor of apoptosis protein 1 and 2 (cIAP1/2), which results in the degradation of NIK. Upon cell activation, TRAF3 degradation takes place allowing for NIK accumulation. NIK is then activated by auto-phosphorylation and in turn phosphorylates IKKα on Ser176 and 180. Activated IKKα then phosphorylates the C-terminal residues in p100 in RelB-p100 complexes. This induces p100 association with the βTRCP complex and its subsequent proteasomal processing to p52, which can then form a transcriptionally active heterodimer with RelB. The dimer translocates to the nucleus, binds to DNA, and mediates transcription of target genes. The generation of mature p52 is IKKα dependent but not IKKβ or NEMO dependent. IKKα kinase activity is not necessary for the activation of the canonical NF-κB pathway by proinflammatory stimuli (56-59) (Figure 1).

1.2.2 Inflammation increases risk of estrogen receptor positive breast cancer

Inflammation is considered as one of the hallmarks of cancer, playing roles in all aspects of tumor biology (e.g. initiation, promotion, and metastasis) (60). Systemic inflammation has been associated with breast cancer risk factors, such as age and menopause. Local inflammation, within the microenvironment of the breast, has been associated with other breast cancer risk factors, such as mammary gland involution after pregnancy and obesity (61). Interestingly, studies have demonstrated that regular intake of nonsteroidal anti-inflammatory drugs (NSAIDS), such as aspirin, reduces the risk of ER+, but not ER- breast cancers, suggesting a significant role of inflammation in the incidence of ER+ tumors (62).

One explanation is that the breast can be a local source estrogen. It has been established that inflammatory factors, such as prostaglandin E2 (PGE2) and cytokines, can stimulate the expression of aromatase within the breast. Aromatase is the enzyme responsible for converting androgen to estrogen. Importantly, the breast microenvironment is a source of inflammatory cytokines, because the breast is an inflammatory organ composed of adipose tissue with embedded hormonally responsive epithelial cells, as well as different types of stromal and immune cells. The infiltrating immune cells can secrete cytokines and chemokines. Tumors respond to the inflammatory microenvironment by activating the inflammatory NF-κB pathway. Tumor cells can also generate an inflammatory microenvironment by producing additional inflammatory cytokines and attracting inflammatory cells under conditions of hypoxia, oncogenic changes, or cancer therapy associated cell death. Thus, inflammatory cytokines produced within tumor microenvironment, can elevate the local estrogen production, which in turn can stimulate the growth of ER+ tumors (61,63).

1.2.3 Role of NF-κB pathway activity in estrogen receptor positive breast cancer

The recognition of the role of NF-κB in cancer was initially delayed, because mutations in the pathway are rare. Interest in the role of NF-κB, however, increased with the discovery of the avian viral oncogene, v-Rel, which exhibits structural homology to the NF-κB Rel transcription factors (52). Currently, NF-κB is considered as a crucial integrator of immunity, inflammation and oncogenesis, and its activity is reported in many types of cancers, including breast cancer, where it is associated with tumor promotion and progression, as well as therapy resistance (54,64).

NF-κB has been shown to be a key regulator of mammary tumor development and progression in animals (55,65-68). In Polyoma middle T oncogene (PyMT) transgenic mice, a

model that can effectively represent human mammary tumors, NF-κB inhibition during tumorigenesis results in increased tumor latency, as well as decreased tumor burden (69). The progression of rat mammary carcinoma cells to malignant phenotype was shown to be accompanied by constitutive activation of the NF-κB pathway (70). Furthermore, increased NF-κB DNA binding was observed in 7,12-dimethylbenzaanthracene (DMBA)-induced rat mammary tumors even before tumors were detectable, emphasizing the early critical role of NF-κB in mammary carcinogenesis (68,71).

Elevated NF-κB DNA-binding and activity has also been reported in human breast tumors, as well as breast cancer cell lines (55,70-73). Furthermore, high IKK kinase activity has been observed in primary human breast tumors and in transformed breast cancer cell lines (74). Several studies reported that elevated NF-κB is primarily associated with an ER- status (70,75). However, published studies indicate that p65 and p50 are expressed in all ER+ tumors (76). Furthermore, these factors were found to be constitutively activated, based on DNA binding activity, in ~15-25% of ER+ breast tumors (77-79). It has been reported that women with ER+ tumors, which have constitutively active p50 and p65, represent a subset of patients with increased risk of recurrence, metastasis, and poor overall survival (77,78).

Constitutive activation of NF-κB in cancer may arise from intrinsic dysregulation of the pathway within the tumor or extrinsic signals in the tumor microenvironment (52,55). Mutations of NF-κB signaling components are one example of intrinsic dysregulation; however, NF-κB activating mutations are rare and are mainly reported in some liquid malignancies (52). An activating mutation of the IKBKE, which encodes for the non-canonical kinase IKK epsilon, has been identified in breast tumors. Yet, the mutation was not found to be associated with ER status (80). On the other hand, several extrinsic signals from the microenvironment have been shown to upregulate expression and/or activity of NF-κB signaling components (52,55). Cancers

with constitutively active NF-κB rely on upstream pathway stimulation, which may involve autocrine and paracrine secretion of inflammatory cytokines, activating mutations of oncogenes, and inactivating mutations of tumor suppressors that crosstalk with NF-κB signaling (52).

Cell based studies related constitutive active NF-κB to cell-derived IL-1, where non-cytokine-dependent activation of EGFR activates NF-κB and results in the expression of the proinflammatory cytokine IL-1, which further activates NF-κB creating a positive feedback loop in human ER- breast cancer cells (81). Another study reported that Annexin1, a member of annexin superfamily of calcium and phospholipid-binding proteins, is a mediator of constitutive activity of NF-κB in basal ER- breast cancer. Annexin1 acts by interacting with NEMO and RIP1 and stabilizing the IKK complex, resulting in high levels IκBα phosphorylation and constitutively active NF-κB (82). Studies in murine breast cancer cell lines proposed overexpression of epidermal growth factor receptor Her2/neu and heregulin as major inducers of constitutive activation of NF-κB (83,84).

The NF-κB pathway is one of the pathways that can influence many, if not all, of the endocrine therapy resistance mechanisms (85). Nakshatri and colleagues reported that the progression of rat mammary cancer cells from an ER+ nonmalignant phenotype to an ER- malignant hormone-independent phenotype is associated with constitutively active NF-κB (70). In ER+ tumors, nuclear expression of NF-κB /p65 was accompanied with resistance to neoadjuvant chemotherapy (77,86). Relating to endocrine therapy, several studies have associated aberrant or constitutively active NF-κB to endocrine therapy resistance. As mentioned above, high DNA binding activity of NF-κB subunits can identify a subset of ER+ tumors with high-risk for early relapse and tamoxifen resistance (78). High basal NF-κB expression and activity were detected in raloxifene resistant cells (87). Higher NF-κB expression is observed in aromatase inhibitor-resistant breast tumors compared to primary tumors before

treatment (88). Furthermore, overexpression of NF-κB induces aromatase inhibitor resistance in breast cancer cell lines (88). Moreover, several preclinical studies have shown that the repression of NF-κB activity restores the sensitivity to endocrine therapy in resistant breast cancer cell lines (89-91). Trinh and colleagues performed a phase II study of the combination of endocrine treatment and the protease inhibitor bortezomib, which is considered as an NF-κB inhibitor. They reported that bortezomib is able to slow disease progression in 22% of ER+ breast cancer patients who developed metastasis during endocrine therapy (92). Thus, the NF-κB pathway plays a critical role in the development of hormone-independence and therapy resistance in ER+ breast tumors.

1.2.4 NF-κB as a therapeutic target

Owing to the role of NF-κB in cancer, targeting the pathway is proposed to be an effective therapeutic strategy. Different points in the pathway can be targeted including IKK activation, IκB degradation, NF-κB nuclear translocation, and DNA binding (93).

1. IKK inhibitors, such as BAY-11-7082, MLN120B, SC-514 and CHS828, are small molecules that can directly bind to and inhibit IKK kinase activity or can block upstream signaling that leads to IKK activation. Most of the compounds are either ATP binding competitors or allosteric inhibitors (93,94). The early recognition of IKKβ as the key driver of NF-κB signaling directed the pharmaceutical companies towards the production of mainly IKKβ inhibitors. Yet, none is in clinical use and only several have published results (52).
2. Proteasome inhibitors, such as bortezomib, inhibit the activity of proteasomes and thus block NF-κB activation at the level of IκB protein degradation. Bortezomib is the first NF-κB inhibitor approved by the FDA and the European Medicines Agency as a treatment of

multiple myeloma (95). In breast cancer, preclinical studies reported that inhibition of NF-κB by bortezomib is able to restore endocrine sensitivity in ER+ resistant breast cancer cell lines (96). A recent study reported that bortezomib inhibits the expression of ER and induces cell death in ER+ breast cancer cells, and proposed the drug for the management of early stage ER+ tumors (97).

3. Nuclear translocation and DNA binding inhibitors. Nuclear translocation inhibitors are small peptides that restrain NF-κB in the cytoplasm even after IκB degradation (e.g. SN-50) (98). DNA binding inhibitors, prevent NF-κB from binding to specific κB sites on DNA (e.g. the sesquiterpene lactone, parthenolide) (99).

Other mechanisms of NF-κB inhibition have also been proposed, such as the use of anti-inflammatory drugs and immunosuppressant drugs. NSAIDs (e.g. sulindac, aspirin, ibuprofen, indomethacin, and COX-2 inhibitors) suppress the inflammatory cell response and thus indirectly suppress NF-κB or directly suppress key points along the NF-κB pathway. Naturally occurring anti-inflammatory compounds (e.g. curcumin and luteolin) belong to this group of NF-κB inhibitors. However, these chemicals are antioxidants and thus their anticancer activity may be due to regulating the redox status of the cell, which in turn may contribute to NF-κB blockade (52).

Gene therapy is another proposed strategy for NF-κB inhibition. This type of therapy directly targets the components of NF-κB pathway. Approaches may involve adenoviral delivery of IκB-super repressor, which is a synthetic non-degradable IκBα, or the use of RNA interference directed against IKKα, IKKβ, or the upstream TAK1. The clinical use of gene therapy, however, mandates the development of specific and efficient targeted delivery systems (52).

A major obstacle in effectively targeting the NF-κB pathway in the clinic is the lack of specificity. Most NF-κB targeting drugs are not NF-κB specific, and the mechanism of inhibition for most drugs is not well established (52). For example, studies have shown that proteasome inhibitors may enhance NF-κB activity in an IKK-dependent manner. Importantly, NF-κB targeting drugs interfere with the physiological role of NF-κB in inflammation, immunity and cellular homeostasis, resulting in side effects such as immunodeficiency. Thus targeting the pathway for cancer prevention and treatment represents a major challenge (52,54,93,100).

NF-κB inhibition alone is generally insufficient to treat cancer, because most of the inhibitors have intrinsic limited chemotherapeutic effect. Thus, NF-κB inhibition is being examined mainly for use in combination with endocrine or chemotherapy. It is reported that therapeutics or radiation activate NF-κB, which inhibits the anticancer activities of the therapeutic agents. Therefore, blocking NF-κB may overcome these complications and result in enhanced anticancer effect. However, selective methods of NF-κB inhibition are still desired for reducing systemic toxicity (93). There is no NF-κB inhibitor approved for the clinical use with ER+ breast cancers. Clinical trials, examining the effect of combined treatment with bortezomib and endocrine therapy or chemotherapy, are ongoing. Other trials on the use of natural products like curcumin are also underway (clinicaltrials.gov).

1.3 Estrogen receptor and NF-κB crosstalk

Studies indicate a critical role for NF-κB in ER+ breast cancer. Hence, understanding the crosstalk between NF-κB and ER, and the effect of each on the other's activity and function, may provide the tools to overcome ER+ tumor progression and endocrine resistance in patients.

1.3.1 Estrogen receptor and NF-κB transrepression

Generally, the activation profiles of both ER and NF-κB in breast cancer are inversely correlated (70,79). In fact, numerous studies suggest a mutual inhibition between ER and NF-κB signaling, where NF-κB represses ER activity and ER represses NF-κB activity (101-103).

1.3.1.a Inhibition of NF-κB by estrogen receptor

Inhibition of NF-κB by ER occurs through different mechanisms that can affect NF-κB pathway activation, NF-κB nuclear translocation, and DNA binding or NF-κB transcriptional activity. ER may maintain a steady state of IκBα levels and thus, inhibit NF-κB activation (104). ER may prevent DNA binding of c-Rel and p65 to the promoter of the NF-κB target gene, IL-6. The interaction of ER with RHD of NF-κB is suggested as a possible mechanism for this observation (105). Furthermore, E2 may inhibit NF-κB activation by increasing the level of the inhibitory p105 subunit in MCF-7 cells. The ankyrin repeats at the C-terminus of p105 can then block the nuclear translocation of NF-κB (106).

On the transcriptional level, ER can regulate the induction of NF-κB transcription by interacting with transcriptional enhancers or repressors. In MCF-7 cells, ER can displace p65 and bind with transcriptional coactivator CREB-binding protein (CBP) on the promoters of NF-κB target genes (107). ER is also able to recruit the corepressor glucocorticoid receptor interacting protein 1 (GRIP1) to NF-κB complexes on the TNFα gene promoter and hence, repress the expression of TNFα (108). ER can also repress NF-κB transcriptional activity at target genes through direct protein-protein interaction. This observation was reported in osteocarcinoma cells, where the RHD proved to be the mediator of the interaction between the two transcription factors (109). Estrogen receptor can also regulate the NF-κB pathway at the transcriptional level

of its constituents. Estrogen receptor has been shown to inhibit de novo RelB synthesis in breast cancer cell lines (110).

1.3.1.b Inhibition of estrogen receptor by NF-κB

NF-κB inhibits the expression of ER, which might explain the repressive effect of NF-κB on ER signaling. Several mechanisms by which NF-κB can repress ER expression have been reported. First, Belguise and Sonenshein proposed a mechanism where the serine/threonine protein kinase θ (PKCθ), which regulates NF-κB activity in mouse mammary tumors, represses ER expression in ER+ breast cancer cells. PKCθ activates the AKT pathway, which in turn phosphorylates FoxO3a and results in exclusion of FoxO3a from the nucleus and its subsequent degradation in the cytoplasm. FoxO3a activates ER expression by binding to two upstream forkhead elements in the ER promoter (111). Thus, PKCθ inhibits ER expression via inactivation of FoxO3a (112).

A second mechanism of ER repression reports the NF-κB subunit, RelB, as an inhibitor of ER expression in breast cancer cells. The RelB target, Bcl2, interacts with Ras in the mitochondrial membrane stimulating the expression of zinc finger repressor, B-lymphocyte-induced maturation protein (BLIMP1), which binds to the ER promoter and represses ER expression. RelB levels are inversely correlated with ER status in breast cancer cells. Furthermore, the transactivation of RelB promoter by NF-κB and AP-1 is observed in ER- but not ER+ breast cancer cells (113).

A third mechanism has recently been suggested, in which the cytokine TNFα activates the expression of the Enhancer of Zeste Homolog 2 (EZH2), a core member of the polycomb repressor complex 2, in an NF-κB-dependent manner. EZH2 in turn may inhibit ER expression (64). This is supported by the inverse correlation between EZH2 and ER in primary breast

tumors, as well as a study reporting that silencing EZH2 in MCF-7 cells significantly enhances ER expression (114).

1.3.2 Positive crosstalk between estrogen receptor and NF-κB

Although many studies suggest a reciprocal inhibition between ER and NF-κB, positive crosstalk between both signaling pathways has been reported. A gene expression profiling study in ER+ MCF-7 breast cancer cells was performed by Frasor and colleagues. The cells were treated with E2, TNFα, or both. Transrepression, as well as prominent positive crosstalk, between E2 and TNFα signaling were observed. The study pointed out three different modes of positive crosstalk: 1) NF-κB enhanced the expression of ER target genes; 2) ER enhanced the expression of NF-κB target genes, and 3) a synergistic effect of both transcription factors. This group of genes was used to derive a gene signature that was found to be associated with aggressive luminal B breast cancer and resistance to tamoxifen, suggesting that ER/NF-κB crosstalk may underlie poor patient outcome in ER+ disease (115).

Frasor and colleagues further reported three examples for positive crosstalk:

1. Prostaglandin-E synthase-1 (PTGES) is an estrogen regulated gene that acts downstream of COX-1/2 to produce prostaglandin E2 (PGE2) (116). PTGES is upregulated in breast cancer cells in response to individual treatments with E2 or proinflammatory cytokines but to a greater extent by the combination. Enhanced recruitment of ER and p65 to an upstream ERE in the PTGES promoter was observed upon treatment with E2 and TNFα compared to either alone. Thus, combined treatment with E2 and TNFα can upregulate PTGES gene transcription synergistically in an ER and p65 dependent manner. (117).

2. ATP-binding cassette sub-family G member 2 (ABCG2) is a transmembrane transporter that has been related to luminal B subtype breast cancer (115). It is also known as BCRP (breast cancer resistance protein), and causes the efflux of anticancer drugs out of breast cancer cells. ABCG2 is regulated by E2 but not TNFα. However, TNFα significantly potentiates the upregulation of ABCG2 gene expression by E2. ER is required to allow the recruitment of p65 to a latent NF-κB response element on the promoter of the gene. The recruited p65 stabilizes ER occupancy on the promoter leading to enhanced gene expression in the presence of both transcription factors (118).
3. Baculoviral IAP repeat containing 3 (BIRC3), an anti-apoptotic factor in breast cancer cells, is upregulated by TNFα but not by E2 (119). However, TNFα-induced expression of BIRC3 is potentiated by E2. An inherently inactive ER binding site is adjacent to NF-κB binding site on the promoter of BIRC3. p65 is required for CBP mediated histone acetylation and subsequent recruitment of ER to the adjacent ERE, resulting in enhanced gene expression (120). Thus, NF-κB influences ER interaction with DNA, such that both ER and p65 are recruited cooperatively, suggesting a potential pioneering function for NF-κB (85).

Other levels of interaction between ER and NF-κB have been reported. The combined treatment of TNFα and tamoxifen enhances TNFα-induced expression of the mitochondrial antioxidant manganese superoxide dismutase (MnSOD) in breast cancer cells. The combination enhances binding of p65/p50 NF-κB and decreases binding p50/p50 NF-κB to the promoter of the gene compared to TNFα alone. This suggests that the homodimer may cause an inhibitory effect, which is alleviated by replacing it with the heterodimer upon treatment with both tamoxifen and TNFα (121).

Interestingly, cytokine-induced NF-κB signaling can activate ER in the absence of E2. The inflammatory cytokines, IL-1β and TNFα, can activate transcriptional activity of ER, yet with less potency than E2 (122-124). TNFα treatment of endothelial cells induces ERK 1/2-dependent phosphorylation of Ser118 in the AF-1 region of ER, which in turn, activates an ERE-dependent reporter (123). Furthermore, TNFα induces expression of classic ER dependent target genes in Ishikawa cells. This is inhibited by the knockdown of ER or by the mutation of Ser118 (125). Ser118 phosphorylation is known to enhance the sensitivity of ER to E2 and increases binding of coactivators, such as SRC3 (126). Ser118 phosphorylation is of specific importance in endocrine therapy, because it decreases the affinity of ER to tamoxifen and reduces the binding of tamoxifen bound receptor to DNA, as well (127).

In addition to ER phosphorylation, inflammatory signaling by IL-1β can inhibit the ability of tamoxifen to repress E2-dependent transcription. Tamoxifen binding to ER induces a protein conformation that allows ER to interact with corepressors, such as NCoR1 (Nuclear Receptor Corepressor 1), leading to the formation of a repressive complex. IL-1β treatment induces the dismissal of the NCoR1 complex from ER target promoters, which is the proposed mechanism by which pro-inflammatory cytokines abolish the repressive capacity of tamoxifen (128). It can then be suggested that ER activation via cytokine signaling may contribute to endocrine therapy resistance via two mechanisms, (i) by preventing the effect of tamoxifen and (ii) by activating the unliganded receptor, which would be of specific importance in women receiving aromatase inhibitors (85).

The non-canonical kinase IKKα can also induce ER Ser118 phosphorylation. In fact, IKKα mediates E2-induced transcription in breast cancer cells. E2 treatment induces the recruitment of IKKα, ER, and the coactivator AIB1/SRC-3 to the promoters of ER target genes, and transcriptionally active complexes are formed. Subsequent phosphorylation of histone

H3, acetylation of H3 and H4, and phosphorylation of RNA polymerase II are observed which is a process dependent on the kinase activity of IKKα. Knockdown of IKKα inhibits E2-mediated ER Ser118 phosphorylation and reduces E2-induced enhancement of AIB1/SRC-3 phosphorylation at serine 857. These effects of IKKα prove to be critical for E2-mediated proliferation, E2-stimulated cell cycle, and regulation of cell cycle genes, including cyclin D1, E2F1, and E2F1 target genes in breast cancer cells (129,130)

Altogether, this extensive body of evidence suggests that ER and NF-κB work together to coordinate gene expression through a variety of transcriptional mechanisms. This complex crosstalk between the two signaling pathways in breast cancer highlights the need for a better understanding of the biological consequences and therapeutic potential of this crosstalk.

II. HYPOTHESIS

There is an urgent need to understand what drives the progression of ER+ breast cancer to an aggressive, therapy-resistant phenotype, so that we can find new therapeutic targets and strategies to help the large population of women, who experience endocrine therapy resistance. While studies suggest that ER/NF-κB crosstalk may drive progression (64,115), direct evidence supporting this concept is lacking. We hypothesize that specific activation of the canonical arm of the NF-κB pathway will be sufficient to drive progression of ER+ breast cancer. Our focus on the canonical arm is based on studies reporting that women who have ER+ tumors with constitutively active p50 and p65, represent a subset of patients with increased risk of recurrence, metastasis, and poor overall survival (77,78). IKKβ kinase activity has been reported in ER+ breast tumors (74). Moreover, multiple publically available gene expression profiling studies of human tumors suggest that IKKβ mRNA expression may be elevated in ER+ versus ER- tumors (131-134). Furthermore, studies have reported a direct, NF-κB-independent, role of IKKβ as a negative regulator of the tumor suppressors: FoxO3a (135), p53 (136), and the tuberous sclerosis 1 (TSC1) complex (137).

In order to test our hypothesis, we decided to use a constitutively active form of the kinase responsible for the activation of the canonical arm of the NF-κB pathway, CA-IKKβ. We introduced CA-IKKβ into human ER+ breast cancer cell lines in order to study the effects of canonical NF-κB signaling on cellular and tumor phenotypes associated with progression to aggressive disease.

III. MATERIALS AND METHODS

3.1 Materials and reagents

17β-estradiol (E2) and Doxycycline (Dox) were purchased from Sigma (Milwaukee, WI, USA). ICI182,780 (ICI) was purchased from Tocris (Bristol, UK). TNFα was purchased from R&D Systems (Minneapolis, MN, USA). Silencing ribonucleic acid (siRNA) targeting cytokeratin 5 (CK5), cytokeratin 14 (CK14) and a non-targeting control (siNeg) were purchased from Ambion (Grand Island, NY, USA). Recombinant adenoviruses IκBα-DN and the control GFP were purchased from Vector Biolabs (Malverin, PA, USA).

3.2 Cell culture conditions

Cell culture reagents were purchased from Life Technologies (Carlsbad, CA, USA) and culture ware from Corning (Corning, Corning, NY, USA) unless otherwise stated. Estrogen receptor positive breast cancer cell lines MCF-7 and T47D cells were obtained from Dr. Debra Tonetti (UIC). MCF-7 cells are originally isolated from the pleural effusion of a 69 year old female patient (138). T47D cells are originally isolated from the pleural effusion of a 54 year old female patient (139). The cells were routinely maintained in Roswell Park Memorial Institute medium (RPMI) 1640 with phenol red. The medium was supplemented with 10% fetal bovine serum (FBS), or tetracycline approved FBS (Atlanta Biologicals, Norcross, GA, USA), 1% antibiotics penicillin-streptomycin, 1% non-essential amino acids, 2 mM L-glutamine, and 6 ng/ mL insulin. Before treatment with ligand or inhibitors, cells were cultured in phenol red-free RPMI 1640 medium supplemented with 5% charcoal-dextran-stripped FBS and components described above except insulin (i.e. treatment media) for 48 hrs.

Estrogen receptor negative breast cancer cell line MDA-MB-231 was obtained from Dr. Clodia Osipo (Loyola University, Chicago). The cells are originally isolated from pleural effusion

of a 51 year old female patient (140). The cells were routinely maintained in Improved Minimum Essential Medium (IMEM) (Corning) supplemented with 5% FBS, 1% antibiotics penicillin-streptomycin, 2 mM L-glutamine, and 1% non-essential amino acids. Cell line authentication was performed for pRetro-MCF-7 and MCF-7-A3 cell lines (which will be described latter) in December 2014 using short tandem repeat (STR), and ATCC analysis was performed by the DNA Services Facility, Research Resources Center (RRC), UIC.

3.3 Production of CA-IKKβ cells lines

Dox-inducible, constitutively active IKKβ (CA-IKKβ) expressing cell lines were derived using the Retro-X™ Tet-On® Advanced Inducible Expression System (Clontech Laboratories, Inc., Mountain View, CA, USA) (Figure 2). This system is composed of two main elements:

I. The pRetroX-Tet-On Advanced vector, which expresses the tetracycline-controlled transactivator, rtTA-Advanced. The protein contains mutant TetR domain (rTetR) that binds *tet*O sequences in the presence of Dox. pRetro-MCF-7 and pRetro-T47D cells were derived from MCF-7 and T47D cells, respectively, and kindly given to us by Dr. Debra Tonetti. They are stably transduced with geneticin-resistant pRetroX-Tet-On Advanced vector encoding rtTA-Advanced.

II. The response vector, pRetroX-Tight-Pur, which contains the inducible response promoter P_{Tight} that controls the expression of the gene of interest, CA-IKKβ. It contains modified Tet-Responsive Element (TRE_{mod}), joined to a modified minimal CMV promoter ($P_{minCMV\Delta}$). In the presence of Dox, rtTA-Advanced binds to the P_{Tight} promoter on the response vector resulting in the transcription of the downstream gene CA-IKKβ.

The derivation of Dox-inducible CA-IKKβ cell lines was done in the following three steps:

1. **Mutation of IKKβ**

An IKKβ expression vector was purchased from InvivoGen (San Diego, CA, USA). Serine to glutamate mutations, Ser177->Glu / Ser181->Glu were introduced using site-directed mutagenesis (Stratagene, Santa Clara, CA, USA). The mutagenesis primers:

5'-AGGAGCTGGATCAGGGCGAACTTTGCACAGAATTCGTGGGGACCCTGC-3'

and 5'-GCAGGGTCCCCACGAATTCTGTGCAAAGTTCGCCCTGATCCAGCTCCT-3' were used and mutations were confirmed by sequencing. The mutated gene was then amplified with the following primers to introduce a Not-1 site at the 5' end of the gene and a Mlu-1 site on the 3' end of the gene:

5'-CTTAGCGGCCGCATGAGCTGGTCACCTT-3' and 5'-ACATACGCGTTCATGAG GCCTGCTC-3'. After amplification, the product was checked on a 1% agarose gel. The reaction product was then purified using the QIAquick PCR purification kit (Qiagen, Valencia, CA, USA).

2. **Subcloning mutated IKKβ into Tet-On vector to produce pRetroX-Tight-Pur-CA-IKKβ vector**

Constitutively active IKKβ was then subcloned into the puromycin resistant Tet-On vector, pRetroX-Tight-Pur using MluI and NotI restriction sites. The vector was sequenced by the DNA Services Facility at UIC.

3. **Creating double stable RetroX-Tet-On Advanced cell lines.**

The puromycin resistant pRetroX-Tight-Pur-CA-IKKβ was cotransfected along with the viral envelop expression vector, pVSV-G, into GP2-293 packaging cells to

generate retrovirus. The retroviral supernatant was harvested after 48 hrs and filtered. The virus was then used to infect pRetro-MCF-7 and pRetro-T47D cells using 4 μg/mL polybrene. Selection markers geneticin and puromycin were added to the cells and limiting dilutions in 96-well plates was performed. Multiple clones were derived from single cells. Dox-induction of CA-IKKβ was evaluated by Western Blotting and QPCR, as described in the results section. Selection of clones for further study was based on the expression of CA-IKKβ, activation of the NF-κB pathway, and the expression of NF-κB target genes. Four CA-IKKβ cell lines were produced: MCF-7-A3, MCF-7-G2, T47D-C7 and T47D-A3 (Table I).

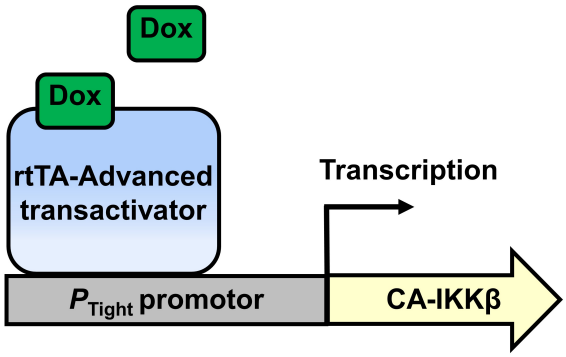

Figure 2: Dox-inducible, CA-IKKβ system. Dox-inducible, CA-IKKβ expressing cell lines were derived using the Retro-X™ Tet-On® Advanced Inducible Expression System (Clontech Laboratories, Inc., Mountain View, CA, USA).

TABLE I: CA-IKKB CELL LINES

Cell line	Description
MCF-7-A3	Dox-inducible, CA-IKKβ expressing cells derived from MCF-7 cell line
MCF-7-G2	Dox-inducible, CA-IKKβ expressing cells derived from MCF-7 cell line
T47D-C7	Dox-inducible, CA-IKKβ expressing cells derived from T47D cell line
T47D-A3	Dox-inducible, CA-IKKβ expressing cells derived from T47D cell line

3.4. Lentiviral transduction and production of stable MCF-7-A3-LUC cell line

The lentiviral expression vector for pFU-Luc2-eGFP (L2G) (141) was obtained from Dr. Angela Tyner (UIC), with the permission of Dr. Michael Clarke (Stanford University). Packaging plasmid (psPAX2) and envelope plasmid (pMD2.G) were obtained from Dr. Chong Wee Liew (UIC). To make the lentivirus, packaging cells (293FT) were transfected with 23 µg of pFU-Luc2-eGFP (L2G), 8 µg of envelope plasmid pMD2.G and 15 µg of psPAX2 using polyethylenimine. MCF-7-A3-LUC cell lines were generated by transducing MCF-7-A3 cells with lentiviral particles using polybrene (4 µg/mL) followed by blasticidin (10 µg/mL) selection. Fluorescence activating cells sorting (FACS) was then performed in Flow Cytometry Service core at UIC using MoFlo Astrios Cell Sorter (Beckman Coulter, Brea, CA, USA).

3.5 siRNA Transfections

Cells were seeded in 6-well plates in treatment media, incubated for 24 hrs, and then transfected with 50 nM (final concentration) siRNA in Dharmafect transfection reagent #1 (Dharmacon, Lafayette, CO, USA). Cells were transfected with a non-targeting control siRNA (siNeg) or siRNA targeting CK5 (siCK5) or CK14 (siCK14) as detailed in the Table II. Media was changed after 24 hrs and cells were treated.

TABLE II: SEQUENCES OF siRNA

Gene	siRNA sequence 5'→ 3'
Non-targeting Control	uaacgacgcgacgacguaatt
CK5	ggagaguagucuagaccaatt
CK14	gaguugaaccugcguaugatt

3.6 Adenovirus transfection

MCF-7-A3 and T47D-C7 cells were seeded at a density of 50,000 and 150,000 cells/well, respectively, in 6-well plates in treatment media. After 24 hrs, cells were infected with recombinant adenovirus IκBα-DN or the control recombinant adenovirus GFP. Multiplicity of infection (MOI) for MCF-7-A3 and T47D-C7 cells were 200 and 20, respectively. After 24 hrs media was changed, and cells were treated.

3.7 DNA growth assay

CA-IKKβ-MCF-7 cells (MCF-7-A3 and MCF-7-G2) and CA-IKKβ-T47D cells (T47D-C7 and T47D-A3) were seeded at a density of 2,500 and 10,000 cells/well, respectively, in 24-well plates in treatment media. Treatment was added 48 hrs after seeding. Cells were retreated every 48hrs. At the end of the experiment, cells were rinsed and then incubated in Hoechst 33342 cell permeable dye (Life Technologies) for 1 hr at 37°C. Fluorescence was read at excitation 355 nm/emission 460 nm on Synergy™ HT Multi-Detection Microplate Reader (BioTek, Winooski, VT, USA). DNA content and cell number were extrapolated from DNA and cell number standard curves, respectively.

3.8 Soft agar colony formation

Cells were seeded in 6-well plates in treatment media. After 48 hrs, cells were treated for 3 days. They were then trypsinized and counted, and 1250 single cells were mixed with 0.45% SeaPlaque agarose (Lonza, Rockland, ME, USA) in 5% tet-approved FBS, phenol red free media. Cells were overlaid on a solidified layer of 0.8% agarose in the bottom of each well of a 24-well plate. Soft agar was covered with treatment media, and cells were retreated every three days. Colony formation was monitored for up to 6 weeks. Colonies (equal to or greater than 60 μm in diameter) were manually counted and imaged using a light microscope, Nikon Eclipse TS100 (Nikon, Melville, NY, USA) supplied with QImaging Micropublisher 3.3 RTV camera (Nikon).

3.9 Clonogenic assay

Cells were seeded in 6-well plates in treatment media. Treatment was added after 48 hrs and continued for 3 days. Cells were trypsinized, counted, and seeded as single cells (1000 cells per well) in 6-well plates. Cells were retreated twice per week for four weeks. Colonies were fixed and stained with crystal violet. Plates were imaged using Molecular Imager Chemidoc XRS (Bio-Rad Laboratories, Hercules, CA, USA). Colonies of more than 50 cells were counted manually. Alternatively, the surface area occupied by the colonies was quantified using image J software (open source from National Institutes of Health, Bethesda, MD, USA). Images were obtained using Quantity One software (Bio-Rad Laboratories).

3.10 Scratch wound healing assay

Cells were plated in 6-well plates in treatment media and cultured until 80-90% confluence was reached. At this point a transverse scratch was created using a 10 μL pipette

tip. Cells were then rinsed gently with phosphate-buffered saline (PBS) to remove any floating debris after scratching. Cells were treated and wounds were monitored and imaged for 96 hrs using Nikon Eclipse TS100 microscope supplied with QImaging Micropublisher 3.3 RTV camera. The wound gaps were measured and calculated as percentage of the initial wound.

3.11 Migration and invasion assay

Falcon transwell inserts (Corning) were used for the migration assay. For the invasion assays, Falcon transwell inserts were coated with100 uL of 300 µg/mL Matrigel (BD Biosciences, San Jose, CA, USA). The inserts were then incubated at 37°C for 2 hrs before use. Cells were seeded in 6-well plates in treatment media. After 48 hrs, treatment was added and continued for 3 days. Cells were then trypsinized, counted, and seeded in the migration or invasion inserts. CA-IKKβ-MCF-7 and CA-IKKβ-T47D cells were seeded in a density of 50,000 and 200,000 cells/insert, respectively. Cells were allowed to migrate or invade for 24 hrs (CA-IKKβ-MCF-7 cells) or 16 hrs (CA-IKKβ-T47D cells). Treatment was maintained during migration or invasion. Non migrating/invading cells were removed from the inside of the inserts using cotton swabs. Migrated/invaded cells on the outer side of the membrane were fixed using 4% p-formaldehyde (Santa Cruz Biotechnology, Santa Cruz, CA, USA), stained using crystal violet (Sigma-Aldrich, St. Loius, MO, USA), washed and allowed to air dry. Using x10 light microscope objective, the total numbers of migrating/invading cells were manually counted anonymously of the identity of the insert. Inserts were counted and imaged using Nikon Eclipse TS100 microscope supplied with QImaging Micropublisher 3.3 RTV camera.

3.12 Western Blotting

Cultured cells were scraped from the culture plates. Whole cell extracts of the cells were prepared in M-PER reagent (Thermo Fisher Scientific, Waltham, MA, USA) with protease inhibitor (Roche, Nutley, NJ, USA) and phosphatase inhibitor (Thermo Fisher Scientific) cocktails. Protein concentration was measured using Pierce BCA protein assay kit (Thermo Fisher Scientific). Proteins were denatured, separated by SDS-PAGE (Bio-Rad Laboratories), and transferred to nitrocellulose membranes (Thermo Fisher Scientific). The membranes were blocked for 1hr in tris-buffered saline and 0.5% Tween 20 (TBST buffer) containing 5% bovine serum albumin (BSA) (Sigma-Aldrich) or 5% nonfat dry milk (LabScientific, Highlands, NJ, USA). Membranes were probed for IKKβ, phospho-p38 (Thr180/ Tyr182), phospho-AKT (Ser473), vimentin, E-cadherin, and ER (rabbit monoclonal, 1:1000, Cell Signaling, Boston, MA, USA), IκBα, AKT-1 and CK 8/18 (mouse monolclonal, 1:1000, Cell Signaling), IKKα, phospho-IκBα (Ser32), phospho-p65 (Ser532), p63-α, phospho-p44/42 MAPK (Erk1/2) (Thr202/Tyr204), p44/42 MAPK (Erk1/2), p38 and TBP (rabbit polyclonal, 1:1000, Cell Signaling), p65 (rabbit polyclonal, 1:200, Santa Cruz Biotechnology), fibronectin (rabbit polyclonal, 1:1000, Santa Cruz Biotechnology), MnSOD (rabbit polyclonal, 1:1000, Abcam, Cambridge, MA, USA) and β-actin (mouse monoclonal, 1:5000, Sigma-Aldrich). The membranes were incubated in the primary antibodies overnight at 4°C. Rabbit and mouse horseradish peroxidase conjugated secondary antibodies were used at 1:10,000 (Pierce/ Thermo Fisher Scientific). The signal was visualized on a Molecular Imager Chemidoc XRS (Bio-Rad Laboratories) following incubation with the Pierce Supersignal West Pico Chemiluminescent Substrate (Thermo Fisher Scientific). Images were obtained using Quantity One software (Bio-Rad Laboratories).

3.13 Quantitative reverse transcription polymerase chain reaction (QRT-PCR)

Total RNA was isolated using Trizol (Sigma-Aldrich). Total RNA (0.5 ug) was reverse transcribed using MMLV-reverse transcriptase (Invitrogen, Life Technologies). The resulting product was then diluted with ddH2O and 2 µL were used for QPCR reaction. SYBR green reaction mixture was used for amplification and detection of the transcripts in the StepOne Plus Real Time PCR machine (Applied Biosystems, Foster City, CA, USA). Standard curve method was applied and fold change was calculated using the ΔΔCt method. 36B4 or GAPDH were used as the internal control. Table III shows the primer sets for each transcript.

3.14 Immunofluorescence and confocal microscopy

Cells were seeded on 0.1% gelatin coated or non-coated glass coverslips in 6-well plates or 24 well plates in treatment media. After treatment, cells were fixed with 4% p-formaldehyde for 10 minutes, permeabilized using 0.1% Triton X-100 and washed with 1% BSA in PBS. Cells were then blocked with 10% goat serum (Thermo Fisher Scientific) in PBS for an hour. After blocking, the cells were incubated overnight with the appropriate primary antibody (diluted in 1% goat serum in PBS) in a humidified chamber at 4ºC. Table IV lists the primary antibodies used. Next day, slides were washed with 1% BSA in PBS, followed by 1 hour incubation with the appropriate antibody, Alexa Fluor 594 conjugated secondary antibody or Alexa Fluor 448 conjugated secondary antibody (dilution 1:1000) (Thermo Fisher Scientific). The coverslips were washed with 1% BSA in PBS then mounted with ProLong Gold anti-fade reagent (Life Technologies) to stain the nuclei with DAPI. Images were then acquired at x63 magnification using LSM710 confocal microscope (Carl Zeiss, Incorporated, North America, Thornwood, NY, USA), in the Department of Physiology and Biophysics, UIC.

TABLE III: SEQUENCES OF PRIMERS

Gene	Forward Sequence 5' → 3'	Reverse Sequence 5' → 3'
36B4	GTGTTCGACAATGGCAGCAT	GACACCCTCCAGGAAGCGA
AR	ATGGTGAGCAGAGTGCCCTATC	ATGGTCCCTGGCAGTCTCCAAA
BIRC3	GAGTGGCTTGCTTTGCCTG	CCTTCGGTTCCCAATTGCT
CCNA2	CTCTACACAGTCACGGGACAAAG	CTGTGGTGCTTTGAGGTAGGTC
CCND1	TCTACACCGACAACTCCATCCG	TCTGGCATTTTGGAGAGGAAGTG
CDC45	TGGATGCTGTCCAAGGACCTGA	CAGGACACCAACATCAGTCACG
CHEK2	GACCAAGAACCTGAGGAGCCTA	GGATCAGATGACAGCAGGAGTTC
CK5	GCTGCCTACATGAACAAGGTGG	ATGGAGAGGACCACTGAGGTGT
E2F1	GGACCTGGAAACTGACCATCAG	CAGTGAGGTCTCATAGCGTGAC
EGR3	TTCTCGTACAGGGTGGCTCC	GGCAGAGAGCAACCTTCCC
ELF5	CCTGATGTCGTGGACTGATCTG	GCTTAGTCCAGTATTCAGGGTGG
ER	TGCCCTACTACCTGGAGAAC	CCATAGCCATACTTCCCTTGTC
EZH2	GACCTCTGTCTTACTTGTGGAGC	CGTCAGATGGTGCCAGCAATAG
FoxA1	GCAATACTCGCCTTACGGCTCT	GGGTCTGGAATACACACCTTGG
FoxC1	AGAAGGACAGGCTGCACCTCAA	GTTCTCGGTCTTGATGTCCTGG
FoxC2	TCACCTTGAACGGCATCTACCAG	TGACGAAGCACTCGTTGAGCGA
FoxM1	TCTGCCAATGGCAAGGTCTCCT	CTGGATTCGGTCGTTTCTGCTG
GAPDH	GTCTCCTCTGACTTCAACAGCG	ACCACCCTGTTGCTGTAGCCAA
Gata3	ACCACAACCACACTCTGGAGGA	TCGGTTTCTGGTCTGGATGCCT
HES1	GGAAATGACAGTGAAGCACCTCC	GAAGCGGGTCACCTCGTTCATG
HEY1	TGTCTGAGCTGAGAAGGCTGGT	TTCAGGTGATCCACGGTCATCTG
ICAM1	TGACGAAGCCAGAGGTCTCAG	AGCGTCACCTTGGCTCTAGG
ID3	CAGCTTAGCCAGGTGGAAATCC	GTCGTTGGAGATGACAAGTTCCG
IL17RB	TTGTCAAATGCACTTCTGCCA	CCCCATGAACGCCACTTAA
MMP13	CCTTGATGCCATTACCAGTCTCC	AAACAGCTCCGCATCAACCTGC
MMP14	CCTTGGACTGTCAGGAATGAGG	TTCTCCGTGTCCATCCACTGGT
MMP9	GCCACTACTGTGCCTTTGAGTC	CCCTCAGAGAATCGCCAGTACT
MnSOD	ACCGAGGAGAAGTACCAGGAG	ACTTGTCAAAGGAACCAAAGTCAC
PR	GTCGCCTTAGAAAGTGCTGTCAG	GCTTGGCTTTCATTTGGAACGCC
PS2	GTGTGCAAATAAGGGCTGCTG	TGGAGGGACGTCGATGGTA
PTGES	CTTCCTTTTCCTGGGCTTCG	GAAGACCAGGAAGTGCATCCA
RelB	TGTGGTGAGGATCTGCTTCCAG	TCGGCAAATCCGCAGCTCTGAT
SNAI1	TGCCCTCAAGATGCACATCCGA	GGGACAGGAGAAGGGCTTCTC
SNAI2	ATCTGCGGCAAGGCGTTTTCCA	GAGCCCTCAGATTTGACCTGTC
SOX9	AGGAAGCTCGCGGACCAGTAC	GGTGGTCCTTCTTGTGCTGCAC
TBX2	AGCAGTGGATGGCTAAGCCTGT	GGATGTCGTTGGCTCGCACTAT
TBX3	GGACACTGGAAATGGCCGAAGA	GCTGCTTGTTCACTGGAGGACT
TP63	CAGGAAGACAGAGTGTGCTGGT	AATTGGACGGCGGTTCATCCCT
TWIST1	GCCAGGTACATCGACTTCCTCT	TCCATCCTCCAGACCGAGAAGG
VGLL1	GGATGAACACTTCTCCAGAGCTC	ATGGAGACGAGTAACGCCACTG
VIM	AGGCAAAGCAGGAGTCCACTGA	ATCTGGCGTTCCAGGGACTCAT
ZEB1	GGCATACACCTACTCAACTACGG	TGGGCGGTGTAGAATCAGAGTC
ZEB2	AATGCACAGAGTGTGGCAAGGC	CTGCTGATGTGCGAACTGTAGG

TABLE IV: ANTIBODIES USED FOR IMMUNOFLUORESCENCE

Antibody	Dilution	Company
CK14, rabbit polyclonal	1:1000	Covance (Princeton, NJ, USA)
CK5, mouse monoclonal	1:50	Leica Biosystems (Buffalo Grove, IL, USA)
CK8/18, mouse monoclonal	1:100	Cell Signaling
E-cadherin, rabbit monoclonal	1:200	Cell Signaling
E-cadherin, rabbit polyclonal	1:250	Santa Cruz Biotechnology
ERα (6F11), mouse monoclonal	1:100	Abcam
FoxA1, mouse monoclonal	10 µg/mL	Abcam
Gata3, rabbit monoclonal	1:1600	Cell Signaling
IKKβ, rabbit polyclonal	1:100	Pierce/Thermo Fisher Scientific
p63-α, rabbit polyclonal	1:100	Cell Signaling
p65, rabbit polyclonal	1:200	Santa Cruz
Phalloidin	1:500	Cytoskeleton Inc. (Denver, CO, USA)
Vimentin, rabbit monoclonal	1:100	Cell Signaling
Vimentin, rabbit monoclonal	1:250	Epitomics (Burlingame, CA, USA)

3.15 Determination of apoptosis

Apoptosis was analyzed using Annexin V-FITC apoptosis detection kit (BD Biosciences). CA-IKKβ-MCF-7 and CA-IKKβ-T47D cells were seeded in treatment media at a density of 280,000 and 820,000 cells/10 cm plate, respectively. After 48 hrs cells were treated for 3 days. The floating cells (cells detached from the plate surface), and attaching cells (harvested by trypsin) were pelleted by centrifugation. The pellet was resuspended in binding buffer and incubated with fluorescein isothiocyanate (FITC)-labeled Annexin V and Propidium Iodide for 15 min at room temperature in the dark. The stained cells were analyzed in Flow Cytometry Service core at UIC using BD LSR Fortessa flow cytometer (BD Biosciences).

3.16 Cell cycle analysis

Cells were seeded in 10 cm plates in treatment media, then treated after 48 hrs for 3 days. They were then trypsinized, washed with PBS and fixed with 1% p-formaldehyde followed by ice cold 70% ethanol, and incubated at 4°C overnight. The cells were then centrifuged, washed, resuspended in 0.5 mL Propidium Iodide staining solution (40 µg/mL Propidium Iodide (Sigma-Aldrich) and 100 µg/mL RNAse A (Thermo Fisher Scientific)), and incubated for 30 min at 37°C. Cell cycle distribution was determined by flow cytometry in Flow Cytometry Service core at UIC using BD LSR Fortessa flow cytometer.

3.17 Xenograft tumor and spontaneous metastasis studies

All procedures and studies involving animals were approved by the Animal Care and Use Committee at UIC according to institutional and national guidelines (ACC protocol #14-134). Female athymic nude mice (6-7 weeks old) (Harlan, Madison, WI, USA) were used for the study. Animals were allowed to acclimatize in the Biologic Resources Laboratory at UIC for 2 weeks. Xenografts were established by injecting 5 x 10^6 MCF-7-A3-LUC cells in 100 µL PBS into the upper thoracic mammary fat pad of the animals (two xenografts/ animal). Pellets containing E2 were implanted at the same time of cell injection to achieve premenopausal E2 levels, which are necessary for growth of the ER+ xenografts. Where appropriate, silastic E2 pellets, or E2 beeswax pellets were used. Silastic E2 pellets, which last for up to 8 weeks in the animals, were prepared by mixing E2 with surgical grade elastomer (Dow Corning, Midland, MI, USA) and inserting the mixture in 1 cm veterinary silicone tubing (Dow Corning) (142). Estrogen beeswax pellets, which will last for up to one year, were prepared by mixing E2 and melted beeswax to yield 30 mg pellets (143). Animals were anesthetized using ketamine (100 mg/kg) mixed with xylazine (6 mg/kg), and the E2 pellets were implanted subcutaneously on animals'

backs. Mice were examined by palpation for the presence of tumors two times per week. Using digital calipers, tumor cross-sectional area was calculated (formula: (length/2) × (width/2) × π). When tumors reached 0.1-0.2 cm^2, Dox (2 mg/mL in 5% sucrose) was introduced into the drinking water of the mice. At the end of the studies or when humane endpoints were reached, mice were euthanized by CO2 inhalation and cervical dislocation. Tumors were excised and fixed in 10% buffered formalin. Soft organs (brain, lung, liver, ovaries, uterus, kidneys, adrenals and spleen), spine and legs bones were removed, ex vivo imaged (as will be discussed later), fixed in 10% formalin for 48 hrs. Spine and bones were decalcified in EDTA/dilute hydrochloric acid solution (Decalcifying Solution, Richard-Allan Scientific, Thermo Fisher Scientific) for 3 hrs prior to fixation. After 48 hrs, tissues were stored in 70% ethanol until processing.

3.18 Experimental metastasis

Female athymic nude mice (6-7 weeks old) (Harlan) were used for the study. Animals were allowed to acclimatize in the Biologic Resources Laboratory at UIC for 2 weeks. Mice were anaesthetized with ketamine (100 mg/kg) mixed with xylazine (6 mg/kg), and E2 silastic pellets were implanted subcutaneously. MCF-7-A3-LUC cells were treated with E2 or E2+Dox in culture for 72 hrs, trypsinized, washed and suspended in PBS. One million cells in 100 µL PBS were injected into the lateral tail vein of the mice 48 hrs post E2 pellet implantation. Mice were anaesthetized with ketamine/xylazine mixture during tail vein injection. Animals were imaged every 1-2 weeks for 6-7 weeks and then euthanized by CO2 inhalation and cervical dislocation. Soft organs (brain, lung, liver, ovaries, uterus, kidneys, adrenals and spleen), spine and legs bones were ex vivo imaged. Soft organs were fixed in 10% formalin; spine and bones were decalcified in EDTA/dilute hydrochloric acid solution (Decalcifying Solution) for 3 hrs prior to fixation. After 48 hrs, tissues were stored in 70% ethanol until processing.

3.19 In vivo preclinical imaging (IVIS)

Non-invasive bioluminescence imaging of live animals was done using the in vivo imaging system, IVIS (Xenogen, Caliper Life Sciences, Hopkinton, MA, USA). Briefly, D-Luciferin potassium salt (Biosynth Chemistry and Biology, Itasca, IL, USA), the substrate for firefly luciferase, was dissolved in Dulbecco's phosphate-buffered saline (DPBS) (Life Technologies) at a concentration of 15 mg/mL. It was then sterilized using a 0.22 μm-pore-size filter. Mice were injected intraperitoneally (150 mg/kg body weight) and anesthetized in an oxygen-rich induction chamber with 2.5% isofluorane. Isoflurane was then reduced to 2% after transferring animals to the imaging chamber. Ten minutes after D-Luciferin injection, bioluminescent images were taken using the IVIS Spectrum (exposure time 1-300 sec, binning 4/8/16, f/stop 1-2, emission filter open). The signal was measured as radiance (photons (p)/second/square centimeter/ steradian (sr)), and analyzed with Living Image Software (Caliper Life Sciences).

For ex vivo imaging, prior to necropsy, animals were injected intraperitoneally with D-Luciferin (150 mg/kg body weight). Ten minutes following injection the mice were euthanized with CO_2 gas followed by cervical dislocation. Tissues of interest were excised, rinsed with DPBS, and soaked in D-Luciferin (300 ug/mL). The tissues were then imaged ex vivo using the IVIS spectrum (exposure time 1-300 sec, binning of 4/8/16, f/stop of 1-2, emission filter open). After ex-vivo imaging, bones were decalcified and the tissues were fixed in 10% neutral-buffered formalin (as mentioned above) for histopathological analysis.

3.20 Histology and immunohistochemistry

Tissues were embedded in paraffin, and 5 μm sections were prepared using Microm HM315 microtome. Tissue sections were deparaffinized, rehydrated, and stained with

hematoxylin and eosin (H&E) using an automated stainer (Sakura). Ki67 staining was performed using Ki67-RM (CRM325) (Biocare Medical, Concord, CA, USA) and green fluorescent protein (GFP) immunohistochemistry (IHC) was performed using the rabbit polyclonal GFP (ab6556) (Abcam). Samples were processed and stained at the Veterinary Diagnostic Laboratory at University of Illinois at Urbana-Champaign under the guidance of our collaborator, Dr. Herbert Whiteley. Images were captured using Olympus BX45 microscope with UPlanApo objective lenses and Olympus DP21-SAL digital camera Olympus (Center Valley, PA, USA).

3.21 Microarray analysis

For gene expression profiling, MCF-7-A3 cells were seeded in 10 cm plates in treatment media (three replicates per treatment). After 48 hrs cells were treated with E2, Dox or E2+Dox for 72 hrs. RNA was extracted, using Trizol followed by the RNeasy RNA Extraction Kit (Qiagen, Valencia, CA, USA) using on-column DNase I digestion. RNA was eluted into RNase free water and quantified. RNA integrity was determined on a Agilent 2200 TapeStation Instrument using RNA screen tape (Agilent, P/N 5067-5576), and RINe ranged from 9.5 to 10 for all samples. Samples were reverse transcribed, amplified, fragmented, and biotin-labeled with the GeneChip® 3' IVT Express Kit (Affymetrix, P/N 901229) according to the manufacturer's protocol. Samples were then hybridized to GeneChip® PrimeView™ Human Gene Expression Arrays (Affymetrix, P/N 901838) and washed and stained using the GeneChip® Hybridization, Wash, and Stain Kit (Affymetrix, P/N 900720) according to the manufacturer's protocol. Arrays were hybridized in a GeneChip® Hybridization Oven 640, washed and stained on a GeneChip® Fluidics Station 450. Then they were scanned on a GeneChip® Scanner 3000 7G. Analysis was performed in Core Genomics Facility at UIC. Data

set was normalized using Robust Multichip Average. Statistical analysis was performed by the laboratory of our collaborator Dr. Chad Creighton (Baylor College of Medicine). Each of the three treatments was compared to vehicle. Genes with fold change more than 1.5 ($p<0.01$) were identified. Supervised clustering was performed in order to group genes having similar expression patterns.

3.22 Gene set enrichment analysis (GSEA)

The Gene Set Enrichment Analysis (GSEA) software was used. The software applies the GSEA technique developed by Subramanian and colleagues (144). GSEA was performed on Molecular Signatures Database (MSigDB) gene set collections using E2 and Dox-regulated gene clusters described above. These collections are made available for use with GSEA by the Broad Institute (145). The parameters used were: 1) number of permutation: 1000, and 2) type of permutation: gene set, because the sample size is 3 per phenotype. Within the GSEA enrichment plots individual genes that contribute to the enrichment score are represented as vertical lines. Genes are ranked left (most positive) to right (most negative) according to signal to noise ratio. Values above 0 indicate a gain in enrichment, and values below 0 indicate reduced enrichment of a gene set.

3.23 Statistical analysis

Statistical analyses were performed using GraphPad Prism 6.0 software (GraphPad Software, Inc., San Diego, CA). Data are presented as mean ± SEM (standard Error of the mean) or ± SD (Standard deviation of the mean). One way or two way ANOVA (followed by Tukey or Sidak's posttest) and t-tests were used where appropriate. Statistics with P values less than 0.05 were considered significant. Error bars represent SEM or SD.

IV. RESULTS

4.1 Characterizing constitutively active IKKβ cell lines

In order to study the effect of NF-κB on ER+ breast cancer, we decided to use the constitutively active form of the kinase IKKβ, which is one of the serine specific catalytic subunits of the IKK complex. IKKβ is activated upon phosphorylation of its Serine residues 177 and 181. Mutation of Ser177 and Ser181 to glutamic acid results in a phosphomimetic state of the molecule, rendering it constitutively active (146,147). In order to control the expression and activity of IKKβ in ER+ breast cancer cells, we developed Doxycycline (Dox)-inducible, CA-IKKβ expressing cell lines using the Retro-X Tet-On Advanced Inducible Expression System. We derived four different cell lines (MCF-7-A3, MCF-7-G2, T47D-C7 and T47D-A3) from the ER+ breast cancer cell lines MCF-7 and T47D (Table I). The majority of our results were replicated in at least 2 cell lines.

In order to characterize the function of CA-IKKβ, cell lines were treated with Dox or the proinflammatory cytokine TNFα, as a positive control. Dox treatment for 24 and 48 hrs induced a substantial increase in IKKβ expression while, as expected, TNFα did not alter IKKβ expression level compared to control. The expression of IKKα, the kinase responsible for activation of the non-canonical arm of the NF-κB pathway, was not affected by Dox, indicating the specificity of Dox induction of the kinase responsible for the canonical arm only. To test the activity of CA-IKKβ, we examined phosphorylation and expression of the NF-κB inhibitor, IκBα. Both Dox and the positive control TNFα increased phospho-IκBα while decreasing total IκBα, indicative of degradation (Figure 3).

IKKβ phosphorylates the NF-κB subunit p65 at Ser536 within the transactivation domain, which facilitates nuclear import and transcriptional activity of the molecule (148,149). Both Dox and TNFα induced p65 phosphorylation at Ser536 (Figure 3). The expression of NF-κB target

genes (e.g. RelB and ICAM1) was detected by QPCR as an indication of NF-κB activity. Dox induced the expression of both genes, confirming the expression of a constitutively active form of IKKβ, which can activate the NF-κB pathway and result in the expression of NF-κB target genes (Figure 4).

Our lab has previously performed a gene expression profiling study in ER+ MCF-7 breast cancer cells, treated with E2, TNFα or both for 2 hrs. We reported a synergistic effect on genes regulated by both E2 and TNFα, and that this gene set is associated with aggressive luminal B breast cancer and resistance to tamoxifen. This suggests that ER/NF-κB crosstalk may underlie poor patient outcome in ER+ disease (115). To determine if CA-IKKβ recapitulates the crosstalk between TNFα and E2, CA-IKKβ expression was induced by treating the cells with Dox for 24 hrs, followed by E2 for an additional 2 hrs. TNFα or E2+TNFα treatment was used as a positive control. Interestingly, we found that CA-IKKβ recapitulates the crosstalk between E2 and TNFα on some genes (e.g. BIRC3 and EGR3). However, it does not recapitulate the crosstalk on other genes (e.g. IL17RB and PTGES) (Figure 5). These results suggest that the canonical arm of NF-κB, activated upon treatment with Dox, regulates some of the genes of the synergy signature previously reported. Other genes may be regulated by the non-canonical arm of the NF-κB pathway or by other pathways regulated by TNFα.

It has been reported that stably transfected cells might exhibit differential expression of the gene of interest on the cellular level, which might affect the phenotype under investigation (150). Therefore, immunofluorescence was used to detect IKKβ expression at the cellular level. Dox treatment for 5 days resulted in high levels of IKKβ expression in all cells, indicating that the Tet-On inducible system is functional in all cells treated with Dox (Figure 6A). Furthermore, Dox treatment enhanced p65 localization in CA-IKKβ cells (Figure 6B), which further indicated IKKβ activity in all cells.

Studies have reported that the NF-κB pathway cooperates with multiple signaling molecules and pathways (e.g. p38, JNK, and AKT) (151). Western Blotting was used to find out whether CA-IKKβ activates signaling pathways other than NF-κB. TNFα activates pathways other than NF-κB, such as AKT, MAPK/ERK and p38 (152-154); hence, TNFα was used as a positive control. Phosphorylation of pathways, such as p38 and MAPK/ERK was observed. However, phosphorylation of other pathways, such as AKT was not observed (Figure 7), suggesting that CA-IKKβ activates downstream pathways other than NF-κB. This could be the direct effect of IKKβ on these pathways (155), or an indirect consequence of growth factors or cytokines produced and secreted in response to IKKβ activation.

These results indicate that multiple ER+ cells lines were produced, in which the expression and activity of IKKβ, one of the main kinases of the NF-κB pathway, could be controlled. These cell lines were then used to determine the in vitro and in vivo effects of the activation of the canonical arm of NF-κB pathway on the phenotype of ER+ breast cancer cells and tumors.

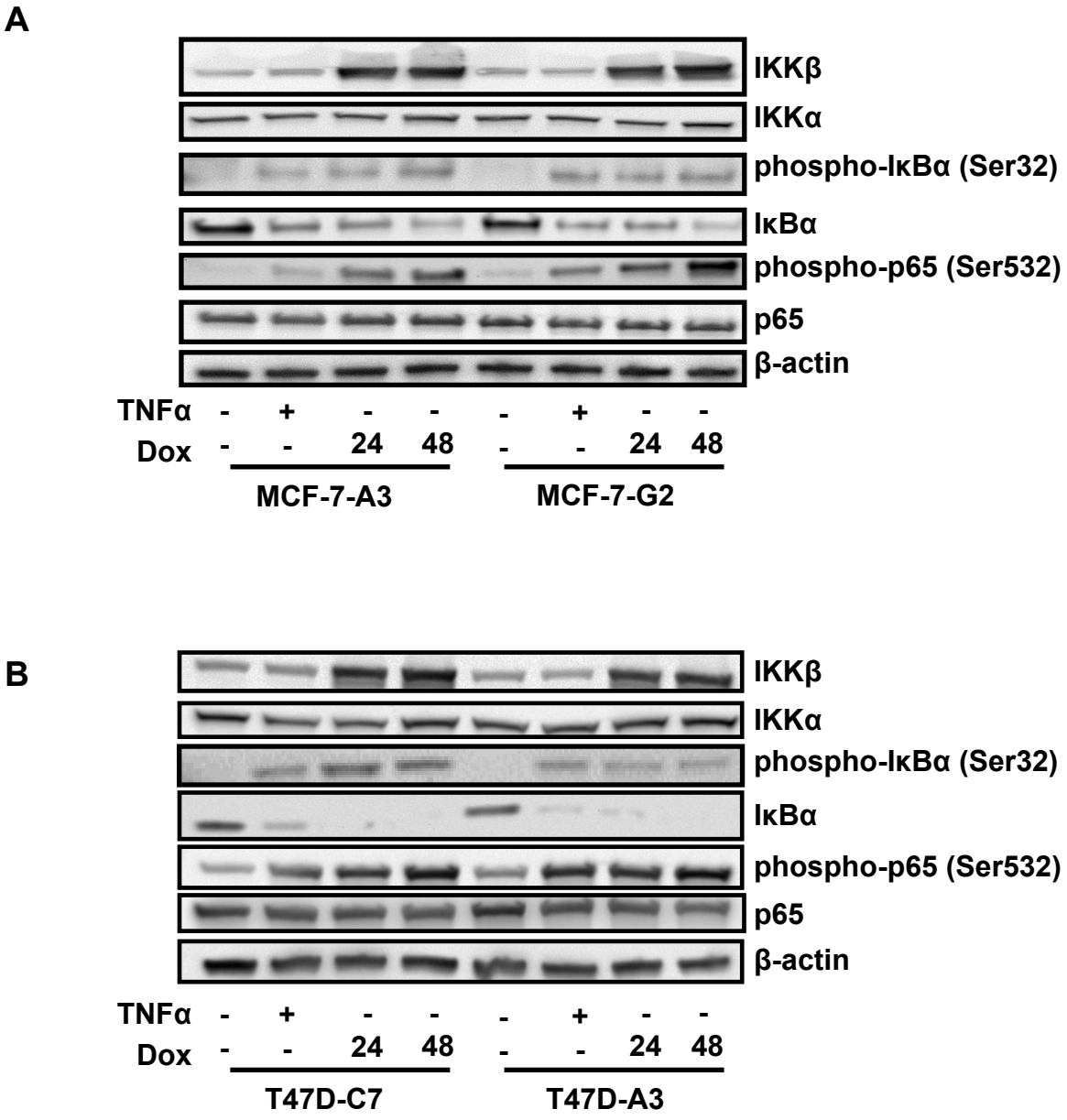

Figure 3: Dox treatment activates the NF-κB pathway in breast cancer cell lines expressing CA-IKKβ. CA-IKKβ-MCF-7 cells (MCF-7-A3 and MCF-7-G2) (A) and CA-IKKβ-T47D cells (T47D-C7 and T47D-A3) (B) were treated with Dox (1 ug/mL) for 24 or 48 hrs or TNFα (10 ng/mL) for 30 min. A, B) Whole cell extract was prepared and IKKβ, IKKα, phospho-IκBα (Ser32), IκBα, phospho-p65 (Ser532), p65, and β-actin expression was detected by Western Blotting.

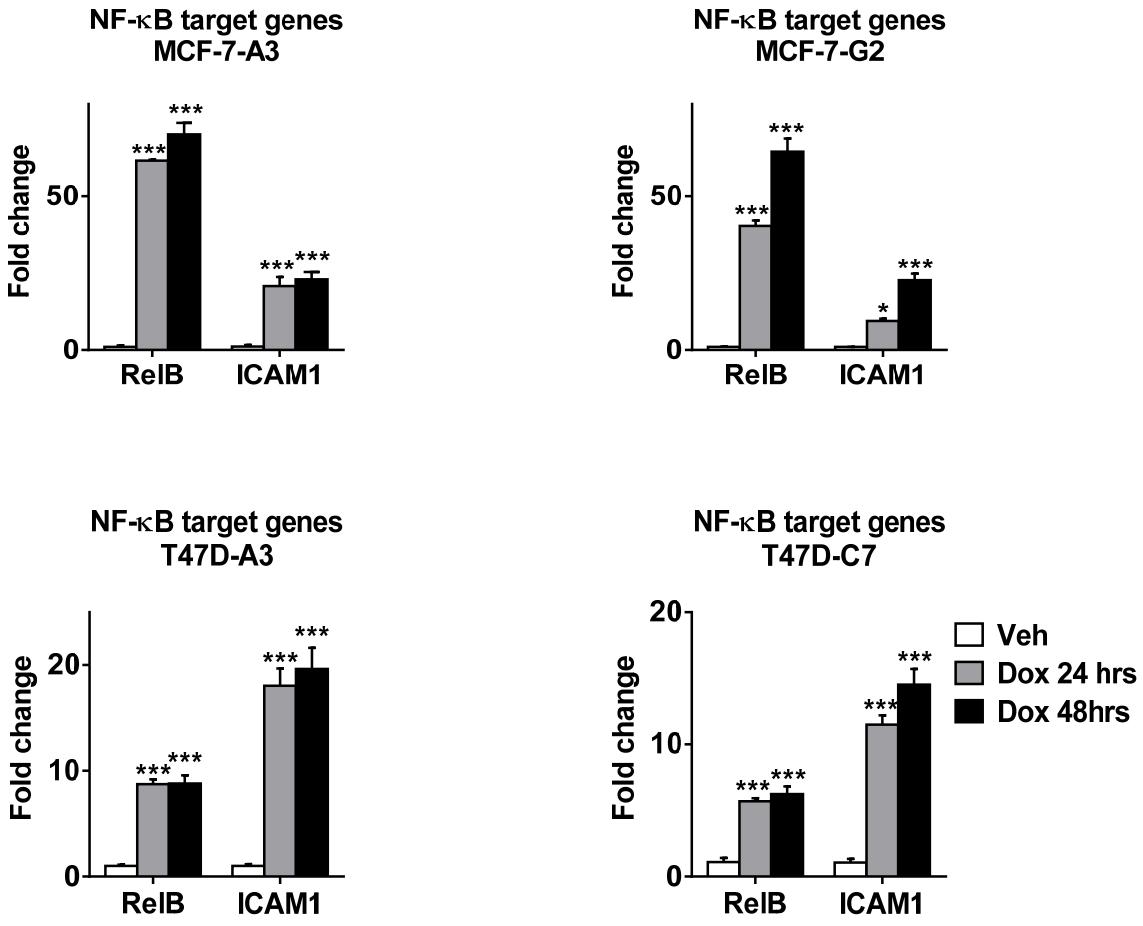

Figure 4: Dox treatment induces the expression of NF-κB target genes in CA-IKKβ cell lines. Each indicated cell line was treated with Dox for 24 hrs and 48 hrs. RelB and ICAM1 mRNA was assessed by QPCR. Fold changes were determined using the ΔΔCt method with 36B4 as an internal control (*p<0.05 and ***p<0.001 for treatment versus vehicle (Veh)).

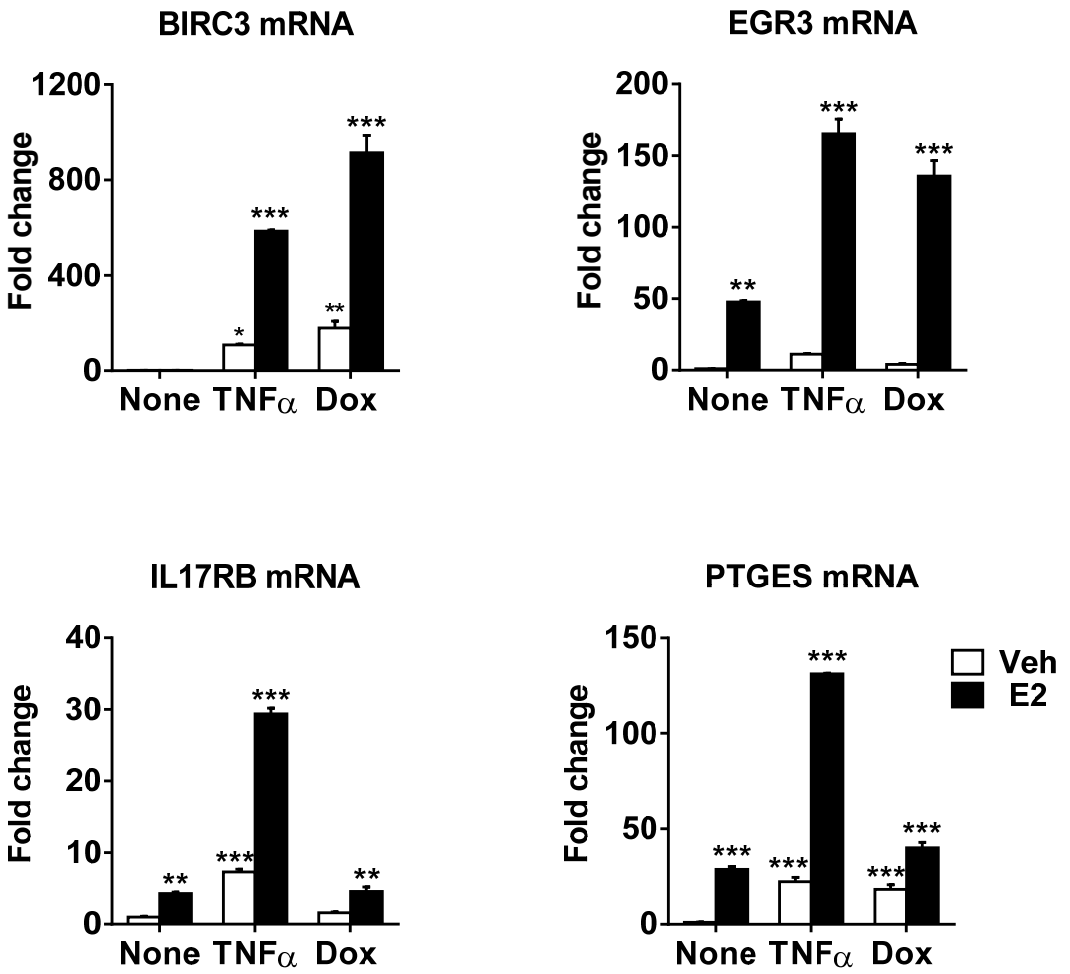

Figure 5: CA-IKKβ recapitulates the crosstalk between E2 and TNFα on some synergy signature genes but not others. MCF-7-A3 cells were treated with Dox for 24 hrs, and then 17β-estradiol (E2) (10 nM), TNFα or E2+TNFα for 2 hrs. mRNA expression of BIRC3, EGR3, IL17RB and PTGES was assessed by QPCR (*p<0.05, **p<0.01 and ***p<0.001 for treatment versus none Veh).

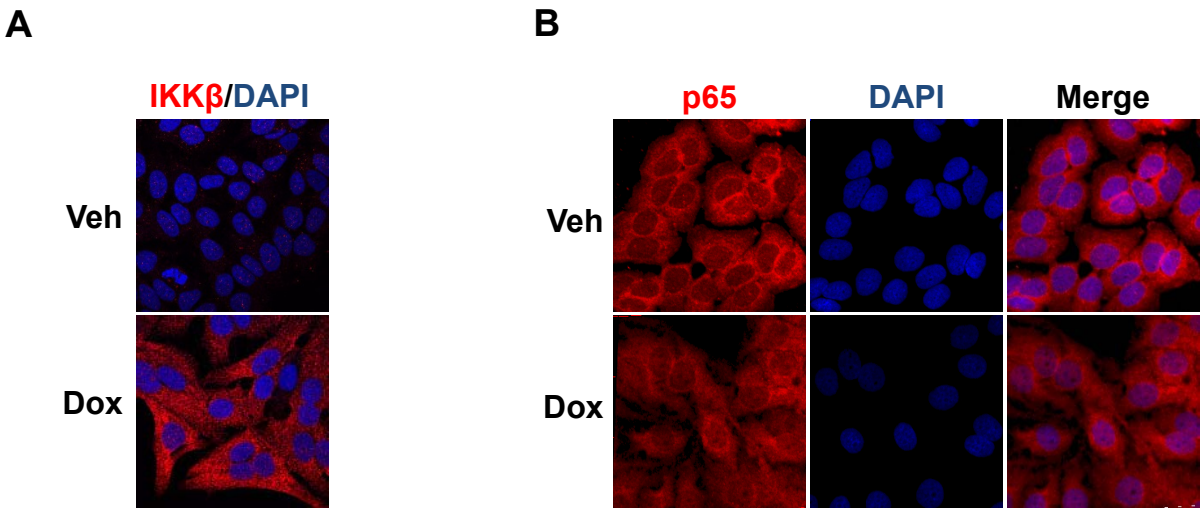

Figure 6: Dox induces IKKβ expression and p65 nuclear localization. MCF-7-A3 cells (A) and MCF-7-G2 cells (B) were treated with Dox for 5 days. Cells were fixed and incubated in primary antibody against IKKβ (red) (A) or p65 (red) (B), then stained with Alexa Fluor 594 conjugated secondary antibody. Nuclei were counterstained with DAPI (blue). Images were captured by x63 objective using confocal microscopy.

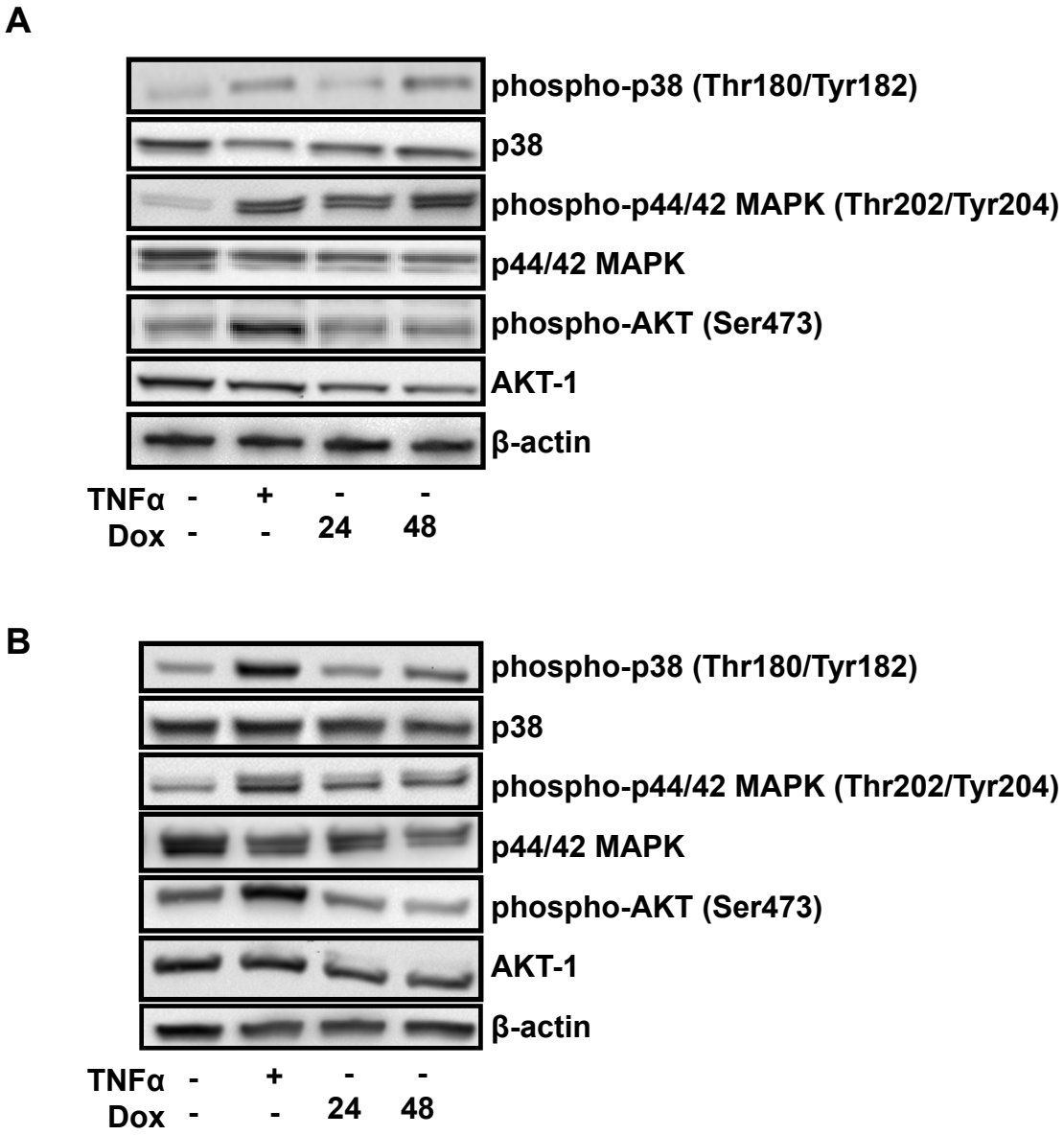

Figure 7: CA-IKKβ activates pathways other than NF-κB. MCF-7-G2 cells (A) and T47D-C7 cells were treated with TNFα for 30 min or Dox for 24 hrs or 48 hrs. Whole cell extract was prepared, and phospho-p38 (Thr180/Tyr182), p38, phospho-p44/42 MAPK (ERK1/2) (Thr202/Tyr204), p44/42 MAPK (ERK1/2), phospho-AKT (Ser473), AKT-1 and β-actin expression was detected by Western Blotting.

4.2. In vitro effects of constitutively active IKKβ on estrogen receptor positive breast cancer cells

4.2.1 Constitutively active IKKβ inhibits estrogen-induced proliferation and enhances cell survival

We hypothesized that the activation of NF-κB pathway is a driver of progression of ER+ breast cancer toward more aggressive phenotypes. Since one of the main hallmarks of aggressive ER+ breast tumors is elevated proliferation (8), we first examined the effect of CA-IKKβ on E2-stimulated breast cancer cell proliferation. Surprisingly, Dox treatment prevented E2-dependent increase in cell number in multiple MCF-7 and T47D clones (Figure 8).This was not observed in control pRetro-MCF-7 and pRetro-T47D cells (Figure 9). This indicates that IKKβ activation, rather than Dox treatment, inhibits E2-induced increase in cell number.

In order to find out whether the observed decrease in cell number is due to CA-IKKβ-induced cell death, we analyzed apoptosis using Annexin V-FITC and Propidium Iodide staining. Annexin V is a Ca2+-dependent phospholipid-binding protein that binds to phosphatidylserine. During early apoptosis, the cell loses membrane symmetry, and phosphatidylserine translocates to the external leaflet. Annexin V, thus, stains early apoptotic cells. The translocation of phosphatidylserine is followed by loss of membrane integrity, a characteristic of the later stages of cell death due to apoptosis or necrosis. The cell becomes permeable to Propidium Iodide, which binds the DNA and thus labels late apoptotic and necrotic cells. Viable cells, however, are not permeable for either stains, and thus are negative for both Annexin V and Propidium Iodide (156). We found that treatment of MCF-7-A3 cells with E2+Dox significantly inhibits early apoptosis and late apoptosis/necrosis versus vehicle (Figure 10A). In T47D-C7 cells, no significant difference in early apoptosis was observed; however, late apoptosis/necrosis was significantly inhibited upon treatment with E2+Dox versus vehicle (Figure 10B). We also

observed that E2 enhances apoptosis in this cell line but not MCF-7-A3 cells, suggesting that the proliferative effect of the cells is accompanied by cell death; yet, the net result is an increase in cell number (Figure 8). These differences may be attributed to inherent differences in the cell line, such as ER levels, p53 status, and/or apoptotic machinery (157- 159). Altogether, our results suggest that activation of IKKβ and treatment with E2 inhibit apoptosis/necrosis and enhance cell survival. Consequently, CA-IKKβ inhibition of E2-induced increase in cell number is not due to apoptosis/necrosis and is potentially due to an anti-proliferative effect of CA-IKKβ.

In order to examine the effect of CA-IKKβ on cellular anchorage-independent growth in vitro, soft agar colony formation assay was performed. The assay measures colony formation and proliferation in a semisolid culture media after 3-4 weeks (160). Cells were pretreated with E2, Dox or E2+Dox, and then they were transferred into soft agar and treatment was maintained for 3 weeks. We found that E2-induced anchorage-independent growth was inhibited upon IKKβ activation. Both the number and size of colonies were reduced in multiple cell lines (Figure 11), which confirmed the anti-proliferative effect of CA-IKKβ.

Cell cycle analysis was performed to understand the anti-proliferative effect of CA-IKKβ on cells treated with E2. As expected, E2 increased the population of cells in the S phase of the cell cycle. CA-IKKβ, however, inhibited E2-induced progression of the cell cycle, as evident by the decrease in E2-induced S phase. Interestingly, CA-IKKβ increased the percentage of cells in the G0/G1 phase, suggesting that activation of IKKβ induces cell cycle arrest (Figure 12). Taken together, our results demonstrate that CA-IKKβ inhibits E2-induced proliferation and progression of the cell cycle, and induces cell cycle arrest in the G0/G1 phase. Activation of IKKβ and treatment with E2, however, enhances cell survival and inhibits apoptosis/necrosis.

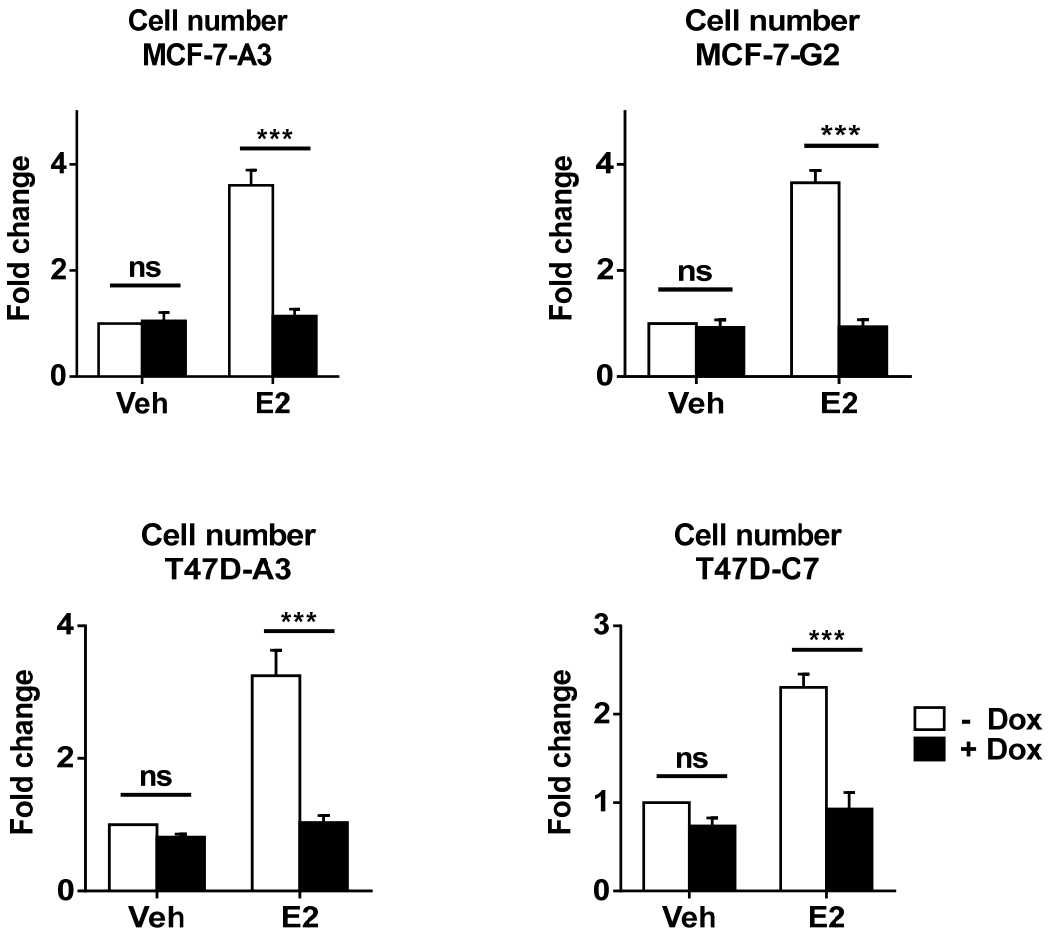

Figure 8: CA-IKKβ inhibits E2-induced increase in cell number. Each cell line indicated was treated with E2, Dox, or E2+Dox for 72 hrs. Cells were counted using a hemocytometer (***p<0.001 and ns=non-significant).

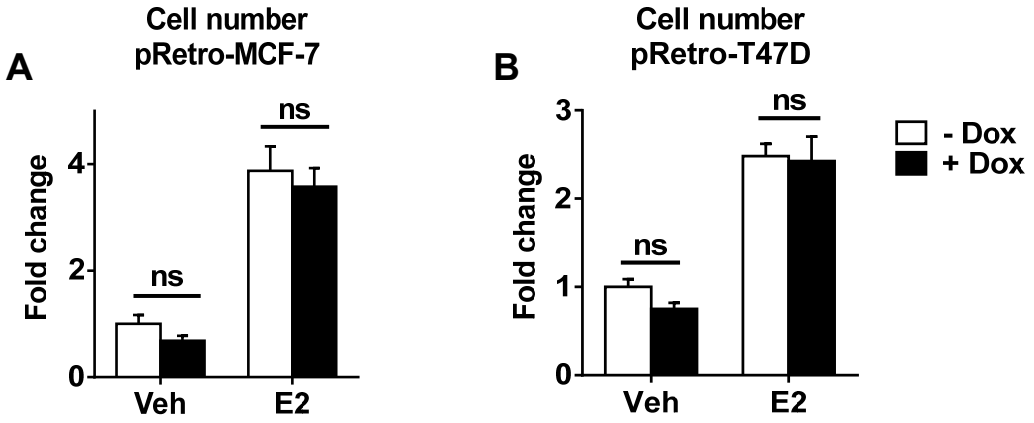

Figure 9: Dox treatment does not inhibit E2-induced increase in cell number of control cells. pRetro-MCF-7 cells (A) and pRetro-T47D cells (B) were treated with E2, Dox, or E2+Dox for 5 days. Hoechst 33342 nucleic acid stain was added to the cells. The incorporated dye was measured using fluorometry. Cell number was extrapolated from standard curves (ns=non-significant).

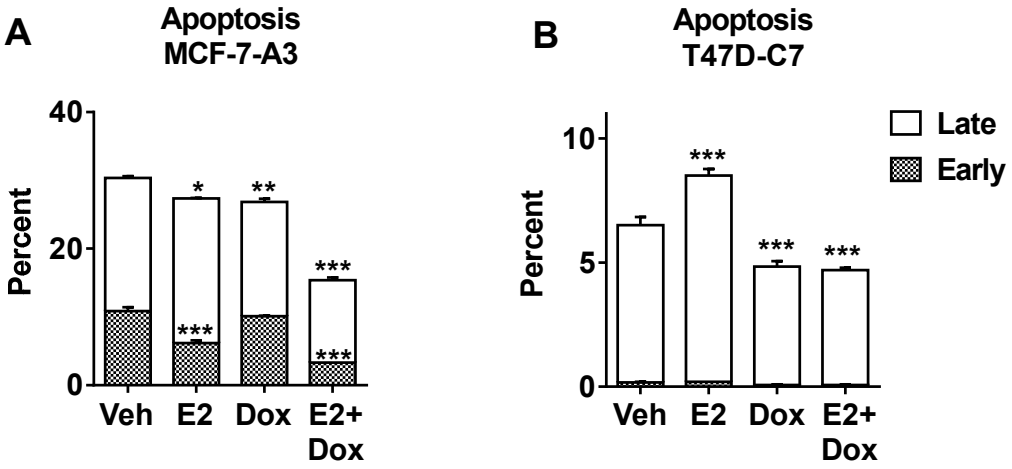

Figure 10: CA-IKKβ inhibits apoptosis. MCF-7-A3 cells (A) and T47D-C7 cells (B) were treated with E2, Dox, or E2+Dox for 72 hrs. Cells were fixed then stained with Annexin V-FITC and Propidium Iodide. The percent of early apoptotic and late apoptotic/necrotic cells was determined using flow cytometry analysis (*p<0.05, **p<0.01, and ***p<0.001 for treatment versus Veh).

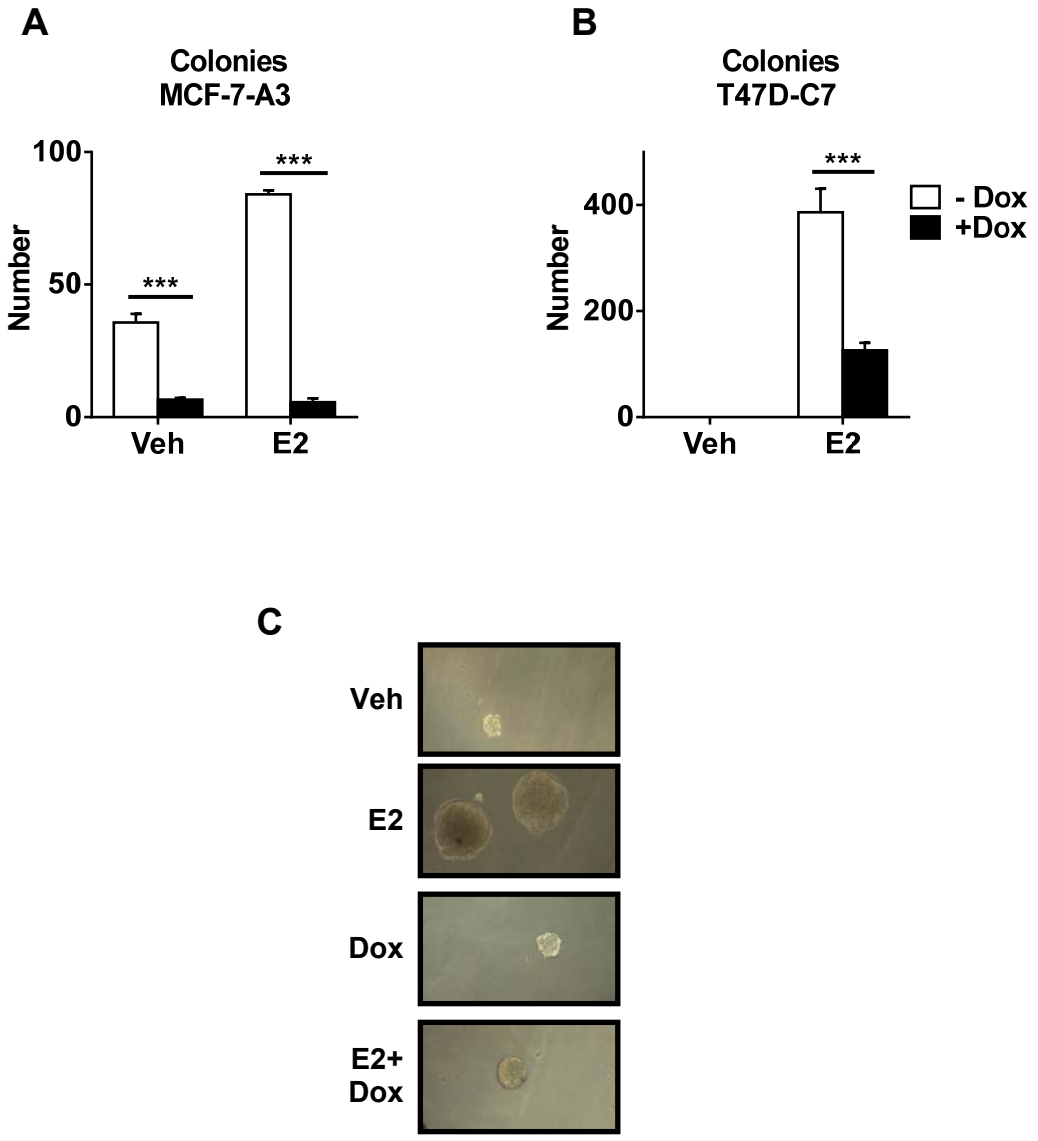

Figure 11: CA-IKKβ inhibits soft agar colony formation. MCF-7-A3 cells (A, C) and T47D-C7 cells (B) were treated with E2, Dox, or E2+Dox for 72 hrs. Cells were trypsinized, counted, seeded as single cells into soft agar, and then retreated every 3 days for 3 weeks. C) Representative images for the size of colonies observed for MCF-7-A3 cells. Images were captured using x10 microscope objective (*** $p<0.001$).

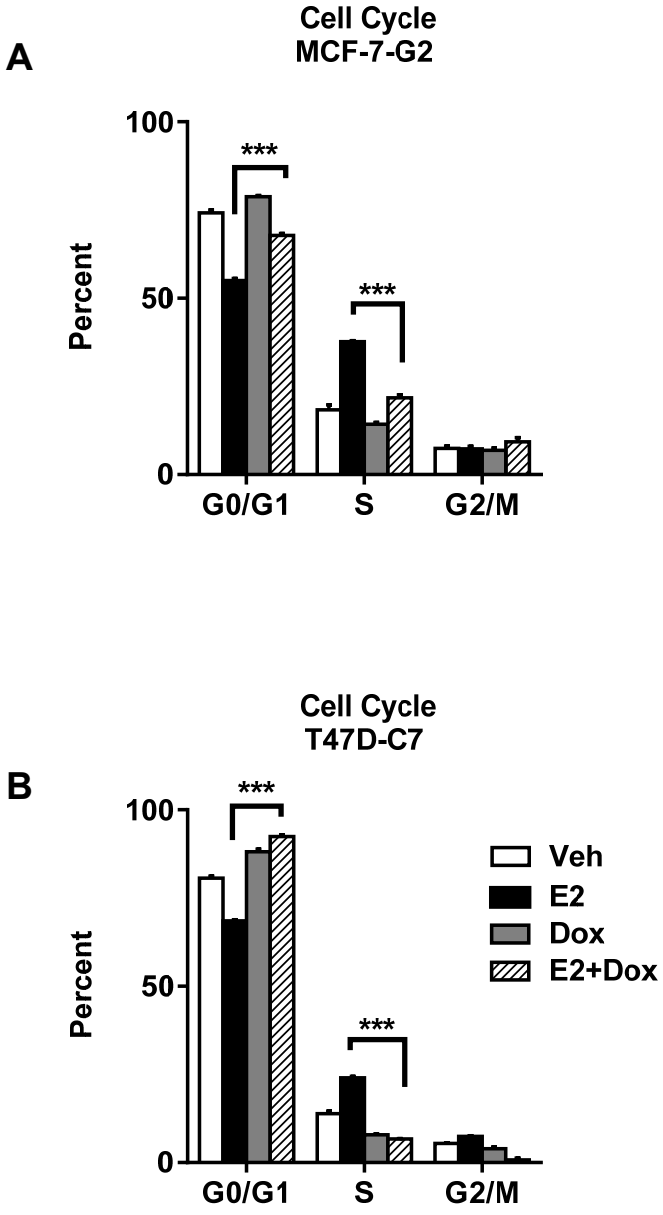

Figure 12: CA-IKKβ inhibits E2-induced cell cycle. MCF-7-G2 cells (A) and T47D-C7 cells (B) were treated with E2, Dox, or E2+Dox for 72hrs. Cells were fixed and stained with Propidium Iodide. Cell cycle analysis was performed using flow cytometry (***p<0.001).

4.2.2 Constitutively active IKKβ induces reversible cellular quiescence

The fact that CA-IKKβ increases the population of cells in the G0/G1 phase of the cell cycle (Figure 12) suggests that CA-IKKβ induces cell cycle arrest. There are two mechanisms of arrest in the G0/G1 phase: 1) cellular quiescence, which is reversible, and 2) cellular senescence, which is irreversible (46). To find out if CA-IKKβ effect on E2-induced proliferation is reversible, cells were treated with E2+Dox briefly, and then Dox was withdrawn to downregulate CA-IKKβ. Cell proliferation was examined using three different approaches: 1) DNA content, 2) clonogenic assay, and 3) soft agar colony formation assay. As expected Dox inhibited the increase in DNA content induced by E2. However, when Dox was withdrawn after 3 days, E2-induced cell proliferation was significantly rescued (Figure 13). The clonogenic assay, which examines both proliferation and survival of the cells, determines the ability of a single cell to survive and grow into a large colony (at least 50 cells) under different conditions and treatments (161,162). As observed in the DNA assay, E2-induced colony formation was also inhibited by CA-IKKβ. Similarly, Dox withdrawal after 8 days of treatment resulted in rescue of the effect of E2 on colony formation (Figure 14). The same finding was observed when we used the soft agar colony formation approach (Figure 15). Prolonged incubation of MCF-7-A3 cells, however, resulted in the aggregation and clumping of vehicle and E2-induced colonies, which rendered them non-countable (Figure 15B). Our results indicate that CA-IKKβ is inducing a reversible growth arrest in ER+ breast cancer cells, suggesting that the phenotype observed is quiescence rather than senescence.

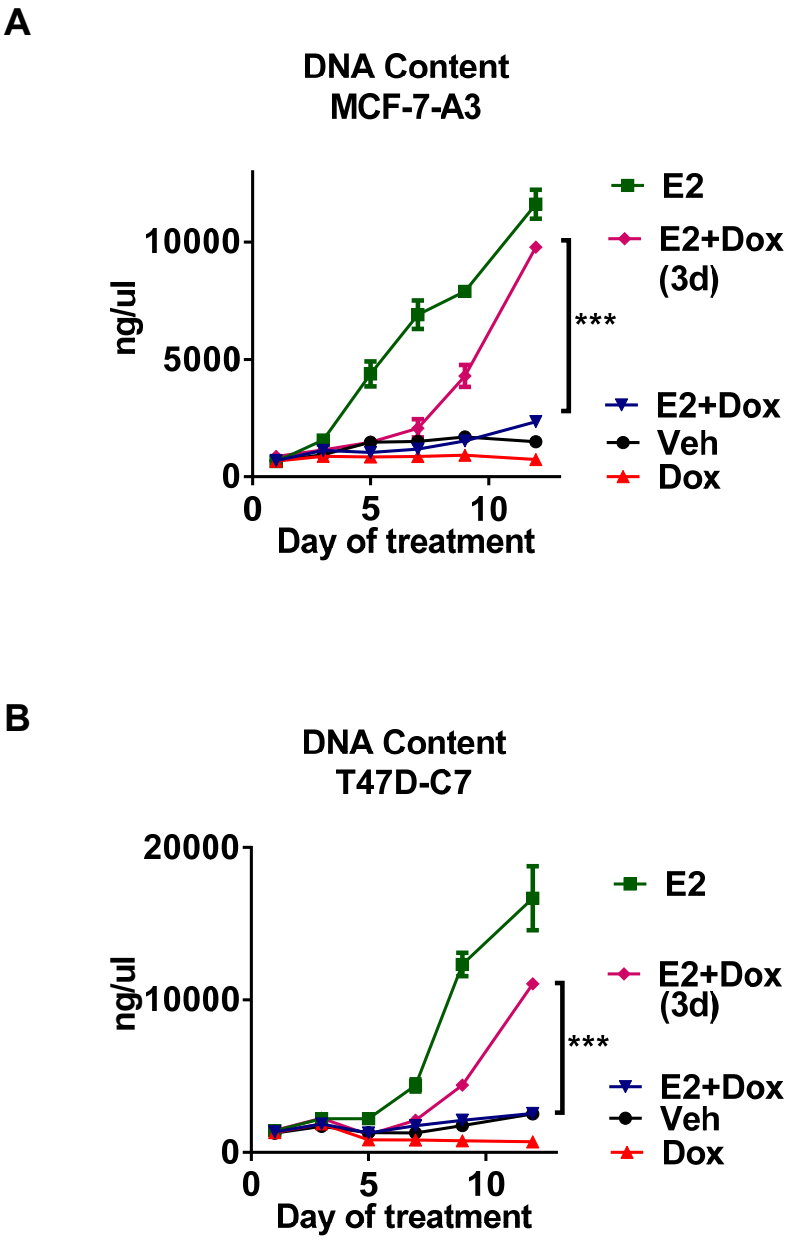

Figure 13: Dox withdrawal rescues E2-induced proliferation. MCF-7-A3 (A) and T47D-C7 (B) cells were treated with E2, Dox, or E2+Dox for 12 days. After 3 days of treatment, Dox was withdrawn from an E2+Dox group. Cells were retreated every 3 days. After 12 days, Hoechst 33342 nucleic acid stain was added to the cells. The incorporated dye was measured using fluorometry. DNA content was extrapolated from standard curves (***$p<0.001$).

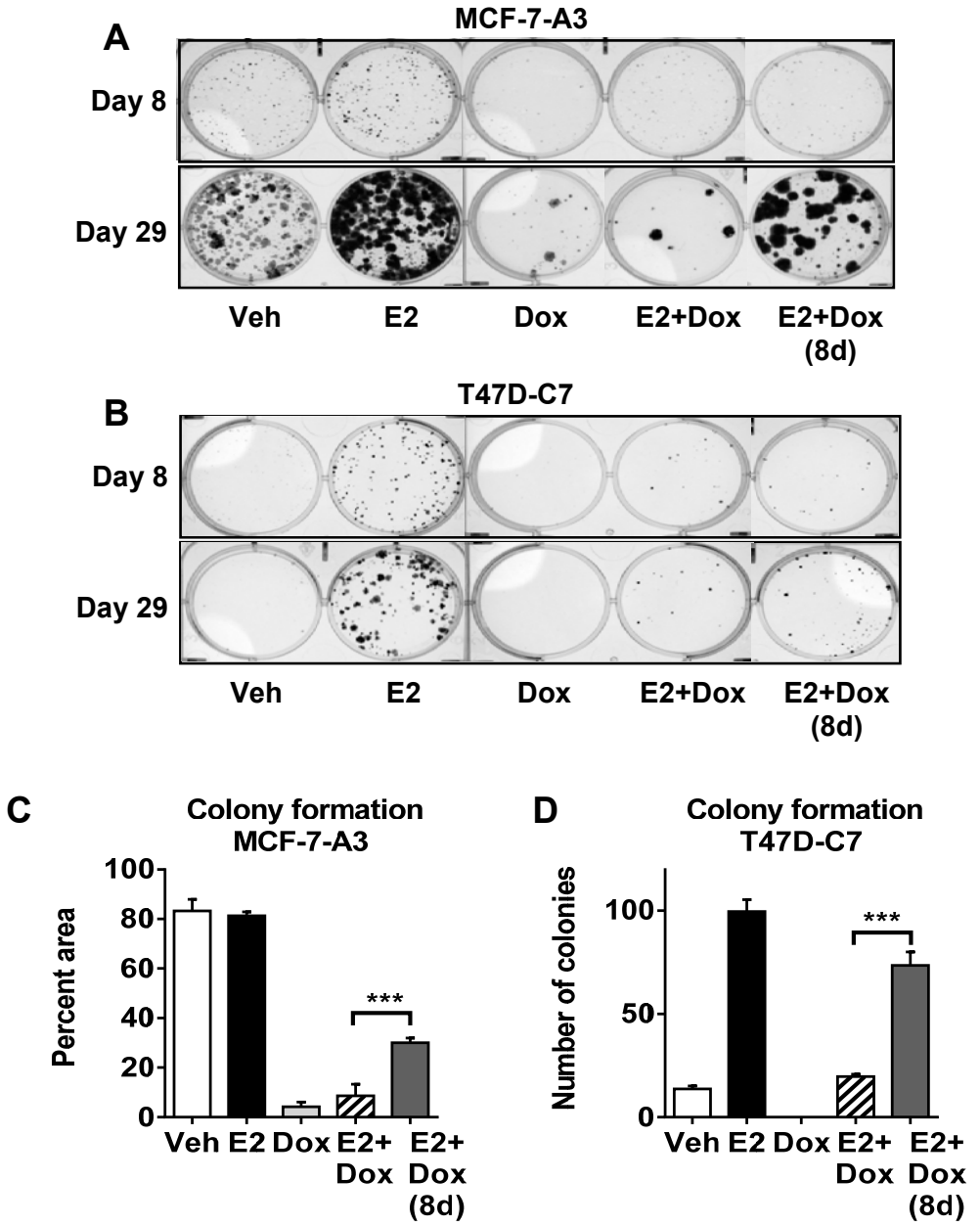

Figure 14: Dox withdrawal rescues E2-induced colony formation. MCF-7-A3 cells (A, C) and T47D-C7 cells (B, D) were treated with E2, Dox, or E2+Dox for 72 hrs. Cells were trypsinized, counted, and seeded as single cells. Colonies were allowed to grow and cells were retreated twice per week. Dox was withdrawn from an E2+Dox group after 8 days. Colony formation was monitored for 29 days, and then the cells were fixed and stained with crystal violet. C) Percent surface area, of the well, occupied by the colonies formed was quantified using Image J. D) Colonies were counted manually (***$p<0.001$).

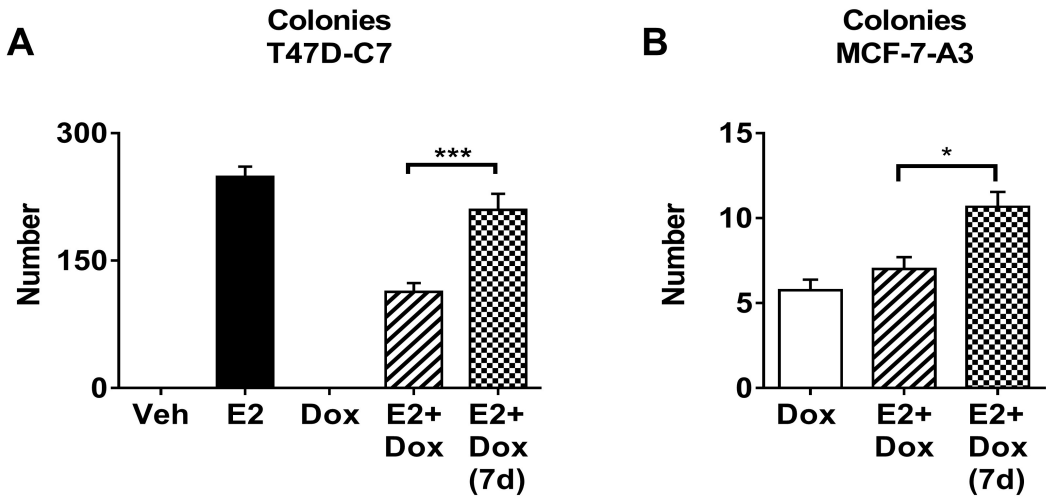

Figure 15: Dox withdrawal rescues E2-induced soft agar colony formation. T47D-C7 cells (A) and MCF-7-A3 cells (B) were treated with E2, Dox, or E2+Dox for 72hrs. Cells were trypsinized, counted, seeded as single cells into soft agar, and then retreated every 3 days. Dox was withdrawn on day 7 from an E2+Dox group. Colonies were counted after 4.5 weeks (A) or 6 weeks (B) (*$p<0.05$ and ***$p<0.001$).

4.2.3 Estrogen and constitutively active IKKβ work together to promote migration and invasion

Interestingly, the observed effect of CA-IKKβ on E2-induced proliferation and survival was associated with a change in the morphology of the cells. MCF-7 cells are characterized by a cobblestone appearance with tight cell-cell contacts. Cells treated with Dox, however, adopted a spindly, elongated, fibroblastic morphology with cellular protrusions (Figure 16A). To investigate the effect of CA-IKKβ on the cytoskeleton, we stained F-actin with phalloidin, which revealed the presence of phalloidin stained stress fibers in the observed protrusions, suggestive of a migratory behavior of the cells (Figure 16B).

To determine the effects of E2 and CA-IKKβ on the migration of the cells, we first performed a scratch wound healing assay. Cells treated with E2+Dox exhibited ~100% wound closure, an effect that was not observed with either E2 or Dox alone over a 96 hrs time course (Figure 17). In the control pRetro-MCF-7 cells, E2 and E2+Dox treatments enhanced closure approximately to the same extent. Doxycycline treatment, however, did not enhance wound closure, indicating that the observed closure in CA-IKKβ cells is an effect of IKKβ activation rather than Dox treatment (Figure 18).

Due to the fact that wound closure can reflect both migration and proliferation of the cells (163), it is likely that the effect of E2 on wound closure may be attributed to E2-induced proliferation. In contrast, the combined effect of E2 and CA-IKKβ inhibited E2-induced proliferation; yet, it resulted in significantly more wound closure compared to E2 alone, suggesting that cells treated with E2+Dox are highly migratory. In order to confirm this finding, we tested the migration of the cells using migration transwell inserts. We found that E2+Dox increased transwell migration compared to either of E2 or Dox alone in multiple cell lines (Figure

19), confirming that the combination of E2 treatment and activation of IKKβ promotes cell migration.

Migration of tumor cells is a prerequisite for cell invasion and eventually, metastasis. For a tumor cell to invade, it has to digest the extracellular matrix (ECM) that otherwise blocks its entry into neighboring tissues in a process involving ECM degradation and proteolysis (164). To examine cell invasion, we used transwell inserts coated with 0.1 mL (300 μg/mL) Matrigel, which resembles the ECM environment found in many tissues. Matrigel is a basement membrane preparation extracted from the Engelbreth-Holm-Swarm (EHS) mouse sarcoma, and it is used to test the invasive activity of tumor cells (165). Similar to migration, E2+Dox treated cells were highly invasive compared to E2 or Dox alone (Figure 20).

Matrix metalloproteinases (MMPs) are zinc-dependent endopeptidases that can degrade all components of the ECM. They play an important role in cancer cells invasion and tumor metastasis. They are classified according to their substrate specificity. Different MMPs are regulated during breast cancer progression (166). The gelatinase MMP9 is a direct transcriptional target of NF-κB (167), and the pathway is associated with expression of collagenase MMP13 in breast cancer (168). Studies have reported that E2 increases the enzymatic activity of the gelatinase MMP2 via the upregulation of MMP14 (169). Examining mRNA expression of MMPs in CA-IKKβ cells, we found that E2 upregulates the expression of MMP14, while CA-IKKβ upregulates the expression of MMP13 and MMP9. Activation of IKKβ and treatment with E2, however, promotes the expression of the three MMPs (Figure 21). This suggests that E2 and CA-IKKβ work together to promote an invasive phenotype in ER+ breast cancer cells, and this may be mediated by the increase in MMPs expression.

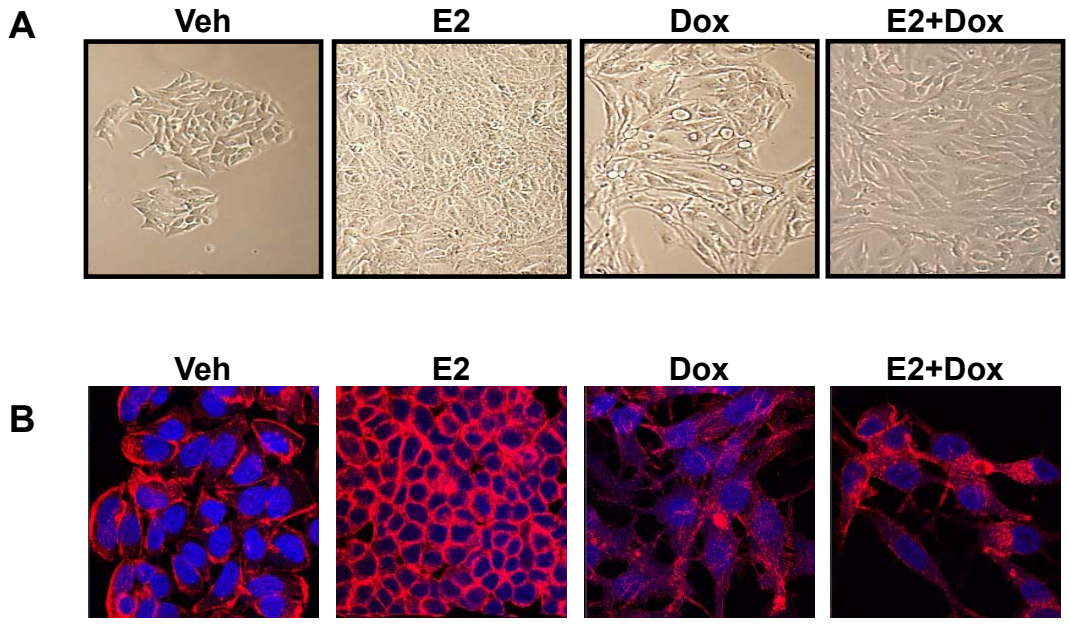

Figure 16: CA-IKKβ induces a change in the morphology of the cells. A) MCF-7-A3 cells were treated with E2, Dox, or E2+Dox for 5 days. Bright field images were captured using x10 microscope objective. B) MCF-7-G2 cells were treated as in A. Cells were fixed, and F-actin was stained with phalloidin (red). Nuclei were visualized with DAPI (blue). Images were captured with x63 microscope objective using confocal microscopy.

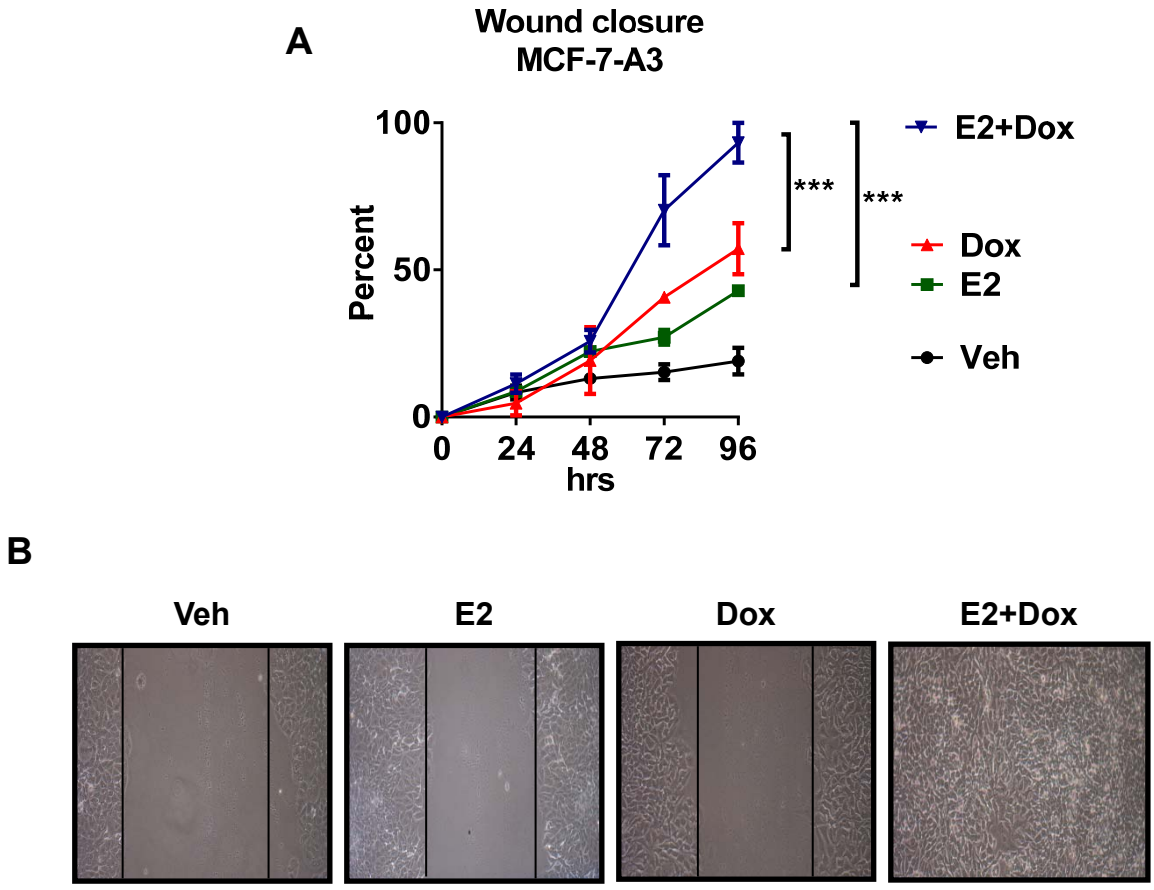

Figure 17: CA-IKKβ+E2 enhance wound closure of ER+ cells. A) MCF-7-A3 cells were grown to 80% confluence. A wound was created, and cells were treated with E2, Dox, or E2+Dox. Cells were retreated every other day, and wound closure was monitored for 96 hrs. Wound closure was measured and expressed as percent of initial wound size. B) Representative bright field images of (A) after 96 hrs captured with x10 microscope (***$p<0.001$).

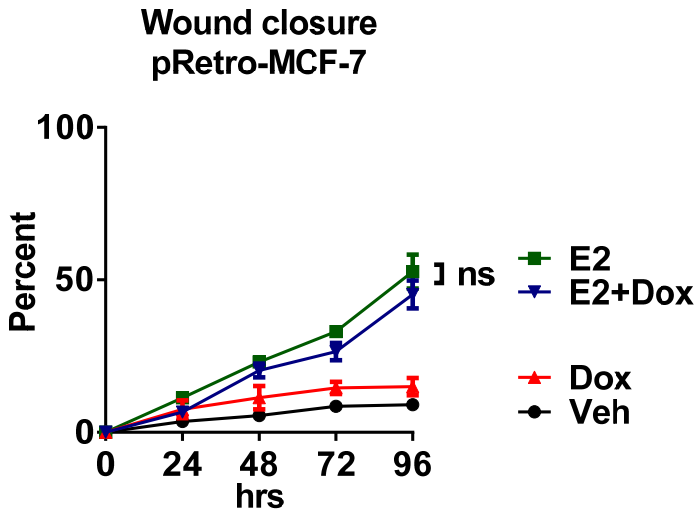

Figure 18: E2, but not Dox, enhances wound closure of control cells. pRetro-MCF-7 cells were grown to 80% confluence. A wound was created, and cells were treated with E2, Dox, or E2+Dox. Cells were retreated every other day, and wound closure was monitored for 96 hrs. Wound closure was measured and expressed as percent of the initial wound (ns=non-significant).

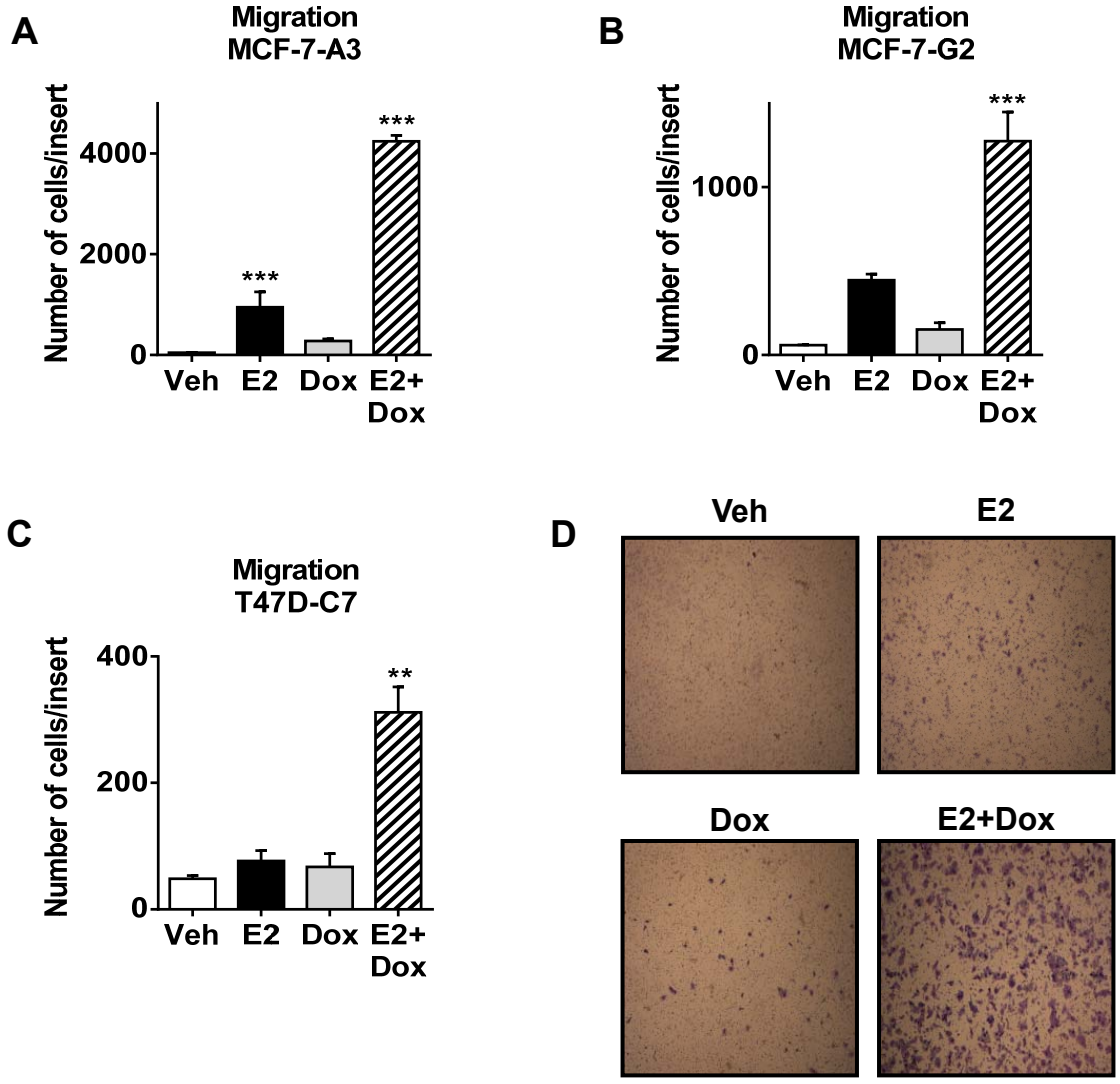

Figure 19: CA-IKKβ+E2 enhance migration of ER+ cells. A-C) Each cell line indicated was treated with E2, Dox, or E2+Dox for 3 days. Equal numbers of cells were transferred to migration inserts and allowed to migrate for 24 hrs (A, B) or 16 hrs (C). Cells were then fixed with 4% p-formaldehyde and stained with 0.1% crystal violet. Cell number per insert was manually counted using x10 microscope objective. D) Representative images of stained inserts of A. Images were taken using x4 microscope objective (**p<0.01 and ***p<0.001 for treatment versus Veh).

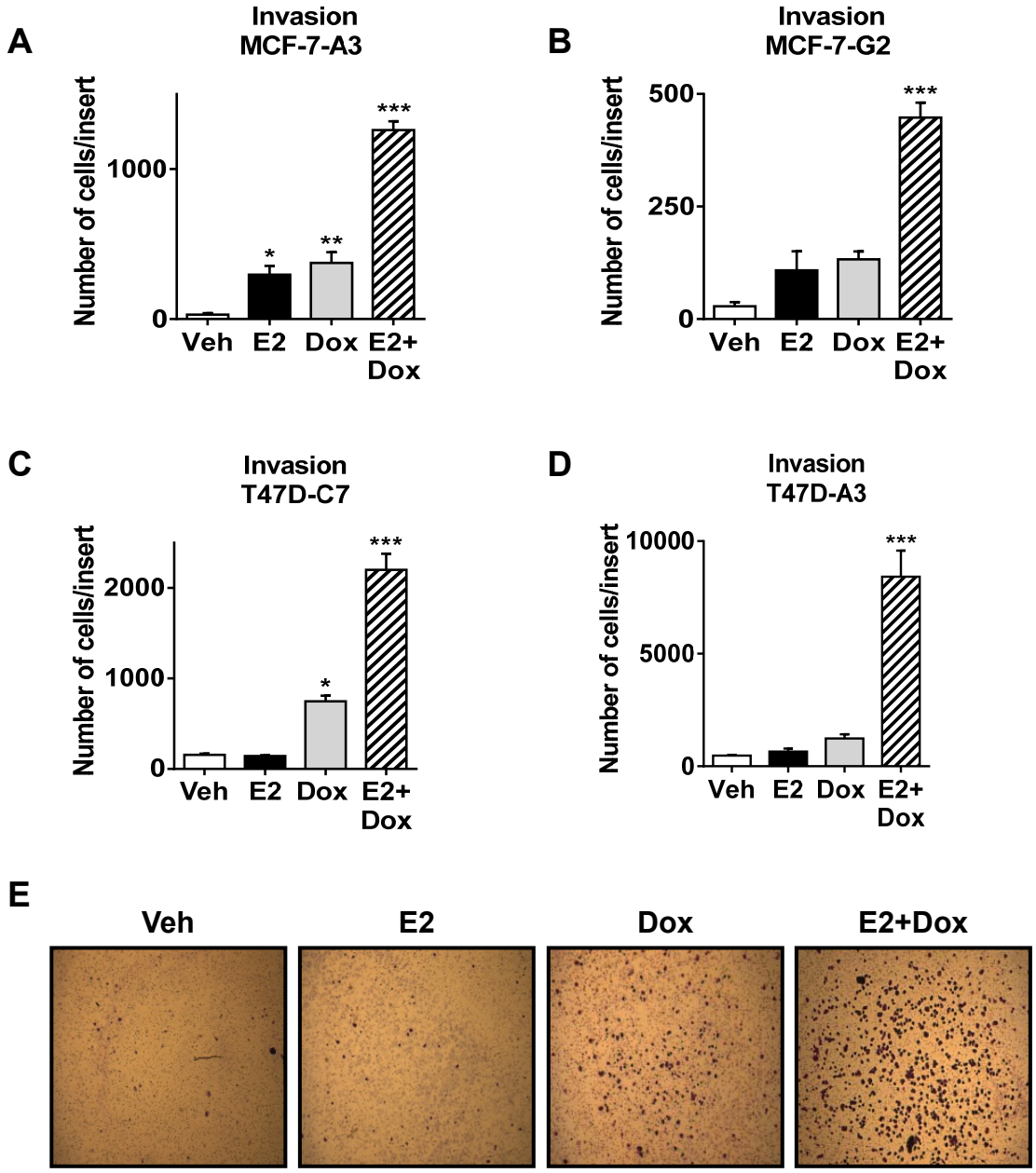

Figure 20: CA-IKKβ+E2 enhance invasion of ER+ cells. A-D) Each cell line indicated was treated with E2, Dox, or E2+Dox for 3 days. Equal numbers of cells were transferred to invasion inserts and allowed to invade for 24 hrs (A, B) or 16 hrs (C, D). Cells were then fixed with 4% p-formaldehyde and stained with 0.1% crystal violet. Cell number per insert was manually counted using x10 microscope objective. E) Representative images of stained inserts of C. Images were taken using x4 microscope objective (*p<0.05, **p<0.01 and ***p<0.001 for treatment versus Veh).

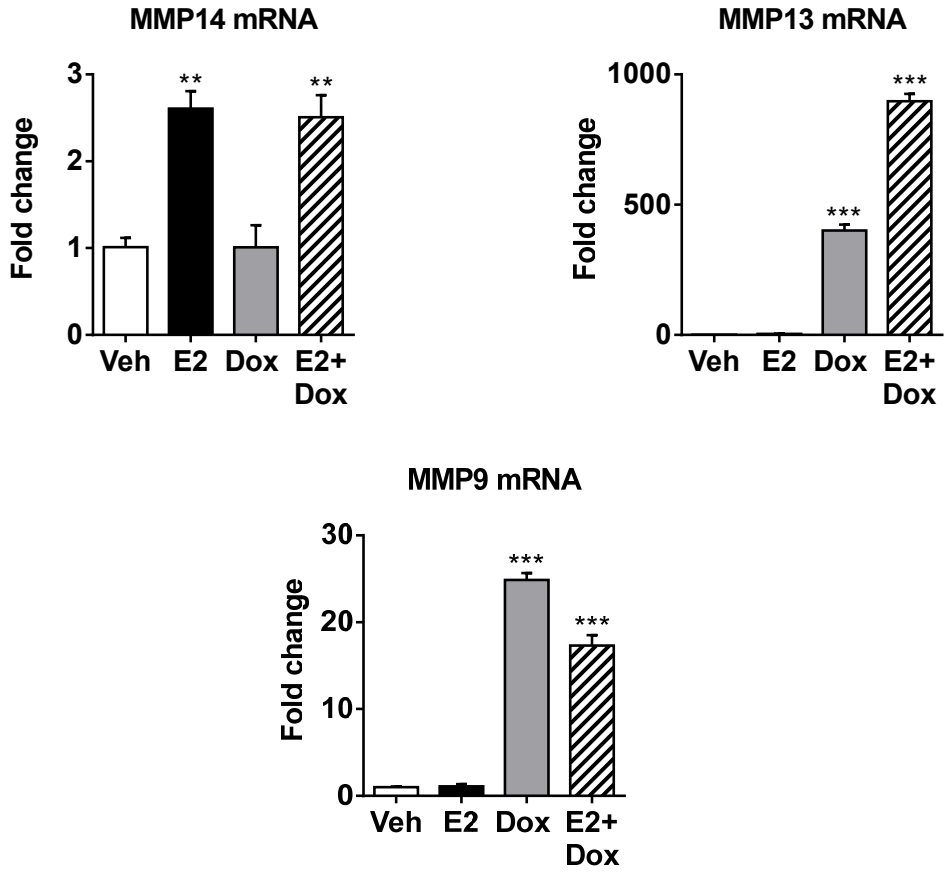

Figure 21: CA-IKKβ+E2 induce the expression of MMPs. MCF-7-A3 cells were treated with E2, Dox, or E2+Dox for 5 days. MMP9, MMP13 and MMP14 mRNA expression was assessed by QPCR. Fold changes were determined using the ΔΔCt method with 36B4 as an internal control (**p<0.01 and ***p<0.001 for treatment versus Veh).

4.3 In vivo effects of constitutively active IKKβ on estrogen receptor positive tumors

4.3.1 Constitutively active IKKβ renders estrogen receptor positive tumors dormant

Results from in vitro studies suggest that IKKβ activation renders ER+ cells in a reversible quiescent and highly invasive state. In order to investigate the effect of CA-IKKβ in vivo, MCF-7-A3 cells dual labeled with GFP and luciferase (MCF-7-A3-LUC) were injected, orthotopically, into the thoracic mammary fat pad of female athymic nude mice. At the same time silastic E2 pellets, which slowly release E2 for up to 8 weeks, were subcutaneously implanted. Palpable tumors were observed 11-14 days after surgery and tumor area was recorded every 3-4 days. Tumors were allowed to grow in the presence of E2 until they reached ~0.1-0.2 cm^2 in area, at which time they were randomized into 3 groups:

1. E2 only: received 5% sucrose in the drinking water.
2. E2+12d Dox: received Dox (2 mg/mL in 5% sucrose) in the drinking water for 12 days and then 5% sucrose throughout the rest of the study.
3. E2+Dox: received Dox (2 mg/mL in 5% sucrose) continuously throughout the experiment.

As expected, tumors in the E2 only group grew continuously (Figure 22A). In contrast, tumors regressed with Dox treatment to the extent that they were not palpable by day 12 (Figure 22A). To determine if viable cells survived, bioluminescence was examined using IVIS (in vivo preclinical imaging system) spectrum. Bioluminescence could be observed at the site of the regressing tumors, indicating that some viable cells had survived (Figure 22B). Tumors in E2+12d Dox group regrew, became palpable ~one week after Dox withdrawal, and continued growing until the end of the experiment (Figures 22A and 22B). The growing tumors of the E2 and E2+12d Dox groups, were dissected, fixed and stained. Tumor cells were confirmed by hematoxylin and eosin (H&E) staining and GFP immunohistochemistry (IHC) (Figure 23A). As

expected, the mitotic marker Ki67 stained the nuclei of E2, as well as E2+12d Dox tumors, confirming that E2-induced tumor growth was rescued upon Dox withdrawal (Figure 23A).

In the group that received continuous Dox, we attempted to identify tumor cells in the area of bioluminescence signal by histology. Tumor cells were not detected in most of the animals. However, one animal showed cancer cells in the auxiliary lymph node and the area surrounding it, as detected by H&E staining and GFP IHC. The tumor cells could be observed surrounding a nerve and invading connective tissue (Figure 23B). To our surprise, the nuclei of the cells stained for Ki67, suggesting that although non palpable, some of the remaining tumor cells may be maintaining a certain rate of mitosis (Figure 23B).

In order to find out if ER+ tumors are still reversibly dormant after long-term of IKKβ activation, MCF-7-A3-LUC cells were injected into the mammary fat pad of athymic nude mice. At the same time beeswax E2 pellets, which release E2 slowly for up to one year, were subcutaneously implanted. When tumors reached ~0.1-0.2 cm^2 in area, Dox was introduced in the drinking water of mice. Tumor burden was monitored by palpation and bioluminescence over 60 days. Dox was then withdrawn, and animals were monitored for an additional 22 days. Similar to our previous observations, Dox causes tumor regression, yet, bioluminescence signal could be detected throughout the entire period of Dox administration. Seven to ten days after Dox withdrawal, palpable tumors were observed (5 out of 6 tumors) and this was accompanied by an increase in the bioluminescence signal (Figures 24A and 24B). The recurrent tumors were confirmed by H&E staining (Figure 24C). Notably, bioluminescence could be observed at metastatic sites in 40% of the animals (Figure 24B), suggesting spontaneous metastasis, which will be discussed in further detail below. Taken together, our findings demonstrate that CA-IKKβ causes tumor regression; yet, cells can survive for long term and are capable of initiating a locally recurrent tumor.

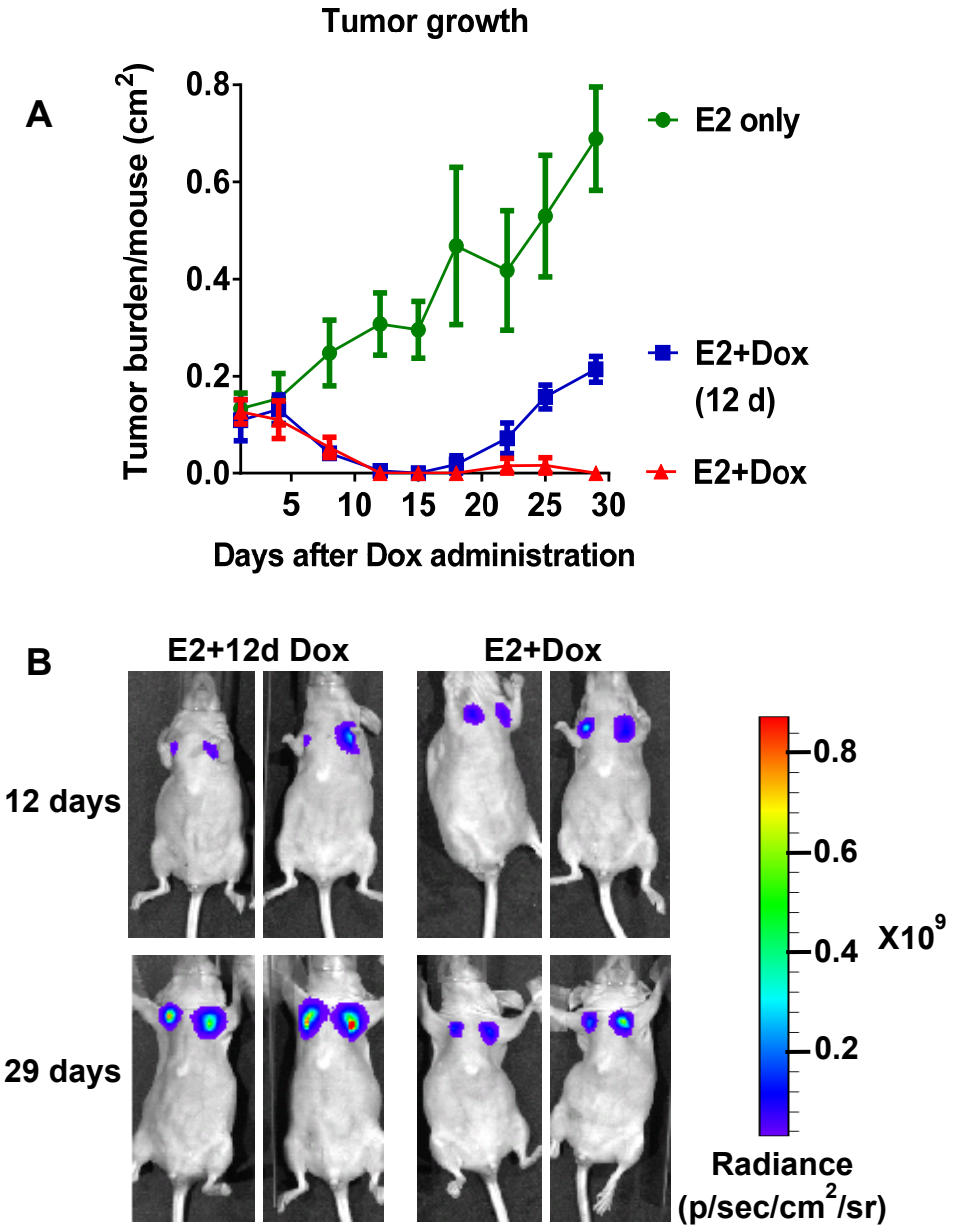

Figure 22: CA-IKKβ causes reversible regression of ER+ xenografts. MCF-7-A3-LUC cells were injected into the mammary fat pad of female athymic nude mice in which E2 pellets were subcutaneously implanted. When tumors reached 0.1-0.2 cm^2 in area, animals were randomized into 3 groups: 1) E2, 2) E2+12 days Dox (2 mg/mL) in the drinking water, 3) E2+Dox continuously. A) Tumor area was monitored 3-4 days per week and plotted as tumor burden/mouse. B) Animals were injected with D-Luciferin (150 mg/kg) and bioluminescence was detected using IVIS spectrum on day 12 and 29 of Dox administration.

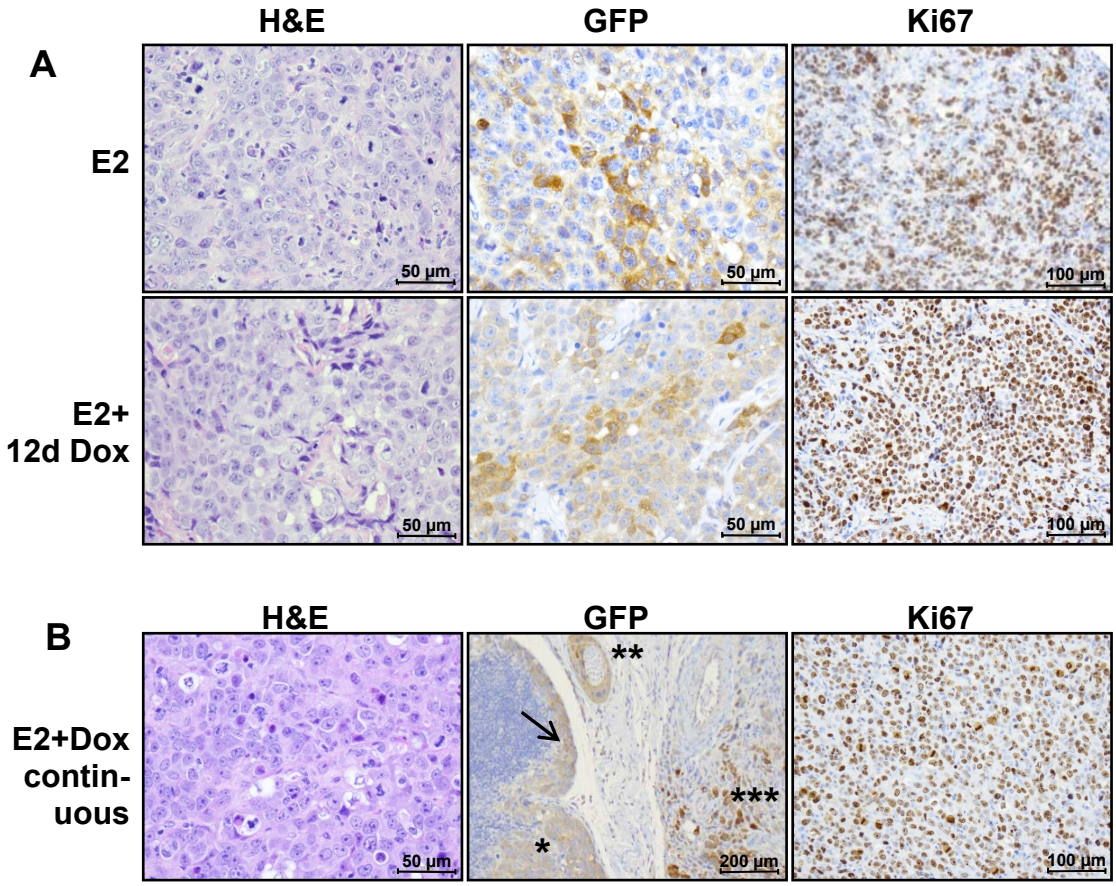

Figure 23: Histologic examination of primary injection site. Tumors were collected after 29 days of Dox treatment, fixed in 10% formalin, embedded in paraffin, and 5 µm sections were prepared. Tissue sections were deparaffinized, rehydrated, and stained with H&E, GFP and Ki67. A) Stained sections of the tumors in animals receiving E2 only and animals receiving E2 and 12 days of Dox. B) Stained sections of the bioluminescent site in animals receiving E2 and continuous Dox (arrow=subcapsular sinus of the lymph node, *= tumor in the lymph node, **=a nerve surrounded by tumor cells, ***=tumor cells invading the connective tissue).

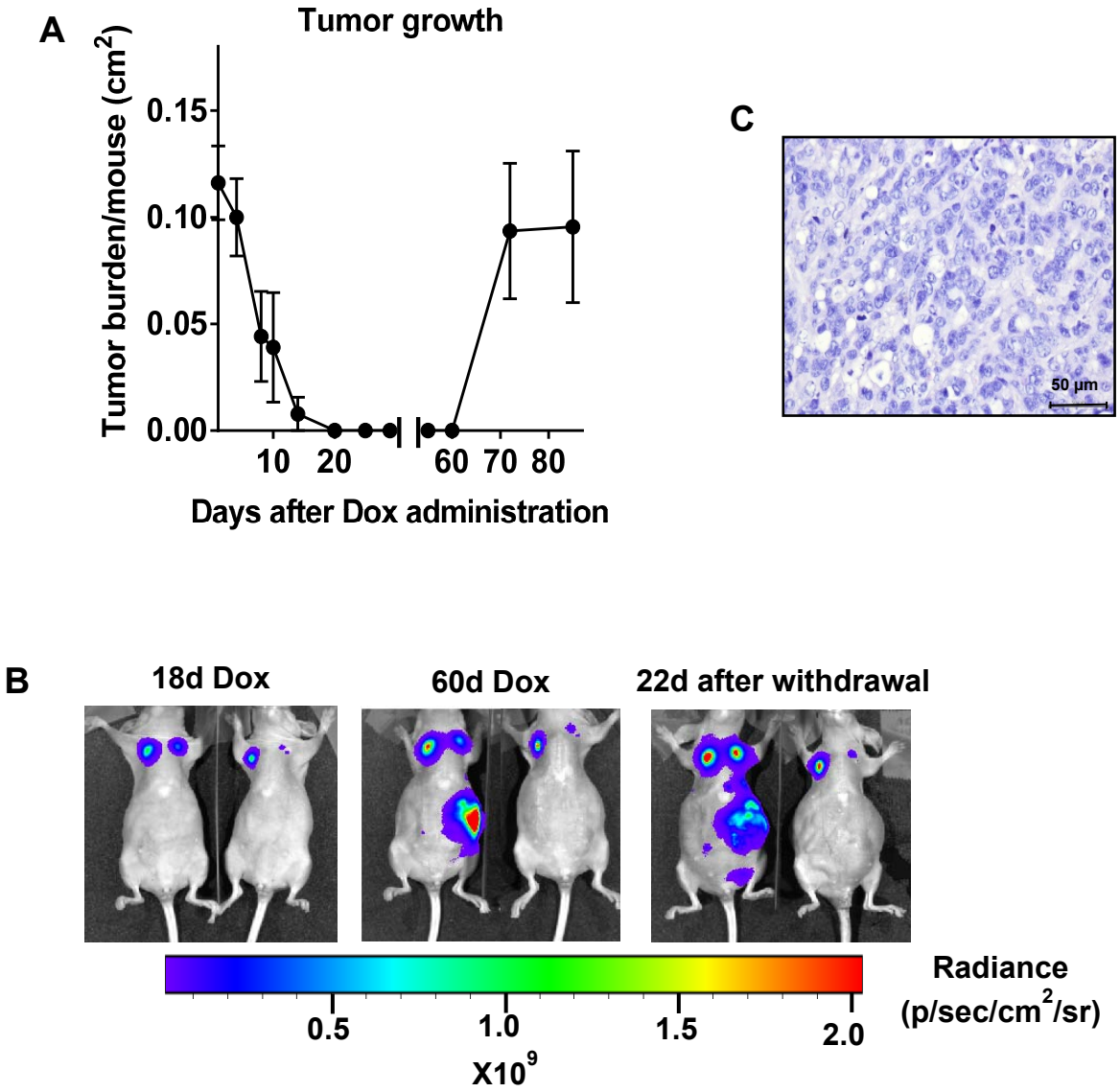

Figure 24: ER+ xenografts recur after 60 days of IKKβ activation. MCF-7-A3-LUC cells were injected into the mammary fat pad of female athymic nude mice, in which E2 pellets were subcutaneously implanted. When tumors reached 0.1-0.2 cm^2, Dox (2 mg/mL) was introduced to the drinking water of the mice. After 60 days, Dox was withdrawn from the drinking water, and animals were monitored for an additional 22 days. A) Tumor area was monitored 3-4 days per week and plotted as tumor burden/mouse. B) Animals were injected with D-Luciferin (150 mg/kg) at different time points and imaged using IVIS spectrum. (C) 22 days after Dox withdrawal, tumors were collected, fixed, embedded in paraffin, and 5 µm sections were prepared. Tissue sections were deparaffinized, rehydrated, and stained with H&E.

4.3.2 Constitutively active IKKβ enhances metastasis of estrogen receptor positive tumors

Our in vitro results suggest that E2 and CA-IKKβ work together to induce a highly invasive phenotype. In vivo data suggest that this translates, potentially, to a metastatic phenotype. We investigated the effect of CA-IKKβ on ER+ tumor metastasis more specifically using both spontaneous and experimental models of metastasis. To investigate spontaneous metastasis, tumor cells are implanted orthotopically, a primary tumor is formed and allowed to grow, and tumor spread in the host is assessed. Spontaneous metastasis, thus, involves all the steps of the metastatic cascade including: the escape of cancer cells from primary tumor, invasion of the surrounding stromal tissue, intravasation into blood vessels, cell survival in the blood stream, extravasation from blood vessels, and colonization in distant organs. Thus, spontaneous metastasis closely resembles clinical disease, because metastatic spread follows natural routes and mechanisms. Experimental metastasis, however, investigates only a part of the metastatic cascade, which is survival of disseminated cells in the circulation, extravasation, and colonization at distant organs. In this approach, cells are directly injected into the circulation of the animals, and thus, they circumvent the initial tumor growth and early stages of the metastatic cascade (170,171).

4.3.2.1 Spontaneous metastasis with in vivo treatment

Spontaneous metastasis of xenograft tumor cells to soft organs was examined in the animals of the tumor growth study, described in Figures 22 and 24. Upon animal sacrifice, lungs, liver, and brain were removed, rinsed, and soaked in D-Luciferin (0.3 mg/mL). Ex vivo bioluminescence imaging was performed using IVIS spectrum. We could not observe a difference in the incidence of metastasis between the three groups: E2, E2+12d Dox, and

E2+Dox (Figure 25A). Bioluminescence could be observed in the lungs of E2 and E2+Dox animals (Figures 25A and 25B). However, we observed bioluminescence in the brains of Dox treated animals only (Figures 25A and 25C), suggesting that CA-IKKβ may enhance metastasis of ER+ cells to the brain. It should be noted that bone metastasis was not investigated in the initial 30 day experiment and that the number of animals was powered for tumor growth. Thus, these results are considered preliminary.

Interestingly, animals receiving Dox for 60 days followed by 22 days of Dox withdrawal exhibited spontaneous metastasis, as well. In vivo imaging revealed metastasis in one animal after 6 weeks of Dox treatment (Figure 24B). Upon animal sacrifice ex vivo imagining revealed incidence of metastases to the lungs and spine in 3 out of 4 animals, and to the brain, liver, adrenals, spleen, ovaries, uterus, and leg bones in 1 out of 4 animals (Figure 25A). Interestingly the bioluminescent ovary was strikingly enlarged, and H&E staining revealed the presence of tumor mass (Figures 25D and 25E). Thus, although the tumors were not palpable for more than 60 days, spontaneous metastasis occurred and the cells survived at the site of metastasis; this suggests a role of IKKβ in metastasis of ER+ breast cancer cells to multiple organs.

4.3.2.1 Spontaneous metastasis of in vitro treated cells

In addition to the above study, we also investigated whether E2+Dox pretreated cells could maintain the invasive phenotype in vivo. To test this, MCF-7-A3-LUC cells were treated with E2 or E2+Dox for 72 hrs (corresponding to the in vitro phenotypic observation of enhanced invasion). Cells were then injected orthotopically into the thoracic mammary fat pad of athymic nude mice. At the same time, slow release silastic E2 pellets were implanted subcutaneously. The study did not involve in vivo administration of Dox to allow for E2-induced tumor growth.

Mice were monitored for tumor development and growth, and no significant difference was observed between the sizes of the tumors by the end of the study (Figure 26A).

Whole animal bioluminescence imaging showed no signs of overt metastasis. Upon animal sacrifice, soft organs including: brain, liver, and lung, were extracted and soaked in D-Luciferin. Ex vivo bioluminescence imaging revealed micrometastasis, with an incidence of 100% in E2+Dox pretreated cells compared to 50% in E2 pretreated cells (Figure 26B). Lung metastasis was observed in both groups although at a higher incidence in E2+Dox pretreated cells (Figures 26B and 26C). Metastasis to liver and brain was observed only in animals with E2+Dox pretreated cells (Figures 26B and 26D). Taken together, our results suggest that IKKβ activation, either continuously in vivo or transiently in vitro, enhances spontaneous metastasis of ER+ tumors to multiple organs.

4.3.2.1 Experimental metastasis of in vitro treated cells

A limiting step in the process of metastasis is for a cell disseminated from the primary tumor to survive in the circulation, extravasate from blood vessels, and settle and colonize at a distant organ. Extravasated tumor cells will face one of the three following fates: 1) cell death, 2) dormancy, which is survival without an increase in cell number, or 3) colony formation, which is the proliferation and growth into macroscopic tumors. The determinants of these alternative fates involve the interactions of cancer cells with their microenvironment, vascularization, and immune surveillance (172). To investigate the effect of CA-IKKβ on survival in the circulation and settlement of cancer cells in different organs, we performed an experimental metastasis study. MCF-7-A3-LUC cells were pretreated with E2 or E2+Dox in culture for 72 hrs (which corresponds to the time point the migratory/invasive phenotype is observed in vitro). Cells were then injected intravenously into the lateral tail vein of animals bearing subcutaneously implanted

silastic E2 pellets. Dox was not administered in the drinking water in order to allow for the proliferation and colonization of cells at the sites, where they extravasate. Lungs are the first vascular bed for the injected cells through the lateral tail vein. Using IVIS spectrum, bioluminescence could be detected in the lungs within 2 hrs of injection, confirming successful tail vein injection. Representative animals are shown in Figure 27A.

Animals were monitored by IVIS spectrum every 1-2 weeks. Whole animal imaging revealed metastasis in 3 out of 8 animals injected with E2+Dox pretreated cells, as opposed to to 1 out of 6 animals injected with E2 pretreated cells. Notably, signals from the legs and spine but not from the lungs were observed (Figure 27B). After 6-7 weeks animals were sacrificed. Upon necroscopy, red nodules/patches could be observed on the surface of the lungs in 5 out 7 animals injected with E2+Dox pretreated cells, but not on the lungs of animals injected with E2 pretreated cells (Fig 28B). Ex vivo imaging was performed and bioluminescent signals were detected from lungs with red nodules but not from clear lungs (Figure 28A). Lungs were then inflated and fixed with 10% formalin. Examination of the fixed lungs under the dissecting microscope confirmed the presence of scattered red nodules/patches in the lungs of ~70% of animals with E2+Dox pretreated cells, but not in the lungs of animals with E2 pretreated cells (Figure 28B). Hematoxylin and eosin staining revealed micrometastases in the lungs with red nodules, which was confirmed by GFP IHC (Figure 28C). Interestingly, H&E staining showed that the red nodules observed are hemorrhagic foci (Figure 28D), suggesting an inflammatory response in lungs harboring metastases from E2+Dox pretreated cells.

In order to detect cancer cell colonization in other organs, bones (including spine, pelvis, femur and tibia) and soft organs (liver, spleen, kidneys, adrenals, ovaries, uterus and brain) were excised during animal necroscopy. Organs were soaked in D-Luciferin and imaged ex vivo. One hundred percent of animals injected with E2+Dox pretreated cells showed

bioluminescence in at least one organ examined. However, only 40% of animals injected with E2 pretreated cells showed bioluminescence, and this was confined to the spine and femur (Figure 29). This suggests that E2+Dox in vitro pretreatment induces a highly invasive cellular phenotype, which can settle and colonize to different organs compared to the cellular phenotype induced by pretreatment of E2 only.

Taken together, our results from both spontaneous and experimental models indicate that activation of IKKβ and treatment with E2 enhance metastasis of ER+ breast cancer to multiple sites. In fact, the enhanced spontaneous and experimental metastasis of E2+Dox pretreated cells, compared to E2 only pretreated cells, suggest that IKKβ activation and treatment with E2 induce a permanent or semi-permanent change in the cells, that lasts long enough to induce a difference in metastatic potential.

A	E2	E2+Dox (12d)	E2+Dox (29d)	E2+Dox (60d)
Incidence of metastasis	2/4	2/4	2/4	3/4
Lung	2/4	0	2/4	3/4
Brain	0	2/4	1/4	1/4
Liver	0	0	0	1/4
Adrenals	nd	nd	nd	1/4
Spleen	nd	nd	nd	1/4
Ovaries	nd	nd	nd	1/4
Uterus	nd	nd	nd	1/4
Bones	nd	nd	nd	2/4
Spine	nd	nd	nd	3/4

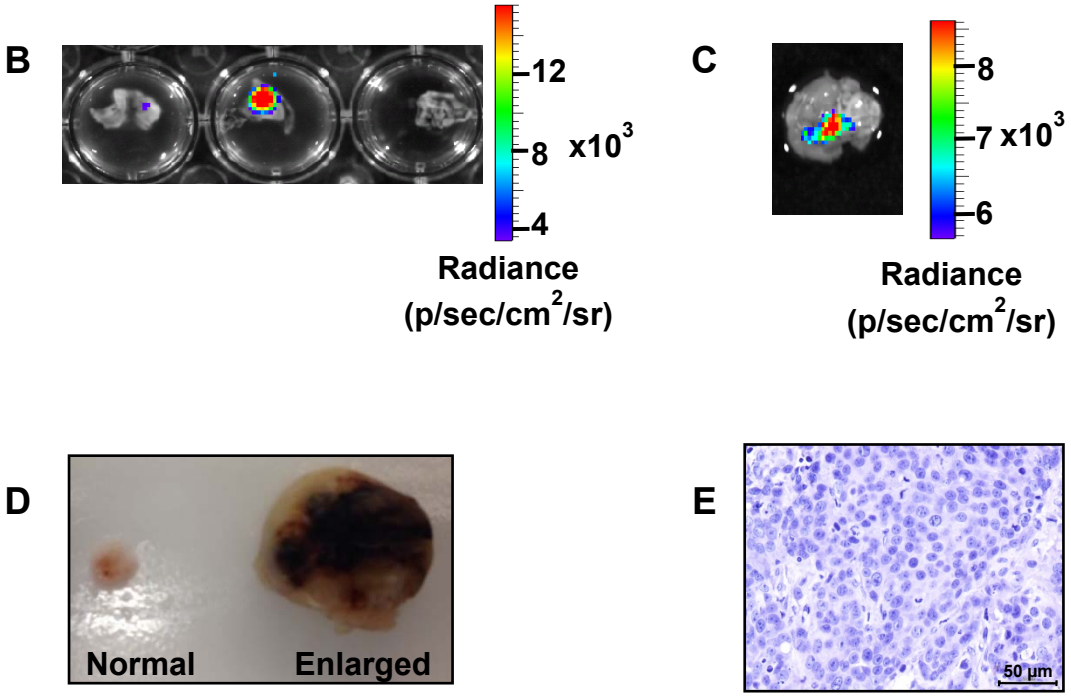

Figure 25: CA-IKKβ enhances spontaneous metastasis of ER+ xenografts. A-C) Ex vivo imaging of tissues from animals described in Figures 22 and 24 using IVIS spectrum. A) Incidence of metastases was recorded (nd=organ not detected by ex vivo). B) Example of the bioluminescence signals obtained from lungs. C) Example of bioluminescence signals obtained from the brain. D) Image of enlarged ovary compared to normal ovary. E) Ovary was fixed, embedded in paraffin and 5 µm sections were prepared. Tissue sections were deparaffinized, rehydrated, and stained with H&E.

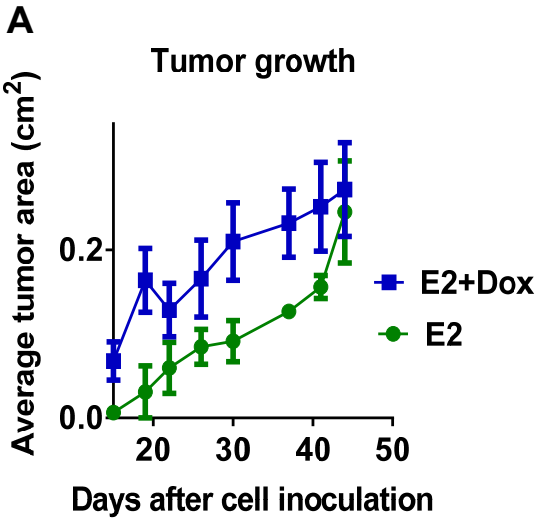

B

	E2 pretreated	E2+Dox pretreated
Incidence of metastasis	2/4	4/4
Lung	2/4	3/4
Brain	0	2/4
Liver	0	2/4

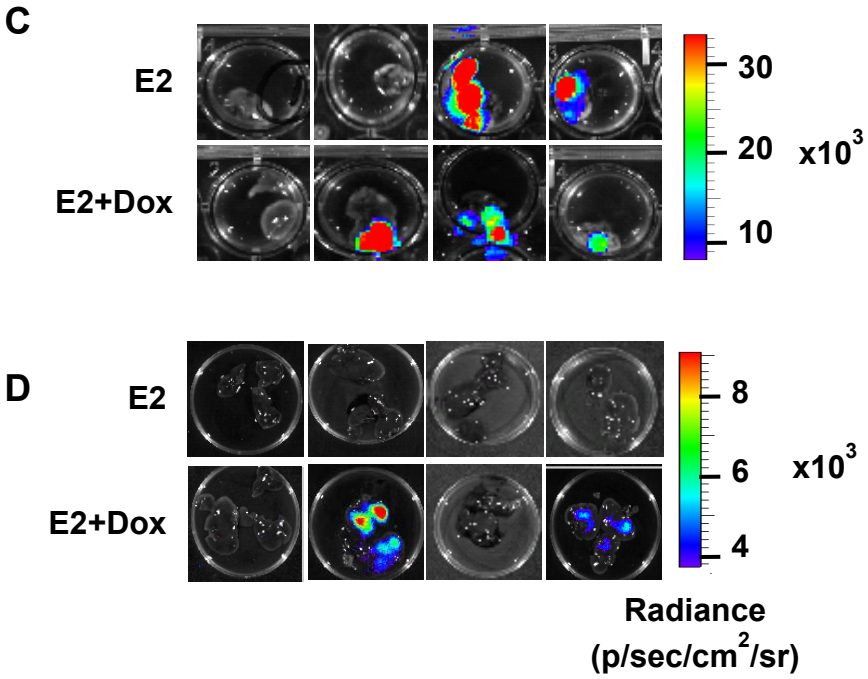

Figure 26: In vitro activation of IKKβ enhances spontaneous metastasis of ER+ xenografts. MCF-7-A3-LUC cells were in vitro treated with E2 or E2+Dox for 72 hrs. Cells were washed with PBS, counted and injected into the mammary fat pad of female athymic nude mice, in which E2 pellets were subcutaneously implanted. A) Tumor area was recorded. B-D) Upon animal sacrifice, lungs, brain, and liver were rinsed with DPBS, soaked in D-Luciferin (300 µg/mL), and ex vivo imaged using IVIS spectrum. A) Metastatic incidence was recorded. C) Bioluminescence from the lungs. D) Bioluminescence from the livers.

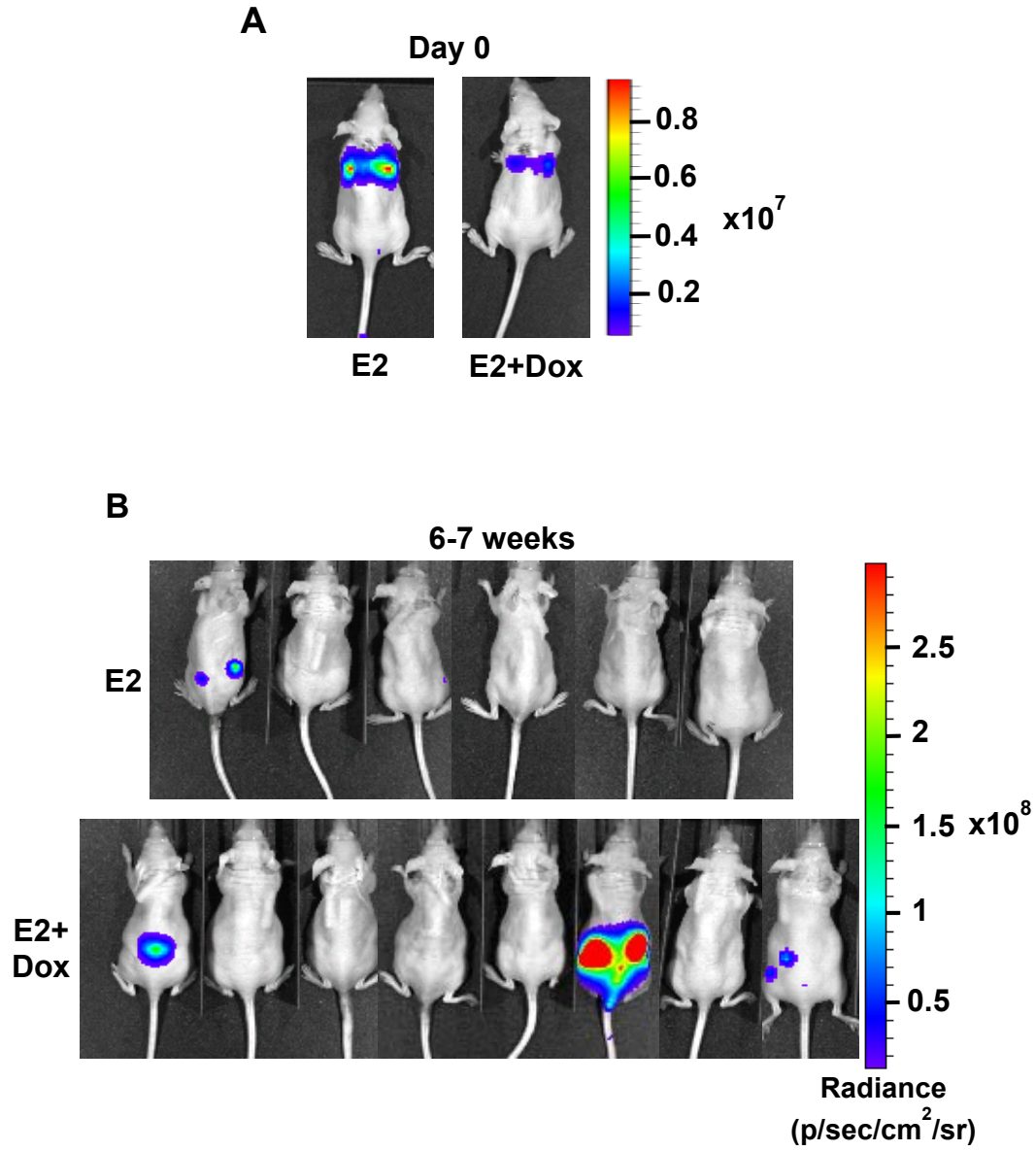

Figure 27: CA-IKKβ enhances experimental metastasis of ER+ cells. MCF-7-A3-LUC cells were treated with E2 or E2+Dox in culture for 72 hrs. Cells were washed with PBS and counted. One million cells were injected intravenously into the lateral tail vein of female athymic nude mice in which silastic E2 pellets were subcutaneously implanted. A) Animals were injected with D-Luciferin and imaged using IVIS spectrum within 2 hrs of intravenous cell injection. B) Animals were injected with D-Luciferin and imaged using IVIS after 6-7 weeks.

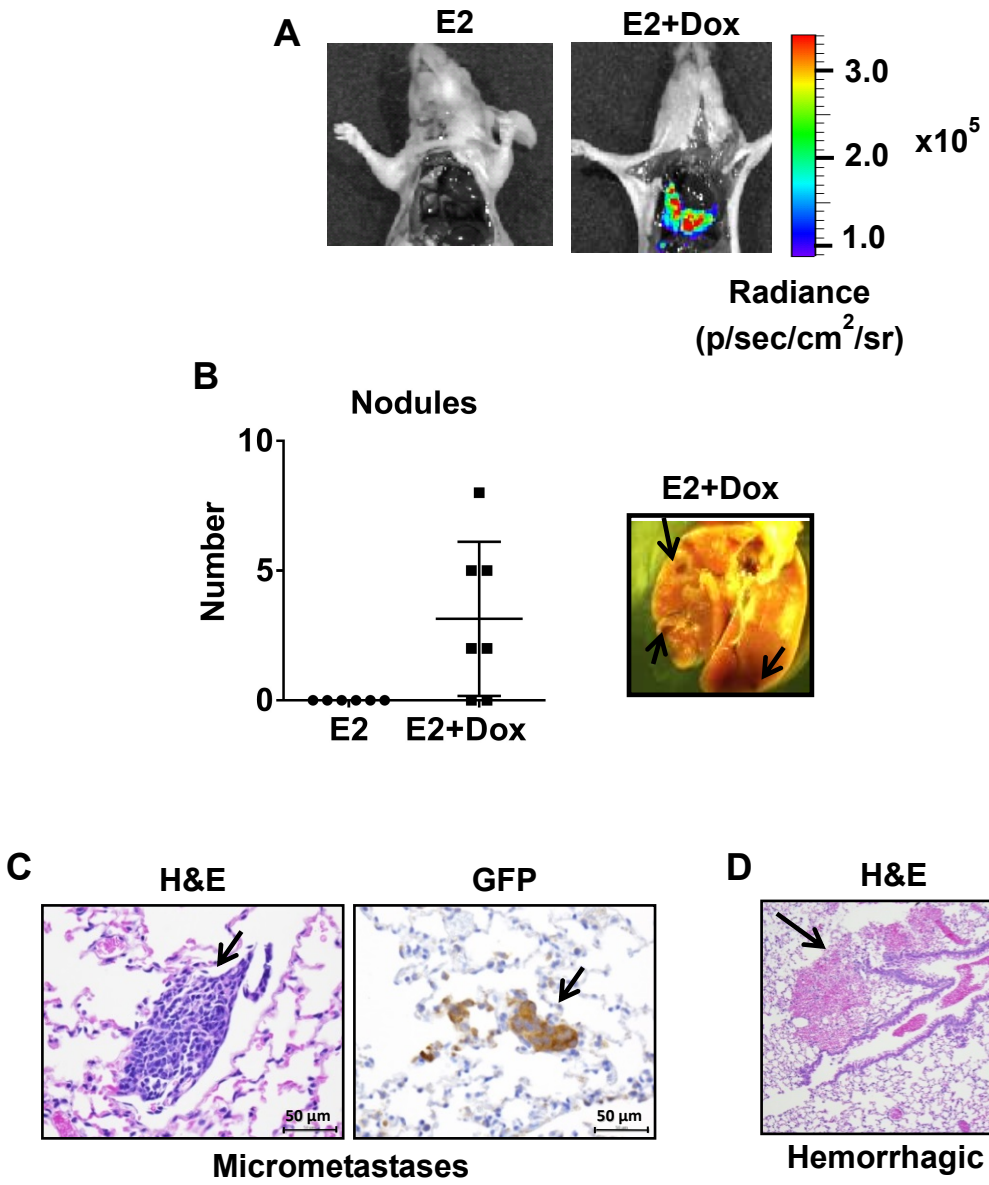

Figure 28: CA-IKKβ pretreated cells metastasize to the lungs. A) Ex-vivo imaging of the lungs of animals upon necroscopy. B) Lungs were inflated with 10% formalin in PBS; red nodules were counted, and imaged using the dissecting microscope. Representative image of red nodules observed in the lungs of animals injected with E2+Dox pretreated cells. Arrows pointing to the nodules. C, D) Fixed lungs were embedded in paraffin blocks and sectioned. C) H&E staining and GFP IHC were performed. Representative images of lungs of animal injected with E2+Dox pretreated cells. Arrow indicates micrometastases. D) Representative images from lungs of animal injected with E2+Dox pretreated cells. Arrow indicates hemorrhagic foci.

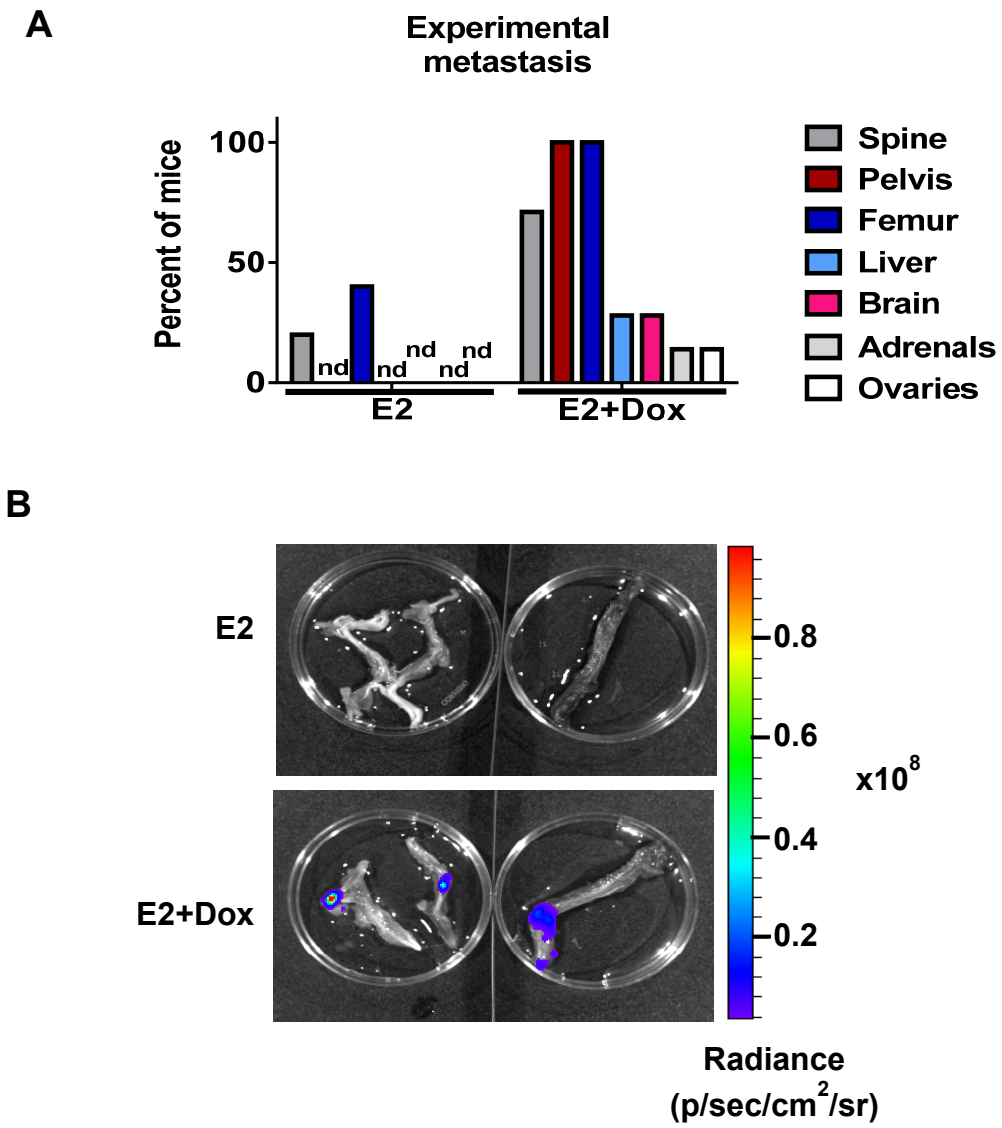

Figure 29: CA-IKKβ enhances experimental metastasis to different organs. A, B) Upon animal sacrifice, bones and soft organs were dissected, rinsed with DPBS, soaked in D-Luciferin, and then ex vivo imaged using IVIS spectrum. A) Percentage of mice with metastasis in each organ was calculated (nd=no signal detected in the organ). B) Bioluminescence observed in the pelvis, femur and spine of representative animals.

4.4 Effect of constitutively active IKKβ on the cellular phenotype of estrogen receptor positive breast cancer cells

Regulatory gene expression programs of differentiation determine the tumor phenotype and the biological identity of cancer cells. Cancer cells inherit the active regulatory programs from the cell of origin. Yet, additional regulatory programs may be repressed or activated by oncogenic pathways and environmental stimuli. The net result is the evolution of a differentiation state that can control the phenotype and clinical traits of the tumor (173). The mammary gland is composed of an inner luminal layer and basal/myoepithelial outer layer. Mammary stem cells are found within the outer layer and are capable of generating all mammary epithelial lineages (174). Many of the transcriptional programs that control the identity of luminal and basal lineages, as well as, the function of stem and progenitor cells in normal mammary gland are active in breast cancer cells (173). Moreover, the epithelial mesenchymal transition (EMT) differentiation program, in which the cells lose epithelial traits in favor of the mesenchymal ones, has been reported in breast cancer cells (175).

Various differentiation programs are linked to each other: mesenchymal traits are linked to the promotion of basal identity and stem cells, while stemness is linked to basal lineage and mesenchymal differentiation. However stemness, EMT, and basal-lineage identity are not necessarily equivalent and cannot be interchangeably used to characterize the breast cancer state (5,174). Thus, breast tumors can be represented on a linear differentiation axis with one end comprising tumors enriched for cells possessing stem cell-like traits, mesenchymal-like characteristics, and basal lineage identity. The other side of the axis comprises differentiated epithelial cells, possessing the luminal lineage identity (Figure 30A) (173). In order to understand the cellular mechanism underlying the quiescent/invasive phenotype observed with IKKβ activation and E2 treatment, we hypothesized that transcriptional programs affecting the

differentiated/epithelial/luminal nature of ER+ cells may be altered. To test this hypothesis, we examined mRNA and protein expression of important genes along the three differentiation axes.

4.4.1 Constitutively active IKKβ and estrogen do not induce epithelial mesenchymal transition

Epithelial mesenchymal transition is a reversible differentiation program that results in the transition of epithelial cells into mesenchymal cells. Cells lose polarity and cell-cell adhesions and these cells undergo cytoskeleton remodeling, which enables the separation of individual cells from the primary tumor mass. The molecular basis of this program is: the direct repression of epithelial genes encoding components of the cell-cell junctions and cell-matrix adhesion (e.g. E-cadherin), reorganization of the cytoskeleton, and the upregulation of mesenchymal markers (e.g. vimentin and fibronectin). Epithelial mesenchymal transition is controlled by a group of transcriptional repressors, such as Zeb1, Zeb2, Twist1, SNAI1, and SNAI2. They induce transcriptional silencing of E-cadherin by recruiting histone deacetylases to the E-cadherin promoter. Consequently, cells become motile and invasive and disseminate as single cells (175,176).

Because a change in the phenotype of cells treated with Dox was observed (Figure 16), we hypothesized that E2+Dox might induce EMT as a cellular mechanism, underlying the highly invasive phenotype observed. Examining the expression of EMT markers revealed that activation of IKKβ and treatment with E2 did not upregulate the expression of the EMT hallmark, vimentin, which is an intermediate filament specific for the mesenchymal cells. However, enhanced expression of other EMT markers, such as the transcription factors SNAI1 and FoxC2 in MCF-7-A3 cells, and SNAI1, SNAI2, FoxC1 and Zeb1 in T47D-C7 cells could be observed. Twist 1 was downregulated in both cell lines (Figures 30B and 30C).

Using Western Blotting and immunofluorescence, no change in the expression of the epithelial hallmark, E-cadherin, was determined (Figures 31A, 31B, 32A and 32B). Neither vimentin nor fibronectin expression was observed in CA-IKKβ-MCF-7 cells treated with E2+Dox, as determined by Western Blotting and immuno-fluorescence (Figures 31A and 31C). Similarly, vimentin was not expressed in CA-IKKβ-T47D cells (Figure 32A and 32C). However, in these cells fibronectin expression was decreased with E2, but not affected by CA-IKKβ with or without E2 (Figure 32A). Results of the mesenchymal MDA-MB-231 cells are shown as a positive control for mesenchymal markers (Figures 31A, 31C, 31D, 32A and 32C).

A change in key hallmarks of EMT was not observed, and therefore, we hypothesized that the cells may be in an early stage of transition and prolonged treatment with E2+Dox may result in complete EMT. Treating the cells with E2+Dox for up to 14 days did not decrease E-cadherin expression nor induce vimentin expression (Figure 31D). Our results suggest that CA-IKKβ and E2 do not induce EMT in ER+ breast cancer cells and that EMT does not underlie the invasive phenotype.

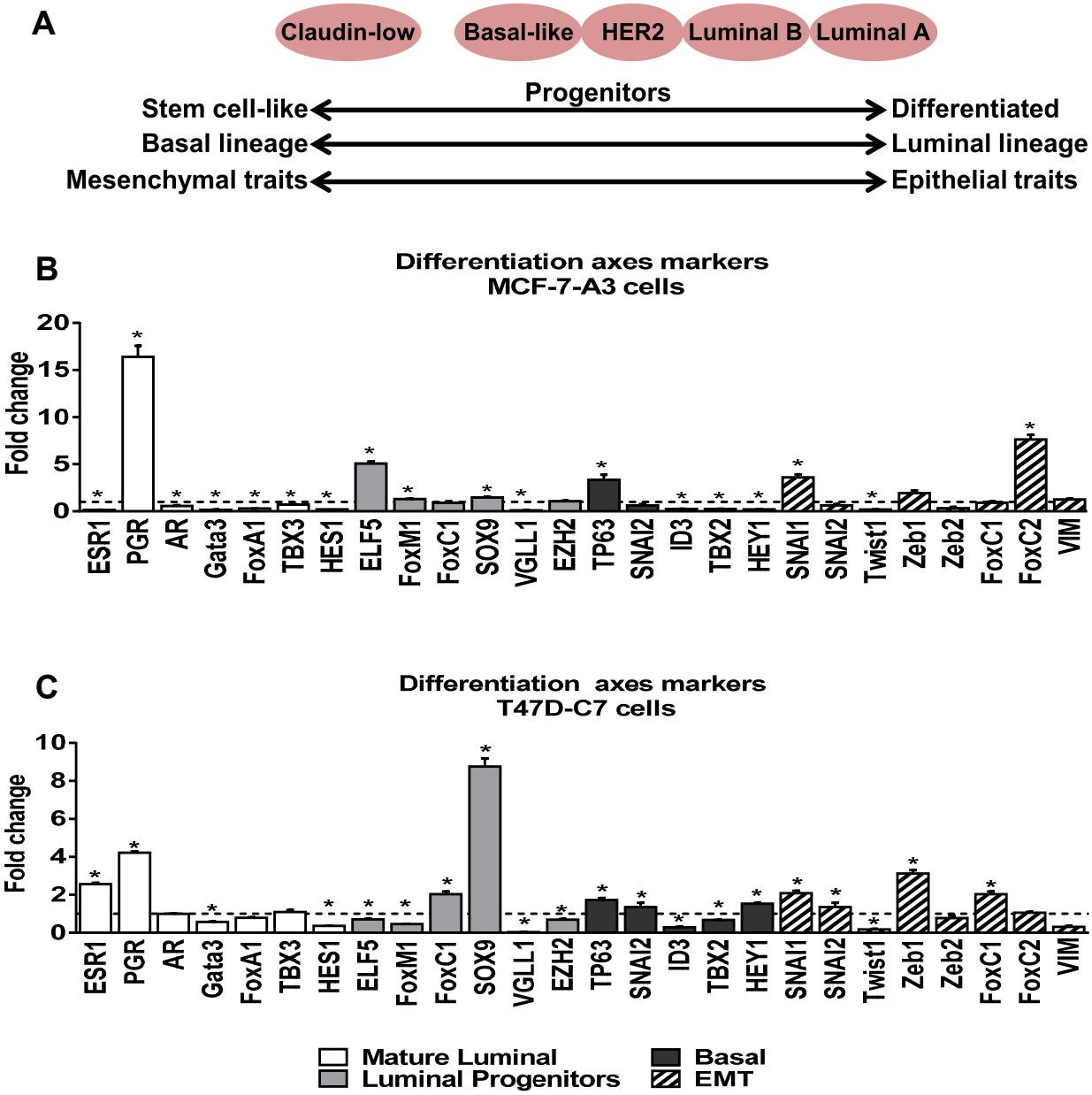

Figure 30: CA-IKKβ induces lineage plasticity in ER+ breast cancer cells. A) Breast cancer subtypes aligned on linear axes representing differentiation states. Adapted and modified from Granit et al., 2014 (173). MCF-7-A3 (B) and T47D-C7 (C) cells were treated with E2+Dox for 72 hrs. mRNA expression of key genes in the differentiation axes was assessed by QPCR. Fold changes were determined using the ΔΔCt method with GAPDH as an internal control (*p<0.05 for E2+Dox compared to vehicle control).

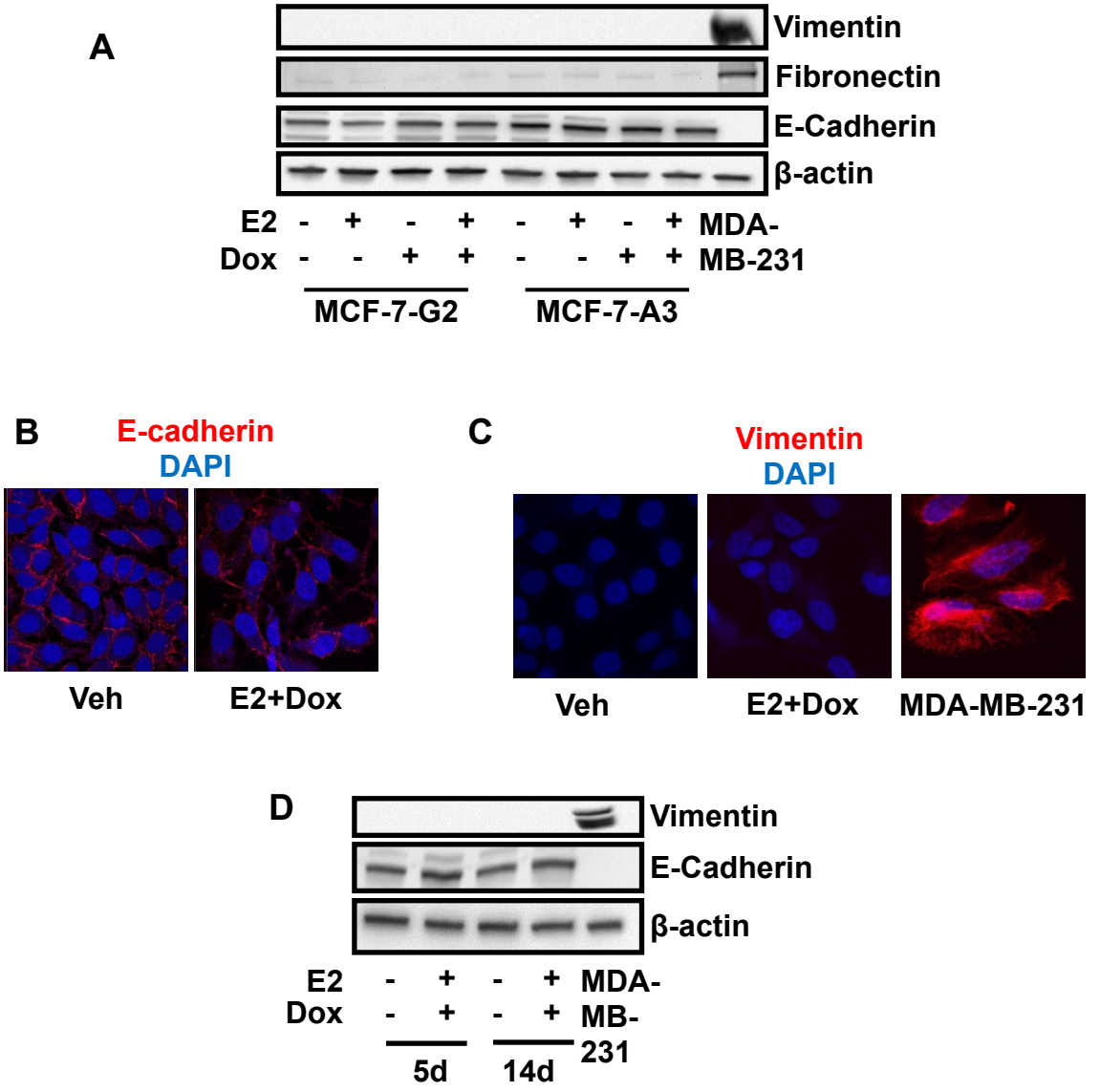

Figure 31: CA-IKKβ does not induce the expression of EMT hallmarks in CA-IKKβ-MCF-7 cells. MCF-7-G2 and MCF-7-A3 cells were treated with E2, Dox, or E2+Dox for 96 hrs. A) Whole cell extract was prepared. Vimentin, fibronectin, E-cadherin, and β-actin expression was detected by Western Blotting. B) Immunofluorescence staining of E-cadherin expression (red) in treated MCF-7-G2 cells was conducted. C) Immunofluorescence staining of vimentin expression (red) in treated MCF-7-G2 cells and control MDA-MB-231 cells was conducted. B, C) Nuclei were visualized with DAPI (blue). Images were captured by x63 objective using confocal microscopy. D) MCF-7-G2 cells were treated with E2+Dox for 5 or 14 days. Whole cell extract was prepared, and vimentin, E-cadherin and β-actin expression was detected by Western Blotting.

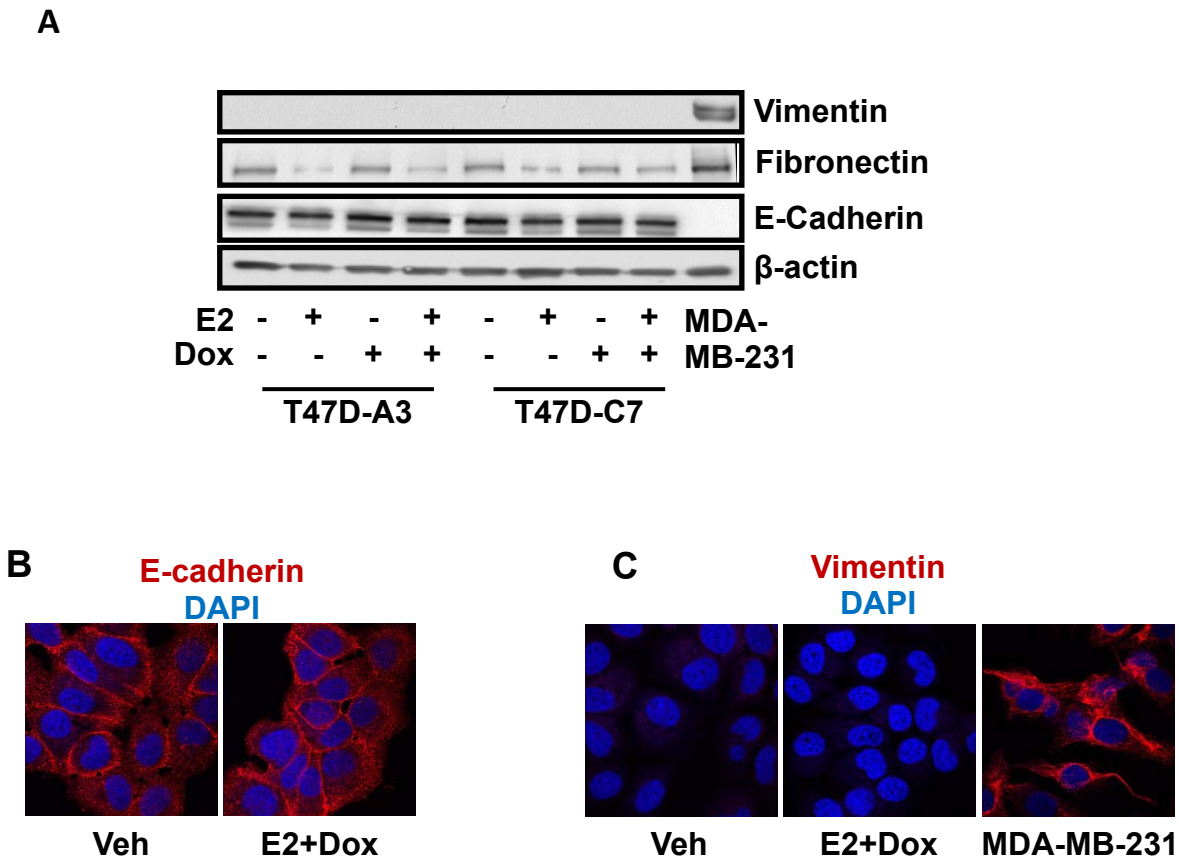

Figure 32: CA-IKKβ does not induce the expression of EMT hallmarks in CA-IKKβ-T47D cells. T47D-A3 and T47D-C7 cells were treated with E2, Dox, or E2+Dox for 96 hrs. A) Whole cell extract was prepared. Vimentin, fibronectin, E-cadherin, and β-actin expression was detected by Western Blotting. B) Immunofluorescence staining of E-cadherin expression (red) in treated T47D-C7 cells was conducted. C) Immunofluorescence staining of vimentin expression (red) in treated T47D-C7 cells and control MDA-MB-231 cells was conducted. B, C) Nuclei were visualized with DAPI (blue). Images were captured by x63 objective using confocal microscopy.

4.4.2 Constitutively active IKKβ and estrogen decrease luminal markers and increase progenitor markers

Luminal cells express hormonal receptors ER, PR, and androgen receptor (AR). They also express regulators of luminal maturation and function such as Gata3, FoxA1 and TBX3 (173). Examining the expression of markers of the luminal lineage, we found that activation of IKKβ and treatment with E2 downregulates ER in MCF-7-A3 cells, but not in T47D-C7 cells (Figures 30B and 30C). This is in agreement with previous studies reporting the same difference in ER regulation between the MCF-7 and T47D cell lines (177), and that E2 drives both transcriptional activation and proteolysis of ER in MCF-7 cells (178). The expression of the E2 target gene PR is upregulated in both cell lines; yet, the expression of all other luminal markers is inhibited in MCF-7-A3 cells, while Gata3 and HES1 are downregulated in T47D-C7 cells (Figures 30B and 30C). Both Gata3 and FoxA1 are reported as important differentiation regulators in ER+ breast cancer. Gata3 is a key lineage regulator required for the differentiation and commitment of luminal epithelial cells in the mammary gland (179). Silencing of FoxA1 represses the expression of luminal markers and induces the expression of basal markers in breast cancer cells (180). HES1 is one of the components of the Notch pathway that has been reported to enhance luminal differentiation (181). This suggests that IKKβ activation and treatment with E2 results in loss of some of the luminal identity of the cells.

Immunofluorescence staining was used to investigate the expression of Gata3 and FoxA1 at the protein level. Results revealed that both Gata3 and FoxA1 are highly expressed in the nuclei of untreated cells, consistent with the luminal nature of the cells. While treatment with E2 or Dox individually downregulated both factors, the combination of E2+Dox further abolished the expression of both. The effect was similar in both MCF-7-A3 and T47D-C7 cells, suggesting

that E2 and CA-IKKβ may alter the luminal nature of ER+ breast cancer cells (Figures 33A and 34).

Interestingly, expression of some luminal progenitor markers is upregulated by E2 and Dox treatment: ELF5, FoxM1 and SOX9 in MCF-7-A3 cells, and FoxC1 and SOX9 in T47D-C7 cells. Yet, a decrease in the expression of other markers, such as VGLL1, could be observed in both cells lines (Figure 30B and 30C). Studies have reported that ELF5, FoxM1 and SOX9 regulate the progenitor state in the mammary gland (182-184). Luminal progenitor cells are capable of giving rise to luminal cells (173). However, growing evidence suggests that cells of the basal cell lineage can also arise from luminal progenitor cells (185). Our results suggest that IKKβ activation and treatment with E2 may endow the cells with some progenitor properties while suppressing others.

Because we do not have hallmark EMT markers, we hypothesized that we have collective motility where the cells migrate/invade as cohesive multicellular strands or networks (186). Studies reported that loss of luminal cytokeratins 8/18 (CK8/18) induces collective invasion in epithelial cells without observed EMT (187). Western blotting and immunofluorescence staining revealed the expression of CK8/18 in MCF-7-A3 and T47D-C7 cells, which is consistent with their luminal identity. In MCF-7-A3 cells, combined treatment with E2 and Dox downregulates CK8/18 to a greater extent than individual treatment with E2 or Dox alone (Figure 33A and 33B). In T47D-C7 cells, treatment with E2 enhances the expression of CK8/18 in the cells, which is inhibited upon treatment with Dox (Figure 34).

Taken together our results demonstrate that activation of IKKβ and treatment with E2 result in a global downregulation of biomarkers of the luminal lineage suggesting that the cells are dedifferentiating away from the luminal phenotype. The repression of luminal CK8/18

expression further suggests that collective invasion rather than EMT may underlie the E2 and CA-IKKβ induced invasive phenotype.

4.4.3 Constitutively active IKKβ and estrogen increase basal markers

This far, our results suggest that the activation of IKKβ and treatment with E2 induce lineage plasticity and shift the cells from the luminal, differentiated, epithelial state without full differentiation to a mesenchymal state. Therefore, we next examined markers of basal lineage. Importantly, studies have reported that the basal markers p63, cytokeratin 14 (CK14), and cytokeratin 5 (CK5) are expressed at the leading edge of the collectively invading breast cancer cells and tumors. And that knockdown of p63 and CK14 inhibits invasion of ER+ breast cancer cells (188). As was the case with luminal markers and luminal progenitor markers, expression of genes from the basal lineage signature revealed upregulation of the expression of some markers, as well as the downregulation of others. The expression of p63 was upregulated, while the expression of ID3 and TBX2 were downregulated in both MCF-7-A3 and T47D-C7 cells (Figures 30B and 30C).

Using both immunofluorescence and Western Blotting, we examined the regulation of p63, CK5, and CK14 by E2 and CA-IKKβ in CA-IKKβ cell lines. For p63, expression was mainly observed in the nuclei of a few E2+Dox treated cells as demonstrated by immunofluorescence (Figures 35A and 36A). Western blotting revealed higher expression of p63 in the nuclear extract of cells treated with E2+Dox compared to E2 or Dox only (Figures 35B and 36B). Cytokeratin 5 expression was observed in the cytoplasm of some cells, mainly in E2+Dox treated cells as demonstrated by immunofluorescence (Figures 35A and 36A). The expression of CK14, however, was observed in scattered groups of cells in MCF-7-A3 cells only (Figure 35A). Interestingly, unlike luminal markers, where the decrease was global in all treated cells

(Figures 33A and 34), the increase in basal markers could be observed in a small population of cells only (Figures 35A and 36A).

Although only a minority of cells within luminal tumors expresses basal epithelial markers, previous studies have reported that the knockdown of these markers inhibits collective invasion (188). Therefore, we hypothesized that the observed basal cell population may be responsible for E2+Dox induced invasion. To test this hypothesis, we knocked down CK5 and CK14 using siRNA. In both MCF-7-A3 and T47D-C7 cells, knockdown of CK5 inhibited E2+Dox induced invasion (Figures 37A and 37B). Knockdown of CK14, however, inhibited E2+Dox induced invasion only in MCF-7-A3 cells (Figure 37A). Our results suggest that CA-IKKβ induces cellular changes in ER+ luminal cells moving their differentiation state from luminal towards progenitor/basal with the expansion of a basal population of cells responsible for the invasive phenotype observed.

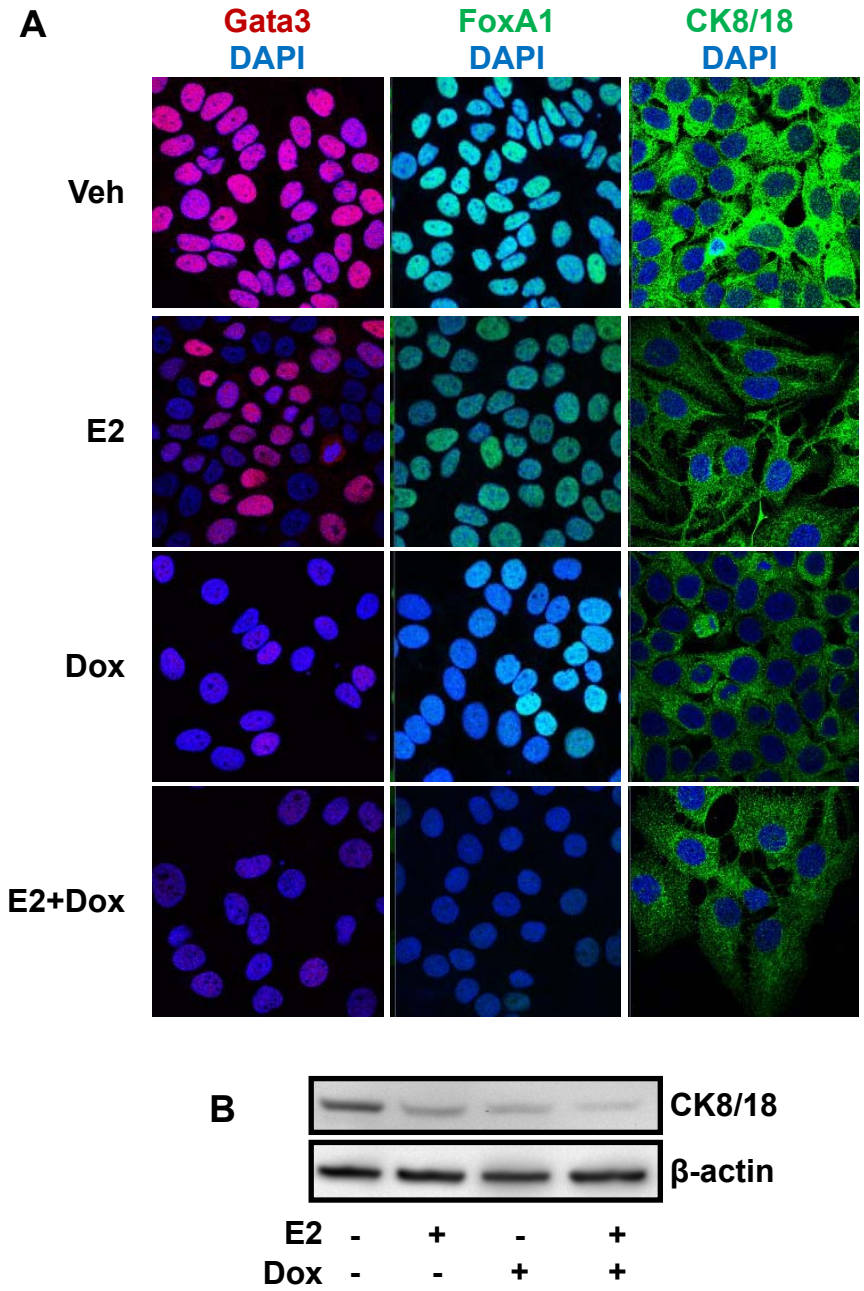

Figure 33: CA-IKKβ+E2 downregulate the expression of luminal markers in CA-IKKβ-MCF-7 cells. MCF-7-A3 cells were treated with E2, Dox, or E2+Dox for 72 hrs. A) Immunofluorescence staining of Gata3 expression (red), FoxA1 expression (green) and CK8/18 expression (green) was conducted. Nuclei were visualized with DAPI (blue). Images were captured by x63 objective using confocal microscopy. B) Whole cell extract was prepared and CK8/18 and β-actin expression was detected by Western Blotting.

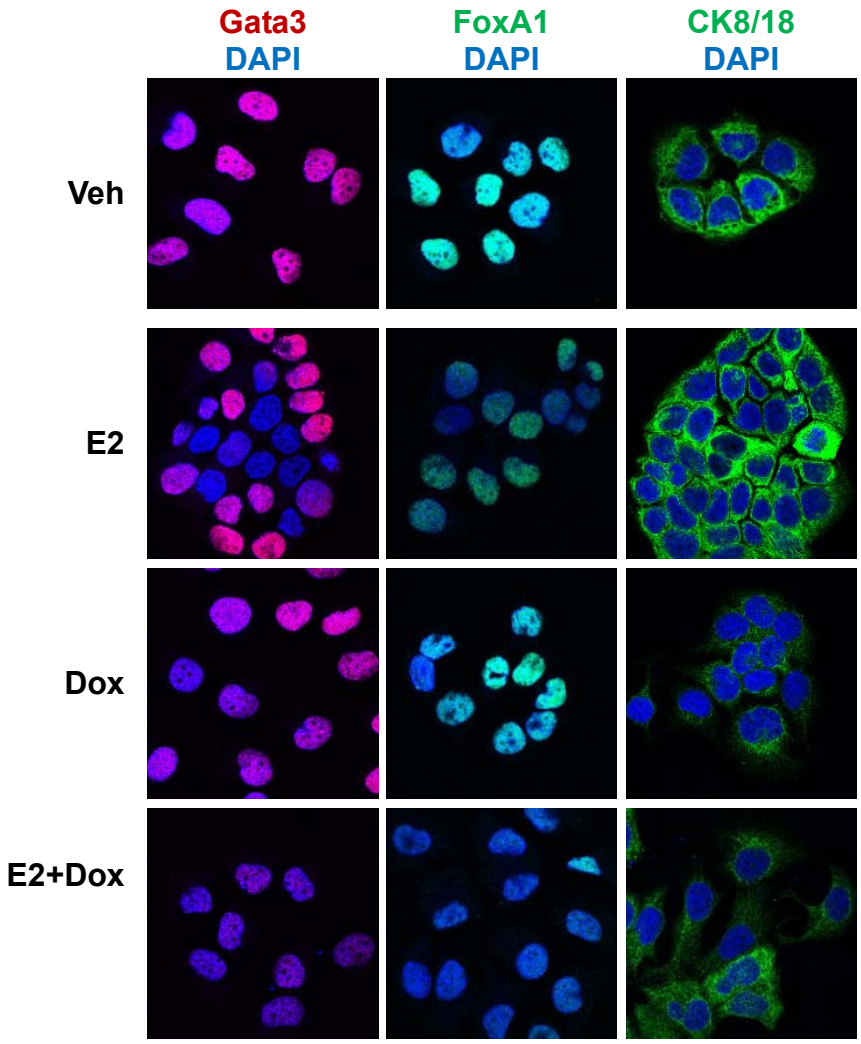

Figure 34: CA-IKKβ+E2 downregulate the expression of luminal markers in CA-IKKβ-T47D cells. T47D-C7 cells were treated with E2, Dox, or E2+Dox for 72 hrs. Immunofluorescence staining of Gata3 expression (red), FoxA1 expression (green) and CK8/18 expression (green) was conducted. Nuclei were visualized with DAPI (blue). Images were captured by x63 objective using confocal microscopy.

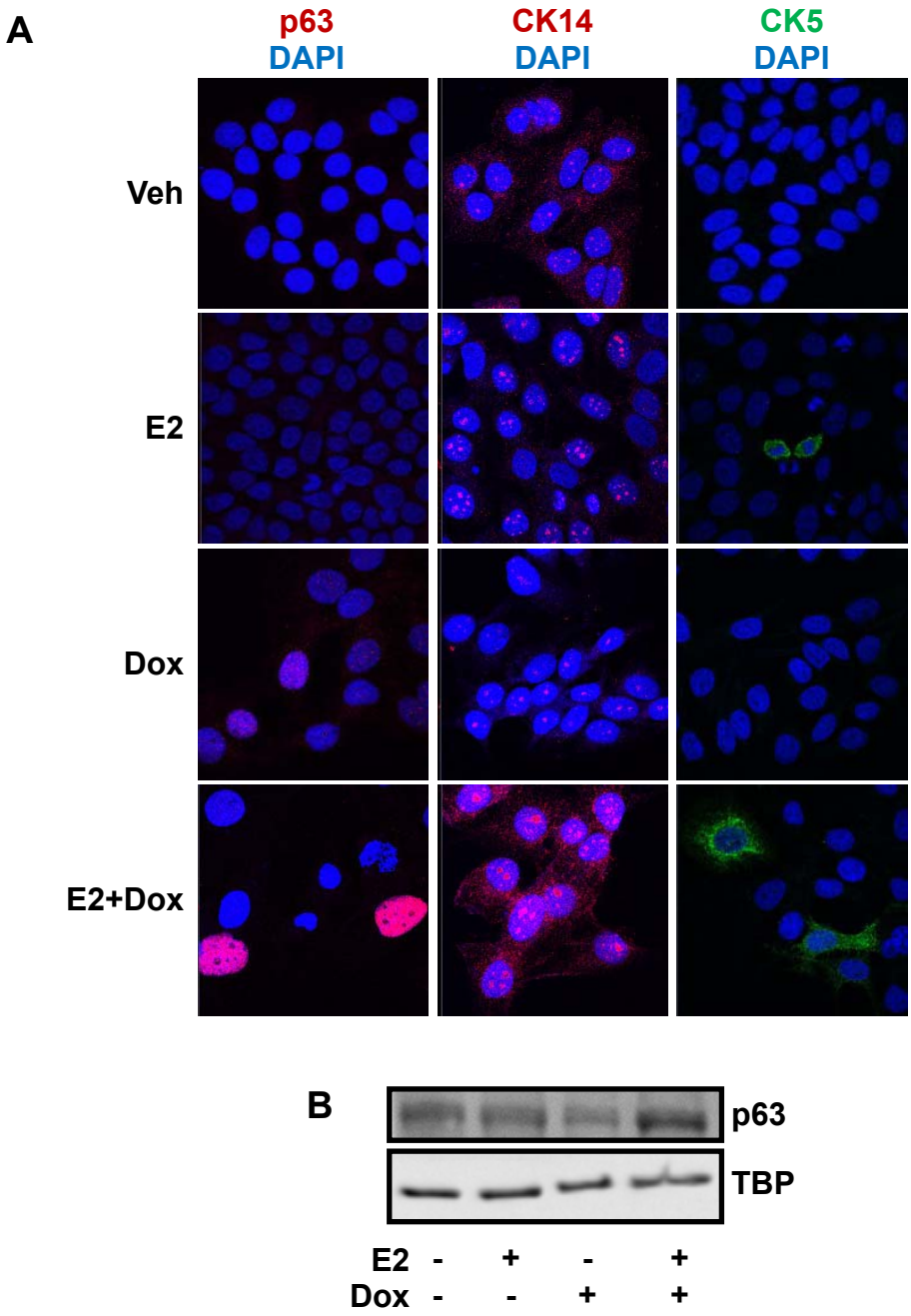

Figure 35: CA-IKKβ+E2 induce the expression of basal markers in CA-IKKβ-MCF-7 cells. MCF-7-A3 cells were treated with E2, Dox, or E2+Dox for 72 hrs. A) Immunofluorescence staining of p63 expression (red), CK14 expression (red) and CK5 expression (green) was conducted. Nuclei were visualized with DAPI (blue). Images were taken by x63 objective using confocal microscopy. B) Nuclear extract was prepared. p63 and TBP expression was detected by Western Blotting.

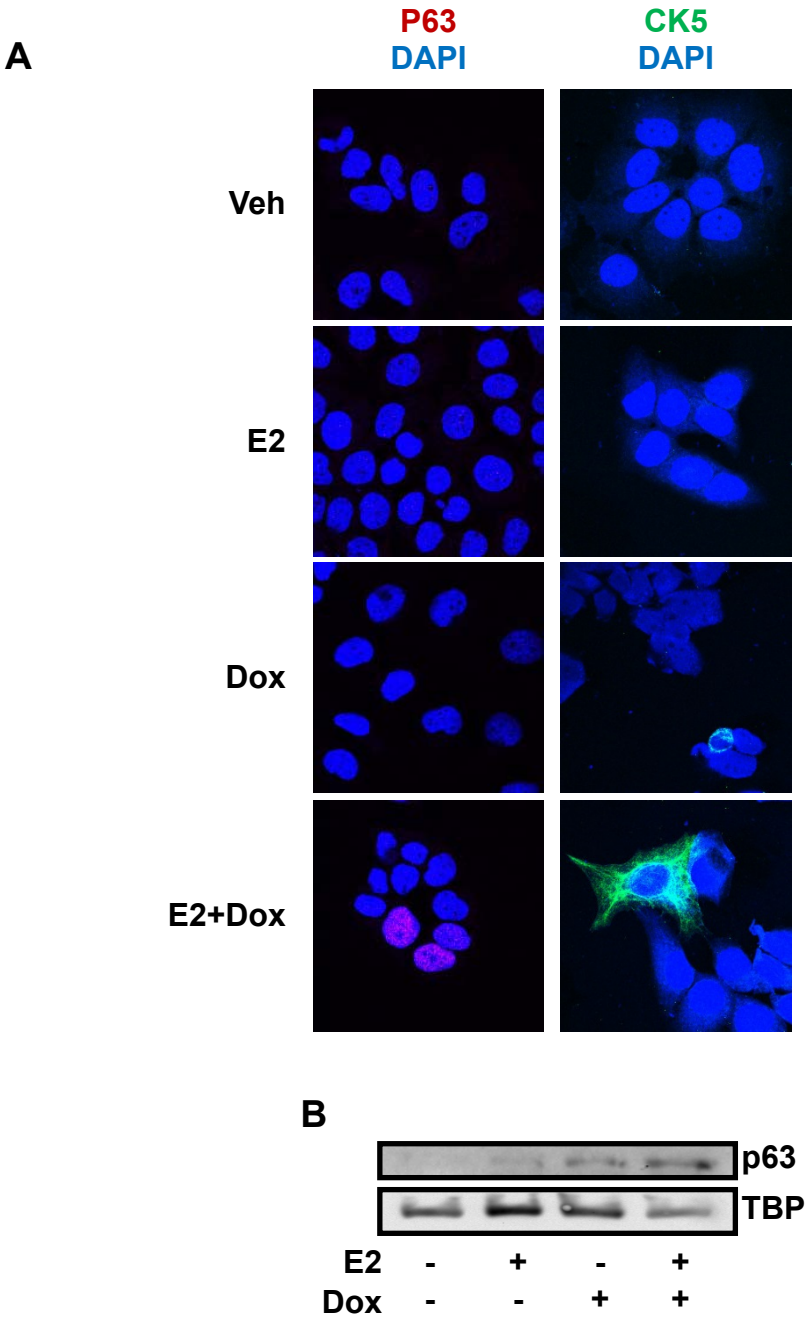

Figure 36: CA-IKKβ+E2 induce the expression of basal markers in CA-IKKβ-T47D cells. T47D-C7 cells were treated with E2, Dox, or E2+Dox for 72 hrs. A) Immunofluorescence staining of p63 expression (red) and CK5 expression (green) was conducted. Nuclei were visualized with DAPI (blue). Images were taken by x63 objective using confocal microscopy. B) Nuclear extract was prepared. p63 and TBP expression was detected by Western Blotting.

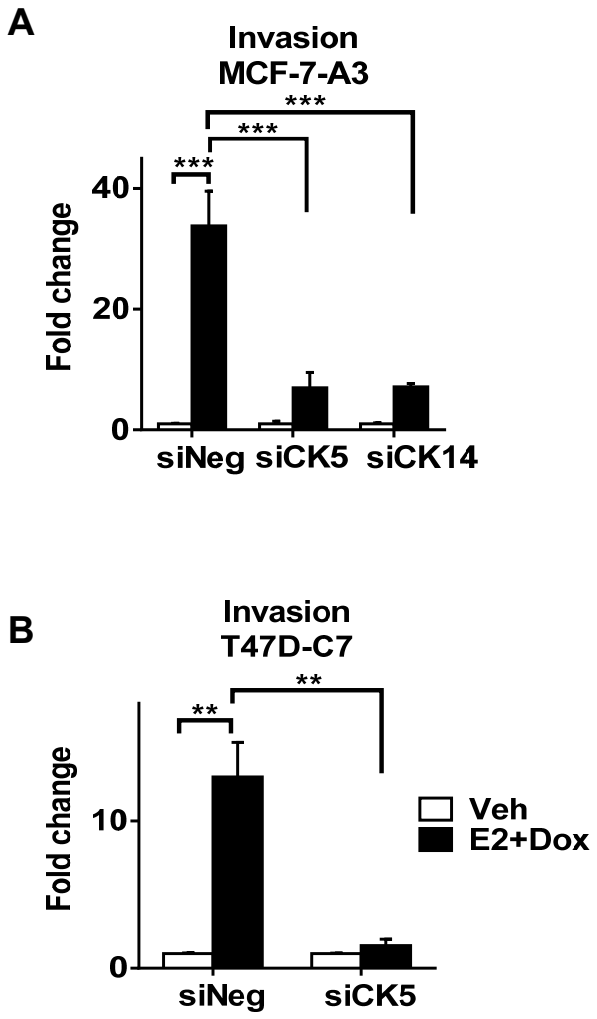

Figure 37: Knockdown of basal markers inhibits CA-IKKβ+E2 induced invasion. A) MCF-7-A3 cells were transfected with a negative control siRNA (siNeg) or siRNA targeting CK5 (siCK5) or CK14 (siCK14). Cells were then treated with E2+Dox for 72 hrs. B) T47D-C7 cells were transfected with siNeg or siCK5 and then treated with E2+Dox for 72 hrs. A, B) After treatment, cells were transferred to invasion inserts in equal densities, allowed to invade for 24 hrs (A) or 16 hrs (B), fixed with 4% p-formaldehyde, and stained with 0.1% crystal violet. Number of invading cells per insert was counted. Fold change in invasion compared to respective vehicle control was calculated (**p<0.01 and ***p<0.001).

4.5 Molecular mechanisms underlying constitutively active IKKβ-induced phenotypes

To this point, all our studies have used E2 treatment and IKKβ activation to determine the effect of CA-IKKβ on the phenotypes of ER+ breast cancer cells. Because E2 and CA-IKKβ oppose each other on proliferation, yet work together to induce a highly invasive/metastatic phenotype, we were interested in finding the role of the downstream mediators, ER and NF-κB transcription factors in these two phenotypes. To do this, two inhibitors were used:

1. ICI 182,780 (ICI), which is a high affinity estrogen receptor antagonist. It is a selective estrogen receptors downregulator (SERD) that induces proteasomal degradation of ER (25).
2. IκBα-DN, which is the dominant-negative phosphorylation mutant of the NF-κB inhibitor IκBα. IκBα-DN cannot be phosphorylated or degraded upon activation of IKKβ so it sequesters NF-κB dimers in the cytoplasm, inhibits their nuclear translocation and subsequent NF-κB target gene expression (150). IκBα-DN acts downstream of CA-IKKβ so it should determine which effects of IKKβ are mediated by NF-κB family members and which are NF-κB-independent.

4.5.1 Inhibition of estrogen-induced proliferation is NF-κB-independent

It is well established that estrogen receptor mediates E2-induced proliferation in ER+ breast cancer cells (189). As expected, ER inhibition by ICI abolished E2-induced proliferation of CA-IKKβ cells (Figure 38). We hypothesized that ER-driven proliferation could be inhibited by CA-IKKβ by downregulating ER. This hypothesis is substantiated by several studies suggesting that activation of NF-κB pathway downregulates ER expression (112,113). We found that CA-IKKβ inhibited ER mRNA and protein expression in CA-IKKβ-MCF-7 cells (Figures 39A, 39C and 39D). Estrogen drives both transcriptional activation and proteolysis of ER in MCF-7 cells

(178), and the observed decrease in ER protein expression levels in E2+Dox is similar to that of E2 alone (Figure 39A). In CA-IKKβ-T47D, CA-IKKβ inhibited E2-induced ER expression in the cells (Figure 39B). However, ER remains transcriptionally active based on the regulation of canonical E2 target genes, such as pS2, and PR (Figure 39E). Thus, although ER is downregulated upon IKKβ activation, this downregulation is not likely to be the mechanism underlying the inhibition of E2-induced proliferation in ER+ breast cancer cells.

To understand the role of NF-κB in the inhibition of E2-induced proliferation by CA-IKKβ, we used IκBα-DN, which does not affect Dox induction of IKKβ expression (Figure 40A). However, it does block Dox-induced NF-κB activation, as indicated by the expression of NF-κB target genes such as RelB (Figure 40B). As expected, activation of IKKβ, upon Dox treatment inhibited E2-induced proliferation. However, IκBα-DN did not restore the proliferative effect of E2 on the cells (Figures 40C and 40D). This suggests that CA-IKKβ inhibits E2-induced proliferation in an NF-κB-independent manner. IKKβ is an active kinase and could phosphorylate targets other than NF-κB and work through them to inhibit the proliferative effect of E2 in the cells.

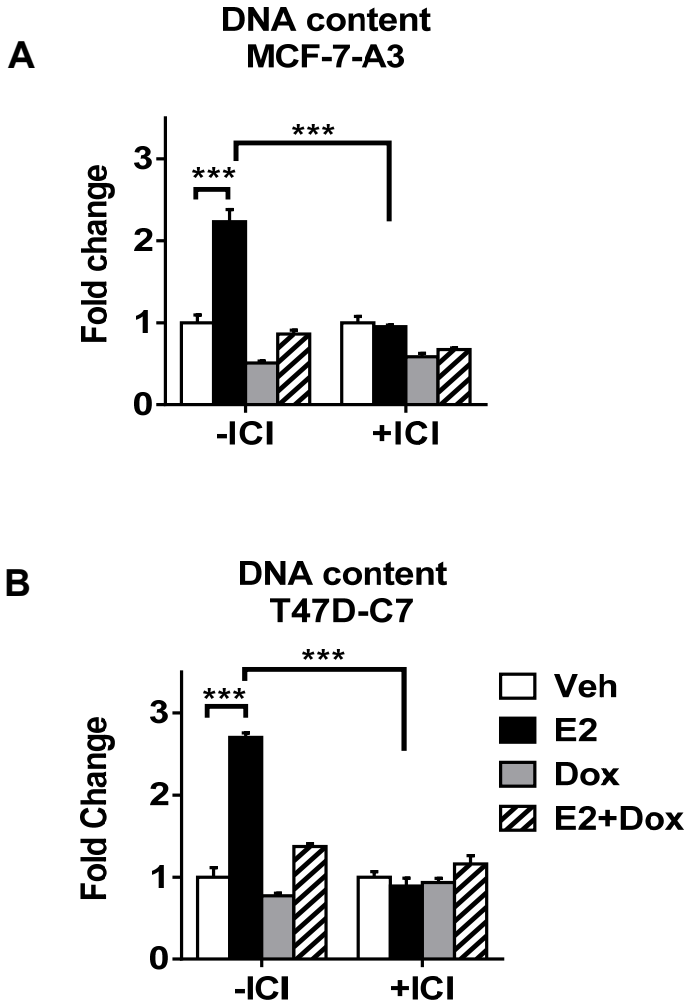

Figure 38: E2-induced proliferation is ER dependent. MCF-7-A3 cells (A) and T47D-C7 cells (B) were treated with E2, Dox, or E2+Dox with or without ICI 182,780 (1uM) for 72 hrs. A, B) Hoechst 33342 nucleic acid stain was added to the cells. The incorporated dye was measured using fluorometry. DNA content was extrapolated from a standard curve. Fold change in DNA content, compared to respective control vehicle, was calculated (***$p<0.001$).

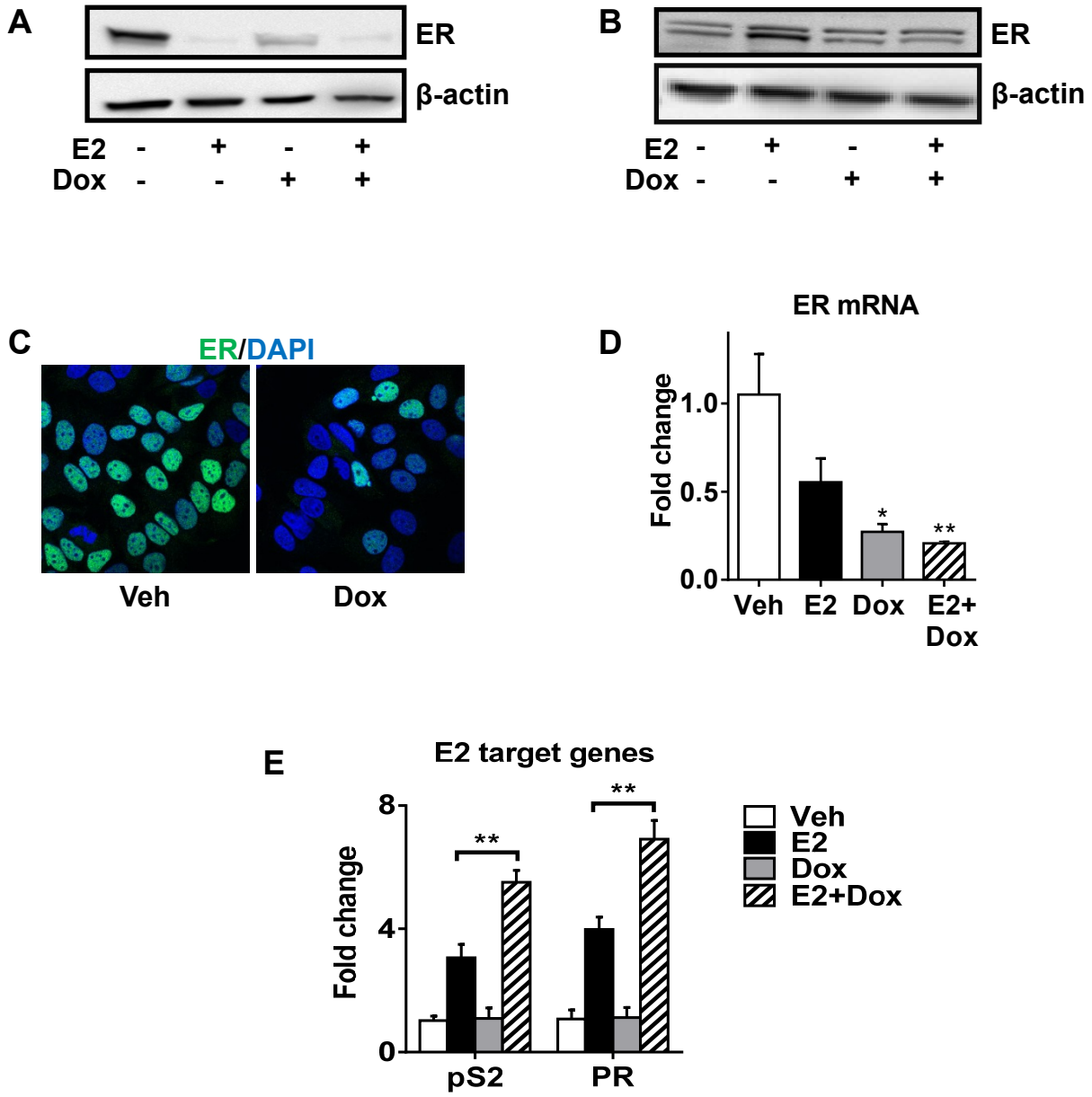

Figure 39: CA-IKKβ downregulates ER, but does not inhibit its transcriptional activity. A) MCF-7-A3 cells were treated with E2, Dox, or E2+Dox for 5 days. Whole cell extract was prepared, and ER and β-actin expression was detected by Western Blotting. B) T47D-C7 cells were treated with E2, Dox, or E2+Dox for 96 hrs. Whole cell extract was prepared, and ER and β-actin expression was detected by Western Blotting. C-E) MCF-7-A3 cells were treated as in A. Immunofluorescence staining of ER expression (green) was conducted. Nuclei were visualized with DAPI (blue). Images were captured by x63 objective using confocal microscopy (C). Expression of ER mRNA (D), and pS2 and PR mRNA (E) was assessed by QPCR. Fold changes were determined using the ΔΔCt method with 36B4 as an internal control. (*p<0.05 and **p<0.01 (treatment versus Veh in D)).

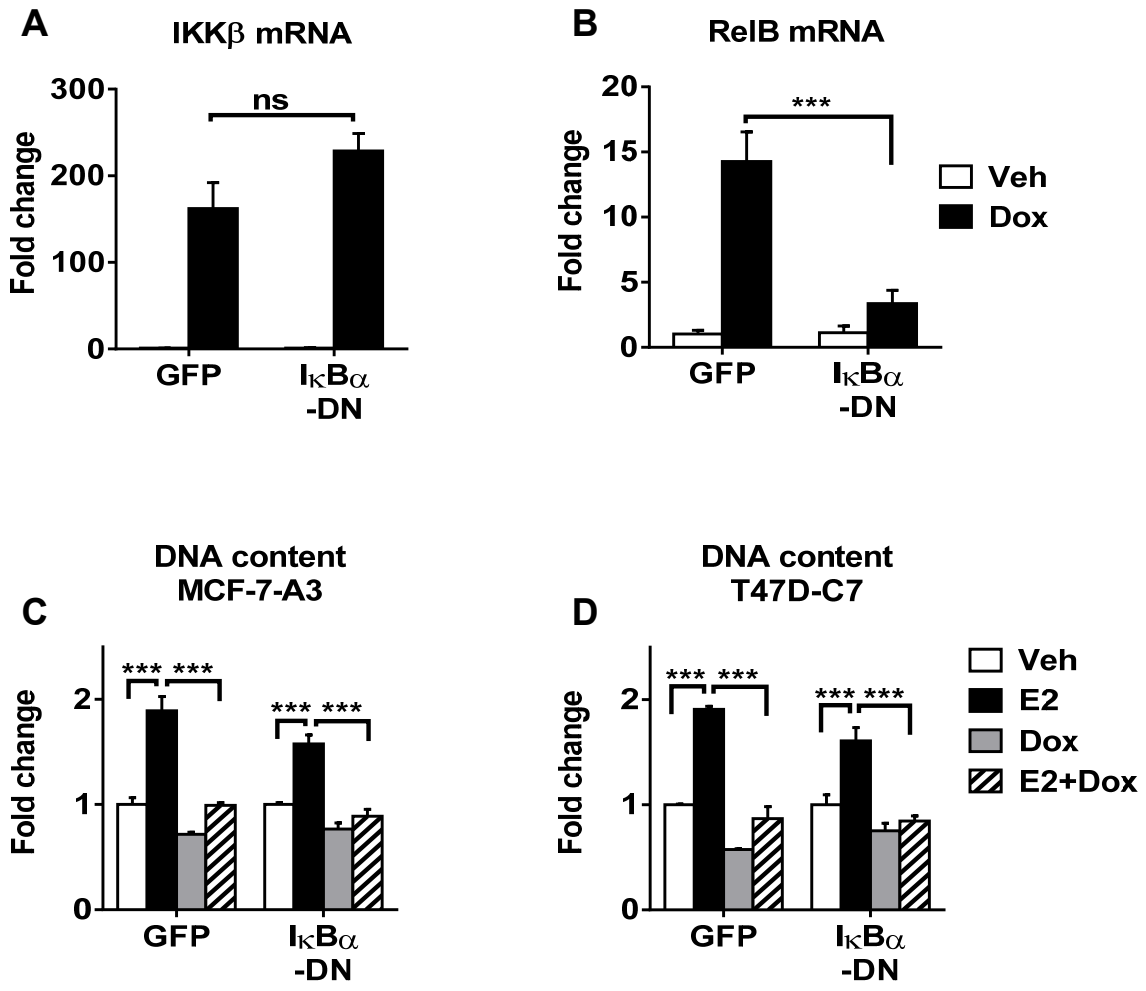

Figure 40: CA-IKKβ inhibits E2-induced proliferation in an NF-κB-independent manner. MCF-7-A3 cells (A,B,C) and T47D-C7 cells (D) were infected with GFP or IκBα-DN adenovirus and treated with E2, Dox, or E2+Dox for 72 hrs. A, B) Expression of IKKβ and RelB mRNA was assessed by QPCR. Fold changes were determined using the ΔΔCt method with 36B4 as an internal control. C, D) Hoechst 33342 nucleic acid stain was added to the cells. The incorporated dye was measured using fluorometry. DNA content was extrapolated from a standard curve. Fold change in DNA content compared to respective control vehicle was calculated (***p<0.001 and ns=non-significant).

4.5.2 Estrogen and constitutively active IKKβ induced invasion is estrogen receptor and NF-κB dependent

We next used ICI and IκBα-DN to understand the role of ER and NF-κB in the invasive phenotype observed upon activation of IKKβ and treatment with E2. ICI inhibited E2-induced invasion of MCF-7-A3 cells, which is in agreement with previous literature emphasizing the role of ER in E2-induced invasion of ER+ breast cancer cells (190-192). ICI did not alter CA-IKKβ-induced invasion; yet, it abolished CA-IKKβ+E2 enhanced invasion in E2+Dox treated cells (Figure 41A). The inhibition of NF-κB by IκBα-DN repressed CA-IKKβ-induced invasion which is consistent with previous literature describing the role of NF-κB in invasion of ER+ breast cancer cells (193). It did not alter E2-induced invasion, but it totally abolished E2+Dox induced invasion (Figure 42A). This suggests that CA-IKKβ+E2 enhanced invasion is both ER and NF-κB dependent. These results were confirmed in T47D-C7 cells, because both ICI and IκBα-DN abolished CA-IKKβ+E2 invasive phenotype (Figures 41B and 42B). Thus, ER and NF-κB work together to induce a highly invasive phenotype in ER+ breast cancer cells.

Interestingly, we observed that in T47D-C7 cells, the inhibition of ER by ICI enhances NF-κB-induced invasion (Figure 41B). As expected, inhibiting IκBα-DN inhibits NF-κB-induced invasion, yet, it significantly enhances E2-induced invasion (Figure 42B). These observations are in agreement with previous studies reporting the transrepression between ER and NF-κB (79,101,103), which appears to be more evident in CA-IKKβ-T47D compared to CA-IKKβ-MCF-7 cells.

Our results have shown that CA-IKKβ and E2 work together to expand a population of cells expressing basal markers, responsible for the invasive phenotype observed in E2+Dox treated cells. To find out the role of ER and NF-κB in the expansion of this basal population, both ICI and IκBα-DN were used. Inhibition of ER and NF-κB totally abolished the induction of

CK5 mRNA expression (Figure 43), indicating that the expansion of CK5+ cell population is ER and NF-κB dependent. Taken together, our results demonstrate that ER and NF-κB work together to expand a population of cells expressing basal markers such as CK5, and this population is responsible for the enhanced invasion observed upon activation of IKKβ and treatment with E2.

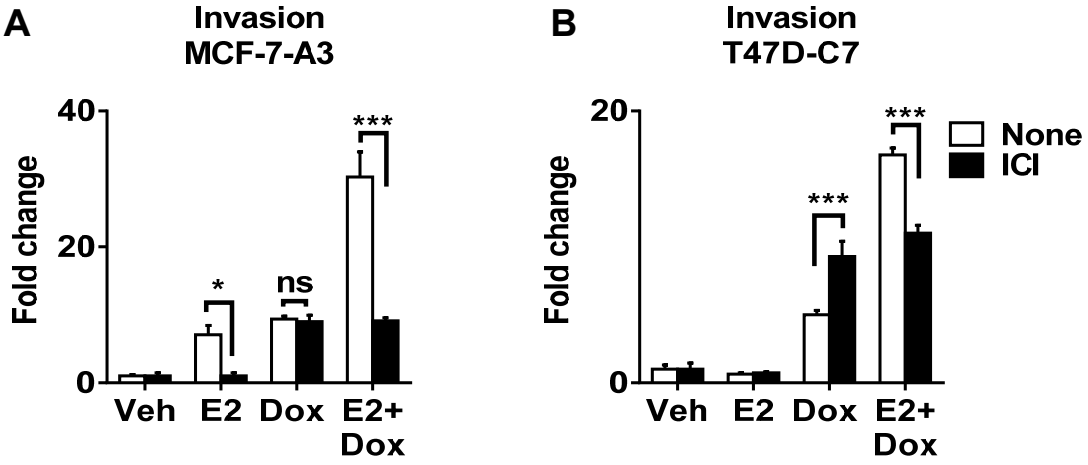

Figure 41: CA-IKKβ+E2 induced invasion is ER dependent. MCF-7-A3 cells (A) and T47D-C7 cells (B) were treated with E2, Dox, or E2+Dox with or without ICI 182,780 for 72 hrs. Cells were transferred into invasion inserts and allowed to invade for 24 hrs (A) or 16 hrs (B), fixed with 4% p-formaldehyde and stained with 0.1% crystal violet. Number of invading cells per insert was counted. Fold change in invasion compared to respective vehicle control was calculated (*$p<0.05$, ***$p<0.001$ and ns= non-significant).

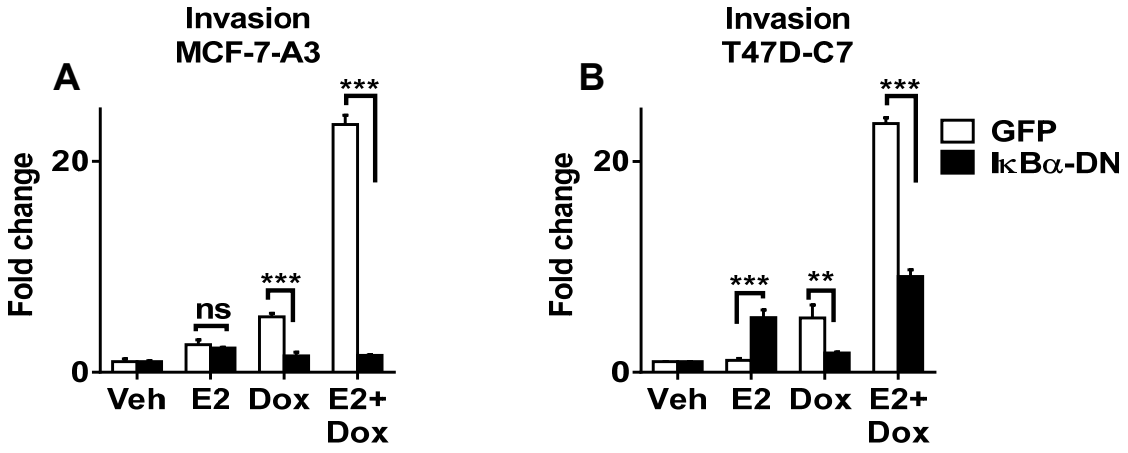

Figure 42: CA-IKKβ+E2 induced invasion is NF-κB-dependent. MCF-7-A3 cells (A) and T47D-C7 cells (B) were infected with GFP or IκBα-DN adenovirus and treated with E2, Dox, or E2+Dox for 72 hrs. Cells were transferred into invasion inserts and allowed to invade for 24 hrs (A) or 16 hrs (B), fixed with 4% p-formaldehyde and stained with 0.1% crystal violet. Number of invading cells per insert was counted. Fold change in invasion compared to respective vehicle control was calculated (**p<0.01, ***p<0.001 and ns= non-significant).

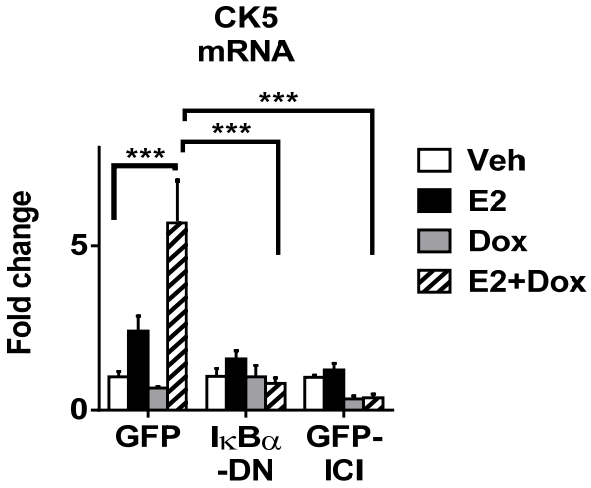

Figure 43: CAIKKβ+E2 induced CK5 expression is ER and NF-κB dependent. MCF-7-A3 cells were infected with adenovirus GFP or IκBα-DN, cells were treated with E2, Dox, or E2+Dox with or without ICI for 72 hrs. Expression of CK5 mRNA was assessed by QPCR. Fold changes were determined using the ΔΔCt method with 36B4 as an internal control (***p<0.001).

4.6 Global gene expression reveals different patterns of gene regulation

Our in vitro results demonstrate that CA-IKKβ opposes ER activity on proliferation but that NF-κB and ER work together to promote invasion. To better understand how ER/CA-IKKβ crosstalk might contribute to these observed phenotypes, we performed a global gene expression profiling study using MCF-7-A3 cells treated with E2, Dox, or E2+Dox for 72 hrs, corresponding to our in vitro phenotypic observation; mRNA was purified, and samples were analyzed on an Affymetrix high-density oligonucleotide array. When the three treatments were compared to vehicle, 12,271 out of 49K gene probes were found to be significantly upregulated ($p<0.01$ and fold change>1.5). Supervised clustering was performed, and multiple discrete regulatory patterns were observed (Figure 44):

1. Genes regulated by E2, not affected by CA-IKKβ alone, but the effect of E2 was reversed by CA-IKKβ.
2. Genes regulated by CA-IKKβ, not affected by E2 alone, but the effect of CA-IKKβ was reversed by E2.
3. Genes regulated by E2 and not affected by CA-IKKβ.
4. Genes regulated by CA-IKKβ and not affected by E2.
5. Genes similarly regulated by E2, CA-IKKβ, and E2+CA-IKKβ.
6. Genes that are oppositely regulated by E2 and CA-IKKβ:
    a) Genes activated by E2, repressed by CA-IKKβ, and not expressed with CA-IKKβ+E2.
    b) Genes activated by CA-IKKβ, repressed by E2, and not expressed with CA-IKKβ+E2.

To understand any potential biological differences between the six patterns, Gene Set Enrichment Analysis (GSEA) was used. GSEA is an analytical method of interpreting gene

expression data that utilizes Molecular Signatures Database (MSigDB), which is a collection of annotated gene sets. GSEA initially calculates an enrichment score that reveals the extent to which an *a priori* defined gene set is overrepresented at the extremes (top or bottom) of a ranked gene set of interest. The enrichment score is then normalized for gene set size, resulting in a normalized enrichment score (NES). False discovery rate (FDR) is then computed by GSEA to estimate the probability that a gene set with a defined NES represents a false positive finding (144). Different patterns of E2 and CA-IKKβ regulated genes were initially examined for enrichment using the hallmark gene sets of the MSigDB. These hallmark sets represent specific defined biological states and processes, and they are considered as the starting point for exploring GSEA (194). In addition to hallmark gene sets, analysis was performed using GO gene sets that comprise genes annotated by GO (Gene Ontology) terms. The sets are derived from the controlled vocabulary of the Gene Ontology project, which defines consistent vocabulary to describe gene sets in terms of the biological functions to which they are associated (194,195). Analysis was also performed using the curated gene sets that are gene signatures collected from publications in PubMed, knowledge of domain experts, and online pathway databases (145,194). Tables V-VII describe the overall results obtained from GSEA, with some key findings highlighted below.

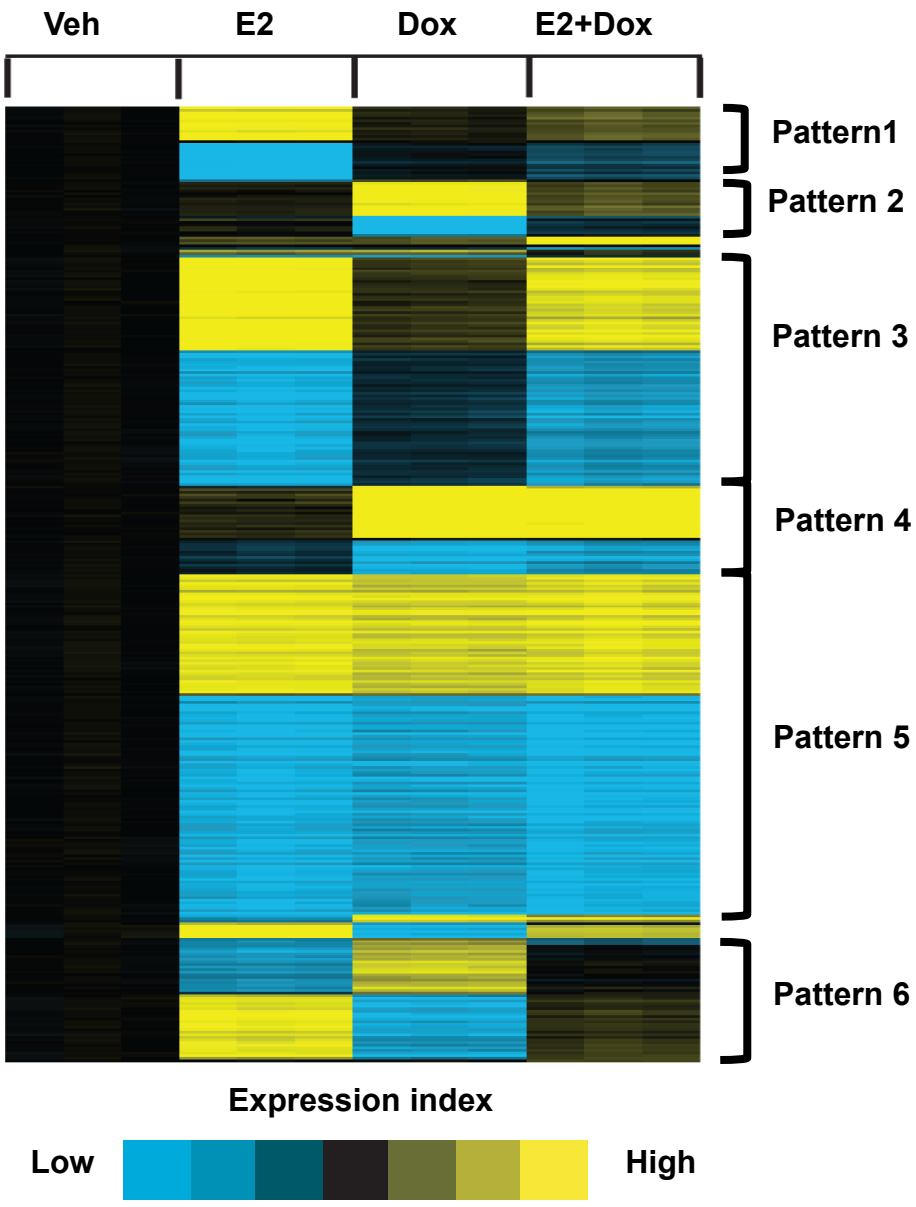

Figure 44: Global gene expression profiling reveals six main patterns of gene regulation. MCF-7-A3 cells were treated with E2, Dox, or E2+Dox for 72 hrs. mRNA was purified, and samples were analyzed on an Affymetrix high-density oligonucleotide array. Treatments were compared to vehicle, and 12,271 gene probes were found significant ($p<0.01$ and fold change>1.5). Supervised clustering was performed. Six different patterns of gene regulation were observed.

TABLE V: GSEA OF DIFFERENT PATTERNS USING HALLMARK GENE SETS OF MSigDB[a]

Response	Pattern 1	Pattern 2	Pattern 3	Pattern 4	Pattern 5	Pattern 6a	Pattern 6b
E2 response	ESTROGEN_ RESPONSE_ LATE ESTROGEN_ RESPONSE_ EARLY		ESTROGEN_ RESPONSE_ LATE ESTROGEN_ RESPONSE_ EARLY		ESTROGEN_ RESPONSE_ LATE ESTROGEN_ RESPONSE_ EARLY	ESTROGEN_ RESPONSE_ LATE ESTROGEN_ RESPONSE_ EARLY	
NF-κB signaling		TNFA_ SIGNALING_ VIA_NF-KB (FDR=0.274)		TNFA_ SIGNALING_ VIA_NF-KB			TNFA_ SIGNALING_ VIA_NF-KB
Inflamma-tion				INFLAMMATO-RY_ RESPONSE	INFLAMMATO-RY_ RESPONSE		
Proliferation	MYC_ TARGETS_V1		G2/M_ CHECKPOINT MYC_ TARGETS_V1 MYC_ TARGETS_V2 E2F_ TARGETS		MYC_ TARGETS_V1 MYC_ TARGETS_V2 E2F_ TARGETS	G2/M_ CHECKPOINT MITOTIC_ SPINDLE MYC_ TARGETS_V1 E2F_ TARGETS	

[a] FDR <0.05 unless otherwise stated.

TABLE V (continued): GSEA OF DIFFERENT PATTERNS USING HALLMARK GENE SETS OF MSigDB[a]

Response	Pattern 1	Pattern 2	Pattern 3	Pattern 4	Pattern 5	Pattern 6a	Pattern 6b
EMT		EPITHELIAL_ MESENCHY-MAL_ TRANSITION	EPITHELIAL_ MESENCHY-MAL_ TRANSITION	EPITHELIAL_ MESENCHY-MAL_ TRANSITION			
Interferon Response				INTERFERON_ GAMMA_ RESPONSE	INTERFERON_ GAMMA_ RESPONSE (FDR=0.066) INTERFERON_ ALPHA_ RESPONSE (FDR=0.063)		INTERFERON_ GAMMA_ RESPONSE INTERFERON_ ALPHA_ RESPONSE
Metabolism	GLYCOLYSIS		OXIDATIVE_ PHOSPHORY-LATION ADIPOGENES-IS XENOBIOTIC_ METABOLISM		OXIDATIVE_ PHOSPHORY-LATION GLYCOLYSIS (FDR=0.061)		

[a] FDR <0.05 unless otherwise stated.

TABLE V (continued): GSEA OF DIFFERENT PATTERNS USING HALLMARK GENE SETS OF MSigDB[a]

Response	Pattern 1	Pattern 2	Pattern 3	Pattern 4	Pattern 5	Pattern 6a	Pattern 6b
Unfolded protein response			UNFOLDED_ PROTEIN_ RESPONSE		UNFOLDED_ PROTEIN_ RESPONSE		
Miscellaneous				ALLOGRAFT_ REJECTION COMPLEMENT KRAS_ SIGNALING_ UP IL2_STAT5_ SIGNALING	MTORC1_ SIGNALING	DNA_REPAIR	UV_ RESPONSE_ DN HYPOXIA

[a] FDR <0.05 unless otherwise stated (DN=downregulated and UP=upregulated).

TABLE VI: GSEA OF PATTERN 6A USING GO GENE SETS OF MSigDB

GO term analysis	NES	FDR
CELL_CYCLE_GO_0007049	2.47	0.001
CELL_CYCLE_PROCESS	2.41	0.001
M_PHASE	2.31	0.001
MITOTIC_CELL_CYCLE	2.3	0.001
DNA_METABOLIC_PROCESS	2.21	0.003
CELL_CYCLE_PHASE	2.19	0.003
DNA_REPLICATION	2.13	0.004
M_PHASE_OF_MITOTIC_CELL_CYCLE	2.13	0.004
MITOSIS	2.12	0.003
DNA_DEPENDENT_DNA_REPLICATION	1.99	0.009
REGULATION_OF_CELL_CYCLE	1.96	0.009
MACROMOLECULAR_COMPLEX_ASSEMBLY	1.83	0.024
CELLULAR_COMPONENT_ASSEMBLY	1.83	0.023
CELL_PROLIFERATION_GO_0008283	1.83	0.023

TABLE VII: GSEA OF DIFFERENT PATTERNS USING CURATED GENE SETS OF MSigDB

GSEA analysis	Pattern	NES	FDR
POOLA_INVASIVE_BREAST_CANCER_UP	4	2.26	0.002
SCHUETZ_BREAST_CANCER_DUCTAL_INVASIVE_UP	4	2.2	0.004
WANG_TUMOR_INVASIVENESS_UP	5	1.87	0.022
SMID_BREAST_CANCER_BASAL_UP	3	1.71	0.050
	4	2.64	0.000
	5	3.18	0.000
CHARAFE_BREAST_CANCER_LUMINAL_VS_BASAL_DN	4	3.02	0.000
	5	2.20	0.004
CHARAFE_BREAST_CANCER_LUMINAL_VS_MESENCHYMAL_DN	4	2.6	0.000
SARRIO_EPITHELIAL_MESENCHYMAL_TRANSITION_UP	5	2.14	0.005
LIM_MAMMARY_STEM_CELL_UP	4	1.91	0.023
PECE_MAMMARY_STEM_CELL_UP	5	1.87	0.023

4.6.1 Estrogen receptor and constitutively active IKKβ crosstalk

As expected, significant enrichment of hallmark gene sets involving early and late response to E2 are observed with E2 treatment in patterns1, 3, 5 and 6a. Similarly, significant enrichment of hallmark TNFα signaling and inflammatory response is observed with CA-IKKβ in patterns 2, 4, 5 and 6b. Gene expression profiling revealed different patterns of crosstalk between E2 and CA-IKKβ:

1) Transrepression was evident with early and late E2 response genes that are reversed and repressed by CA-IKKβ in patterns 1 and 6a, respectively. Similarly, NF-κB target genes were repressed by E2 in group 2 and 6b (Table V). This observation is in agreement with literature describing the transrepression between E2 and NF-κB signaling (70,101).

2) No crosstalk between E2 and CA-IKKβ was evident by early and late E2 response genes in pattern 3 that are not affected by CA-IKKβ. Also, NF-κB target genes in pattern 4 that are not affected by E2.

3) Coregulation was evident by early and late E2 response genes and inflammatory genes that are regulated by E2, CA-IKKβ or both in pattern 5.

Thus, gene expression profiling is in agreement with our previous work, describing the different patterns of crosstalk between E2 and TNFα in ER+ breast cancer cells (115).

4.6.2 Effect of constitutively active IKKβ on estrogen-induced proliferation

Our studies have shown that E2-regulated proliferation is inhibited by CA-IKKβ both in vitro and in vivo. Therefore, we looked for cell cycle and proliferation associated gene sets to uncover the mechanism underlying the effect of CA-IKKβ on proliferation. We observed an enrichment of hallmark proliferation related gene sets, G2/M checkpoint, and mitotic spindle, upon E2 treatment in patterns 3 and pattern 6a (Table V). Target genes of MYC and E2F, both

known mediators of E2 regulated proliferation, were observed in all E2 regulated patterns (Table V) (Figure 45). Studies have reported that both MYC and E2F1 are E2-regulated, and they are associated with E2-induced proliferation and cell cycle progression in breast cancer cells (189,196). Given that CA-IKKβ represses proliferation, we would expect patterns 1 and 6a, which are E2 regulated genes reversed/repressed by CA-IKKβ, to comprise cell cycle genes inhibited by CA-IKKβ. Using GO terms, we found that pattern 6a was enriched for cell cycle, cell cycle process, and cell proliferation GO terms (Table VI) (Figure 46). Moreover, we identified the cell cycle gene cyclin D1 (CCND1), an E2 target gene that facilitates entry to S phase (189,197), in pattern 1. These findings suggest that E2-regulated cell cycle genes in patterns 1 and 6a are repressed by CA-IKKβ and may contribute to the repression of proliferation.

Because our results indicate that CA-IKKβ inhibition of proliferation is NF-κB-independent, we hypothesized that CA-IKKβ would inhibit genes in cell cycle GO signature independently of NF-κB. To test this, we used IκBα-DN and looked at mRNA expression of enriched genes: checkpoint kinase 2 (CHEK2), cyclin A2 (CCNA2), E2F1, and cell division cycle 45 (CDC45). As expected, E2 upregulated the expression of the four genes, and this was prevented by CA-IKKβ. Inhibition of NF-κB with IκBα-DN did not rescue the expression of representative genes. Similarly, E2-induced CCND1 expression was not rescued by IκBα-DN (Figure 47). These results are consistent with our initial finding that CA-IKKβ inhibition of E2-induced proliferation is NF-κB-independent.

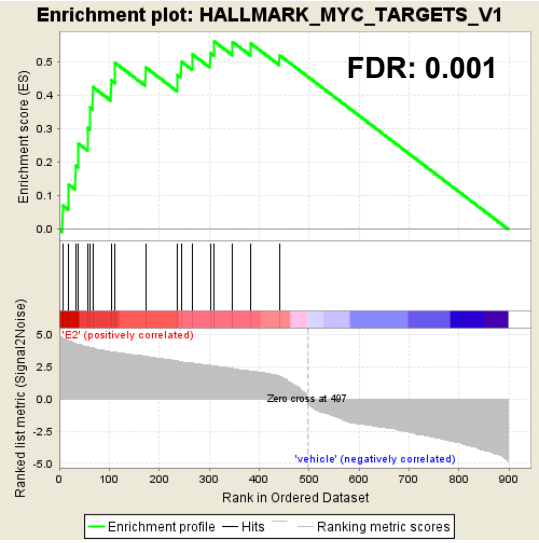

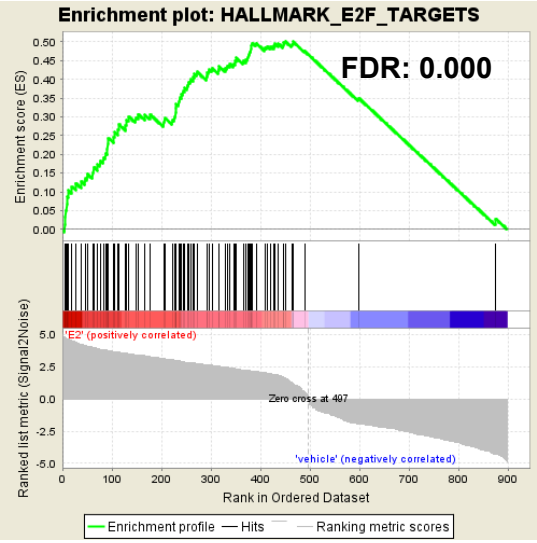

Figure 45: Enrichment of myc and E2F targets in pattern 6a. GSEA analysis was performed for genes regulated in pattern 6a using the hallmark gene sets of the MSigDB. Genes that contribute to the enrichment score are represented as vertical lines. Genes are ranked left (most positive) to right (most negative). Values above 0 indicate a gain in enrichment, and values below 0 indicate reduced enrichment of a gene set.

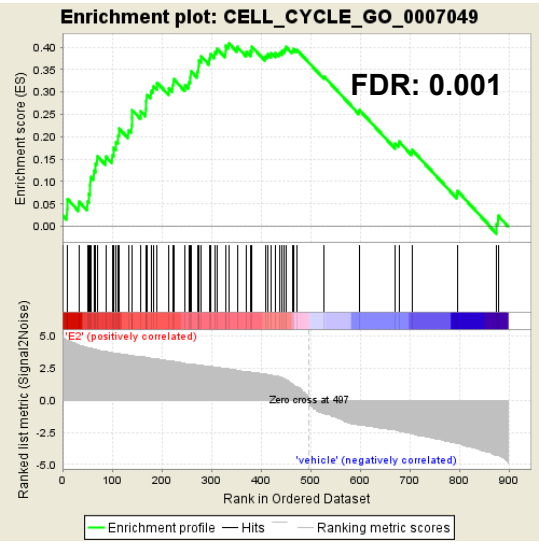

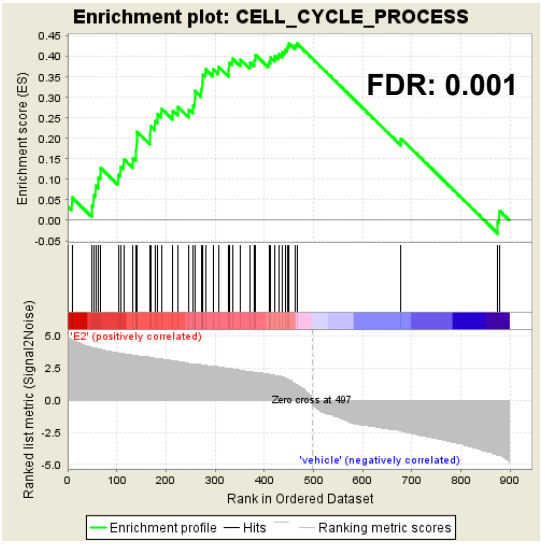

Figure 46: Enrichment of cell cycle GO terms in genes of pattern 6a. GSEA analysis was performed for genes regulated in pattern 6a using the GO gene sets of MSigDB.

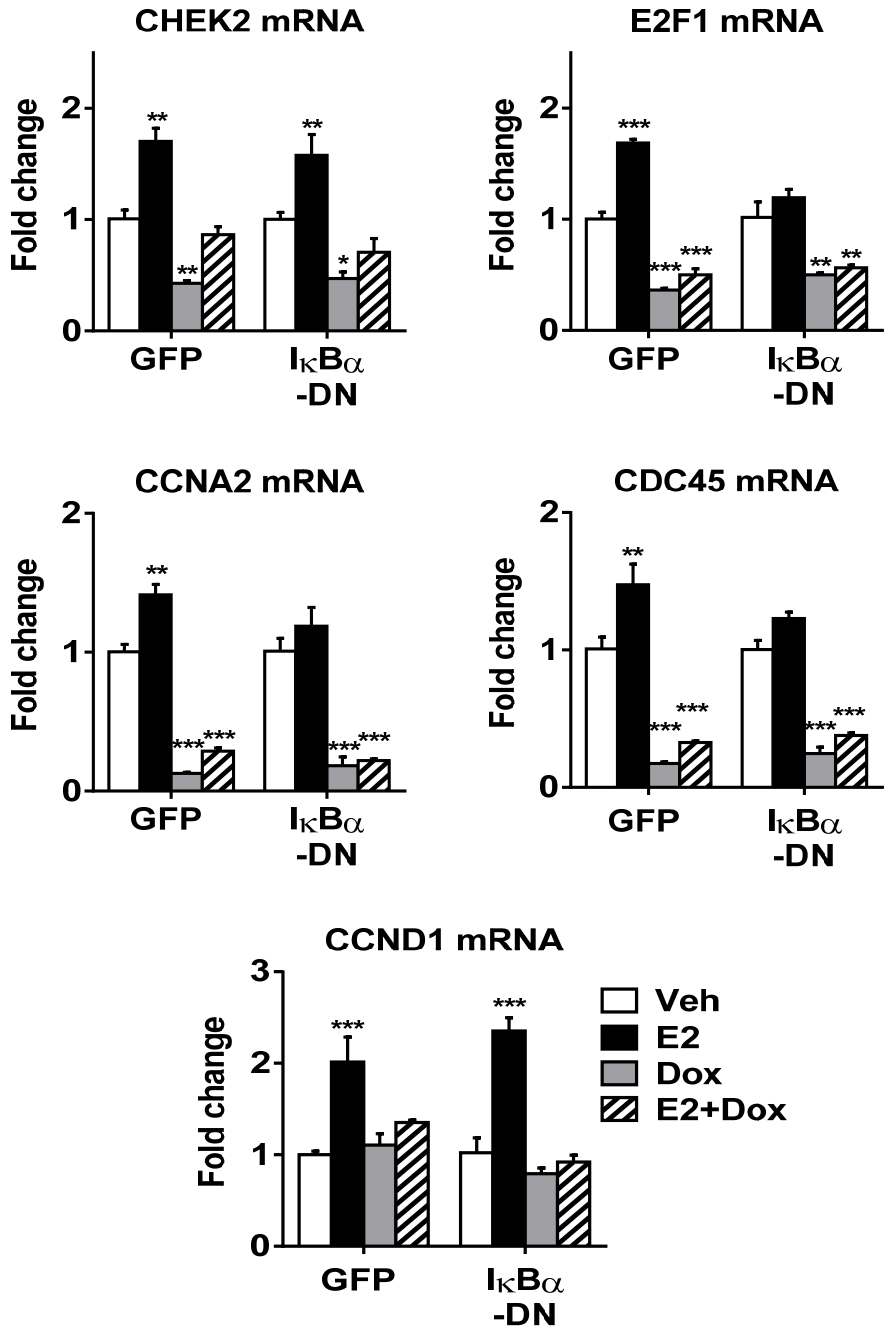

Figure 47: CA-IKKβ inhibition of cell cycle genes is not NF-κB-dependent. MCF-7-A3 cells were infected with adenovirus GFP or IκBα-DN. Cells were treated with E2, Dox, or E2+Dox for 72 hrs. Expression of CHEK2, E2F1, CCNA2, CDC45 and CCND1 mRNA was assessed by QPCR. Fold changes were determined using the ΔΔCt method with 36B4 as an internal control (*p<0.05, **p<0.01 and ***p<0.001 for treatment versus respective Veh).

4.6.3 Effect of estrogen and constitutively active IKKβ on invasion and metastasis

Constitutively active IKKβ and ER work together to increase invasion in vitro and metastasis in vivo. GSEA did not reveal enrichment of motility/migration GO terms; however, enrichment of three curated GSEA gene sets for invasive breast cancer was observed (Figure 48) (Table VII):

1. POOLA_INVASIVE_BREAST_CANCER_UP. This gene set includes genes upregulated in atypical ductal hyperplastic tissues from patients who had breast cancer, compared to the tissues from patients who did not have the cancer. Women with atypical ductal hyperplastic tissues have approximately 5 times higher incidence of invasive breast cancer than women who did not have atypical ductal hyperplasia (198). The enrichment was significantly observed in pattern 4, which comprises genes regulated by CA-IKKβ and not affected by E2 treatment.
2. SCHUETZ_BREAST_CANCER_DUCTAL_INVASIVE_UP. These genes are upregulated in invasive ductal carcinoma, compared to ductal carcinoma in situ, which is non-invasive (199). Significant enrichment was observed in pattern 4, which represents genes regulated by CA-IKKβ and not affected by E2 treatment.
3. WANG_TUMOR_INVASIVENESS_UP. These are genes upregulated in the invasive subpopulation of polyoma middle T oncogene-derived mammary tumor cells, compared to the whole population of the cells in the primary tumors (200). Significant enrichment of this set was observed in pattern 5, which contains genes coregulated by CA-IKKβ and E2.

Thus, GSEA suggests that CA-IKKβ and CA-IKKβ+E2 regulated genes may be clinically relevant to invasive breast cancer.

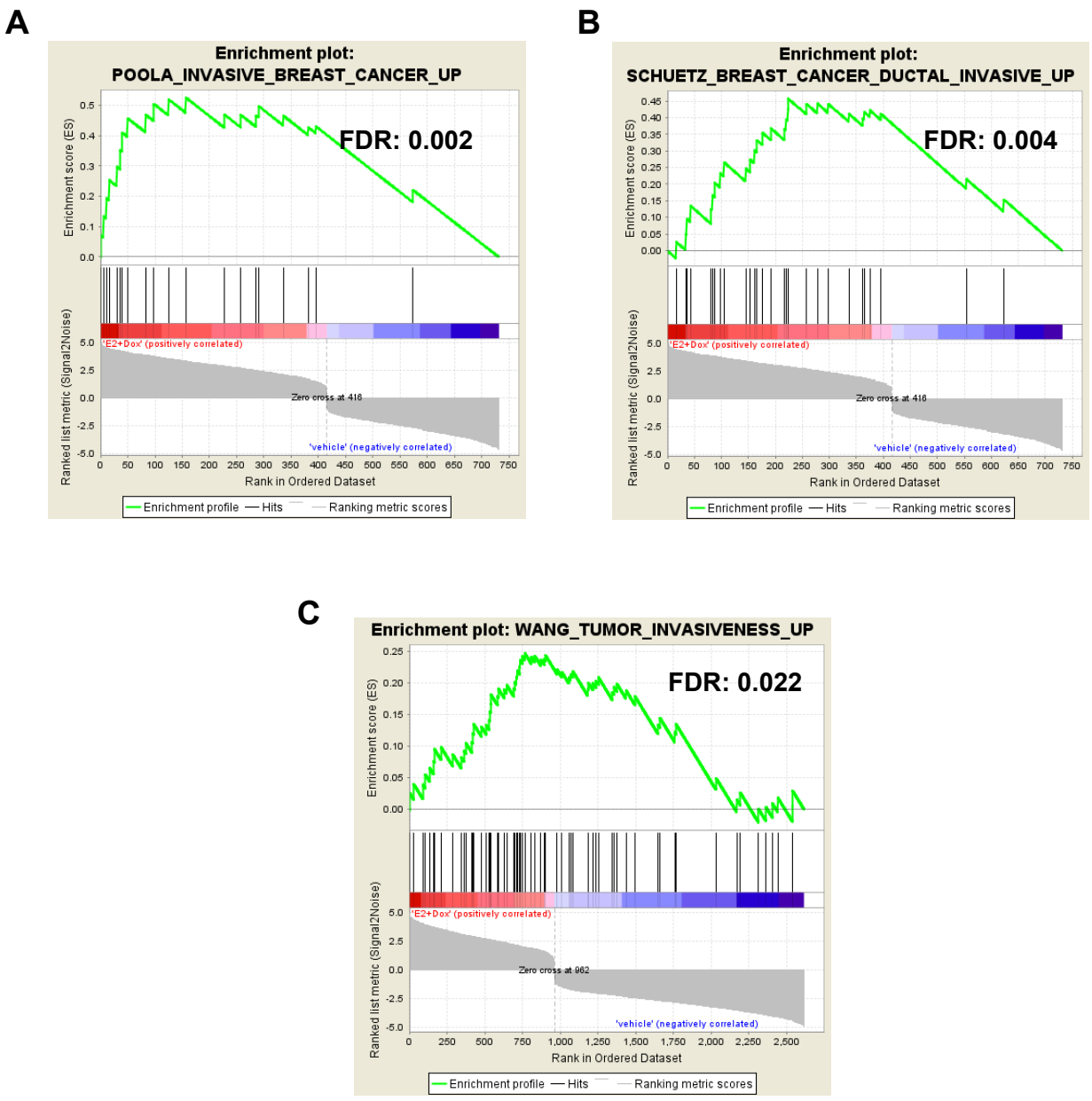

Figure 48: Enrichment of invasion gene sets in cells treated with E2+Dox. GSEA analysis was performed for genes regulated in pattern 4 (A, B) and pattern 5 (C) using the curated gene sets of MSigDB.

4.6.4 Effect of estrogen and constitutively active IKKβ on the cellular phenotype

Our cell based studies indicate that activation of IKKβ and treatment with E2 shift the differentiation state of ER+ cells from luminal towards basal/mesenchymal/ luminal progenitor without gaining a full basal or mesenchymal state. Consistent with these findings, GSEA revealed enrichment of two basal versus luminal breast cancer gene signatures (Figure 49) (Table VII):

1. SMID_BREAST_CANCER_BASAL_UP. This gene set includes genes upregulated in basal subtype breast tumors versus the other breast cancer subtypes (201). Significant enrichment of this gene set was observed in genes of patterns 3, 4 and 5.
2. CHARAFE_BREAST_CANCER_LUMINAL_VS_BASAL_DN. These are genes downregulated in luminal-like versus the basal-like breast cancer cell lines (202). Significant enrichment of this gene set was observed in patterns 4 and 5.

Although EMT was not observed upon activation of IKKβ and treatment with E2, enrichment of EMT gene sets was observed in CA-IKKβ regulated patterns 2 and 4 (Table V). The regulation by CA-IKKβ is in agreement with studies reporting that NF-κB activation is associated with the induction of EMT (150,203). Some studies have reported that E2 inhibits EMT (204-206), while others reported that E2 induces EMT (207,208). This controversy is evident in our GSEA results, since one set is reversed by E2 (pattern 2), a second set is regulated by E2 (pattern 3), and a third set is not affected by E2 (pattern 4) (Table V). Moreover, significant enrichment of mesenchymal gene signatures was also observed (Figure 50) (Table VII):

1. CHARAFE_BREAST_CANCER_LUMINAL_VS_MESENCHYMAL_DN, which are genes downregulated in luminal-like versus the mesenchymal-like breast

cancer cell lines (202). Significant enrichment could be observed in genes regulated by CA-IKKβ and not affected by E2 (pattern 4).

2. SARRIO_EPITHELIAL_MESENCHYMAL_TRANSITION_UP, which are genes upregulated in MCF10A cells undergoing EMT (209). Significant enrichment of this gene set was observed in genes coregulated by E2 and CA-IKKβ (pattern 5).

Together, these findings are consistent with our mRNA and protein studies, in which we found that E2 and CA-IKKβ upregulate the expression of some EMT genes and downregulate others, without inducing the protein expression of EMT hallmarks. Thus, despite changes in mRNA levels, there is no conclusive evidence that EMT is occurring.

Significant enrichment of stem cells gene sets were observed (Figure 51) (Table VII):

1. LIM_MAMMARY_STEM_CELL_UP, which represents genes upregulated in human and mouse mammary stem cells (210). Significant enrichment could be observed in genes regulated by CA-IKKβ and not affected by E2 (pattern 4).
2. PECE_MAMMARY_STEM_CELL_UP, which represents genes upregulated in human normal mammary stem cells (211). Significant enrichment was observed in genes coregulated by E2 and CA-IKKβ (pattern 5).

Overall, GSEA results are in agreement with our cell based studies, and suggest that activation of IKKβ and treatment with E2 result in dedifferentiation of luminal cells, and their shift along the differentiation axis toward the basal/mesenchymal states with the gain of stem-like characteristics.

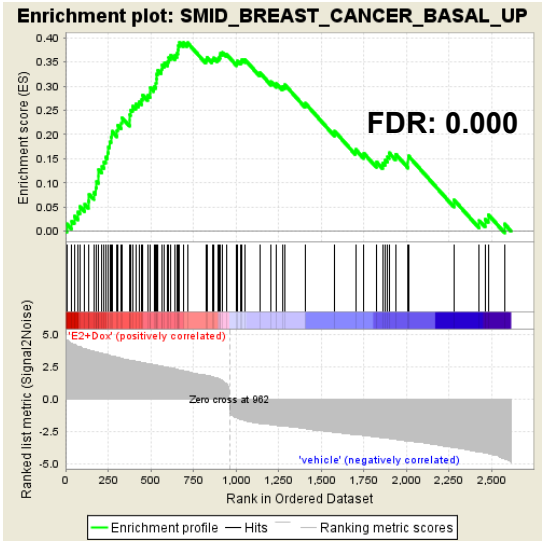

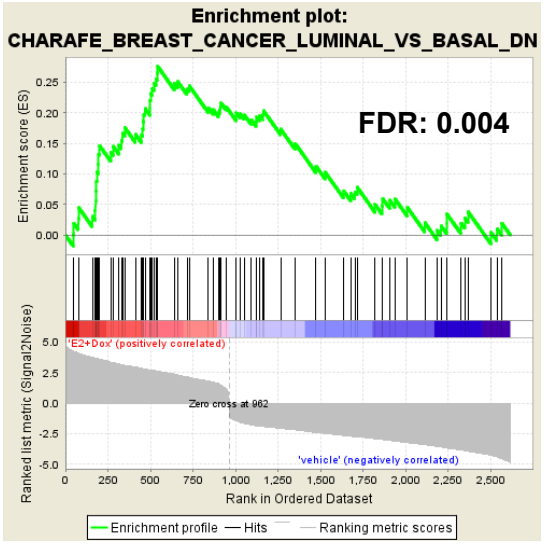

Figure 49: Enrichment of basal gene sets in genes of pattern 5. GSEA analysis was performed for genes regulated in pattern 5 using the curated gene sets of MSigDB.

A

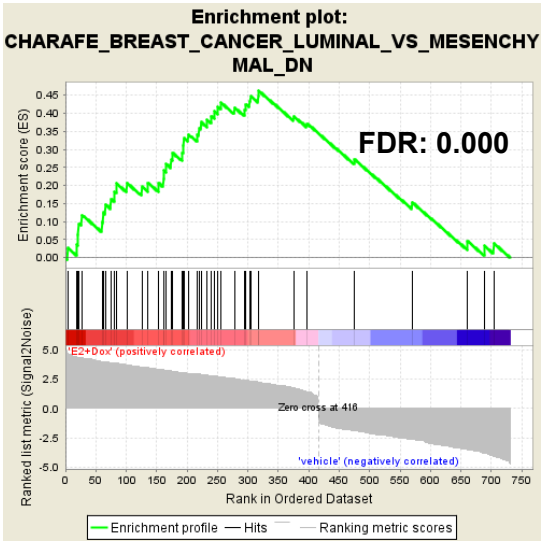

B

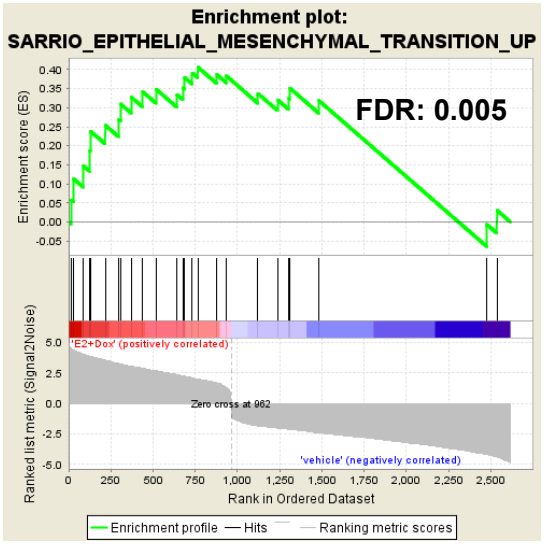

Figure 50: Enrichment of mesenchymal gene sets in cells treated with E2+Dox. GSEA analysis was performed for genes regulated in pattern 4 (A) and pattern 5 (B) using the curated gene sets of MSigDB.

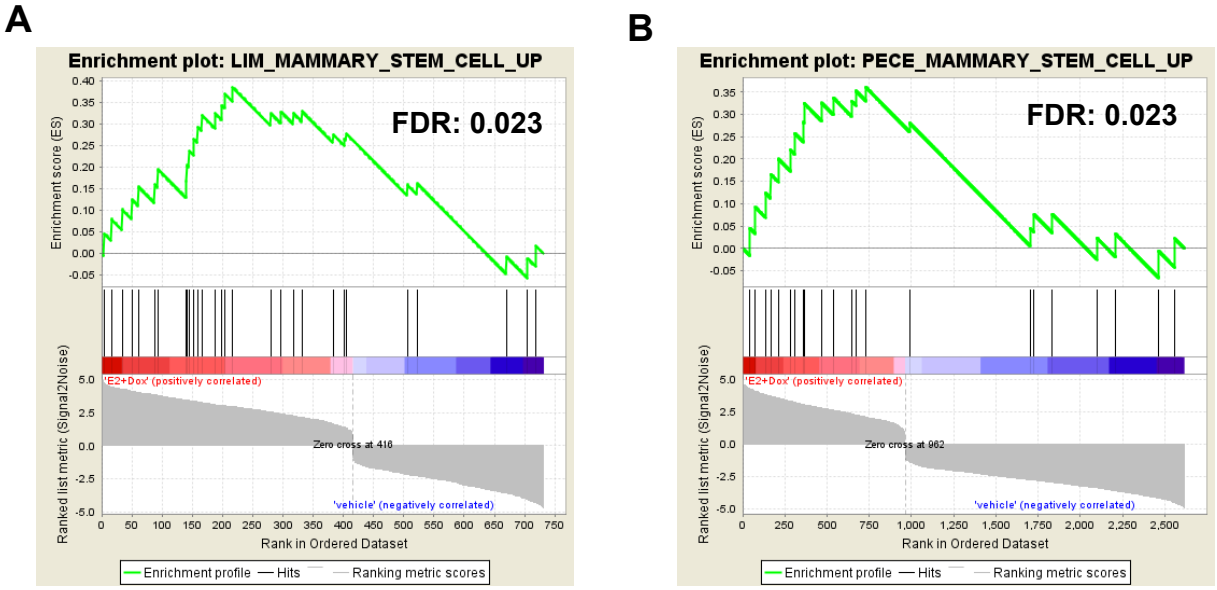

Figure 51: Enrichment of stem gene sets in cells treated with E2+Dox. GSEA analysis was performed for genes regulated in pattern 4 (A) and pattern 5 (B) using the curated gene sets of MSigDB.

4.6.5 Effect of estrogen and constitutively active IKKβ on glycolysis, unfolded protein response, and interferon response

One interesting finding that we have observed is that gene sets representing the metabolic processes, oxidative phosphorylation and glycolysis, are regulated by ER and CA-IKKβ. In the presence of oxygen, cells metabolize glucose to pyruvate, which is used up by the mitochondria to produce high amount of ATP. This process is termed oxidative phosphorylation and is considered the main source of energy in normal cells. Under conditions of limited oxygen, cells redirect pyruvate away from the mitochondrial oxidative phosphorylation and generate lactic acid in a process called anaerobic glycolysis. Cancer cells could have high glycolysis rate in the presence of oxygen, and this process is termed aerobic glycolysis (212). Lactic acid is considered a signaling molecule, playing an important role in migration and metastasis (213).

Enrichment of oxidative phosphorylation gene sets was observed in genes regulated by E2 and not affected by CA-IKKβ (pattern 3), and genes coregulated by E2 and CA-IKKβ (pattern 5). Enrichment of glycolysis gene sets was observed in genes regulated by E2 and reversed by CA-IKKβ (pattern 1), as well as genes coregulated by E2 and CA-IKKβ (Table V) (Figure 52). Recent studies have reported that mitochondrial enzyme manganese superoxide dismutase (MnSOD /SOD2) sustains the metabolic shift to glycolysis in breast cancer (214). Analysis of MnSOD expression in CA-IKKβ cells revealed that E2+Dox enhance the expression of MnSOD at both the mRNA and protein levels (Figure 53), suggesting a potential role for CA-IKKβ and E2 in inducing glycolysis in ER+ breast cancer cells via MnSOD upregulation.

Another observation of interest is the enrichment of Unfolded Protein Response (UPR) genes observed in genes regulated by E2 (pattern 3) and genes regulated by both E2 and CA-IKKβ (pattern 5) (Table V) (Figure 54). In conditions of endoplasmic reticulum stress, the function of the endoplasmic reticulum is disrupted, leading to the accumulation of unfolded

proteins. Cells react to the stress by activating UPR as a survival response to restore endoplasmic reticulum homeostasis. Cell death mechanisms are activated, if the stress persists. Endoplasmic reticulum stress is recognized in cancer, and UPR plays an important role in cancer cell survival (215). Estrogen promotes an adaptive UPR response that protects breast cancer cells against UPR-mediated apoptosis (216). Studies reported that proinflammatory stimuli (e.g. cytokines) trigger endoplasmic reticulum stress, which initiates or amplifies inflammatory responses by activating NF-κB signaling (217,218). GSEA demonstrated that a set of UPR genes is regulated by both E2 and CA-IKKβ, suggesting a role for UPR in E2 and CA-IKKβ enhanced cell survival.

GSEA further revealed enrichment of interferon response genes in the gene set regulated by CA-IKKβ (pattern 4 and pattern 6b), as well as the gene sets regulated by both E2 and CA-IKKβ (pattern 5) (Table V) (Figure 55). Interferons are cytokines produced by immune cells in response to viral/microbial infections as well as tumors. Dysregulation of interferon signaling, resulting in constitutive overexpression of interferon-stimulated genes, is associated with endocrine resistance. Interferon-stimulated genes IFITM1 and PLSCR1 are constitutively overexpressed in aromatase inhibitor resistant breast cancer cells and tumors. Knockdown of IFITM1 significantly inhibits cell proliferation, migration and invasion (219). Although gene enrichment in pattern 5 is insignificant, both IFITM1 and PLSCR1 are included in the group of interferon alpha response enriched genes observed in cells regulated by E2 and CA-IKKβ (pattern 5), suggesting a role of CAIKKβ and E2 in endocrine therapy resistance.

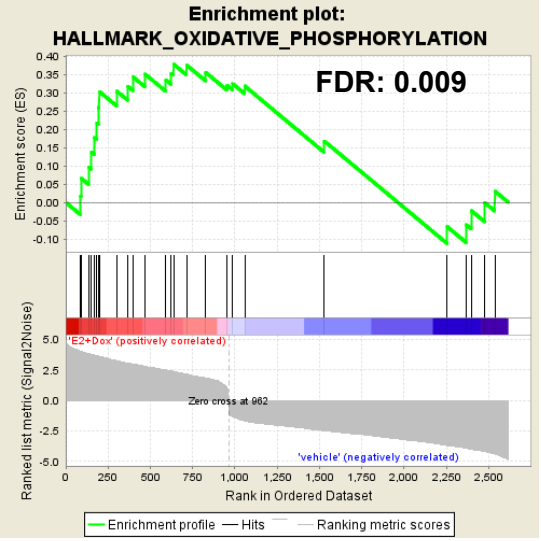

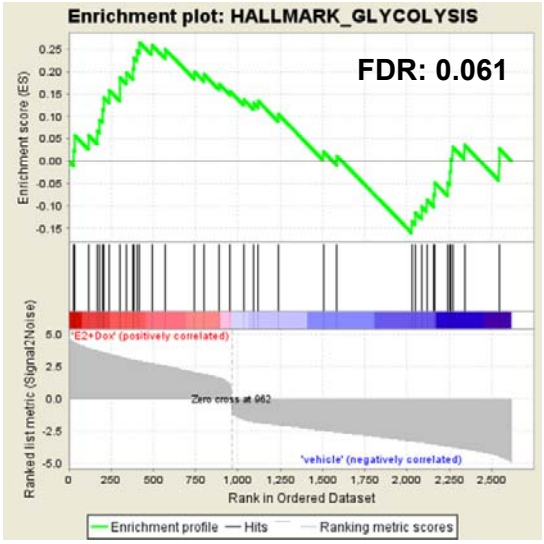

Figure 52: Enrichment of both oxidative phosphorylation and glycolysis gene sets in genes of pattern 5. GSEA analysis was performed for genes regulated in pattern 5 using the hallmark gene sets of MSigDB.

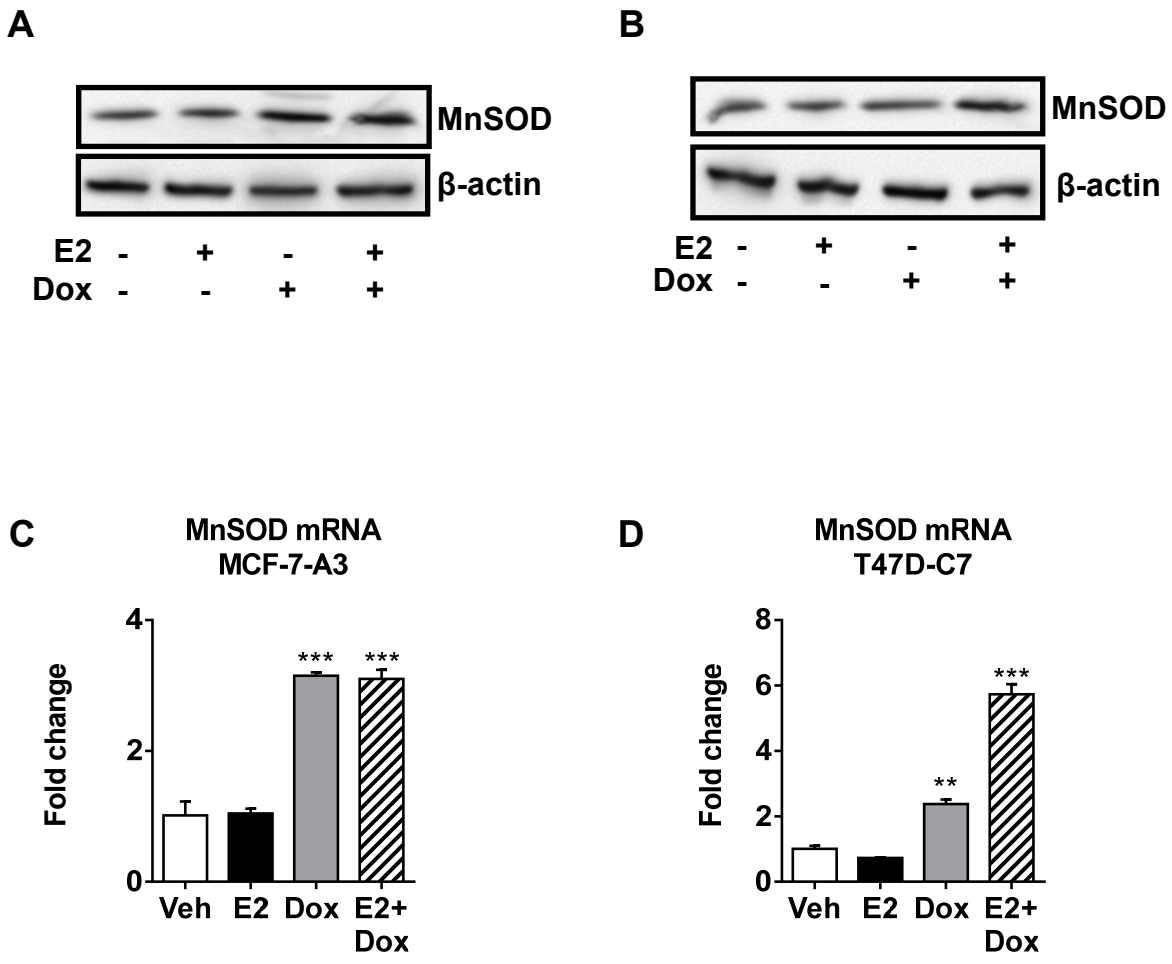

Figure 53: CA-IKKβ+E2 enhances the expression of MnSOD in ER+ breast cancer cells. MCF-7-A3 (A, C) cells and T47D-C7 cells (B, D), were treated with E2, Dox or E2+Dox for 72 hrs. A, B) Whole cells extract was prepared and the expression of MnSOD and β-actin was detected by Western Blotting. C, D) mRNA expression of MnSOD was assessed by QPCR. Fold changes were determined using the ΔΔCt method with 36B4 as an internal control (**p<0.01 and ***p<0.001 for treatment versus Veh).

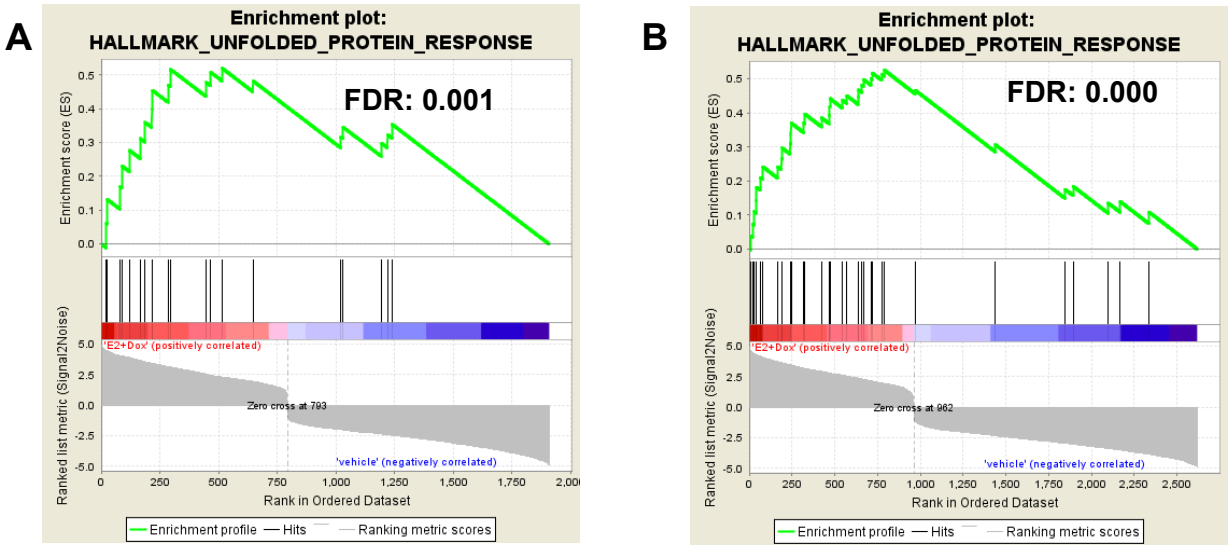

Figure 54: Enrichment of unfolded protein response gene sets in cells treated with E2+Dox. GSEA of genes in pattern 3 (A) and pattern 5 (B) using the hallmark gene sets of MSigDB.

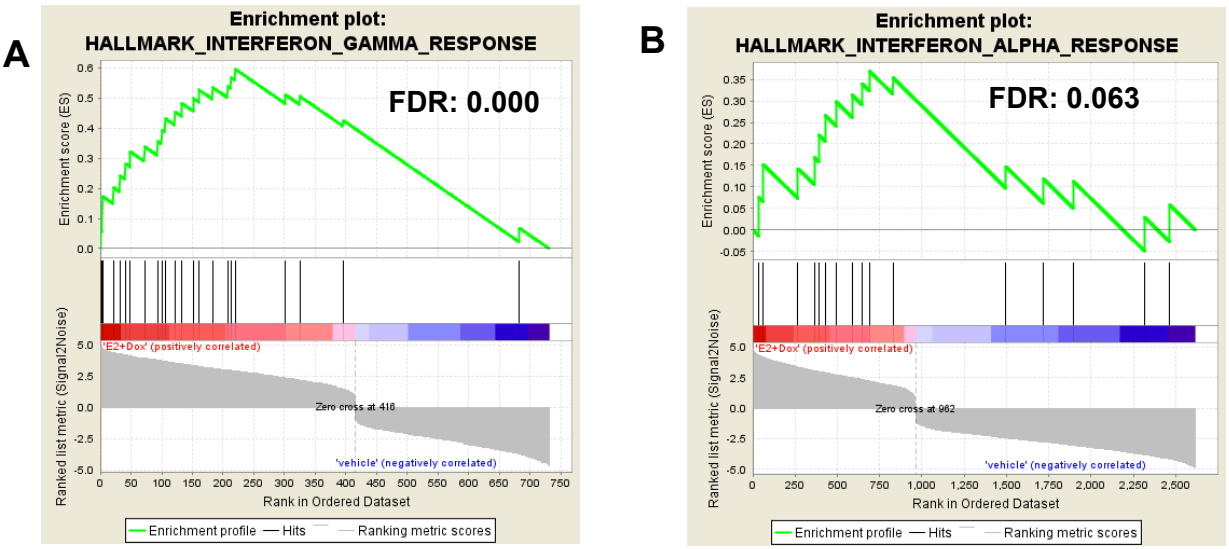

Figure 55: Enrichment of interferon response gene sets in cells treated with E2+Dox. GSEA of genes in pattern 4 (A) and pattern 5 (B) using the hallmark gene sets of MSigDB.

V. DISCUSSION

NF-κB activation, as well as ER-NF-κB crosstalk, is highly associated with aggressive disease and poor patient outcome in women with ER+ breast cancer (77,78,115). However, it is not clear whether NF-κB is a driver or a consequence of aggressive ER+ disease. In this study, we developed multiple ER+ breast cancer cell lines that express an inducible, constitutively active form of the kinase IKKβ, which allowed us to specifically activate the canonical arm of the NF-κB pathway in a controlled fashion. Using these cells, we found that the CA-IKKβ blocks E2-dependent cell proliferation in vitro and tumor growth in vivo. However, ER and CA-IKKβ also work together to promote cell survival. This was particularly evident in vivo, where cells at the primary implantation site survived for up to 60 days despite no palpable tumor growth. These results, in conjunction with the finding that the anti-proliferative effects of CA-IKKβ were reversible, suggest the possibility that CA-IKKβ induced dormant ER+ disease. Moreover, we found that coactivation of ER and the canonical NF-κB pathway promote cell migration and invasion in vitro, through a mechanism involving expansion of a basal-like cell population, as well as both spontaneous and experimental metastasis in vivo. Together, these findings suggest that coactivation of ER and the canonical arm of the NF-κB pathway may promote a dormant, metastatic phenotype in ER+ breast cancer. These findings also implicate IKKβ as a driver of certain features of aggressive ER+ breast cancer and suggest IKKβ as both a potential biomarker and a novel therapeutic target in ER+ breast cancer.

5.1 Constitutively active IKKβ promotes cellular quiescence and tumor dormancy in estrogen receptor positive breast cancer models

Proliferation of ER+ breast cancer cells is known to be driven by estrogen through regulating the expression of E2-target genes involved in G1 to S transition of the cell cycle

(189,196), as well as, rapid membrane-initiated signaling (220). Our findings indicate that activation of IKKβ halts this process in a reversible manner. An anti-proliferative effect of IKKβ is consistent with previous reports from the literature, showing that CA-IKKβ inhibits the proliferation of normal human fibroblasts (221), and that immortalized mouse embryo fibroblasts derived from IKKβ knockout mice exhibit increased proliferation (222).

In contrast to proliferation, we find that IKKβ activation enhances E2-induced cell survival. It has been shown that NF-κB promotes cell survival by inhibiting apoptosis. Several NF-κB target genes, such as cIAP1, cIAP2 and Bcl-xL are known to have anti-apoptotic effects (54,223,224). Studies reported that NF-κB promotes cell survival in a variety of models, including mitotically arrested HeLa cells (223) and Ras transformed mammary cells (150). Furthermore, several studies have emphasized a specific role for IKKβ on cell survival. For example, it has been shown that IKKβ is responsible for promoting survival of ER+ breast cancer cells after irradiation by facilitating double strand break repair (225). Similarly, Sakamoto and colleagues reported that a portion of activated IKKβ can translocate to the nucleus and directly phosphorylate ataxia-telangiectasia mutated (ATM), a critical molecule involved in DNA double-strand break signaling and repair, to promote DNA repair. Thus, IKKβ can inhibit DNA damage mediated apoptosis to promote cell survival and maintain cellular homeostasis (226). Thus, both anti-proliferative and pro-survival effects of IKKβ are consistent with previous findings.

Non-dividing viable cells, as we find with activation of both ER and IKKβ, can be categorized as quiescent or senescent based on the ability of the cell to exit the non-dividing state (46). Our findings that CA-IKKβ reversibly inhibits E2-induced cell proliferation, while enhancing cell survival, indicate that IKKβ-induced growth arrest is due to quiescence rather than senescence. Whether IKKβ induces cellular quiescence in vivo is less clear given that we

were unable to locate cancer cells by histological examination of tissues. We found that primary tumors regress to undetectable levels after 12 days of Dox administration, suggesting cell death to reduce the bulk of the tumor. However, a bioluminescent signal was detectable at the site of the regressing tumors, indicating that at least a portion of the cells survived and were capable of seeding a recurrent tumor upon IKKβ inactivation.

Cellular quiescence has been proposed as one growth arrest mechanism underlying tumor dormancy, which can be defined as the presence of clinically undetectable cancer cells in specific organs that eventually give rise to recurrent tumors after a period of time (46,227). In addition to cellular quiescence, other mechanisms contributing to dormancy include tumor dormancy, in which there is a balance between proliferation and cell death, or cancer cells may undergo very slow proliferation. In both cases there is no increase in tumor burden. One proposed mechanism is angiogenic dormancy, which results from a balance between the pro-angiogenic and anti-angiogenic factors (30,46,228). Immune dormancy has also been proposed, whereby an active immune system keeps proliferating tumor cells in low number (46,229). A common theme in the proposed dormancy mechanisms is the crosstalk between cancer cells and their microenvironment. The exact mechanisms of dormancy termination are poorly understood; however, studies have reported avenues through which the tumor escapes dormancy: i) onset of angiogenesis (angiogenic switch), ii) escape from immunosurveillance, iii) the initiation of interaction with the ECM, iv) genetic and epigenetic changes (30,230).

Our finding, that IKKβ causes both tumor regression and long term cell survival, is controversial. Generally, if cell death exceeds division, then tumors would regress; however, our in vitro results demonstrate that CA-IKKβ enhances survival, and inhibits apoptosis and probably necrosis. How IKKβ causes tumor regression is not clear, but a possible scenario could be that activation of IKKβ induces the expression of NF-κB target genes, such as TNFα

and MMP9, and reverses the tumor associated macrophages (in the microenvironment) from the pro-tumorigenic state to the anti-tumorigenic state, resulting in tumor regression (231,232). An alternative scenario is the enhanced metastatic potential induced by IKKβ activation that might result in cancer cells escaping from the primary tumor. This could explain the decrease of the palpable area of the tumor, which is already non-proliferative.

Dormancy explains the long disease-free interval between the initial diagnosis and treatment of the disease, and occurrence of local or metastatic relapse. Locoregional and distant recurrence require both a tumor initiating potential and a strong proliferative signal which results in the accumulation of a tumor mass exceeding the detection limit (30,227,230). Our animal study results indicate that turning off the activity of IKKβ, by withdrawing Dox from the drinking water of the animals, rescues the strong proliferative signal of E2, resulting in locoregional recurrence of the tumor. Studies have shown that in ovariectomized mice, intracardially injected ER+ breast cancer cells can seed distant organs. Yet, the cells lie dormant as micrometastases and do not exhibit detectable metastases until they are supplemented with E2 (47,233). These findings are in agreement with clinical studies, reporting that stopping endocrine therapy after 5 years of treatment may contribute to late recurrence (42). Indeed, it is proposed that the homing and survival of ER+ cells does not require E2 (47); however, the pathways and mechanisms which allow homing of ER+ breast cancer cells and maintenance of both anti-proliferative and pro-survival pathways in these sites are unknown. Our results propose that CA-IKKβ is a mediator of ER+ breast cancer dormancy by enhancing the survival of the cells and inhibiting the proliferative/growth signal of E2.

5.2 Estrogen and constitutively active IKKβ work together to promote migration, invasion, and metastasis in ER+ breast cancer.

Our results demonstrate that E2 and CA-IKKβ work together to promote cell migration and invasion in vitro, as well as both spontaneous and experimental metastasis in vivo. Individually, we found only modest effects of either E2 treatment or IKKβ activation on migration and invasion. It is generally accepted that ER+ breast cancer cell lines are non-invasive and non-metastatic (234), and that ER signaling inhibits invasion in invasive breast cancer cell lines (110). Yet, several studies have shown that E2 induces migration, invasion, and metastasis of ER+ breast cancer cells in an ER dependent manner (47,190,192,235). We find that E2 treatment of breast cancer cells has a slight to modest effect on cell migration and invasion in vitro and metastasis in vivo. Similarly, we find that activation of IKKβ enhances migration and invasion in vitro. It should be noted that we were unable to test the individual role of IKKβ on metastasis in vivo because the growth of ER+ breast cancer cells is E2-dependent. Nevertheless, our in vitro results are supported by literature, which shows that NF-κB promotes migration and invasion in breast cancer by directly upregulating the expression of mediators, such as IL-6 and miR-21 (236). Generally NF-κB induces the expression of cytokines, such as IL-6 and TNFα, which results in an inflammatory response favoring tumor invasion and metastasis (237). Studies reported that the inhibition of NF-κB using DN-IκBα reduced the invasion of 7,12-dimethylbenz (a) anthracene (DMBA) transformed mammary tumor cells driven by c-Rel subunit (238) and metastasis in Ras transformed epithelial cells (150).

Importantly, we find that coactivation of both ER and IKKβ greatly enhanced migration and invasion in vitro and metastasis to soft organs and bones in vivo. These findings are completely novel and suggest that activation of IKKβ renders ER+ breast cancer more aggressive. This is supported by studies reporting that women with ER+ tumors, which have

constitutively active p50 and p65, represent a subset of patients with increased risk of metastasis (77,78). Also of interest is our finding that cells with ER and IKKβ activation are more likely to metastasize to bone versus ER alone, suggesting that the activation of IKKβ enhances the affinity of the cells to microenvironment of the bone.

Although our findings suggest that ER and CA-IKKβ expand a population of cells expressing basal markers (luminobasal cells) and that this population is responsible for the invasive phenotype observed, it does not explain why the cells preferentially home to the bones. This is because CK5 and CK14 expressions are not clinically associated with bone metastasis in ER+ breast cancer (239,240). And preclinical studies also demonstrate that cardiac injection of initially ER+PR+CK5- cells results in the development of heterogeneous metastases comprising ER-PR-CK5+ population. This observation was not organ specific, yet raises questions about the identity of the cells responsible for metastasis. Thus, we suggest that the luminobasal population induced by activation of IKKβ and treatment with E2 is necessary for the initial invasion of the cells. However, additional signals and factors, known to be regulated by NF-κB, may be responsible for the preferential metastasis to the bones in vivo. One of these factors might be CXCR4, a direct transcriptional target of NF-κB identified as an important determinant in a gene expression signature of breast cancer colonizing to the bones (241). Moreover, NF-κB targets, such as granulocyte macrophage-colony stimulating factor (GM-CSF) (242) and vascular cell adhesion molecule 1 (VCAM-1), have been reported to promote the osteolytic bone metastasis of breast cancer cells in the bones by stimulating osteoclast development (243). Therefore, activation of IKKβ results in the upregulation of NF-κB target genes, mediating the preferential colonization of the cells to the bones. This is of specific clinical implication because the major site of metastases of ER+ luminal cancer is the bone (13,30), which is considered to be the major reservoir of disseminating tumor cells (30).

Interestingly, we identified a substantial number of hemorrhagic lesions on the surface of lungs as a result of ER and IKKβ activation, versus none with E2 alone. Hemorrhage, due to the presence of pulmonary metastatic lesions, has been previously reported in animals (244). We propose that the pulmonary metastases, initiating from IKKβ and E2 activated cells, create a surrounding inflammatory microenvironment resulting in vessel injury and hemorrhagic foci. Several studies have associated hemorrhage to inflammation (245,246). Low levels of TNFα have been shown to mediate hemorrhage in shock-induced acute lung injury (246). TNFα is also reported to inhibit thromobosis and delay arterial occlusion, which enhances bleeding upon vascular injury in mice (247).Therefore, it is likely that TNFα expression in IKKβ activated cells is inducing vessel injury and hemorrhagic lesions. This is clinically important because hemorrhage is considered as one of the radiographic features of pulmonary metastasis in patients (248).

Our results demonstrate that the incidence of metastasis was higher in tumors initiating from E2 and IKKβ activated cells, versus E2 activated cells only. In fact, only a brief pretreatment to activate IKKβ in vitro, rather than a continuous activation of IKKβ in vivo, was sufficient to enhance metastasis compared to E2 treatment. This suggests that transient activation of IKKβ endows the cells with permanent or semi-permanent changes that persist long enough to induce a difference in metastasis between the two treatment groups. The changes are due to differences in metastatic potential and not related to growth because both E2 and E2+Dox pretreated cells formed xenografts with similar growth rates. We suggest three possible explanations for this observation. First, it is possible that CA-IKKβ has long half-life and remains active for prolonged periods in vivo without administration of Dox. Second, the expansion of the luminobasal population of cells, as described below, may be a permanent change, and this population is maintained even in the absence of IKKβ activation. Third, CA-

IKKβ may be expanding the stem-like cell population which enhances metastases. This is supported by studies reporting that stable expression of p65 or CA-IKKβ increases mammosphere formation capacity, a feature of stem-like cells, in ER+ breast cancer cells (249). Other studies reveal that IκBα-DN decreases the portion of CD44+ cells, a marker of stem-like cells, in mouse tumors compared to control. We have not studied the stem-like properties of the luminobasal population expanded upon activation of IKKβ and treatment with E2. Yet, studies have reported an overlap, although not complete, between the CK5+ cells and the tumor initiating cell marker CD44 (250,251). This suggests that the cancer stem-like properties of the expanded luminobasal population may play a role in the metastatic phenotype observed.

5.3. Activation of IKKβ and estrogen receptor promote expansion of cells with a luminobasal phenotype that are responsible for enhanced invasion

To understand how activation of ER and IKKβ might promote metastases, cellular changes associated with invasion were investigated. We initially hypothesized that EMT, the reversible differentiation process by which the cells lose epithelial markers (e.g. E-cadherin) and express mesenchymal markers (e.g. vimentin), might underlie ER and IKKβ induced migration and invasion. This is based on the fact that induction of invasion (252) and metastasis by NF-κB in breast cancer has been previously linked to EMT (150,238). Huber and colleagues used an in vivo model of mammary carcinogenesis to show that inhibition of NF-κB prevented EMT, while constitutive activation of IKKβ promoted EMT, even in the absence of TGFβ, a known EMT regulator (150). In addition, NF-κB has been shown to induce the expression of EMT-related genes, such as MMP9 (167) and serine protease urokinase-type plasminogen activator (uPA) in breast cancer cells (253), and Zeb1, Zeb2, vimentin (203), Twist1 (252), and SNAI1 in mammary epithelial cells (254). In contrast to NF-κB, the effect of E2 on breast cancer EMT is

less clear. Some studies have reported that E2 induces reversible EMT like changes (207) and EMT associated mechanisms in ER+ breast cancer cell (208), while others have reported that ER maintains the expression of E-cadherin and inhibits EMT (204-206). In vivo metastasis studies demonstrated that ER+ breast cancer cells retain their cohesive epithelial nature throughout the metastatic cascade and do not undergo EMT (47).

Our findings indicate that although E2 treatment and IKKβ activation altered cellular morphology in an EMT-like manner and regulated mRNA expression of some EMT markers, they did not regulate the expression of key EMT hallmarks (E-cadherin, vimentin, and fibronectin) at the protein level. One possibility is that the cells might undergo partial or incomplete EMT, which has been shown in primary human carcinomas (255). However, we tested this possibility by the activation of IKKβ and E2 treatment for two weeks, and we found that prolonged treatment does not induce hallmark EMT markers on the protein level. Thus, we did not observe any conclusive evidence of EMT upon IKKβ activation and E2 treatment. This suggests that the observed invasion is not EMT-mediated and that other modes of cancer cell migration and invasion may be involved.

Several studies have reported collective motility in breast cancer (188,256,257). In fact, the majority of solid tumors exhibit features of collective invasion, in which the cells invade surrounding tissues as a cohesive multicellular unit (186,188). Although we did not confirm that the cells are undergoing collective motility, we did examine a series of luminal-basal markers that have been shown to mediate collective motility. Fortier and colleagues reported that the inhibition of the luminal cytokeratins 8 and 18 induced collective invasion in epithelial cells (187); whereas, Cheung and colleagues reported that breast cancer cells expressing basal epithelial markers, such as CK5, CK14 and p63, lead collective invasion. Using a three-dimensional organoid assay, they showed that although only a minority of cells within the organoid

expressed basal markers, the knockdown of either CK14 or p63 was sufficient to inhibit the observed invasion (188). Similar to these reported findings, our results demonstrate that activation of ER and IKKβ inhibits expression of luminal CK8/18 globally and induces expression of basal markers CK5, CK14 and p63 in a small population of cells. Moreover, knockdown of basal markers abolishes the invasive phenotype. These findings demonstrate that CA-IKKβ and E2 work together to expand a population of cells with basal markers responsible for inducing invasion, and this suggests that the cells may be undergoing collective invasion. One difference noted between CA-IKKβ-MCF-7 and CA-IKKβ-T47D cells was the lack of CK14 induction in CA-IKKβ-T47D. Generally, many studies reported differences in protein expression and cellular energetics between MCF-7 and T47D cell lines (157,258).

It has been shown that the expansion of the basal population responsible for collective invasion within the luminal breast cancer cells is not due to proliferation, but rather due to direct acquisition of basal markers by luminal cells (188). In fact, plasticity between luminal and basal cell populations has been suggested in breast cancer (173,185). Although luminal breast cancers primarily consist of ER+/PR+/CK18+ cells, studies have reported that a subpopulation of ER-/PR-/CK5+ cells, termed luminobasal cells, exists in ER+ tumors, and this population is more resistant to both endocrine and chemotherapy compared to the bulk CK5- tumor cells (259). Our studies show that ER and IKKβ cause expansion of CK5+ cells; whereas, reports in the literature indicate this is a progesterone mediated effect. Progesterone induces the expansion of ER-PR-CK5+ cell population, and a transitional ER+PR+CK5+ population is reported (251), which emphasizes the plasticity between the two lineages. ER-PR-CK5+ cells are quiescent, have enhanced invasiveness and self-renewal properties, and are considered as progenitor/stem cells (250). We have not examined the ER or PR status of the observed CK5+ population. However, the above mentioned previous studies suggest this population might be

ER-PR-. Consequently, the CK5+ population observed upon activation of IKKβ and treatment with E2 may not only be mediating invasion, but CK5+ cells may also be progenitor/resistant cells that can escape therapy and initiate new tumors in distant sites. Overall our GSEA reveals enrichment of stem cell gene sets, suggesting the role of IKKβ activation and E2 treatment in conferring stem/progenitor characteristics on ER+ breast cancer cells.

One important finding is the downregulation of two breast cancer differentiation regulators, FoxA1 and Gata3. We propose that the downregulation of Gata3 and FoxA1 is also important in shifting the cell phenotype from a luminal towards a basal identity. This is substantiated by studies reporting that Gata3 is required for the differentiation and commitment of luminal epithelial cells in the mammary gland (179). Knockdown of FoxA1 represses the expression of luminal markers and induces the expression of basal markers in breast cancer cells (180). Therefore, activation of IKKβ and treatment with E2 downregulate the expression FoxA1 and Gata3, and this may be the mechanism underlying the shift in the luminal identity of the cells. This is important clinically because each of Gata3 and FoxA1 is considered as a strong predictor of good clinical outcome in ER+ breast cancer (260) (261).

We also propose that downregulation of Gata3 and FoxA1 may be promoting the invasive metastatic phenotype observed. This is because Gata3 expression in human breast cancer cell lines is inversely correlated with their metastatic capability (262). Ectopic expression of Gata3 inhibits invasion/metastasis of MDA-MB-231 breast cancer cells, and the knockdown of Gata3 in MCF-7 inhibits E-cadherin expression and enhances motility/metastasis of the cells (263). Similarly, the silencing of FoxA1 induces a migratory/invasive phenotype, and enhances the aggressiveness of breast cancer cell lines (180). These studies suggest a role for Gata3 and FoxA1 downregulation in the observed invasion, potentially indirectly, by shifting the

identity of the cells and allowing for the expansion of the basal population responsible for invasion.

5.4 Mechanisms of estrogen receptor and constitutively active IKKβ crosstalk that may underlie a dormant, metastatic phenotype

Our findings demonstrate that ER and CA-IKKβ both work together and oppose one another to have profound effects on breast cancer cell phenotype: i) CA-IKKβ represses ER dependent proliferation in an NF-κB-independent manner, ii) CA-IKKβ enhances E2-dependent cell survival, and iii) E2 and CA-IKKβ, acting via ER and NF-κB, respectively, work together to promote cell migration and invasion.

Our results indicate that CA-IKKβ inhibits E2-induced proliferation, independently of downstream NF-κB activity, and this is associated with a decrease in the expression cyclin D1, and E2F target genes. Several potential NF-κB-independent roles of IKKβ have been reported that could explain the anti-proliferative effect observed. For example, IKKβ phosphorylates aurora kinase A (AURKA), a key regulator of a number of steps in mitosis such as bipolar spindle assembly and centrosome maturation (264). IKKβ-induced phosphorylation targets AURKA for βTRCP-mediated degradation (265). Downregulation of AURKA significantly inhibits E2-induced S phase of the cell cycle, as well as anchorage-dependent and -independent growth of MCF-7 cells (266). Recently, it has been shown that the knockdown of AURKA decreases the expression of cyclin D1, an important E2 target in early G1 phase that facilitates activation of cyclin-dependent kinases (CDK) and entry to S phase, in breast cancer cells. Notably, significant positive correlation of AURKA with cyclin D1 expression could be observed in ER+ breast tumors (267,268). Thus, AURKA downregulation/ degradation by IKKβ, may result in downregulation of cyclin D1, inhibition of cell cycle entry, and E2-induced proliferation.

A second possible mechanism involves the repression of E2F activity. Downstream of active CDK is the retinoblastoma/E2F pathway. Early in the G1 phase, the activated cyclin D-CDK4 complex phosphorylates retinoblastoma leading to its degradation and the release of E2F, which mediates the transcription of genes necessary for S phase entry and DNA replication and synthesis (269). Araki and colleagues reported that CA-IKKβ inhibits the proliferation of normal human fibroblasts by suppressing the expression of E2F responsive genes. Constitutively active IKKβ directly phosphorylates the E2F repressor, E2F4. This results in the nuclear accumulation of E2F4 and enhances DNA binding of the E2F4/p130 repressor complex. This suggests that the direct effect of CA-IKKβ on E2F mediated gene expression may also play a role in the observed anti-proliferative phenotype (221).

Estrogen stimulates both proliferation and survival of ER+ breast tumors. In stimulating survival, ER regulates the expression of genes that prevent apoptosis and maintain the mitochondrial membrane integrity, such as Bcl-2 and Bcl-xL (270,271). Frasor and colleagues performed a gene expression profiling study in MCF-7 cells and reported a wide range of E2-dependent cell survival regulation, including the upregulation of anti-apoptotic factors and the downregulation pro-apoptotic factors (272). Our results reveal that CA-IKKβ inhibited ER dependent proliferation. Yet, these two players worked together to enhance cell survival both in vitro and in vivo. Each of ER and NF-κB are potent, pro-survival factors in breast cancer (150,270). Previous studies reported that ER and NF-κB cooperate to promote survival of breast cancer cells in an inhibitor of apoptosis (IAP)-dependent manner. More specifically, E2 and TNFα synergistically upregulated one IAP family member, BIRC3 (cIAP2), which plays an essential role in breast cancer cell survival (115,119). Our results demonstrate that E2 and CA-IKKβ recapitulate the effect of E2 and TNFα on the BIRC3 gene expression, suggesting a potential role for BIRC3 in E2 and CA-IKKβ enhanced cell survival. One difference noted

between CA-IKKβ-MCF-7 and CA-IKKβ-T47D cells was that E2 enhanced apoptosis of CA-IKKβ-T47D cells, an effect that was abolished upon IKKβ activation. The apoptotic effect of E2 on CA-IKKβ-T47D cells appears to be associated with E2-induced proliferation, because the net result is an increase in cell number upon treatment with E2. This could be attributed to the reported differences in the apoptotic mechanisms between MCF-7 and T47D cell lines (159). Moreover, T47D cells have been reported to express a mutant form of the tumor suppressor p53 compared to MCF-7 that express the wild type (158).

Cooperation between ER and NF-κB also proved to underlie the invasive phenotype observed upon activation of both ER and IKKβ. Inhibition of either transcription factor abolished the invasive phenotype, indicating that both are necessary for invasion by causing an expansion of a small population of cells possessing basal markers and mediating invasion. This population was too small to be quantified; yet, we were able to observe the increase in mRNA expression of CK5 in CA-IKKβ-MCF-7 cells. This increase proved to be ER and NF-κB dependent. Axlund and colleagues reported that the expansion of CK5+ population in ER+ breast cancer cells is PR and not ER dependent (250). Thus we propose that the increase in CK5 population could be indirectly mediated by ER and NF-κB. This is because we observe that the activation of IKKβ and treatment with E2 upregulate the expression of the progesterone receptor (PR) concomitantly with the expansion of CK5 population. It is reported that direct phosphorylation of PR by kinases, like MAPK and CDK2, modifies its transcriptional activity, and this may result in ligand-independent activity of the receptor (273). Interestingly, CA-IKKβ activates MAPK, suggesting a ligand-independent effect of PR, as an underlying mechanism of the expansion of CK5+ population.

Underlying these profound phenotypic changes are equally profound gene regulatory changes. In fact, gene expression profiling revealed different patterns of CA-IKKβ and E2

crosstalk: i) transrepression (i.e. genes regulated by E2 or CA-IKKβ that are reversed/repressed by CAIKKβ or E2, respectively), ii) no crosstalk (i.e. genes regulated by E2 or CA-IKKβ and not affected by CA-IKKβ or E2, respectively), and iii) coregulation (i.e. genes regulated similarly by CA-IKKβ and E2). Our results are in agreement with previous studies by our lab (115) reporting that the responses to E2 and NF-κB signaling can potentially create novel synergistic and antagonistic responses. Frasor and colleagues reported that in MCF-7 cells treated with E2 and TNFα, transrepression, as well as prominent positive crosstalk between ER and NF-κB, could be observed. Gene-specific studies revealed that ER and p65 cooperate in order to synergistically regulate expression of genes involved in cell survival and endocrine resistance. Three examples of co-operation upon treatment with E2 and TNFα have been reported: 1) enhanced recruitment of both p65 and ER to PTGES estrogen response elements (117), 2) ER mediated recruitment of p65 to a latent NF-κB response element on the promoter of ABCG2 (118), and 3) p65 mediated stabilization of ER occupancy on the promoter of BIRC3 (120). Recently, by using global run-on coupled with deep sequencing technology (GRO-seq), the Kraus group reported that TNFα signaling altered the transcriptome of MCF-7 cells through extensive remodeling of ER enhancer landscape in an NF-κB and FoxA1 dependent manner. TNFα induced redistribution of the pioneer factor FoxA1, creating new possibilities for ER binding. In fact, TNFα signaling exposed latent ER enhancers, which allowed ER to access sets of ER enhancers demarcated by FoxA1 or NF-κB (274).

GSEA revealed enrichment of different gene sets representing responses that may be playing a role in the quiescent/invasive phenotype observed upon activation of IKKβ and treatment with E2:

1. Enrichment of unfolded protein response (UPR) gene sets: UPR may play a role in the enhanced survival observed with CA-IKKβ and E2. It has been shown that

cells activate UPR in response to endoplasmic reticulum stress to both promote cell survival and to restore endoplasmic reticulum homeostasis. However, if stress persists and homeostatsis cannot be restored, cell death mechanisms are activated. Studies have reported that estrogen promotes an adaptive UPR response that protects breast cancer cells against UPR-mediated apoptosis (216). It is reported that if coupled with tumor dormancy, UPR protects the tumor cells from apoptosis (215). Elevated expression of UPR gene signature is correlated with tamoxifen resistance, reduced time to recurrence, and poor survival in ER+ breast cancer (216).

2. Enrichment of glycolysis gene sets: Under conditions of limited oxygen, cells redirect pyruvate away from the mitochondrial oxidative phosphorylation and generate lactic acid in a process called glycolysis. Lactic acid, a byproduct of glycolysis, is known to play an important role cancer cell migration, immune escape, and metastasis (213). Thus, glycolysis may be playing a role in the metastatic phenotype observed.

3. Enrichment of interferon response gene sets: Dysregulation of interferon signaling, resulting in constitutive overexpression of interferon-stimulated genes contributes to endocrine resistance. Interferon-stimulated genes IFITM1 and PLSCR1 are constitutively overexpressed in aromatase inhibitor resistant breast cancer cells and tumors. Knockdown of IFITM1 significantly inhibits cell proliferation, migration and invasion of the cells (219). Both IFITM1 and PLSCR1 are included in the group of interferon alpha response enriched genes up-regulated by E2 and Dox, suggesting a role of CA-IKKβ and E2 in endocrine therapy resistance.

Future studies are needed to investigate the roles of UPR, glycolysis, and interferon signaling in the dormant/metastatic phenotype induced by CA-IKKβ and E2.

5.5 Clinical significance

Our study presents several novel findings that may be of direct clinical relevance. First, we find that activation of IKKβ induces dormancy in ER+ breast cancer. This is significant because dormancy is a major clinical problem in ER+ breast cancer. Late recurrence occurs in more than 50% of the patients with ER+ tumors, from 5 to more than 20 years after initial diagnosis (30,42,230). This suggests that the cells lie dormant until they are triggered by a proliferation stimulatory signal that initiates the growth of clinically detectable tumors locoregionally or at distant sites. Clinical studies report that stopping endocrine therapy after 5 years may contribute to late recurrence (42). In fact results from the Adjuvant Tamoxifen: Longer Against Shorter (ATLAS) clinical trial demonstrate that continuing tamoxifen for 10 years reduces recurrence and mortality in patients compared to 5 years of tamoxifen only (275). This could be explained by preclinical studies demonstrating that E2 is necessary for growth of tumors and metastases, but not for homing and survival of dormant cancer cells. Yet, the pathways and mechanisms which allow for maintenance of both anti-proliferative and pro-survival pathways in these sites are unknown. Our study demonstrates IKKβ as a mediator of dormancy by inhibiting the proliferative effect of E2 and enhancing the survival of tumor cells.

Second, we find that activation of IKKβ and E2 enhances the metastasis of ER+ tumors compared to E2 alone. This is clinically significant because ~90% of breast cancer related deaths are due to metastasis and not the primary tumor itself. Estrogen receptor positive tumors represent ~75% of breast cancers. Indeed, ~70% of distant recurrent metastatic breast tumors are ER+ (13).

Third, we find that activation of IKKβ enhances metastasis to the spine and bones. This is clinically significant because post-operative distant recurrence arises from disseminated tumor cells, which are frequently found in bone marrow of patients, yet, without any clinical signs of metastasis (30). Most importantly, the bones are the main sites of metastasis in ER+ tumors, representing more than 49% of ER+ breast cancer metastases (13,233).

Fourth, we find that activation of IKKβ inhibits E2-induced proliferation and renders the cells quiescent/invasive. This is clinically significant because chemotherapy and endocrine therapy target proliferating cells. Cells with activated IKKβ are, thus, potentially non-targetable by these drugs. This suggests that dormant cells with activated IKKβ may escape from the primary tumor, potentially before the clinical detection of the tumors, and resist treatment for a long period of time. They are then triggered by an unknown signal and/or the termination of endocrine therapy, resulting in emergence of locoregional or distant metastases and recurrence.

Taken together, constitutively active IKKβ may prove to be a useful biomarker, clinically. It could potentially be used to predict tumors destined to recur and develop metastasis. So far none of the developed IKKβ inhibitors made its way to the clinic, potentially, due to the non-specificity of these drugs. Thus, further studies into the role of CA-IKKβ in ER+ breast cancer metastasis and dormancy may define new specific therapeutic targets and therapeutic strategies with minimum side effects in order to help women with ER+ breast tumors.

5.6 Future directions

Our findings raise several important and interesting questions that can be addressed in future work. First, our results suggest that the activation of IKKβ results in a more aggressive/dormant/metastatic phenotype of ER+ breast cancer; however, the critical mediators of CA-IKKβ-induced dormancy maintenance and escape are not clear. To investigate this, we

propose to use a genome-wide library of CRISPR-Cas9 sgRNAs of CA-IKKβ expressing cells in a xenograft model. Mutagenesis followed by DNA sequencing will help us identify genes and mediators necessary for maintaining IKKβ dormancy.

Second, our results suggest that activation of IKKβ inhibits E2-induced proliferation and induces quiescence, which potentially renders the cells non-targetable by therapy. Yet, we have not examined the effect of endocrine therapy on the invasive/metastatic phenotype observed, which is ER dependent. Tamoxifen is an ER agonist/antagonist. Thus, it is questionable whether activation of IKKβ and treatment with tamoxifen enhances migration/invasion/ metastasis or not. In order to study this, we propose to investigate the effect of tamoxifen treatment and activation of IKKβ on ER+ cells, both in vitro and in vivo.

Third, our results suggest that activation of IKKβ induces a dormant, metastatic phenotype are based on two ER+ cell lines that have long been used as preclinical models of ER+ breast cancer. In order to relate our findings to the clinic, we need to investigate the relationship between IKKβ expression and activity, and patient outcome. Since IKKβ activated cells are metastatic, they could potentially be detected by IHC in the positive lymph nodes removed from patients during surgery. To do this, we propose to investigate the expression of IKKβ and its activated/phosphorylated form in lymph node specimens from patients. Kaplan-Meier analysis could be used to compare staining patterns to time of recurrence. Associations among staining scores and other clinical variables, such as tumor grade, tumor size, nodal status, and expression of hormone receptors (ER, PR) could also be performed.

CITED LITERATURE

1. Department of Defense Breast Cancer Research Program, May 2013. The Breast Cancer Landscape. 2013.

2. National Cancer Institute. SEER Stats Fact Sheets: Breast Cancer. 2015; Available at: http://seer.cancer.gov/statfacts/html/breast.html. Accessed 06/28, 2015.

3. American Cancer Society. Breast Cancer Facts & Figures. 2015; Available at: http://www.cancer.org/acs/groups/content/@editorial/documents/document/acspc- 044552.pdf. Accessed 06/28, 2015.

4. Susan G. Komen. Breast Cancer Statistics. 2015; Available at: http://ww5.komen.org/BreastCancer/Statistics.html. Accessed 06/28, 2015.

5. Prat A, Perou CM. Deconstructing the molecular portraits of breast cancer. Mol Oncol 2011 Feb;5(1):5-23.

6. Perou CM, Sorlie T, Eisen MB, van de Rijn M, Jeffrey SS, Rees CA, et al. Molecular portraits of human breast tumours. Nature 2000 Aug 17;406(6797):747-752.

7. Sorlie T, Tibshirani R, Parker J, Hastie T, Marron JS, Nobel A, et al. Repeated observation of breast tumor subtypes in independent gene expression data sets. Proc Natl Acad Sci U S A 2003 Jul 8;100(14):8418-8423.

8. Sorlie T, Perou CM, Tibshirani R, Aas T, Geisler S, Johnsen H, et al. Gene expression patterns of breast carcinomas distinguish tumor subclasses with clinical implications. Proc Natl Acad Sci U S A 2001 Sep 11;98(19):10869-10874.

9. Rouzier R, Perou CM, Symmans WF, Ibrahim N, Cristofanilli M, Anderson K, et al. Breast cancer molecular subtypes respond differently to preoperative chemotherapy. Clin Cancer Res 2005 Aug 15;11(16):5678-5685.

10. Prat A, Parker JS, Karginova O, Fan C, Livasy C, Herschkowitz JI, et al. Phenotypic and molecular characterization of the claudin-low intrinsic subtype of breast cancer. Breast Cancer Res 2010;12(5):R68.

11. Herschkowitz JI, Simin K, Weigman VJ, Mikaelian I, Usary J, Hu Z, et al. Identification of conserved gene expression features between murine mammary carcinoma models and human breast tumors. Genome Biol 2007;8(5):R76.

12. Dunnwald LK, Rossing MA, Li CI. Hormone receptor status, tumor characteristics, and prognosis: a prospective cohort of breast cancer patients. Breast Cancer Res 2007;9(1):R6.

13. Kennecke H, Yerushalmi R, Woods R, Cheang MCU, Voduc D, Speers CH, et al. Metastatic behavior of breast cancer subtypes. J Clinical Oncol Oncology 2010;28(20):3271-3277.

14. Garcia-Becerra R, Santos N, Diaz L, Camacho J. Mechanisms of Resistance to Endocrine Therapy in Breast Cancer: Focus on Signaling Pathways, miRNAs and Genetically Based Resistance. Int J Mol Sci 2012 Dec 20;14(1):108-145.

15. Carroll JS, Hall GF, Wang Q, Bekiranov S, Sementchenko V, Fox EA, et al. Genome-wide analysis of estrogen receptor binding sites. Nat Genet 2006;38(11):1289-1297.

16. Khan S, Abdelrahim M, Samudio I, Safe S. Estrogen receptor/Sp1 complexes are required for induction of cad gene expression by 17beta-estradiol in breast cancer cells. Endocrinology 2003 Jun;144(6):2325-2335.

17. Kushner PJ, Agard DA, Greene GL, Scanlan TS, Shiau AK, Uht RM, et al. Estrogen receptor pathways to AP-1. J Steroid Biochem Mol Biol 2000 Nov 30;74(5):311-317.

18. Dahlman-Wright K, Qiao Y, Jonsson P, Gustafsson JA, Williams C, Zhao C. Interplay between AP-1 and estrogen receptor alpha in regulating gene expression and proliferation networks in breast cancer cells. Carcinogenesis 2012 Sep;33(9):1684-1691.

19. Hsu P, Pereira JS, Lopez R, Russo J, Wang Q, Lamartiniere CA, et al. Estrogen-mediated epigenetic repression of large chromosomal regions through DNA looping. Genome Res 2010;20(6):733-744.

20. Weigel NL, Zhang Y. Ligand-independent activation of steroid hormone receptors. J Mol Med 1998;76(7):469-479.

21. Barone I, Brusco L, Fuqua SAW. Estrogen receptor mutations and changes in downstream gene expression and signaling. Clin Cancer Res 2010;16(10):2702-2708.

22. Prossnitz ER, Arterburn JB, Smith HO, Oprea TI, Sklar LA, Hathaway HJ. Estrogen signaling through the transmembrane G protein-coupled receptor GPR30. Annu Rev Physiol 2008;70(1):165-190.

23. Vrtacnik P, Ostanek B, Mencej-Bedrac S, Marc J. The many faces of estrogen signaling. Biochem Med (Zagreb) 2014 Oct 15;24(3):329-342.

24. Jordan VC. Selective estrogen receptor modulation: concept and consequences in cancer. Cancer cell 2004;5(3):207-213.

25. Wittmann BM, Sherk A, McDonnell DP. Definition of functionally important mechanistic differences among selective estrogen receptor down-regulators. Cancer Res 2007 Oct 1;67(19):9549-9560.

26. Goss PE, Strasser K. Aromatase inhibitors in the treatment and prevention of breast cancer. J Clinical Oncol 2001;19(3):881-894.

27. Blok EJ, Derks MG, van der Hoeven JJ, van de Velde CJ, Kroep JR. Extended adjuvant endocrine therapy in hormone-receptor positive early breast cancer: current and future evidence. Cancer Treat Rev 2015 Mar;41(3):271-276.

28. Vogel VG, Costantino JP, Wickerham DL, Cronin WM, Cecchini RS, Atkins JN, et al. Effects of tamoxifen vs raloxifene on the risk of developing invasive breast cancer and other disease outcomes: the NSABP Study of Tamoxifen and Raloxifene (STAR) P-2 trial. JAMA 2006 Jun 21;295(23):2727-2741.

29. Clarke R, Wang Y, Hilakivi-Clarke LA, Liu MC, Bouker KB, Gu Z, et al. Antiestrogen resistance in breast cancer and the role of estrogen receptor signaling. Oncogene 2003;22(47):7316-7339.

30. Zhang XH, Giuliano M, Trivedi MV, Schiff R, Osborne CK. Metastasis dormancy in estrogen receptor-positive breast cancer. Clin Cancer Res 2013 Dec 1;19(23):6389-6397.

31. Gutierrez MC, Detre S, Johnston S, Mohsin SK, Shou J, Allred DC, et al. Molecular changes in tamoxifen-resistant breast cancer: relationship between estrogen receptor, HER-2, and p38 mitogen-activated protein kinase. J Clin Oncol 2005 Apr 10;23(11):2469-2476.

32. Schiff R, Massarweh S, Shou J, Osborne CK. Breast cancer endocrine resistance: how growth factor signaling and estrogen receptor coregulators modulate response. Clin Cancer Res 2003 Jan;9(1 Pt 2):447S-54S.

33. Santen RJ, Fan P, Zhang Z, Bao Y, Song RX, Yue W. Estrogen signals via an extra-nuclear pathway involving IGF-1R and EGFR in tamoxifen-sensitive and -resistant breast cancer cells. Steroids 2009 Jul;74(7):586-594.

34. Murphy LC, Seekallu SV, Watson PH. Clinical significance of estrogen receptor phosphorylation. Endocr Relat Cancer 2011 Jan 19;18(1):R1-14.

35. Le Romancer M, Poulard C, Cohen P, Sentis S, Renoir JM, Corbo L. Cracking the estrogen receptor's posttranslational code in breast tumors. Endocr Rev 2011 Oct;32(5):597-622.

36. Arpino G, Wiechmann L, Osborne CK, Schiff R. Crosstalk between the estrogen receptor and the HER tyrosine kinase receptor family: molecular mechanism and clinical implications for endocrine therapy resistance. Endocr Rev 2008 Apr;29(2):217-233.

37. Zhang XH, Giuliano M, Trivedi MV, Schiff R, Osborne CK. Metastasis dormancy in estrogen receptor-positive breast cancer. Clin Cancer Res 2013 Dec 1;19(23):6389-6397.

38. Karrison TG, Ferguson DJ, Meier P. Dormancy of mammary carcinoma after mastectomy. J Natl Cancer Inst 1999 Jan 6;91(1):80-85.

39. Mittempergher L, Saghatchian M, Wolf DM, Michiels S, Canisius S, Dessen P, et al. A gene signature for late distant metastasis in breast cancer identifies a potential mechanism of late recurrences. Mol Oncol 2013 Oct;7(5):987-999.

40. Blows FM, Driver KE, Schmidt MK, Broeks A, van Leeuwen FE, Wesseling J, et al. Subtyping of breast cancer by immunohistochemistry to investigate a relationship between subtype and short and long term survival: a collaborative analysis of data for 10,159 cases from 12 studies. PLoS Med 2010 May 25;7(5):e1000279.

41. Early Breast Cancer Trialists' Collaborative Group (EBCTCG), Davies C, Godwin J, Gray R, Clarke M, Cutter D, et al. Relevance of breast cancer hormone receptors and other factors to the efficacy of adjuvant tamoxifen: patient-level meta-analysis of randomised trials. Lancet 2011 Aug 27;378(9793):771-784.

42. Burstein HJ, Griggs JJ. Deep time: the long and the short of adjuvant endocrine therapy for breast cancer. J Clin Oncol 2012 Mar 1;30(7):684-686.

43. Bliss JM, Kilburn LS, Coleman RE, Forbes JF, Coates AS, Jones SE, et al. Disease-related outcomes with long-term follow-up: an updated analysis of the intergroup exemestane study. J Clin Oncol 2012 Mar 1;30(7):709-717.

44. Mauriac L, Keshaviah A, Debled M, Mouridsen H, Forbes JF, Thurlimann B, et al. Predictors of early relapse in postmenopausal women with hormone receptor-positive breast cancer in the BIG 1-98 trial. Ann Oncol 2007 May;18(5):859-867.

45. Regan MM, Neven P, Giobbie-Hurder A, Goldhirsch A, Ejlertsen B, Mauriac L, et al. Assessment of letrozole and tamoxifen alone and in sequence for postmenopausal women with steroid hormone receptor-positive breast cancer: the BIG 1-98 randomised clinical trial at 8.1 years median follow-up. Lancet Oncol 2011 Nov;12(12):1101-1108.

46. Aguirre-Ghiso JA. Models, mechanisms and clinical evidence for cancer dormancy. Nat Rev Cancer 2007 Nov;7(11):834-846.

47. Ganapathy V, Banach-Petrosky W, Xie W, Kareddula A, Nienhuis H, Miles G, et al. Luminal breast cancer metastasis is dependent on estrogen signaling. Clin Exp Metastasis 2012;29(5):493-509.

48. Zheng WQ, Lu J, Zheng JM, Hu FX, Ni CR. Variation of ER status between primary and metastatic breast cancer and relationship to p53 expression*. Steroids 2001 Dec;66(12):905-910.

49. Hoehn JL, Plotka ED, Dickson KB. Comparison of estrogen receptor levels in primary and regional metastatic carcinoma of the breast. Ann Surg 1979 Jul;190(1):69-71.

50. Yu M, Bardia A, Aceto N, Bersani F, Madden MW, Donaldson MC, et al. Cancer therapy. Ex vivo culture of circulating breast tumor cells for individualized testing of drug susceptibility. Science 2014 Jul 11;345(6193):216-220.

51. Toy W, Shen Y, Won H, Green B, Sakr RA, Will M, et al. ESR1 ligand-binding domain mutations in hormone-resistant breast cancer. Nat Genet 2013 Dec;45(12):1439-1445.

52. Erstad DJ, Cusack JCJ. Targeting the NF-kB Pathway in Cancer Therapy. Sur Oncol Clin N Am 2013;22(4):705-746.

53. Li Q, Verma IM. NF-kappaB regulation in the immune system. Nat Rev Immunol 2002 Oct;2(10):725-734.

54. DiDonato JA, Mercurio F, Karin M. NF-kappaB and the link between inflammation and cancer. Immunol Rev 2012 Mar;246(1):379-400.

55. Karin M, Cao Y, Greten FR, Li ZW. NF-kappaB in cancer: from innocent bystander to major culprit. Nat Rev Cancer 2002 Apr;2(4):301-310.

56. Chariot A. The NF-kappaB-independent functions of IKK subunits in immunity and cancer. Trends Cell Biol 2009 Aug;19(8):404-413.

57. Oeckinghaus A, Hayden MS, Ghosh S. Crosstalk in NF-kappaB signaling pathways. Nat Immunol 2011 Jul 19;12(8):695-708.

58. Vallabhapurapu S, Karin M. Regulation and function of NF-kappaB transcription factors in the immune system. Annu Rev Immunol 2009;27:693-733.

59. Espinosa L, Margalef P, Bigas A. Non-conventional functions for NF-kappaB members: the dark side of NF-kappaB. Oncogene 2015 Apr 30;34(18):2279-2287.

60. Hanahan D, Weinberg RA. Hallmarks of Cancer: The Next Generation. Cell 2011;144(5):646-674.

61. Baumgarten SC, Frasor J. Minireview: Inflammation: an instigator of more aggressive estrogen receptor (ER) positive breast cancers. Mol Endocrinol (Baltimore, Md.) 2012;26(3):360-371.

62. Terry MB, Gammon MD, Zhang FF, Tawfik H, Teitelbaum SL, Britton JA, et al. Association of frequency and duration of aspirin use and hormone receptor status with breast cancer risk. JAMA 2004 May 26;291(20):2433-2440.

63. Irahara N, Miyoshi Y, Taguchi T, Tamaki Y, Noguchi S. Quantitative analysis of aromatase mRNA expression derived from various promoters (I.4, I.3, PII and I.7) and its association with expression of TNF-alpha, IL-6 and COX-2 mRNAs in human breast cancer. Int J Cancer 2006 Apr 15;118(8):1915-1921.

64. Sas L, Lardon F, Vermeulen P, Hauspy J, Van Dam P, Pauwels P, et al. The interaction between ER and NFκB in resistance to endocrine therapy. Breast Cancer Res 2012;14(4):212-212.

65. Hennighausen L, Robinson GW. Signaling pathways in mammary gland development. Dev Cell 2001;1(4):467-475.

66. Sindhu Singh, Qian Shi, Shannon T. Bailey, Marek J. Palczewski, Arthur B. Pardee, J. Dirk Iglehart, et al. Nuclear factor-κB activation: a molecular therapeutic target for estrogen receptor–negative and epidermal growth factor receptor family receptor–positive human breast cancer. Mol Cancer Ther 2007;6(7):1973.

67. Cao Y, Luo J, Karin M. IkappaB kinase alpha kinase activity is required for self-renewal of ErbB2/Her2-transformed mammary tumor-initiating cells. Proc Natl Acad Sci U S A 2007;104(40):15852.

68. Kim DW, Sovak MA, Zanieski G, Nonet G, Romieu-Mourez R, Lau AW, et al. Activation of NF-kappaB/Rel occurs early during neoplastic transformation of mammary cells. Carcinogenesis 2000 May;21(5):871-879.

69. Connelly L, Barham W, Onishko HM, Sherrill T, Chodosh LA, Blackwell TS, et al. Inhibition of NF-kappa B activity in mammary epithelium increases tumor latency and decreases tumor burden. Oncogene 2011;30(12):1402-1412.

70. Nakshatri H, Bhat-Nakshatri P, Martin D, Goulet R,Jr, Sledge G,Jr. Constitutive activation of NF-kappaB during progression of breast cancer to hormone-independent growth. Mol Cell Biol 1997;17(7):3629-3639.

71. Sovak MA, Bellas RE, Kim DW, Zanieski GJ, Rogers AE, Traish AM, et al. Aberrant nuclear factor-kappaB/Rel expression and the pathogenesis of breast cancer. J Clin Invest 1997;100(12):2952-2960.

72. Nakshatri H, Goulet RJ,Jr. NF-kappaB and breast cancer. Curr Probl Cancer 2002 Sep-Oct;26(5):282-309.

73. Cogswell PC, Guttridge DC, Funkhouser WK, Baldwin J,A S. Selective activation of NF-kappa B subunits in human breast cancer: potential roles for NF-kappa B2/p52 and for Bcl-3. Oncogene 2000;19(9):1123.

74. Romieu-Mourez R, Landesman-Bollag E, Seldin DC, Traish AM, Mercurio F, Sonenshein GE. Roles of IKK kinases and protein kinase CK2 in activation of nuclear factor-kappaB in breast cancer. Cancer Res 2001;61(9):3810.

75. Biswas DK, Dai SC, Cruz A, Weiser B, Graner E, Pardee AB. The nuclear factor kappa B (NF-kappa B): a potential therapeutic target for estrogen receptor negative breast cancers. Proc Natl Acad Sci U S A 2001 Aug 28;98(18):10386-10391.

76. Zhou XL, Fan W, Yang G, Yu MX. The clinical significance of PR, ER, NF- kappa B, and TNF- alpha in breast cancer. Dis Markers 2014;2014:494581.

77. Jones RL, Rojo F, A'Hern R, Villena N, Salter J, Corominas JM, et al. Nuclear NF-kappaB/p65 expression and response to neoadjuvant chemotherapy in breast cancer. J Clin Pathol 2011 Feb;64(2):130-135.

78. Zhou Y, Eppenberger-Castori S, Marx C, Yau C, Scott GK, Eppenberger U, et al. Activation of nuclear factor-kappaB (NFkappaB) identifies a high-risk subset of hormone-dependent breast cancers. Int J Biochem Cell Biol 2005 May;37(5):1130-1144.

79. Biswas DK, Shi Q, Baily S, Strickland I, Ghosh S, Pardee AB, et al. NF-kappa B activation in human breast cancer specimens and its role in cell proliferation and apoptosis. Proc Natl Acad Sci U S A 2004 Jul 6;101(27):10137-10142.

80. Boehm JS, Zhao JJ, Yao J, Kim SY, Firestein R, Dunn IF, et al. Integrative genomic approaches identify IKBKE as a breast cancer oncogene. Cell 2007 Jun 15;129(6):1065-1079.

81. Streicher KL, Willmarth NE, Garcia J, Boerner JL, Dewey TG, Ethier SP. Activation of a nuclear factor kappaB/interleukin-1 positive feedback loop by amphiregulin in human breast cancer cells. Mol Cancer Res 2007 Aug;5(8):847-861.

82. Bist P, Leow SC, Phua QH, Shu S, Zhuang Q, Loh WT, et al. Annexin-1 interacts with NEMO and RIP1 to constitutively activate IKK complex and NF-kappaB: implication in breast cancer metastasis. Oncogene 2011 Jul 14;30(28):3174-3185.

83. Bhat-Nakshatri P, Sweeney CJ, Nakshatri H. Identification of signal transduction pathways involved in constitutive NF-kappaB activation in breast cancer cells. Oncogene 2002 Mar 27;21(13):2066-2078.

84. Pianetti S, Arsura M, Romieu-Mourez R, Coffey RJ, Sonenshein GE. Her-2/neu overexpression induces NF-kappaB via a PI3-kinase/Akt pathway involving calpain-mediated degradation of IkappaB-alpha that can be inhibited by the tumor suppressor PTEN. Oncogene 2001 Mar 15;20(11):1287-1299.

85. Frasor J, El-Shennawy L, Stender JD, Kastrati I. NFkappaB affects estrogen receptor expression and activity in breast cancer through multiple mechanisms. Mol Cell Endocrinol 2014 Oct 18, doi: 10.1016/j.mce.2014.09.013.

86. Montagut C, Tusquets I, Ferrer B, Corominas JM, Bellosillo B, Campas C, et al. Activation of nuclear factor-kappa B is linked to resistance to neoadjuvant

chemotherapy in breast cancer patients. Endocr Relat Cancer 2006 Jun;13(2):607-616.

87. Liu H, Lee ES, Gajdos C, Pearce ST, Chen B, Osipo C, et al. Apoptotic action of 17beta-estradiol in raloxifene-resistant MCF-7 cells in vitro and in vivo. J Natl Cancer Inst 2003 Nov 5;95(21):1586-1597.

88. Kubo M, Kanaya N, Petrossian K, Ye J, Warden C, Liu Z, et al. Inhibition of the proliferation of acquired aromatase inhibitor-resistant breast cancer cells by histone deacetylase inhibitor LBH589 (panobinostat). Breast Cancer Res Treat 2013 Jan;137(1):93-107.

89. Oida K, Matsuda A, Jung K, Xia Y, Jang H, Amagai Y, et al. Nuclear factor-kB plays a critical role in both intrinsic and acquired resistance against endocrine therapy in human breast cancer cells. Sci Rep 2014 Feb 17;4:4057.

90. Riggins RB, Zwart A, Nehra R, Clarke R. The nuclear factor kappa B inhibitor parthenolide restores ICI 182,780 (Faslodex; fulvestrant)-induced apoptosis in antiestrogen-resistant breast cancer cells. Mol Cancer Ther 2005 Jan;4(1):33-41.

91. deGraffenried L, Chandrasekar B, Friedrichs W, Donzis E, Silva J, Hidalgo M, et al. NF-κB inhibition markedly enhances sensitivity of resistant breast cancer tumor cells to tamoxifen. Ann Oncol 2004;15(6):885-190.

92. Trinh XB, Sas L, Van Laere SJ, Prové A, Deleu I, Rasschaert M, et al. A Phase II Study of the Combination of Endocrine Treatment and Bortezomib in Patients with Endocrine Resistant Metastatic Breast Cancer. Oncol Rep 2012 Mar;27(3):657-663.

93. Lin Y, Bai L, Chen W, Xu S. The NF-kappaB activation pathways, emerging molecular targets for cancer prevention and therapy. Expert Opin Ther Targets 2010;14(1):45-55.

94. Klein CA. Parallel progression of primary tumours and metastases. Nat Rev Cancer 2009 Apr;9(4):302-312.

95. Field-Smith A, Morgan GJ, Davies FE. Bortezomib (Velcadetrade mark) in the Treatment of Multiple Myeloma. Ther Clin Risk Manag 2006 Sep;2(3):271-279.

96. Zhou Y, Yau C, Gray JW, Chew K, Dairkee SH, Moore DH, et al. Enhanced NFκB and AP-1 transcriptional activity associated with antiestrogen resistant breast cancer. BMC Cancer 2007;7(1):59-59.

97. Thaler S, Thiede G, Hengstler JG, Schad A, Schmidt M, Sleeman JP. The proteasome inhibitor Bortezomib (Velcade) as potential inhibitor of estrogen receptor-positive breast cancer. Int J Cancer 2015 Aug 1;137(3):686-697.

98. Lin YZ, Yao SY, Veach RA, Torgerson TR, Hawiger J. Inhibition of nuclear translocation of transcription factor NF-kappa B by a synthetic peptide containing a cell membrane-permeable motif and nuclear localization sequence. J Biol Chem 1995 Jun 16;270(24):14255-14258.

99. Zhang S, Won YK, Ong CN, Shen HM. Anti-cancer potential of sesquiterpene lactones: bioactivity and molecular mechanisms. Curr Med Chem Anticancer Agents 2005 May;5(3):239-249.

100. Greten FR, Arkan MC, Bollrath J, Hsu LC, Goode J, Miething C, et al. NF-kappaB is a negative regulator of IL-1beta secretion as revealed by genetic and pharmacological inhibition of IKKbeta. Cell 2007 Sep 7;130(5):918-931.

101. Evans MJ, Eckert A, Lai K, Adelman SJ, Harnish DC. Reciprocal antagonism between estrogen receptor and NF-kappaB activity in vivo. Circ Res 2001;89(9):823.

102. Sas L, Lardon F, Vermeulen P, Hauspy J, Van Dam P, Pauwels P, et al. The interaction between ER and NFκB in resistance to endocrine therapy. Breast Cancer Res 2012;14(4):212-212.

103. Steven J. Van Laere, Luc Y. Dirix, Ilse Van der Auwera, Gert G. Van den Eynden, Hilde J. Elst, Joost Weyler, et al. Nuclear Factor-κB Signature of Inflammatory Breast Cancer by cDNA Microarray Validated by Quantitative Real-time Reverse Transcription-PCR, Immunohistochemistry, and Nuclear Factor-κB DNA-Binding. Clin Cancer Res 2006;12(11):3249.

104. Sun WH, Keller ET, Stebler BS, Ershler WB. Estrogen Inhibits Phorbol Ester-Induced IκBα Transcription and Protein Degradation. Biochem and Biophys Res Commun 1998;244(3):691-695.

105. Galien R, Garcia T. Estrogen receptor impairs interleukin-6 expression by preventing protein binding on the NF-kappaB site. Nucleic Acids Res 1997;25(12):2424-2429.

106. Hsu SM, Chen YC, Jiang MC. 17 beta-estradiol inhibits tumor necrosis factor-alpha-induced nuclear factor-kappa B activation by increasing nuclear factor-kappa B p105 level in MCF-7 breast cancer cells. Biochem Biophys Res Commun 2000;279(1):47.

107. Nettles KW, Gil G, Nowak J, Métivier R, Sharma VB, Greene GL. CBP Is a Dosage-Dependent Regulator of Nuclear Factor-κB Suppression by the Estrogen Receptor. Mol Endocrinol 2008;22(2):263-272.

108. Cvoro A, Tzagarakis-Foster C, Tatomer D, Paruthiyil S, Fox MS, Leitman DC. Distinct Roles of Unliganded and Liganded Estrogen Receptors in Transcriptional Repression. Mol Cell 2006;21(4):555-564.

109. Quaedackers ME, van den Brink CE, van der Saag PT, Tertoolen LGJ. Direct interaction between estrogen receptor α and NF-κB in the nucleus of living cells. Mol Endocrinol 2007;273(1):42-50.

110. Wang X, Belguise K, Kersual N, Kirsch KH, Mineva ND, Galtier F, et al. Oestrogen signalling inhibits invasive phenotype by repressing RelB and its target BCL2. Nat Cell Biol 2007;9(4):470.

111. Guo S. SGE. Forkhead box transcription factor FOXO3a regulates estrogen receptor alpha expression and is repressed by the Her-2/neu/phosphatidylinositol 3-kinase/Akt signaling pathway. Mol Cell Biol 2004;24:8681.

112. Belguise K, Sonenshein GE. PKCθ promotes c-Rel–driven mammary tumorigenesis in mice and humans by repressing estrogen receptor α synthesis. J Clin Invest 2007;117(12):4009-4021.

113. Wang X, Trinkaus-Randall V, Chalbos D, Sonenshein GE, Belguise K, O'Neill CF, et al. RelB NF-kappaB represses estrogen receptor alpha expression via induction of the zinc finger protein Blimp1. Mol Cell Biol 2009;29(14):3832.

114. Reijm E, Jansen M, Ruigrok-Ritstier K, van Staveren I, Look M, van Gelder M, et al. Decreased expression of EZH2 is associated with upregulation of ER and favorable outcome to tamoxifen in advanced breast cancer. Breast Cancer Res Treat 2011;125(2):385-394.

115. Frasor J, Weaver A, Pradhan M, Dai Y, Miller L, Lin C, et al. Positive Cross-Talk between Estrogen Receptor and NF-kB in Breast Cancer. Cancer Res 2009;69(23):8918-8925.

116. Park JY, Pillinger MH, Abramson SB. Prostaglandin E2 synthesis and secretion: the role of PGE2 synthases. Clin Immunol 2006;119(3):229-240.

117. Frasor J, Weaver AE, Pradhan M, Mehta K. Synergistic up-regulation of prostaglandin E synthase expression in breast cancer cells by 17beta-estradiol and proinflammatory cytokines. Endocrinology 2008;149(12):6272.

118. Pradhan M, Bembinster LA, Baumgarten SC, Frasor J. Proinflammatory Cytokines Enhance Estrogen-dependent Expression of the Multidrug Transporter Gene ABCG2 through Estrogen Receptor and NFκB Cooperativity at Adjacent Response Elements. J Biol Chem 2010;285(41):31100-31106.

119. Stanculescu A, Bembinster L, Borgen K, Bergamaschi A, Wiley E, Frasor J. Estrogen promotes breast cancer cell survival in an inhibitor of apoptosis (IAP)-dependent manner. Horm Cancer 2010;1(3):127-135.

120. Pradhan M, Baumgarten SC, Bembinster LA, Frasor J. CBP mediates NF-κB-dependent histone acetylation and estrogen receptor recruitment to an estrogen response element in the BIRC3 promoter. Mol Cell Biol 2012;32(2):569-575.

121. Daosukho C, Kiningham K, Kasarskis EJ, Ittarat W, St Clair DK. Tamoxifen enhancement of TNF-alpha induced MnSOD expression: modulation of NF-kappaB dimerization. Oncogene 2002;21(22):3603.

122. King AE, Collins F, Klonisch T, Sallenave JM, Critchley HO, Saunders PT. An additive interaction between the NFkappaB and estrogen receptor signalling pathways in human endometrial epithelial cells. Hum Reprod 2010 Feb;25(2):510-518.

123. Gori I, Pellegrini C, Staedler D, Russell R, Jan C, Canny GO. Tumor necrosis factor-alpha activates estrogen signaling pathways in endometrial epithelial cells via estrogen receptor alpha. Mol Cell Endocrinol 2011 Oct 15;345(1-2):27-37.

124. Feldman I, Feldman GM, Mobarak C, Dunkelberg JC, Leslie KK. Identification of proteins within the nuclear factor-kappa B transcriptional complex including estrogen receptor-alpha. Am J Obstet Gynecol 2007 Apr;196(4):394.e1-11; discussion 394.e11-3.

125. Weitsman GE, Li L, Skliris GP, Davie JR, Ung K, Niu Y, et al. Estrogen receptor-alpha phosphorylated at Ser118 is present at the promoters of estrogen-regulated genes and is not altered due to HER-2 overexpression. Cancer Res 2006 Oct 15;66(20):10162-10170.

126. Shah YM, Rowan BG. The Src kinase pathway promotes tamoxifen agonist action in Ishikawa endometrial cells through phosphorylation-dependent stabilization of estrogen receptor (alpha) promoter interaction and elevated steroid receptor coactivator 1 activity. Mol Endocrinol 2005 Mar;19(3):732-748.

127. Likhite VS, Stossi F, Kim K, Katzenellenbogen BS, Katzenellenbogen JA. Kinase-specific phosphorylation of the estrogen receptor changes receptor interactions with ligand, deoxyribonucleic acid, and coregulators associated with alterations in estrogen and tamoxifen activity. Mol Endocrinol 2006 Dec;20(12):3120-3132.

128. Zhu P, Baek SH, Bourk EM, Ohgi KA, Garcia-Bassets I, Sanjo H, et al. Macrophage/cancer cell interactions mediate hormone resistance by a nuclear receptor derepression pathway. Cell 2006 Feb 10;124(3):615-629.

129. Park KJ, Krishnan V, O'Malley BW, Yamamoto Y, Gaynor RB. Formation of an IKKalpha-dependent transcription complex is required for estrogen receptor-mediated gene activation. Mol Cell 2005 Apr 1;18(1):71-82.

130. Tu Z, Prajapati S, Park KJ, Kelly NJ, Yamamoto Y, Gaynor RB. IKK alpha regulates estrogen-induced cell cycle progression by modulating E2F1 expression. J Biol Chem 2006 Mar 10;281(10):6699-6706.

131. Cancer Genome Atlas Network. Comprehensive molecular portraits of human breast tumours. Nature 2012 Oct 4;490(7418):61-70.

132. Curtis C, Shah SP, Chin SF, Turashvili G, Rueda OM, Dunning MJ, et al. The genomic and transcriptomic architecture of 2,000 breast tumours reveals novel subgroups. Nature 2012 Apr 18;486(7403):346-352.

133. Minn AJ, Gupta GP, Siegel PM, Bos PD, Shu W, Giri DD, et al. Genes that mediate breast cancer metastasis to lung. Nature 2005 Jul 28;436(7050):518-524.

134. Lu X, Lu X, Wang ZC, Iglehart JD, Zhang X, Richardson AL. Predicting features of breast cancer with gene expression patterns. Breast Cancer Res Treat 2008 Mar;108(2):191-201.

135. Hu MC, Saso H, Kobayashi R, Hung M, Lee D, Xia W, et al. IkappaB kinase promotes tumorigenesis through inhibition of forkhead FOXO3a. Cell 2004;117(2):225.

136. Xia Y, Padre RC, De Mendoza TH, Bottero V, Tergaonkar VB, Verma IM. Phosphorylation of p53 by IkappaB kinase 2 promotes its degradation by beta-TrCP. Proc Natl Acad Sci U S A 2009 Feb 24;106(8):2629-2634.

137. Lee DF, Kuo HP, Chen CT, Hsu JM, Chou CK, Wei Y, et al. IKK beta suppression of TSC1 links inflammation and tumor angiogenesis via the mTOR pathway. Cell 2007 Aug 10;130(3):440-455.

138. Soule HD, Vazguez J, Long A, Albert S, Brennan M. A human cell line from a pleural effusion derived from a breast carcinoma. J Natl Cancer Inst 1973 Nov;51(5):1409-1416.

139. Keydar I, Chen L, Karby S, Weiss FR, Delarea J, Radu M, et al. Establishment and characterization of a cell line of human breast carcinoma origin. Eur J Cancer 1979 May;15(5):659-670.

140. Cailleau R, Young R, Olive M, Reeves WJ,Jr. Breast tumor cell lines from pleural effusions. J Natl Cancer Inst 1974 Sep;53(3):661-674.

141. Liu H, Patel MR, Prescher JA, Patsialou A, Qian D, Lin J, et al. Cancer stem cells from human breast tumors are involved in spontaneous metastases in orthotopic mouse models. Proc Natl Acad Sci U S A 2010 Oct 19;107(42):18115-18120.

142. Robinson SP, Jordan VC. Antiestrogenic action of toremifene on hormone-dependent, -independent, and heterogeneous breast tumor growth in the athymic mouse. Cancer Res 1989 Apr 1;49(7):1758-1762.

143. DeRose YS, Gligorich KM, Wang G, Georgelas A, Bowman P, Courdy SJ, et al. Patient-derived models of human breast cancer: protocols for in vitro and in vivo applications in tumor biology and translational medicine. Curr Protoc Pharmacol 2013 Mar;Chapter 14:Unit14.23.

144. Subramanian A, Tamayo P, Mootha VK, Mukherjee S, Ebert BL, Gillette MA, et al. Gene set enrichment analysis: a knowledge-based approach for interpreting genome-wide expression profiles. Proc Natl Acad Sci U S A 2005 Oct 25;102(43):15545-15550.

145. Liberzon A, Subramanian A, Pinchback R, Thorvaldsdottir H, Tamayo P, Mesirov JP. Molecular signatures database (MSigDB) 3.0. Bioinformatics 2011 Jun 15;27(12):1739-1740.

146. Mercurio F, Zhu H, Murray BW, Shevchenko A, Bennett BL, Li J, et al. IKK-1 and IKK-2: cytokine-activated IkappaB kinases essential for NF-kappaB activation. Science 1997 Oct 31;278(5339):860-866.

147. Delhase M, Hayakawa M, Chen Y, Karin M. Positive and negative regulation of IkappaB kinase activity through IKKbeta subunit phosphorylation. Science 1999 Apr 9;284(5412):309-313.

148. Sakurai H, Chiba H, Miyoshi H, Sugita T, Toriumi W. IkappaB kinases phosphorylate NF-kappaB p65 subunit on serine 536 in the transactivation domain. J Biol Chem 1999 Oct 22;274(43):30353-30356.

149. Yang F, Tang E, Guan K, Wang CY. IKK beta plays an essential role in the phosphorylation of RelA/p65 on serine 536 induced by lipopolysaccharide. J Immunol 2003 Jun 1;170(11):5630-5635.

150. Huber MA, Azoitei N, Baumann B, Grünert S, Sommer A, Pehamberger H, et al. NF-κB is essential for epithelial-mesenchymal transition and metastasis in a model of breast cancer progression. J Clin Invest 2004;114(4):569-581.

151. Hoesel B, Schmid JA. The complexity of NF-kappaB signaling in inflammation and cancer. Mol Cancer 2013 Aug 2;12:86-4598-12-86.

152. Ozes ON, Mayo LD, Gustin JA, Pfeffer SR, Pfeffer LM, Donner DB. NF-kappaB activation by tumour necrosis factor requires the Akt serine-threonine kinase. Nature 1999 Sep 2;401(6748):82-85.

153. Yanagawa Y, Iijima N, Iwabuchi K, Onoe K. Activation of extracellular signal-related kinase by TNF-alpha controls the maturation and function of murine dendritic cells. J Leukoc Biol 2002 Jan;71(1):125-132.

154. Zhou FH, Foster BK, Zhou XF, Cowin AJ, Xian CJ. TNF-alpha mediates p38 MAP kinase activation and negatively regulates bone formation at the injured growth plate in rats. J Bone Miner Res 2006 Jul;21(7):1075-1088.

155. Beinke S, Robinson MJ, Hugunin M, Ley SC. Lipopolysaccharide activation of the TPL-2/MEK/extracellular signal-regulated kinase mitogen-activated protein kinase cascade is regulated by IkappaB kinase-induced proteolysis of NF-kappaB1 p105. Mol Cell Biol 2004 Nov;24(21):9658-9667.

156. Vermes I, Haanen C, Steffens-Nakken H, Reutelingsperger C. A novel assay for apoptosis. Flow cytometric detection of phosphatidylserine expression on early apoptotic cells using fluorescein labelled Annexin V. J Immunol Methods 1995 Jul 17;184(1):39-51.

157. Aka JA, Lin SX. Comparison of functional proteomic analyses of human breast cancer cell lines T47D and MCF7. PLoS One 2012;7(2):e31532.

158. Vojtesek B, Lane DP. Regulation of p53 protein expression in human breast cancer cell lines. J Cell Sci 1993 Jul;105(Pt 3):607-612.

159. Mooney LM, Al-Sakkaf KA, Brown BL, Dobson PR. Apoptotic mechanisms in T47D and MCF-7 human breast cancer cells. Br J Cancer 2002 Oct 7;87(8):909-917.

160. Borowicz S, Van Scoyk M, Avasarala S, Karuppusamy Rathinam MK, Tauler J, Bikkavilli RK, et al. The soft agar colony formation assay. J Vis Exp 2014 Oct 27;(92):e51998. doi(92):e51998.

161. Munshi A, Hobbs M, Meyn RE. Clonogenic cell survival assay. Methods Mol Med 2005;110:21-28.

162. Franken NA, Rodermond HM, Stap J, Haveman J, van Bree C. Clonogenic assay of cells in vitro. Nat Protoc 2006;1(5):2315-2319.

163. Zahm JM, Kaplan H, Herard AL, Doriot F, Pierrot D, Somelette P, et al. Cell migration and proliferation during the in vitro wound repair of the respiratory epithelium. Cell Motil Cytoskeleton 1997;37(1):33-43.

164. Kramer N, Walzl A, Unger C, Rosner M, Krupitza G, Hengstschlager M, et al. In vitro cell migration and invasion assays. Mutat Res 2013 Jan-Mar;752(1):10-24.

165. Kleinman HK, Martin GR. Matrigel: basement membrane matrix with biological activity. Semin Cancer Biol 2005 Oct;15(5):378-386.

166. Noel A, Albert V, Bajou K, Bisson C, Devy L, Frankenne F, et al. New functions of stromal proteases and their inhibitors in tumor progression. Surg Oncol Clin N Am 2001 Apr;10(2):417-32, x-xi.

167. Ricca A, Biroccio A, Del Bufalo D, Mackay A, Santoni A, Cippitelli M. bcl-2 over-expression enhances NF-kappaB activity and induces mmp-9 transcription in human MCF7(ADR) breast-cancer cells. Int J Cancer 2000;86(2):188-196.

168. Ito-Kureha T, Koshikawa N, Yamamoto M, Semba K, Yamaguchi N, Yamamoto T, et al. Tropomodulin 1 expression driven by NF-kappaB enhances breast cancer growth. Cancer Res 2015 Jan 1;75(1):62-72.

169. Grandas OH, Mountain DH, Kirkpatrick SS, Cassada DC, Stevens SL, Freeman MB, et al. Regulation of vascular smooth muscle cell expression and function of

matrix metalloproteinases is mediated by estrogen and progesterone exposure. J Vasc Surg 2009 Jan;49(1):185-191.

170. Francia G, Cruz-Munoz W, Man S, Xu P, Kerbel RS. Mouse models of advanced spontaneous metastasis for experimental therapeutics. Nat Rev Cancer 2011 Feb;11(2):135-141.

171. Mohanty S, Xu L. Experimental metastasis assay. Journal of visualized experiments : JoVE 2010(42).

172. Shibue T, Weinberg RA. Metastatic colonization: settlement, adaptation and propagation of tumor cells in a foreign tissue environment. Semin Cancer Biol 2011 Apr;21(2):99-106.

173. Granit RZ, Slyper M, Ben-Porath I. Axes of differentiation in breast cancer: untangling stemness, lineage identity, and the epithelial to mesenchymal transition. Wiley Interdiscip Rev Syst Biol Med 2014 Jan-Feb;6(1):93-106.

174. Visvader JE. Keeping abreast of the mammary epithelial hierarchy and breast tumorigenesis. Genes Dev 2009 Nov 15;23(22):2563-2577.

175. Bill R, Christofori G. The relevance of EMT in breast cancer metastasis: Correlation or causality? FEBS Lett 2015 Jun 22;589(14):1577-1587.

176. Kalluri R, Weinberg RA. The basics of epithelial-mesenchymal transition. J Clin Invest 2009 Jun;119(6):1420-1428.

177. Pink JJ, Jordan VC. Models of estrogen receptor regulation by estrogens and antiestrogens in breast cancer cell lines. Cancer Res 1996 May 15;56(10):2321-2330.

178. Valley CC, Métivier R, Solodin NM, Fowler AM, Mashek MT, Hill L, et al. Differential Regulation of Estrogen-Inducible Proteolysis and Transcription by the Estrogen Receptor a N Terminus. Mol Cell Biol 2005;25(13):5417-5428.

179. Chou J, Provot S, Werb Z. GATA3 in development and cancer differentiation: cells GATA have it! J Cell Physiol 2010 Jan;222(1):42-49.

180. Bernardo GM, Bebek G, Ginther CL, Sizemore ST, Lozada KL, Miedler JD, et al. FOXA1 represses the molecular phenotype of basal breast cancer cells. Oncogene 2013 Jan 31;32(5):554-563.

181. Bouras T, Pal B, Vaillant F, Harburg G, Asselin-Labat ML, Oakes SR, et al. Notch signaling regulates mammary stem cell function and luminal cell-fate commitment. Cell Stem Cell 2008 Oct 9;3(4):429-441.

182. Chakrabarti R, Wei Y, Romano RA, DeCoste C, Kang Y, Sinha S. Elf5 regulates mammary gland stem/progenitor cell fate by influencing notch signaling. Stem Cells 2012 Jul;30(7):1496-1508.

183. Carr JR, Kiefer MM, Park HJ, Li J, Wang Z, Fontanarosa J, et al. FoxM1 regulates mammary luminal cell fate. Cell Rep 2012 Jun 28;1(6):715-729.

184. Guo W, Keckesova Z, Donaher JL, Shibue T, Tischler V, Reinhardt F, et al. Slug and Sox9 cooperatively determine the mammary stem cell state. Cell 2012 Mar 2;148(5):1015-1028.

185. Molyneux G, Geyer FC, Magnay FA, McCarthy A, Kendrick H, Natrajan R, et al. BRCA1 basal-like breast cancers originate from luminal epithelial progenitors and not from basal stem cells. Cell Stem Cell 2010 Sep 3;7(3):403-417.

186. Friedl P, Locker J, Sahai E, Segall JE. Classifying collective cancer cell invasion. Nat Cell Biol 2012 Aug;14(8):777-783.

187. Fortier AM, Asselin E, Cadrin M. Keratin 8 and 18 loss in epithelial cancer cells increases collective cell migration and cisplatin sensitivity through claudin1 up-regulation. J Biol Chem 2013 Apr 19;288(16):11555-11571.

188. Cheung KJ, Gabrielson E, Werb Z, Ewald AJ. Collective invasion in breast cancer requires a conserved basal epithelial program. Cell 2013 Dec 19;155(7):1639-1651.

189. Prall OW, Rogan EM, Musgrove EA, Watts CK, Sutherland RL. c-Myc or cyclin D1 mimics estrogen effects on cyclin E-Cdk2 activation and cell cycle reentry. Mol Cell Biol 1998 Aug;18(8):4499-4508.

190. Sanchez AM, Flamini MI, Baldacci C, Goglia L, Genazzani AR, Simoncini T. Estrogen receptor-alpha promotes breast cancer cell motility and invasion via focal adhesion kinase and N-WASP. Mol Endocrinol 2010 Nov;24(11):2114-2125.

191. Giretti MS, Fu XD, De Rosa G, Sarotto I, Baldacci C, Garibaldi S, et al. Extra-nuclear signalling of estrogen receptor to breast cancer cytoskeletal remodelling, migration and invasion. PLoS One 2008 May 21;3(5):e2238.

192. Zheng S, Huang J, Zhou K, Zhang C, Xiang Q, Tan Z, et al. 17beta-Estradiol enhances breast cancer cell motility and invasion via extra-nuclear activation of actin-binding protein ezrin. PLoS One 2011;6(7):e22439.

193. Tafani M, Russo A, Di Vito M, Sale P, Pellegrini L, Schito L, et al. Up-regulation of pro-inflammatory genes as adaptation to hypoxia in MCF-7 cells and in human mammary invasive carcinoma microenvironment. Cancer Sci 2010 Apr;101(4):1014-1023.

194. Broad Institute. MSigDB Collections. Available at: http://www.broadinstitute.org/gsea/msigdb/collections.jsp#H. Accessed 08/4, 2015.

195. Ashburner M, Ball CA, Blake JA, Botstein D, Butler H, Cherry JM, et al. Gene ontology: tool for the unification of biology. The Gene Ontology Consortium. Nat Genet 2000 May;25(1):25-29.

196. Stender JD, Frasor J, Komm B, Chang KC, Kraus WL, Katzenellenbogen BS. Estrogen-regulated gene networks in human breast cancer cells: involvement of E2F1 in the regulation of cell proliferation. Mol Endocrinol 2007 Sep;21(9):2112-2123.

197. Altucci L, Addeo R, Cicatiello L, Dauvois S, Parker MG, Truss M, et al. 17beta-Estradiol induces cyclin D1 gene transcription, p36D1-p34cdk4 complex activation and p105Rb phosphorylation during mitogenic stimulation of G(1)-arrested human breast cancer cells. Oncogene 1996 Jun 6;12(11):2315-2324.

198. Poola I, DeWitty RL, Marshalleck JJ, Bhatnagar R, Abraham J, Leffall LD. Identification of MMP-1 as a putative breast cancer predictive marker by global gene expression analysis. Nat Med 2005 May;11(5):481-483.

199. Schuetz CS, Bonin M, Clare SE, Nieselt K, Sotlar K, Walter M, et al. Progression-specific genes identified by expression profiling of matched ductal carcinomas in situ and invasive breast tumors, combining laser capture microdissection and oligonucleotide microarray analysis. Cancer Res 2006 May 15;66(10):5278-5286.

200. Wang W, Wyckoff JB, Goswami S, Wang Y, Sidani M, Segall JE, et al. Coordinated regulation of pathways for enhanced cell motility and chemotaxis is conserved in rat and mouse mammary tumors. Cancer Res 2007 Apr 15;67(8):3505-3511.

201. Smid M, Wang Y, Zhang Y, Sieuwerts AM, Yu J, Klijn JG, et al. Subtypes of breast cancer show preferential site of relapse. Cancer Res 2008 May 1;68(9):3108-3114.

202. Charafe-Jauffret E, Ginestier C, Monville F, Finetti P, Adelaide J, Cervera N, et al. Gene expression profiling of breast cell lines identifies potential new basal markers. Oncogene 2006 Apr 6;25(15):2273-2284.

203. Chua HL, Bhat-Nakshatri P, Clare SE, Morimiya A, Badve S, Nakshatri H. NF-kappaB represses E-cadherin expression and enhances epithelial to mesenchymal transition of mammary epithelial cells: potential involvement of ZEB-1 and ZEB-2. Oncogene 2007;26(5):711.

204. Bouris P, Skandalis SS, Piperigkou Z, Afratis N, Karamanou K, Aletras AJ, et al. Estrogen receptor alpha mediates epithelial to mesenchymal transition, expression of specific matrix effectors and functional properties of breast cancer cells. Matrix Biol 2015 Apr;43:42-60.

205. Fujita N, Jaye DL, Kajita M, Geigerman C, Moreno CS, Wade PA. MTA3, a Mi-2/NuRD complex subunit, regulates an invasive growth pathway in breast cancer. Cell 2003;113(2):207-219.

206. Ye Y, Xiao Y, Wang W, Yearsley K, Gao JX, Barsky SH. ERalpha suppresses slug expression directly by transcriptional repression. Biochem J 2008 Dec 1;416(2):179-187.

207. Planas-Silva MD, Waltz PK. Estrogen promotes reversible epithelial-to-mesenchymal-like transition and collective motility in MCF-7 breast cancer cells. J Steroid Biochem Mol Biol 2007;104(1-2):11-21.

208. Jimenez-Salazar JE, Posadas-Rodriguez P, Lazzarini-Lechuga RC, Luna-Lopez A, Zentella-Dehesa A, Gomez-Quiroz LE, et al. Membrane-initiated estradiol signaling of epithelial-mesenchymal transition-associated mechanisms through regulation of tight junctions in human breast cancer cells. Horm Cancer 2014 Jun;5(3):161-173.

209. Sarrio D, Rodriguez-Pinilla SM, Hardisson D, Cano A, Moreno-Bueno G, Palacios J. Epithelial-mesenchymal transition in breast cancer relates to the basal-like phenotype. Cancer Res 2008 Feb 15;68(4):989-997.

210. Lim E, Wu D, Pal B, Bouras T, Asselin-Labat ML, Vaillant F, et al. Transcriptome analyses of mouse and human mammary cell subpopulations reveal multiple conserved genes and pathways. Breast Cancer Res 2010;12(2):R21.

211. Pece S, Tosoni D, Confalonieri S, Mazzarol G, Vecchi M, Ronzoni S, et al. Biological and molecular heterogeneity of breast cancers correlates with their cancer stem cell content. Cell 2010 Jan 8;140(1):62-73.

212. Zheng J. Energy metabolism of cancer: Glycolysis versus oxidative phosphorylation (Review). Oncol Lett 2012 Dec;4(6):1151-1157.

213. Marchiq I, Pouyssegur J. Hypoxia, cancer metabolism and the therapeutic benefit of targeting lactate/H symporters. J Mol Med (Berl) 2015 Jun 24.

214. Hart PC, Mao M, de Abreu AL, Ansenberger-Fricano K, Ekoue DN, Ganini D, et al. MnSOD upregulation sustains the Warburg effect via mitochondrial ROS and AMPK-dependent signalling in cancer. Nat Commun 2015 Feb 5;6:6053.

215. Vandewynckel YP, Laukens D, Geerts A, Bogaerts E, Paridaens A, Verhelst X, et al. The paradox of the unfolded protein response in cancer. Anticancer Res 2013 Nov;33(11):4683-4694.

216. Andruska N, Zheng X, Yang X, Helferich WG, Shapiro DJ. Anticipatory estrogen activation of the unfolded protein response is linked to cell proliferation and poor survival in estrogen receptor alpha-positive breast cancer. Oncogene 2014 Sep 29;0:10.1038/onc.2014.292.

217. Hu P, Han Z, Couvillon AD, Kaufman RJ, Exton JH. Autocrine tumor necrosis factor alpha links endoplasmic reticulum stress to the membrane death receptor pathway through IRE1alpha-mediated NF-kappaB activation and down-regulation of TRAF2 expression. Mol Cell Biol 2006 Apr;26(8):3071-3084.

218. Zhang K, Shen X, Wu J, Sakaki K, Saunders T, Rutkowski DT, et al. Endoplasmic reticulum stress activates cleavage of CREBH to induce a systemic inflammatory response. Cell 2006 Feb 10;124(3):587-599.

219. Choi HJ, Lui A, Ogony J, Jan R, Sims PJ, Lewis-Wambi J. Targeting interferon response genes sensitizes aromatase inhibitor resistant breast cancer cells to estrogen-induced cell death. Breast Cancer Res 2015 Jan 15;17:6-014-0506-7.

220. Cortez V, Mann M, Brann DW, Vadlamudi RK. Extranuclear signaling by estrogen: role in breast cancer progression and metastasis. Minerva Ginecol 2010 Dec;62(6):573-583.

221. Araki K, Kawauchi K, Tanaka N. IKK/NF-kappaB signaling pathway inhibits cell-cycle progression by a novel Rb-independent suppression system for E2F transcription factors. Oncogene 2008 Sep 25;27(43):5696-5705.

222. Chen F, Lu Y, Castranova V, Li Z, Karin M. Loss of Ikkbeta promotes migration and proliferation of mouse embryo fibroblast cells. J Biol Chem 2006 Dec 1;281(48):37142-37149.

223. Mistry P, Deacon K, Mistry S, Blank J, Patel R. NF-kappaB promotes survival during mitotic cell cycle arrest. J Biol Chem 2004 Jan 9;279(2):1482-1490.

224. Karin M, Greten FR. NF-kappaB: linking inflammation and immunity to cancer development and progression. Nat Rev Immunol 2005 Oct;5(10):749-759.

225. Wu L, Shao L, An N, Wang J, Pazhanisamy S, Feng W, et al. IKKbeta regulates the repair of DNA double-strand breaks induced by ionizing radiation in MCF-7 breast cancer cells. PLoS One 2011 Apr 7;6(4):e18447.

226. Sakamoto K, Hikiba Y, Nakagawa H, Hirata Y, Hayakawa Y, Kinoshita H, et al. Promotion of DNA repair by nuclear IKKbeta phosphorylation of ATM in response to genotoxic stimuli. Oncogene 2013 Apr 4;32(14):1854-1862.

227. Sosa MS, Bragado P, Aguirre-Ghiso JA. Mechanisms of disseminated cancer cell dormancy: an awakening field. Nat Rev Cancer 2014 Sep;14(9):611-622.

228. Holmgren L, O'Reilly MS, Folkman J. Dormancy of micrometastases: balanced proliferation and apoptosis in the presence of angiogenesis suppression. Nat Med 1995 Feb;1(2):149-153.

229. Weinhold KJ, Goldstein LT, Wheelock EF. The tumor dormant state. Quantitation of L5178Y cells and host immune responses during the establishment and course of dormancy in syngeneic DBA/2 mice. J Exp Med 1979 Mar 1;149(3):732-744.

230. Gelao L, Criscitiello C, Fumagalli L, Locatelli M, Manunta S, Esposito A, et al. Tumour dormancy and clinical implications in breast cancer. Ecancermedicalscience 2013;7:10.3332/ecancer.2013.320.

231. Leifler KS, Svensson S, Abrahamsson A, Bendrik C, Robertson J, Gauldie J, et al. Inflammation induced by MMP-9 enhances tumor regression of experimental breast cancer. J Immunol 2013 Apr 15;190(8):4420-4430.

232. Shime H, Matsumoto M, Oshiumi H, Tanaka S, Nakane A, Iwakura Y, et al. Toll-like receptor 3 signaling converts tumor-supporting myeloid cells to tumoricidal effectors. Proc Natl Acad Sci U S A 2012 Feb 7;109(6):2066-2071.

233. Ogba N, Manning NG, Bliesner BS, Ambler SK, Haughian JM, Pinto MP, et al. Luminal breast cancer metastases and tumor arousal from dormancy are promoted by direct actions of estradiol and progesterone on the malignant cells. Breast Cancer Res 2014 Dec 5;16(6):489-014-0489-4.

234. Ziegler E, Hansen MT, Haase M, Emons G, Grundker C. Generation of MCF-7 cells with aggressive metastatic potential in vitro and in vivo. Breast Cancer Res Treat 2014 Nov;148(2):269-277.

235. Harrell JC, Dye WW, Allred DC, Jedlicka P, Spoelstra NS, Sartorius CA, et al. Estrogen receptor positive breast cancer metastasis: altered hormonal sensitivity and tumor aggressiveness in lymphatic vessels and lymph nodes. Cancer Res 2006 Sep 15;66(18):9308-9315.

236. Niu J, Shi Y, Tan G, Yang CH, Fan M, Pfeffer LM, et al. DNA damage induces NF-kappaB-dependent microRNA-21 up-regulation and promotes breast cancer cell invasion. J Biol Chem 2012 Jun 22;287(26):21783-21795.

237. Bollrath J, Greten FR. IKK/NF-kappaB and STAT3 pathways: central signalling hubs in inflammation-mediated tumour promotion and metastasis. EMBO Rep 2009 Dec;10(12):1314-1319.

238. Shin SR, Sanchez-Velar N, Sherr DH, Sonenshein GE. 7,12-dimethylbenz(a)anthracene treatment of a c-rel mouse mammary tumor cell line induces epithelial to mesenchymal transition via activation of nuclear factor-kappaB. Cancer Res 2006 Mar 1;66(5):2570-2575.

239. Sihto H, Lundin J, Lundin M, Lehtimaki T, Ristimaki A, Holli K, et al. Breast cancer biological subtypes and protein expression predict for the preferential distant metastasis sites: a nationwide cohort study. Breast Cancer Res 2011 Sep 13;13(5):R87.

240. Savci-Heijink CD, Halfwerk H, Hooijer GK, Horlings HM, Wesseling J, van de Vijver MJ. Retrospective analysis of metastatic behaviour of breast cancer subtypes. Breast Cancer Res Treat 2015 Apr;150(3):547-557.

241. Kang Y, Siegel PM, Shu W, Drobnjak M, Kakonen SM, Cordon-Cardo C, et al. A multigenic program mediating breast cancer metastasis to bone. Cancer Cell 2003 Jun;3(6):537-549.

242. Park BK, Zhang H, Zeng Q, Dai J, Keller ET, Giordano T, et al. NF-kappaB in breast cancer cells promotes osteolytic bone metastasis by inducing osteoclastogenesis via GM-CSF. Nat Med 2007 Jan;13(1):62-69.

243. Lu X, Mu E, Wei Y, Riethdorf S, Yang Q, Yuan M, et al. VCAM-1 promotes osteolytic expansion of indolent bone micrometastasis of breast cancer by engaging alpha4beta1-positive osteoclast progenitors. Cancer Cell 2011 Dec 13;20(6):701-714.

244. Matsuda Y, Yoshimura H, Ueda J, Naito Z, Korc M, Ishiwata T. Nestin delineates pancreatic cancer stem cells in metastatic foci of NOD/Shi-scid IL2Rgamma(null) (NOG) mice. Am J Pathol 2014 Mar;184(3):674-685.

245. Goerge T, Ho-Tin-Noe B, Carbo C, Benarafa C, Remold-O'Donnell E, Zhao BQ, et al. Inflammation induces hemorrhage in thrombocytopenia. Blood 2008 May 15;111(10):4958-4964.

246. Son Y, Lee HJ, Rho JK, Chung SY, Lee CG, Yang K, et al. The ameliorative effect of silibinin against radiation-induced lung injury: protection of normal tissue without decreasing therapeutic efficacy in lung cancer. BMC Pulm Med 2015 Jul 5;15:68-015-0055-6.

247. Cambien B, Bergmeier W, Saffaripour S, Mitchell HA, Wagner DD. Antithrombotic activity of TNF-alpha. J Clin Invest 2003 Nov;112(10):1589-1596.

248. Seo JB, Im JG, Goo JM, Chung MJ, Kim MY. Atypical pulmonary metastases: spectrum of radiologic findings. Radiographics 2001 Mar-Apr;21(2):403-417.

249. Storci G, Chieco P, Marcu KB, Bonafè M, Sansone P, Mari S, et al. TNFalpha up-regulates SLUG via the NF-kappaB/HIF1alpha axis, which imparts breast cancer cells with a stem cell-like phenotype. J Cell Physiol 2010;225(3):682-691.

250. Axlund SD, Yoo BH, Rosen RB, Schaack J, Kabos P, Labarbera DV, et al. Progesterone-inducible cytokeratin 5-positive cells in luminal breast cancer exhibit progenitor properties. Horm Cancer 2013 Feb;4(1):36-49.

251. Horwitz KB, Dye WW, Harrell JC, Kabos P, Sartorius CA. Rare steroid receptor-negative basal-like tumorigenic cells in luminal subtype human breast cancer xenografts. Proc Natl Acad Sci U S A 2008 Apr 15;105(15):5774-5779.

252. Li C, Ding Q, Wang Y, Lai Y, LaBaff AM, Wu T, et al. Epithelial-mesenchyme transition induced by TNF-α requires NF-κB-mediated transcriptional upregulation of Twist1. Cancer Res 2012;72(5):1290-1300.

253. Sliva D, Rizzo MT, English D. Phosphatidylinositol 3-kinase and NF-kappaB regulate motility of invasive MDA-MB-231 human breast cancer cells by the secretion of urokinase-type plasminogen activator. J Biol Chem 2002 Feb 1;277(5):3150-3157.

254. Kim HJ, Litzenburger BC, Cui X, Delgado DA, Grabiner BC, Lin X, et al. Constitutively active type I insulin-like growth factor receptor causes transformation and xenograft growth of immortalized mammary epithelial cells and is accompanied by an epithelial-to-mesenchymal transition mediated by NF-kappaB and snail. Mol Cell Biol 2007 Apr;27(8):3165-3175.

255. Tsai JH, Yang J. Epithelial-mesenchymal plasticity in carcinoma metastasis. Genes Dev 2013 Oct 15;27(20):2192-2206.

256. Westcott JM, Prechtl AM, Maine EA, Dang TT, Esparza MA, Sun H, et al. An epigenetically distinct breast cancer cell subpopulation promotes collective invasion. J Clin Invest 2015 May;125(5):1927-1943.

257. Kim KJ, Godarova A, Seedle K, Kim MH, Ince TA, Wells SI, et al. Rb suppresses collective invasion, circulation and metastasis of breast cancer cells in CD44-dependent manner. PLoS One 2013 Dec 4;8(12):e80590.

258. Radde BN, Ivanova MM, Mai HX, Salabei JK, Hill BG, Klinge CM. Bioenergetic differences between MCF-7 and T47D breast cancer cells and their regulation by oestradiol and tamoxifen. Biochem J 2015 Jan 1;465(1):49-61.

259. Kabos P, Haughian JM, Wang X, Dye WW, Finlayson C, Elias A, et al. Cytokeratin 5 positive cells represent a steroid receptor negative and therapy resistant subpopulation in luminal breast cancers. Breast Cancer Res Treat 2011 Jul;128(1):45-55.

260. Mehra R, Varambally S, Ding L, Shen R, Sabel MS, Ghosh D, et al. Identification of GATA3 as a breast cancer prognostic marker by global gene expression meta-analysis. Cancer Res 2005 Dec 15;65(24):11259-11264.

261. Albergaria A, Paredes J, Sousa B, Milanezi F, Carneiro V, Bastos J, et al. Expression of FOXA1 and GATA-3 in breast cancer: the prognostic significance in hormone receptor-negative tumours. Breast Cancer Res 2009;11(3):R40.

262. Kouros-Mehr H, Bechis SK, Slorach EM, Littlepage LE, Egeblad M, Ewald AJ, et al. GATA-3 links tumor differentiation and dissemination in a luminal breast cancer model. Cancer Cell 2008 Feb;13(2):141-152.

263. Yan W, Cao QJ, Arenas RB, Bentley B, Shao R. GATA3 inhibits breast cancer metastasis through the reversal of epithelial-mesenchymal transition. J Biol Chem 2010 Apr 30;285(18):14042-14051.

264. Ducat D, Zheng Y. Aurora kinases in spindle assembly and chromosome segregation. Exp Cell Res 2004 Nov 15;301(1):60-67.

265. Irelan JT, Murphy TJ, DeJesus PD, Teo H, Xu D, Gomez-Ferreria MA, et al. A role for IkappaB kinase 2 in bipolar spindle assembly. Proc Natl Acad Sci U S A 2007 Oct 23;104(43):16940-16945.

266. Lee HH, Zhu Y, Govindasamy KM, Gopalan G. Downregulation of Aurora-A overrides estrogen-mediated growth and chemoresistance in breast cancer cells. Endocr Relat Cancer 2008 Sep;15(3):765-775.

267. Zheng XQ, Guo JP, Yang H, Kanai M, He LL, Li YY, et al. Aurora-A is a determinant of tamoxifen sensitivity through phosphorylation of ERalpha in breast cancer. Oncogene 2014 Oct 16;33(42):4985-4996.

268. Doisneau-Sixou SF, Sergio CM, Carroll JS, Hui R, Musgrove EA, Sutherland RL. Estrogen and antiestrogen regulation of cell cycle progression in breast cancer cells. Endocr Relat Cancer 2003 Jun;10(2):179-186.

269. Ferreira R, Naguibneva I, Pritchard LL, Ait-Si-Ali S, Harel-Bellan A. The Rb/chromatin connection and epigenetic control: opinion. Oncogene 2001 May 28;20(24):3128-3133.

270. Gompel A, Somai S, Chaouat M, Kazem A, Kloosterboer HJ, Beusman I, et al. Hormonal regulation of apoptosis in breast cells and tissues. Steroids 2000 Oct-Nov;65(10-11):593-598.

271. Teixeira C, Reed JC, Pratt MA. Estrogen promotes chemotherapeutic drug resistance by a mechanism involving Bcl-2 proto-oncogene expression in human breast cancer cells. Cancer Res 1995 Sep 1;55(17):3902-3907.

272. Frasor J, Danes JM, Komm B, Chang KCN, Lyttle CR, Katzenellenbogen BS. Profiling of estrogen up- and down-regulated gene expression in human breast cancer cells: insights into gene networks and pathways underlying estrogenic control of proliferation and cell phenotype. Endocrinology 2003;144(10):4562-4574.

273. Hagan CR, Lange CA. Molecular determinants of context-dependent progesterone receptor action in breast cancer. BMC Med 2014 Feb 20;12:32-7015-12-32.

274. Franco HL, Nagari A, Kraus WL. TNFalpha signaling exposes latent estrogen receptor binding sites to alter the breast cancer cell transcriptome. Mol Cell 2015 Apr 2;58(1):21-34.

275. Davies C, Pan H, Godwin J, Gray R, Arriagada R, Raina V, et al. Long-term effects of continuing adjuvant tamoxifen to 10 years versus stopping at 5 years after diagnosis of oestrogen receptor-positive breast cancer: ATLAS, a randomised trial. Lancet 2013 Mar 9;381(9869):805-816.

VITA

NAME: Lamiaa Khamies Mohamed Ali El-Shennawy

EDUCATION:

Ph.D., Biopharmaceutical Sciences, College of Pharmacy, University of Illinois at Chicago, Chicago, IL, 2015

M.S., Environmental Studies, Biological Sciences Branch, Institute of Graduate Studies and Research, University of Alexandria, Alexandria, Egypt, 2008

Diploma of Environmental Studies, Institute of Graduate Studies and Research, University of Alexandria, Alexandria, Egypt, 2005

Diploma of Biotechnology, Institute of Graduate Studies and Research, University of Alexandria, Alexandria, Egypt, 1999

Bachelor of Pharmaceutical Sciences, Faculty of Pharmacy, University of Alexandria, Alexandria, Egypt, 1997

TEACHING EXPERIENCE:

Department of Biopharmaceutical Sciences, College of Pharmacy, University of Illinois at Chicago, Chicago, IL: Pharmaceutics Laboratory for Doctor of Pharmacy Students, 2015

Department of Biopharmaceutical Sciences, College of Pharmacy, University of Illinois at Chicago, Chicago, IL: Principles of Drug Action and Therapeutics V and VII for Doctor of Pharmacy Students, 2014

Department of Biopharmaceutical Sciences, College of Pharmacy, University of Illinois at Chicago, Chicago, IL: Pharmaceutics Laboratory for Doctor of Pharmacy Students, 2013

Department of Environmental Sciences, Institute of Graduate Studies and Research, University of Alexandria, Alexandria, Egypt: Applied Statistics, Biochemistry and Toxicology for Graduate Students, 2004-2010

Department of Pharmaceutics, College of Pharmacy, University of Alexandria, Alexandria, Egypt: Pharmaceutics Laboratory for Pharmaceutical Sciences Students, 1998

HONORS:

Susan G. Komen Scholar-In-Training Award for early-career scientists, American Association of Cancer Research 106th Annual Meeting 2015, Philadelphia, PA, 2015

Endocrine Society Travel Award for abstract presentation, Great Lakes Nuclear Receptor Meeting (GLNRM), University of Wisconsin-Madison, Madison, WI, 2014

Poster competition, second place, Student Research Forum, University of Illinois at Chicago, Chicago, IL, 2014

Poster competition, first place, International Fulbright Science and Technology Awardees Capstone Meeting, US Department of State, Washington DC, 2013

International Fulbright Science and Technology Award, 2010-2013

Graduation with Honors, Institute of Graduate Studies and Research, University of Alexandria, Alexandria, Egypt, 2008

Graduation with Distinction Honors, Faculty of Pharmacy, University of Alexandria, Alexandria, Egypt, 1997

PROFESSIONAL MEMBERSHIP:

American Association of Cancer Research (AACR)
Women in Cancer Research (WICR)
Endocrine Society
Egyptian Pharmacist Syndicate

LEADERSHIP:

Member of College of Pharmacy Graduate Student Committee, University of Illinois at Chicago, Chicago, IL

ABSTRACTS:

El-Shennawy L and Frasor J. Constitutively active NF-κB signaling switches estrogen receptor positive breast cancer cells from a proliferative to an invasive phenotype through luminal/basal plasticity. American Association of Cancer Research 106th Annual Meeting 2015, Philadelphia, PA, 2015.

El-Shennawy L and Frasor J. Constitutively active NF-κB signaling switches estrogen receptor positive breast cancer cells from a proliferative to an invasive phenotype through luminal/basal plasticity. College of Pharmacy Research Day, University of Illinois at Chicago, Chicago, IL, 2015.

El-Shennawy L and Frasor J. Constitutively active NF-κB signaling switches estrogen receptor positive breast cancer cells from a proliferative to an invasive phenotype. College of Medicine Research Day, University of Illinois at Chicago, Chicago, IL, 2014.

El-Shennawy L and Frasor J. Constitutively active NF-κB signaling switches estrogen receptor positive breast cancer cells from a proliferative to an invasive phenotype. Great Lakes Nuclear Receptor Meeting, University of Wisconsin-Madison, Madison, WI, 2014.

El-Shennawy L and Frasor J. Constitutive activation of the canonical NF-κB pathway switches the phenotype of estrogen receptor positive breast cancer cells from estrogen-induced proliferation to estrogen-induced migration. The Endocrine Society Annual Meeting and Expo, Chicago, IL, 2014.

El-Shennawy L and Frasor J. Constitutive activation of the canonical NF-κB pathway switches the phenotype of estrogen receptor positive breast cancer cells from estrogen-induced proliferation to estrogen-induced migration/invasion. Cancer Center Research Forum, University of Illinois at Chicago, Chicago, IL, 2014.

El-Shennawy L and Frasor J. Constitutive activation of the canonical NF-κB pathway switches the phenotype of estrogen receptor positive breast cancer cells from estrogen-induced proliferation to estrogen-induced migration/invasion. Student Research Forum, University of Illinois at Chicago, Chicago, IL, 2014.

El-Shennawy L and Frasor J. Constitutive activation of the canonical NF-κB pathway switches the phenotype of estrogen receptor positive breast cancer cells from estrogen-induced proliferation to estrogen-induced migration/invasion. College of Pharmacy Research Day, University of Illinois at Chicago, Chicago, IL, 2014.

El-Shennawy L and Frasor J. Constitutively active IKKβ switches estrogen action from proliferation to migration in estrogen receptor positive breast cancer cells. College of Medicine Research Day, University of Illinois at Chicago, Chicago, IL, 2013.

Beck WT, Arslan AD, Ho T, Majumdar N, El-Shennawy L, Maggio M and He X. Identification of small molecule inhibitors of splicing factor PTBP1 as potential therapeutic agents to treat ovarian cancer. 9th AACR-Japanese Cancer Association Joint Conference, Maui, HI, 2013.

El-Shennawy L, Felice DL, Swanson SM, Unterman, TG and Frasor J. Growth hormone potentiates the proliferative effect of estrogen in breast cancer cells in an AKT-dependent manner. Great Lakes Nuclear Receptor Meeting, Chicago, IL, 2012.

Felice DL, El-Shennawy L, Zhao S, Lantvit DL, Shen Q, Unterman, TG, Swanson, SM and Frasor J. Growth Hormone activates ERK via EGFR, not IGF-1R to potentiate estrogen dependent breast cancer cell proliferation. American Association for Cancer Research 103rd Annual Meeting 2012, Chicago, IL, 2012.

Yousef MI, Saad AA and El-Shennawy L. Grape seed proanthocyanidin extract prevents doxorubicin-induced oxidative stress in rats. 10th International Conference, Functional Foods and Bioactive Compounds in Health and Disease: Science and Practice, University of California Santa Barbara, CA, 2012.

Yousef MI, Saad AA and El-Shennawy L. Grape seed proanthocyanidin extract protects against doxorubicin-induced damage in heart genomic DNA and cardiotoxicity in rats. 10th International Conference, Functional Foods and Bioactive Compounds in Health and Disease: Science and Practice, University of California, Santa Barbara, CA, 2012.

PUBLICATIONS:

El-Shennawy L, Kastrati I, Wiley EL, Whiteley H, Frasor J. Activation of IKKbeta induces dormancy and metastasis in estrogen receptor positive breast cancer. Manuscript in preparation.

El-Shennawy L, Felice DL, Frasor J. Growth Hormone signals through AKT/FoxO in breast cancer cells. Manuscript in preparation.

Kastrati I, Siklos MI, El-Shennawy L, Thayer E, Thatcher GRJ, Frasor J. Dimethyl fumarate inhibits the Nuclear Factor κB pathway in breast cancer cells by covalent modification of p65. Submitted to J Biol Chem, 2015.

Frasor J, El-Shennawy L, Stender JD, Kastrati I. NFκB affects estrogen receptor expression and activity in breast cancer through multiple mechanisms. Mol Cell Endocrinol 2014 Oct 18, doi: 10.1016/ j.mce.2014.09.013.

Felice DL, El-Shennawy L, Zhao S, Lantvit DL, Shen Q, Unterman TG, Swanson SM, Frasor J. Growth hormone potentiates 17β-estradiol-dependent breast cancer cell proliferation independently of IGF-I receptor signaling. Endocrinology 2013 Sep;154(9): 3219-3227.

Saad A, Youssef MI, El-Shennawy L. Cisplatin induced damage in kidney genomic DNA and nephrotoxicity in male rats: the protective effect of grape seed proanthocyanidin extract. Food Chem Toxicol 2009 Jul;7(7):1499-1506.

Saad A, Youssef MI, El-Shennawy L. Protective effect of grape seed proanthocyanidin extract against oxidative stress induced by cisplatin in rats. Food Chem Toxicol 2009 Jun 47(6):1176-1183.

ORAL PRESENTATIONS:

El-Shennawy L and Frasor J. Constitutive activation of the canonical NF-κB pathway switches the phenotype of estrogen receptor positive breast cancer cells from estrogen-induced proliferation to estrogen-induced migration/invasion. Annual Pharmaceutics Graduate Student Research Meeting, University of Illinois at Chicago, Chicago, IL, 2014.

El-Shennawy L, Felice DL, Swanson SM, Untermann TG and Frasor J. Growth hormone potentiates the proliferative effect of breast cancer cells in an AKT-dependent manner. International Fulbright Science and Technology Awardees Capstone Meeting, US Department of State, Washington DC, 2013.

Arslan AD, Maggio M, El-Shennawy L, He X and Beck WT. Knockdown of polypyrimidine tract-binding protein (PTB) sensitizes ovarian cancer cells to chemotherapeutic agents in vitro. American Association for Cancer Research 103rd Annual Meeting 2012, Chicago, IL, 2012.